DOCTORAL THESIS

MicroRNA profiling of multiple sclerosis: from brain to blood

Sanders, Katherine

Award date:
2017

MicroRNA Profiling of Multiple Sclerosis: from Brain to Blood

Katherine Anne Sanders

Submitted in total fulfilment of the requirements of the degree of Doctor of Philosophy

April 2017

Faculty of Health Sciences and Medicine,

Supervised by Associate Professor Lotti Tajouri, Associate Professor Jeannette Lechner-Scott and Professor Rodney J Scott

This research was supported by an Australian Government Research Training Program Scholarship.

ABSTRACT

microRNA (miRNA) are short, non-coding RNAs that can significantly affect gene expression. In Multiple Sclerosis (MS), an autoimmune disease targeting the central nervous system, much is understood about how the immune system promotes neurodegeneration in early stages of disease. However, studies on secondary progressive MS (SPMS) demonstrate that the continued role of the immune system in disease progression is not well characterised. As key regulators of gene expression, identifying changes of miRNA expression patterns in SPMS tissues will provide insight into disease mechanisms at this stage.

Using next-generation sequencing, a comprehensive miRNA expression profile of CD4+ T-cells was attained, and the NanoString nCounter miRNA array was used to the same effect in normal appearing white matter (NAWM) of SPMS individuals. RT-qPCR confirmed results from these methods, and further explored associated gene expression changes, such as common targets of dysregulated miRNAs, and genes essential to miRNA biogenesis and DNA methylation. The role of DNA methylation on miRNA dysregulation was also explored using Illumina 450k arrays.

A convergence of several factors, led by changes in miRNA expression, was found to reduce activity of CD4+ T-cells in SPMS. Broad down-regulation of miRNAs was identified, a novel observation in MS miRNA studies, caused by a reduction of miRNA biogenesis molecules. This resulted in: up-regulation of *SOCS6*, negatively regulating T-cell activation; and *de novo* hypermethylation driven by miR-29b-associated up-regulation of *DNMT3b*. These findings point towards CD4+ T-cells having a diminished role in SPMS. Additionally, analysis of miRNA expression in NAWM also identified miR-29b down-regulation, amongst other miRNAs, that may act to prevent oligodendrocyte maturation and thus hinder remyelination. This suggests that neurodegenerative mechanisms are fully operational in NAWM during SPMS.

In conclusion, the mechanisms of disease progression in SPMS are now better understood. miRNA down-regulation prompts CD4+ T-cells to take a backseat, and neurodegeneration assisted by miRNA dysregulation, is primed to occur in NAWM.

KEYWORDS

microRNA, multiple sclerosis, secondary progressive, progression, CD4+ T-cells, normal appearing white matter, DNA methylation, next-generation sequencing.

DECLARATION BY AUTHOR

This thesis is submitted to Bond University in fulfilment of the requirements of the degree of Doctor of Philosophy. This thesis represents my own original work towards this research degree and contains no material which has been previously submitted for a degree or diploma at this University or any other institution, except where due acknowledgement is made.

KATHERINE ANNE SANDERS

18 April 2017

DECLARATION OF AUTHOR CONTRIBUTIONS

Signed statement of authorship for the published paper that constitutes Chapter Two.

Title: Next-generation sequencing reveals broad down-regulation of microRNAs in secondary progressive multiple sclerosis CD4+ T- cells.

Publication details: Sanders KA, Benton MC, Lea RA, Maltby VE, Agland S, Griffin N, Scott RJ, Tajouri L, Lechner-Scott J. *Next-generation sequencing reveals broad down-regulation of microRNAs in secondary progressive multiple sclerosis CD4+ T-cells.* Clinical epigenetics. 2016;8(1):87.

Principal author	Katherine A Sanders		
Contribution to paper	Collected and processed samples, performed experiments, analysed and interpreted data, and wrote manuscript.		
Overall percentage	75%		
Signature		Date	10/12/2016

Co-author contributions:

Name	Miles C Benton		
Contribution to paper	Analysed NGS data and wrote manuscript.		
Signature		Date	12/12/2016

Name	Rod A Lea		
Contribution to paper	Analysed NGS data and wrote manuscript.		
Signature		Date	10/12/2016

Name	Vicki E Maltby		
Contribution to paper	Performed experiments.		
Signature		Date	12/12/2016

Name	Susan Agland		
Contribution to paper	Collected samples.		
Signature		Date	12/12/2016

Name	Nathan Griffin		
Contribution to paper	Performed experiments.		
Signature		Date	12/12/2016

Name	Rodney J Scott		
Contribution to paper	Supervised the study.		
Signature		Date	13/12/2016

Name	Lotti Tajouri		
Contribution to paper	Supervised the study.		
Signature		Date	12/12/2016

Name	Jeannette Lechner-Scott		
Contribution to paper	Supervised the study.		
Signature		Date	13/12/2016

RESEARCH OUTPUTS AND PUBLICATIONS DURING CANDIDATURE

Peer-review publications

Sanders KA, Benton MC, Lea RA, Maltby VE, Agland S, Griffin N, Scott RJ, Tajouri L, Lechner-Scott J. *Next-generation sequencing reveals broad down-regulation of microRNAs in secondary progressive multiple sclerosis CD4+ T-cells.* Clinical epigenetics. 2016;8(1):87.

Maltby VE, Graves MC, Lea RA, Benton MC, Sanders KA, Tajouri L, Scott RJ, Lechner-Scott J. *Genome-wide DNA methylation profiling of CD8+ T cells shows a distinct epigenetic signature to CD4+ T cells in multiple sclerosis patients.* Clinical epigenetics. 2015;5(7):118.

Published and Presented Conference Abstracts

Sanders KA, Miles BC, Lea RA, Maltby VE, Agland S, Scott RJ, Tajouri L, Lechner-Scott J. *A negative regulator of T-cell activation, SOCS6, is up-regulated in response to decreased microRNA expression in SPMS CD4+ T-cells.* Poster presented at: American Congress of Treatment and Research in Multiple Sclerosis (ACTRIMS); 2016 February 18-20; New Orleans, USA.

Sanders KA, Miles BC, Lea RA, Maltby VE, Agland S, Scott RJ, Tajouri L, Lechner-Scott J. *MicroRNA sequencing identifies four down-regulated microRNA in CD4+ T-cells of secondary progressive multiple sclerosis patients.* Oral presentation at: Multiple Sclerosis Research Australia – progress in MS research; 2015 October 29-30; Melbourne, Australia.

Sanders KA, Miles BC, Lea RA, Maltby VE, Agland S, Scott RJ, Tajouri L, Lechner-Scott J. *MicroRNA sequencing identifies down-regulated microRNA in CD4+ T-cells of secondary progressive multiple sclerosis patients.* Poster presented at: European Congress of Treatment and Research in Multiple Sclerosis (ECTRIMS); 2015 October 7-10; Barcelona, Spain.

Sanders KA, Miles BC, Lea RA, Maltby VE, Agland S, Scott RJ, Tajouri L, Lechner-Scott J. *MicroRNA sequencing identifies down-regulation of miR-21, miR-29b and*

miR-155 in CD4+ T-cells of multiple sclerosis patients. Poster presented at: Australian Society of Medical Research Satellite Symposium; 2015 April 2; Newcastle, Australia.

Sanders KA, Miles BC, Lea RA, Maltby VE, Agland S, Scott RJ, Tajouri L, Lechner-Scott J. *Using next generation sequencing to identify deregulated microRNA in the CD4+ T-cells of secondary progressive multiple sclerosis patients.* Poster presented at: 16th European Molecular Biology Laboratory (EMBL) PhD Symposium; 2014 October 24-26; Heidelberg, Germany.

Sanders KA, Miles BC, Lea RA, Maltby VE, Agland S, Scott RJ, Lechner-Scott J, Tajouri L. *Identification of deregulated microRNA in the CD4+ T-cells of multiple sclerosis patients using next generation sequencing.* Oral presentation at: Inaugural EMBL Australia PhD Symposium; 2014 December 3-5; Sydney, Australia.

Sanders KA, Miles BC, Lea RA, Maltby VE, Agland S, Scott RJ, Tajouri L, Lechner-Scott J. *Next generation sequencing of microRNA in the CD4+ T-cells of secondary progressive multiple sclerosis individuals.* Poster presented at: ACTRIMS-ECTRIMS Joint Meeting; 2014 September 10-13; Boston, USA.

Sanders KA, Scott RJ, Lechner-Scott J, and Tajouri L. *Is relapse during pregnancy in Multiple Sclerosis associated with the PROGINS polymorphism of the progesterone receptor gene.* Poster presented at: 2nd ECTRIMS Summer School; 2014 June 25-27; Tallinn, Estonia.

ETHICS DECLARATION

The research associated with this thesis received ethics approval from:

Bond University Human Research Ethics Committee. RO-1382

Hunter New England Human Research Ethics Committee. 09/04/15/5.13

University of Newcastle Human Research Ethics Committee. H-2009-0365

ACKNOWLEDGEMENTS

This PhD would not have been possible without the support and guidance of many wonderful people. First, I must thank my supervisory team: Lotti Tajouri, without whom this project would never have existed – your constant encouragement and faith in my ability gave me the confidence to see this through. Jeannette Lechner-Scott, for making me so welcome in Newcastle and ensuring I had every opportunity to spread my wings and explore the international world of MS research, this experience was made so much richer for that. And Rodney Scott, for supporting my ideas, and giving me a place to work filled with amazing people.

I must also give a special thank you to Vicki Maltby, I'm not sure I ever would have finished if you hadn't been there to push me along. You motivated me to get into the lab on days when I felt like this PhD was completely impossible. Most of all, you made it fun. I'm really going to miss our duets and dance-offs at the prep bench!

Thank you to the MS team and your unerring belief that I could do it, and to the members of Information-Based Medicine at HMRI, you have made this an unforgettable experience. Particular thanks to Karen, Susan and Trish for your help collecting and processing samples. It was a job that seemed endless, but we made it.

Additionally, this project was made achievable by the financial generosity of a number of organisations. Thank you to Multiple Sclerosis Research Australia and the Trish MS Research Foundation for my Postgraduate Fellowship, and to Bond University's Health Sciences and Medicine Faculty who supported me from the start. Thank you also to the Bloomfield Foundation and the John Hunter Hospital Charitable Trust for funding my research.

Finally, I have to give thanks to those closest to me. Firstly, to Hattie and Tim for being there for celebrations and commiserations, and most importantly for gin and tonics. And to my parents, for always having confidence in my capability, and listening to me babble about failed experiments. I know you didn't understand half of what I was on about, but it allowed me to formulate ideas that made this thesis what it is. Your everlasting encouragement of the pursuit of my dreams has made me who I am today.

TABLE OF CONTENTS

LIST OF TABLES AND FIGURES

Chapter Three

Chapter Four

Chapter Five

Appendix Two

Appendix Three

Appendix Four

LIST OF ABBREVIATIONS

AD	Alzheimer's disease
Ago	Argonaute protein
AHSCT	Autologous hematopoietic stem cell therapy
ALS	Amyotrophic lateral sclerosis
BBB	Blood-brain barrier
BEC	Brain endothelial cell
BIH	Benign intracranial hypertension
bp	Base pair
cDNA	Complementary DNA
circRNA	Circular RNA
CIS	Clinically isolated syndrome
CNS	Central nervous system
CpG	5’-C-phosphate-G-3’
CSF	Cerebrospinal fluid
DC	Discovery cohort
DGCR8	DiGeorge syndrome critical region 8
DMP	Differentially methylated position
DMR	Differentially methylated region
DMT	Disease modifying therapy
DNA	Deoxyribonucleic acid
DNMT	DNA methyltransferase
DTI	Diffusion tensor imaging
EAE	Experimental autoimmune encephalopathy
EBV	Epstein-Barr virus

EDSS	Expanded disability status scale
FDR	False discovery rate
FFPE	Formalin-fixed, paraffin-embedded
FIN	Fingolimod
GA	Glatiramer acetate
Gd+	Gadolinium-enhancing
GDP	Guanosine diphospate
GTP	Guanosine triphosphate
GWAS	Genome-wide association study
HC	Healthy controls
HLA	Human leukocyte antigen
IFN-β	Interferon-beta
IFN-γ	Interferon-gamma
IQR	Interquartile range
K-S test	Kolmogorov-Smirnov test
LCM	Laser capture microdissection
LFB-PAS	Luxol fast blue – periodic acid Schiffs
MHC	Major histocompatibility complex
miRNA	MicroRNA
MRI	Magnetic resonance imaging
mRNA	Messenger RNA
MS	Multiple sclerosis
MSRA	Multiple Sclerosis Research Australia
NAWM	Normal appearing white matter
NGS	Next-generation sequencing
NMOSD	Neuromyelitis optica spectrum disorder

nt	Nucleotide
NTZ	Natalizumab
OND	Other neurological disease
OPC	Oligodendrocyte precursor cell
PBMC	Peripheral blood mononuclear cell
PFC	Pre-frontal cortex
PMI	Post-mortem interval
PML	Progressive multifocal leukoencephalopathy
PPMS	Primary progressive MS
QC	Quality control
qPCR	Quantitative polymerase chain reaction
RISC	RNA induced silencing complex
RNA	Ribonucleic acid
RNase	Ribonuclease
RRMS	Relapsing-remitting MS
RT-qPCR	Reverse transcription quantitative polymerase chain reaction
SD	Standard deviation
SLE	Systemic lupus erythematosus
sncRNA	Short non-coding RNA
snoRNA	Small nucleolar RNA
SNP	Single nucleotide polymorphism
SOCS6	Suppressor of cytokine signalling 6
SPMS	Secondary progressive MS
TEMP	Temporal lobe
Th	T-helper cell
TLDA	TaqMan Low Density Arrays

TRBP	TAR RNA binding protein
T-reg	T-regulatory cell
TSS	Transcription start site
UTR	Untranslated region
UV	Ultraviolet
VC	Validation cohort
WM	White matter

CHAPTER ONE - INTRODUCTION

Multiple Sclerosis (MS) is a complex autoimmune disease affecting the central nervous system, and risk of developing MS is determined by genetics, environment and epigenetic factors. A key epigenetic factor of interest is microRNAs (miRNAs), which regulate gene expression by binding to messenger RNA (mRNA) thus repressing translation to proteins or triggering mRNA degradation. Each miRNA can regulate multiple mRNAs and an mRNA can be targeted by multiple miRNAs. Dysregulation of miRNA levels plays an important role in disease by causing altered cell growth, apoptosis and tissue differentiation.

MiRNA species are short (~22nt), non-coding RNAs that are remarkably stable and there is great potential for them to be used as biomarkers to diagnose and predict disease outcome in MS. Analysis of miRNA expression has been conducted in peripheral blood mononuclear cells (PBMCs), whole blood, T regulatory cells (T-regs), plasma, serum and white matter. However, miRNA studies in heterogeneous cell populations fall short of identifying the effect miRNA dysregulation has on particular cell types. Furthermore, MS pathology initiates in the normal appearing white matter (NAWM) before development of symptomatic lesions, yet studies in white matter have looked at a limited panel of microRNAs and/or in small sample cohorts, and potentially missed significant dysregulation in the MS brain.

The significance of this research lays in identifying microRNA changes in CD4+ T-cells and the NAWM of secondary progressive MS (SPMS) patients, how these changes are correlated, and understanding how this dysregulation plays a role in disease progression.

Multiple sclerosis

MS is an autoimmune disease caused by multifocal inflammatory attacks on the central nervous system (CNS) resulting in demyelination and axonal damage. Propagation of action potentials along the axon is hindered when the insulating myelin sheath is damaged. This results in physical symptoms including muscle weakness, vision impairment and lack of coordination. MS typically affects young Caucasian individuals with disease onset between 20 to 50 years of age. Females account for more cases of MS than males with a ratio ranging from 2:1 to 3:1 (1) and are predisposed to higher relapse activity than males (2). MS has moderate heritability; the concordance rate for developing MS is only 25% in monozygotic twins, whom share 100% of their genes (3, 4), indicating that factors other than genetics significantly contribute to the development of MS, such as environment and epigenetics.

Several forms of MS define varying degrees of symptomatic debilitation over time: relapsing-remitting MS (RRMS), secondary progressive MS (SPMS) and primary progressive MS (PPMS). The most common form of MS is RRMS, accounting for ~85% of initial diagnoses. RRMS is characterised by relapses followed by periods of remission. New symptoms appear spontaneously while existing symptoms become more severe. Relapses can occur over days, weeks or months and recovery can be slow, gradual or instantaneous. The remission phase of RRMS is highly variable in duration, ranging from months to years. Age of disease onset and the use of disease modifying therapies (DMT) influence the risk of RRMS patients converting to a SPMS disease course; risk decreases with DMT treatment (5), whereas higher age of disease onset increases the likelihood of transition to SPMS (5, 6). Onset of progression is more dependent on age rather than the duration of pre-progression symptomatic disease course (7). Over half of RRMS patients will transition to SPMS within 33 years of disease onset; SPMS has no remitting phase and is characterised by demonstrated disability accumulation in the absence of relapses (8). At this stage, the disease is considered to be more neurodegenerative than inflammatory (9) (figure 1.1). Once diagnosed with SPMS, treatment with a DMT is usually halted, as disease progression is less sensitive to current treatment options (10).

PPMS is progressive from disease onset. Disease course is relentlessly progressive without interspersed relapses or significant recovery, and symptoms gradually

worsen. This type of MS is the most severe form and accounts for 15% of MS cases (11). The age of onset of PPMS is typically later than in RRMS, presenting itself in the late thirties or early forties (12). PPMS onset is slow and followed by gradually worsening symptoms and almost no remissions (13).

A single episode of neurological symptoms is defined as Clinically Isolated Syndrome (CIS) (14). On further laboratory or imaging investigation, the clinician may find evidence of a second attack that defines RRMS. Repeat investigations after an interval or a second attack may be necessary to diagnose MS in very early cases.

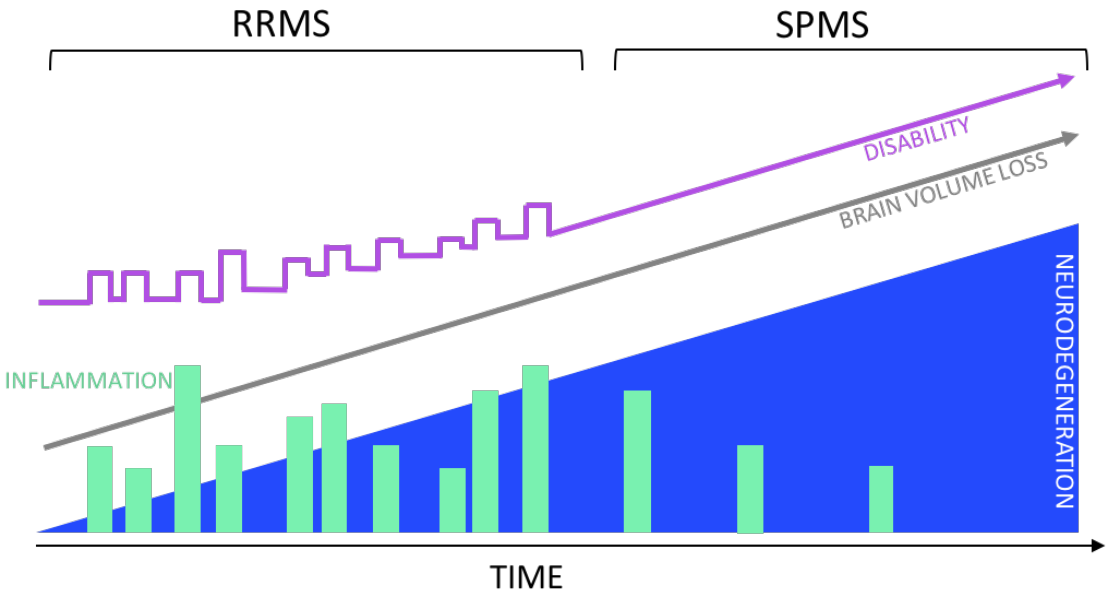

Figure 1.1: Schematic detailing the relationship between disability, neurodegeneration, inflammatory events, brain volume, and disease course.

Diagnosis

MS is diagnosed according to the McDonald criteria that combines neurological history and examination, disseminating lesions in space and time, paraclinical laboratory examinations and magnetic resonance imaging (MRI) (15, 16). Disease severity is measured using the Expanded Disability Status Scale (EDSS), which ranges from 0 to 10 and is based on measures of impairment in seven functional systems as well as walking ability. A score of 0 to 5.5 indicates the MS patient can walk unaided, though walking distance is reduced between EDSS 4.0 to 5.5. A score of 6.0 to 9.5 indicates impairment to walking through to confinement to bed and other

functional deficiencies (17). Following RRMS, EDSS increase in the absence of relapse, over the course of at least three months, indicates the patient has transitioned to SPMS disease course (8).

Pathogenesis and progression

MS is an autoimmune disease that attacks the CNS, however the initial mechanism of pathogenesis is not fully established. Does the immune system attack the CNS unprompted, or is there a starting point in the CNS that cascades down to activation of the immune system?

Homeostasis of the CNS is largely controlled by the blood-brain barrier (BBB) that actively limits movement of mediators and lymphocytes from the periphery to the CNS. The BBB is a highly specialised component of the neurovascular system and is disrupted in MS allowing immune activity within the CNS. In RRMS, CD4+ T-cells are amongst the primary infiltrators moving from the periphery, through the BBB into the CNS (18). These cells then initiate an immune response that results in localised demyelination and corresponding symptoms.

Several neurodegenerative disorders have BBB dysfunction as a component of their pathogenesis including Alzheimer's (AD) and Parkinson's diseases and Amyotrophic Lateral Sclerosis (ALS) (19). Studies have thus far defined a number of pathways for lymphocyte entry from blood to the CNS (20-22) and results of a study in experimental autoimmune encephalopathy (EAE) in mice (animal model of MS) suggest that infiltration of the BBB occurs in parenchymal capillaries and post-capillary venules (21). Recently, a lymphatic system within the CNS was discovered (23), presenting a further potential path for lymphocyte infiltration into the CNS.

Endothelial cells in the BBB express tight junction and adherens junction proteins which act to reduce paracellular permeability (24). Astrocytes play an important role in maintaining the integrity of the BBB through contact-dependant mechanisms and secretion of essential factors, however in neuroinflammatory disorders such as MS, astrocytes can also release inflammatory cytokines causing endothelial cell activation and BBB dysregulation (24, 25). In MS, activated T-cells produce cytokines, reactive oxygen species and matrix metalloproteinases that either disrupt BBB components or act on receptors expressed by endothelial cells of the BBB (for in-depth review see

(26)). In contrast, resting T-cells have limited capability to cross the BBB (27). Advancement of brain endothelial cells towards an inflammation phenotype is considered to be mediated by proinflammatory cytokines such as TNFα and IFN-γ, secreted from lymphocytes and CNS-resident cells. These induce the expression of chemoattractant cytokines (e.g. CXCL10, CX3CL1 and CCL3) on the brain endothelium, promoting adhesion of lymphocytes to the BBB and increased permeability (26, 28, 29). Furthermore, it should be noted that lymphocyte infiltration of the BBB increases the barrier's permeability, facilitating subsequent crossings (30). Consequently, a permissive environment is created for the trafficking of inflammatory molecules and circulating lymphocytes into the CNS, causing demyelination and axonal loss.

Many studies have focused on the activity of lymphocytes, particularly CD4+ T-cells (31), in RRMS, and their pathway into the CNS. However, the interplay between the immune system and CNS in SPMS is an incomplete puzzle. While it is recognised that neurodegeneration is a significant driving force in accumulation of disability (increased EDSS) in SPMS, the continued role of CD4+ T-cells and the immune system in disease progression is poorly established (32).

Myelin is synthesised by mature oligodendrocytes and forms the extended membrane of oligodendrocyte cells; it is composed of a lipid bilayer and proteins. The function of myelin is to insulate neurons providing rapid conduction of action potentials along the axon. Damage to axons occurs very early on in disease (33) and repeated demyelination events eventually destroy the axon (34). Over the course of MS, a series of remyelination events occur whereby oligodendrocyte precursor cells (OPC) migrate to surround active lesions in response to semaphorin 3A and 3F (35), temporally coinciding with the phagocytic removal of myelin. These OPCs then differentiate to mature oligodendrocytes and remyelinate the naked axons. Cycles of demyelination and remyelination eventually exhaust the capacity for tissue repair and the degree of recovery associated with remyelination decreases after each event (36).

Histologically, MS presents as lesions throughout the CNS (figure 1.2). Demyelinated lesions form most commonly in the white matter but can also form in grey matter and across white and grey matter (leukocortical) (37). The diameter of lesions can vary greatly, from one millimetre to several centimetres and occur throughout the CNS but

most predominantly in the periventricular white matter and optic nerve (38). Formation of lesions is associated with degeneration of myelin and resulting impaired neuronal function causing physical symptoms of MS. There are three main types of lesions: active, chronic active and chronic. Active lesions are filled with macrophages containing myelin debris, demonstrate infiltration by lymphocytes, and BBB disruption (39). Unlike active lesions, chronic active lesions exhibit well demarcated margins and myelin-containing macrophages are commonly found here. The centre of a chronic active lesion may be either absent of myelin or contain remyelinated fibres originating from the lesion edge. Chronic lesions have no inflammatory component and a fibrous centre, as with chronic active lesions, remyelination can also occur throughout the whole lesion; this is known as a shadow plaque (40).

Normal appearing white matter (NAWM) is defined as a region that appears unaltered upon light microscopic analysis. However, in-depth molecular analyses of NAWM indicate that MS pathology initiates within this tissue before development of symptomatic lesions. A study focused on microglia analysed the phenotype *ex vivo* and the immune responsiveness *in vitro* of microglia from MS NAWM. This study found elevated levels of the immunoregulatory molecule CD45, however contrasting low levels of additional markers such as CD206 were also observed. These findings, combined with increased mRNA levels of the inhibitory CD32b isoform, demonstrate that microglia within MS brain NAWM are in an alerted state but displaying features of immunosuppression (further characterised by unresponsiveness to bacterial lipopolysaccharide) (41), likely preventing full activation of the inflammatory response responsible for lesion formation. In murine EAE models, severe nerve fibre pathology was detected in the NAWM, comparable to that found in white matter lesions (42).

MRI techniques have also been used to observe NAWM and monitor its influence on MS pathology. Diffusion tensor imaging (DTI) can assess the micro-structural integrity of white matter in MS. The degree of axonal degradation and white matter pathology is resolved by observing the extent to which water diffuses preferentially along axons and is constrained by cell walls (43). DTI is sensitive to myelin content and axon count (44), and to the evolution of tissue damage within lesions (45). DTI of NAWM also correlates with processing speed in MS individuals (46).

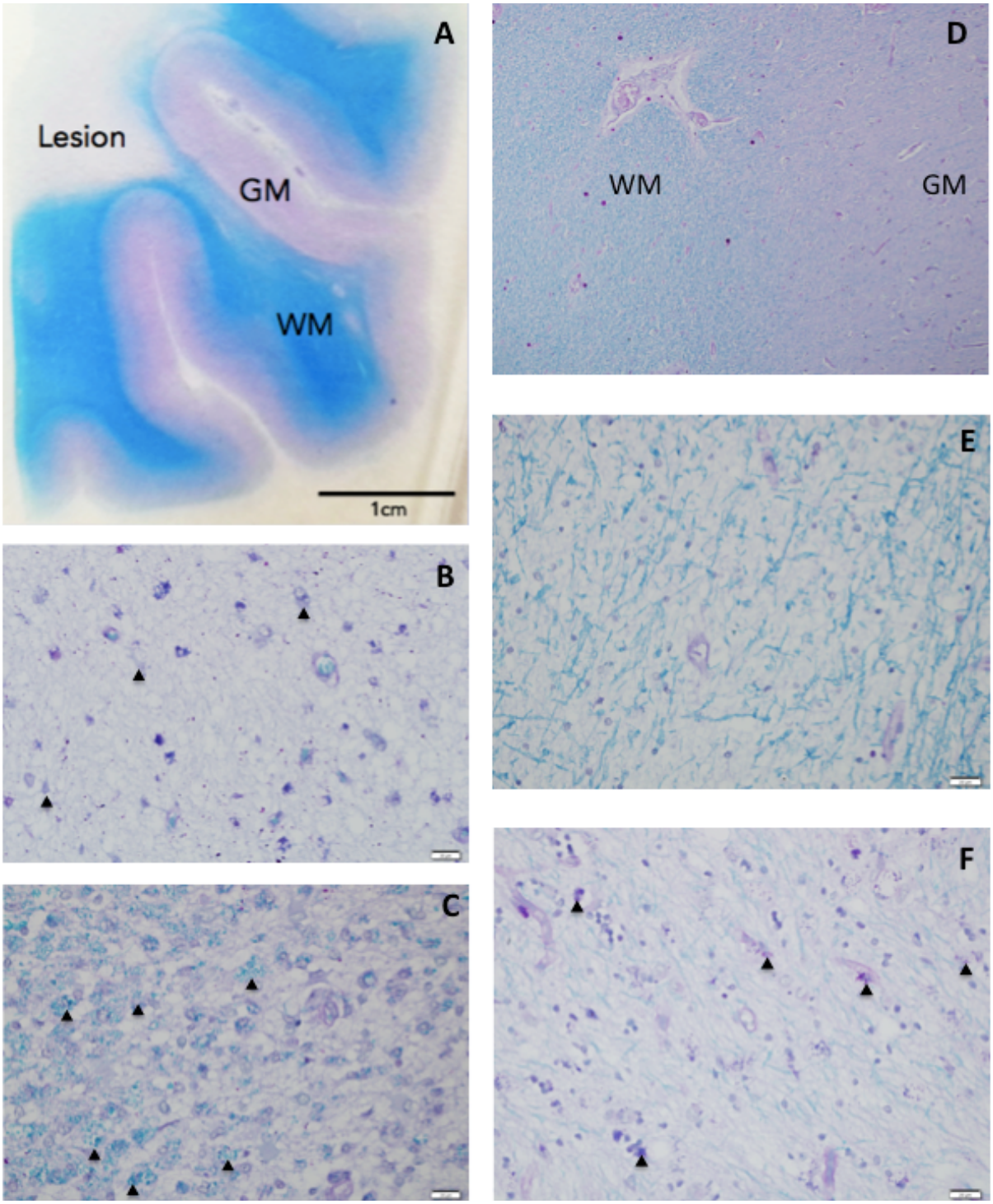

Figure 1.2: Brain sections stained with Luxol Fast Blue – Periodic acid Schiff (LFB-PAS) depicting MS pathology. **(A)** Whole section showing white matter (WM), grey matter (GM) and a chronic lesion. **(B)** Chronic lesion (x400) astrocytes (arrows) present. **(C)** Active lesion (x400) LFB+ macrophages (arrows). **(D)** Normal appearing WM (NAWM) (x200) with consistent myelin coverage and normal oligodendrocyte morphology. GM adjacent. **(E)** Remyelinated region (x400) patchy areas of myelin

and oligodendrocytes difficult to locate. **(F)** Recently active region (x400), macrophages (arrows) containing PAS positive material. These images were produced by Katherine Sanders from samples and methods described in Chapter Five.

Environmental risk factors

Many studies have shown that environmental influences can cause significant changes to epigenetic traits (47-49), which in turn may impact of risk of developing MS, disease course and progression. Factors such as vitamin D deficiency, smoking and Epstein-Barr virus (EBV) infection show strong and consistent association with development of MS (in-depth review (50)).

The prevalence of MS is significantly lower in countries in close proximity to the equator (51); this observed latitudinal effect complements the finding that MS risk decreases with increasing vitamin D levels in serum (52). Vitamin D is produced in the skin as a result of exposure to ultraviolet-B (UV) radiation and it has been shown that vitamin D regulates expression of histone modifying enzymes (53), demonstrating a probable link between vitamin D and epigenetic regulation in MS. Disease course in MS also appears to be influenced by levels of vitamin D; degree of disability (54) and frequency of relapses are augmented by lower levels of vitamin D (54, 55). However, it should be noted that serum vitamin D levels are often used as a proxy for patient's UV exposure. UV has immunomodulatory mechanisms that can be vitamin D independent (56). Therefore, caution must be exercised when describing effects of UV and vitamin D as the same factor, as they can operate independently.

Cigarette smoke is a very heterogeneous substance containing many toxins and carcinogens; this makes it difficult to associate any specific substance with a particular mechanism of action. However, analysis of the large scale Nurses' Health Study clearly demonstrated significantly increased risk of getting MS in smokers compared to those who never smoked (57). Cigarette smoke also has a significant impact on epigenetic mechanisms including DNA methylation (49), microRNA (miRNA) expression (58-60) and histone modification (61-63).

EBV infection is very common and persists latently in memory B cells after infection. Seropositivity for EBV in adults is approximately 95% in the normal population complicating studies into the effect of EBV on MS risk. Seronegativity is associated with very low risk of MS development (64), whereas a symptomatic response to EBV (infectious mononucleosis) nearly doubles the risk of getting MS (65). Changes in DNA methylation occur in response to EBV infection via the up-regulation of several DNA methyltransferase genes (66), and miRNA expression in B cells is dysregulated (67). EBV was the first virus in which miRNAs were found (68) and the Sanger database presently lists EBV as encoding 44 mature miRNAs. Several EBV-encoded miRNAs have been found to be dysregulated in the B cells of RRMS individuals (69).

Other potential environmental risk factors for MS have been identified, including sodium intake (70, 71), alcohol consumption (72) and childhood obesity (73, 74). However, further studies are necessary to corroborate their effect on MS risk.

Genetic risk factors

MS is a complex disease and incidence is influenced by many factors including genetics, though polymorphisms alone cannot fully determine MS risk. As demonstrated above, environmental factors are strongly associated with MS risk and some have also been associated with epigenetic modifications. There are a number of genetic loci that predetermine an individual's MS risk baseline before environmental risk factors are accounted for. The human leukocyte antigen (HLA) gene cluster located at chromosome 6p21.3 in the major histocompatibility region (MHC), has strong association to MS susceptibility with the primary signal located at the HLA-DRB1 gene (75); some HLA-DRB1 alleles are associated with an up to three-fold increased risk of developing MS (76). The gene products of the MHC locus are involved in antigen presentation which ties-in with the autoimmune status of MS. HLA-DRB1*15 has been identified as a risk allele for MS; its frequency is higher in females than males and transmission is more common from mother to daughter compared with father to daughter inheritance (77). Also, the HLA-DRB1*15 allele is related with lower age of onset (78). In contrast, the HLA-DRB1*08 allele is prevalent in RRMS and associated with lower relapse rate and degree of disability (79).

New genetic susceptibility variants for MS continue to be discovered; in 2013 the International Multiple Sclerosis Genetics Consortium identified 48 new susceptibility single nucleotide polymorphisms (SNPs) (80) bringing the total number of variants outside the MHC locus to 110 (80-84). Variants were identified in a number of loci including nuclear factor-κB that plays a role in controlling gene expression relevant to autoimmune disease (85). Furthermore, two SNP variants in the MHC produce a two-fold increase in the likelihood of positive oligoclonal bands in the cerebrospinal fluid (CSF); a key diagnostic marker of MS (86). Other genomic regions containing susceptibility variants are related to functions including antigen presentation and processing, the MHC, oxidative phosphorylation, synaptic transmission, cellular transport and translational initiation (for a detailed review see (87)). A large proportion of these variants were in regions not previously associated with known function, though they are predominantly found in close proximity to immunologically relevant genes (83). Many of these variants have no known function and may not have any consequence for the gene in which they are located. However, it is now becoming apparent that some of these variants are associated with control of gene expression (88). Perturbation of gene expression control would have wide consequences and could be significantly contributing to MS. Interestingly, these genetic studies have identified susceptibility factors strongly concentrated on the immune system. Though why the immune system specifically targets the CNS in MS is still not clear.

Epigenetics

Epigenetics causes modification of the expression of genes without altering the genetic code itself. Epigenetic factors are capable of creating or influencing chemical modifications on the genome, affecting the way genes are expressed. There are numerous epigenetic mechanisms including DNA methylation, histone modifications (methylation and adenylation), post-transcriptional alterations (polyadenylation) and RNA interfering molecules such as miRNAs.

DNA methylation

DNA methylation is the addition of a methyl group to cytosine at 5'-C-phospate-G-3' (CpG) dinucleotides, often concentrated in hundreds of dinucleotide repeats (CpG islands) near gene promoter regions. Hypermethylation in promoter regions suppresses gene expression (89). DNA methylation is mediated by DNA methyltransferases (DNMTs). Maintenance of DNA methylation patterns is performed by DNMT1 during cell replication, whereas *de novo* methylation of unmethylated sites is carried out by DNMT3a and DNMT3b (90). Methylation patterns are dynamic and can change with age (91), environmental pressures (92), and disease, including MS (93).

A study of discordant monozygotic twins identified no significant differential DNA methylation (94) suggesting other epigenetic mechanisms play a crucial role in MS risk, however it should be noted that the study only looked at three pairs of twins and did not perform MRI on the unaffected twin to show discordance. In fact, other DNA methylation studies have identified differentially methylated regions (DMRs) in numerous MS tissues compared to healthy controls (HC) (95-101). Genome-wide DNA methylation analyses have been conducted in CD4+ and CD8+ T-cells of RRMS patients (98, 99, 101), and a hypomethylated DMR in the MHC region, specifically HLA-DRB1, was identified in CD4+ T-cells (98). Furthermore, hypo- and hypermethylated DMRs in NAWM of MS patients have a demonstrated effect on associated gene transcription (100).

However, while DNA methylation changes clearly play a role in MS pathology, it does not account for all remaining risk, and other epigenetic factors such as miRNAs must also be considered. Interestingly, epigenetic mechanisms can regulate or influence one another. DNA methylation can control expression of miRNAs (102), and vice versa (103), though there are currently no studies in MS cross-referencing DNA methylation and miRNA expression patterns.

MicroRNA

miRNAs are endogenous short (~22nt), non-coding RNAs that play a role as post-transcriptional regulators. Gene silencing occurs when they bind to the 3' untranslated region (UTR) of target mRNAs, suppressing translation or marking the mRNA for degradation. According to miRBase v21, over 1800 miRNAs have been identified in the human genome (104) and it is estimated that miRNAs regulate at least half of human genes. Dysregulation of one or many miRNAs will affect cellular gene expression, resulting in abnormal phenotype that may contribute to disease onset, progression and exacerbation.

One miRNA can target many mRNA; likewise, a mRNA may have binding sites for multiple miRNAs. The target sites on mRNAs are only partially complementary to the miRNA itself and this makes predicting the target genes of miRNAs difficult. However, nucleotides 2-7 of the miRNA (known as the seed region) are critical for target recognition (105). Software packages are available that utilise prediction algorithms to identify potential targets and are often used in combination to select target mRNAs for experimental validation. For example, miRSystem, a freely accessible online tool, incorporates seven miRNA gene target prediction programs to robustly predict gene targets (106).

MicroRNA biogenesis and mechanism of action

MiRNA-coding sequences are commonly found within or overlapping with mRNA or other RNA genes; these are referred to as the host genes for miRNAs. In most cases, miRNA genes are transcribed by RNA polymerase II producing the primary miRNA transcript (pri-miRNA) (107). There are two pathways that lead to the processing of mature miRNAs, canonical and non-canonical. The majority of miRNAs are processed in the canonical pathway and shall be described (Figure 1.2).

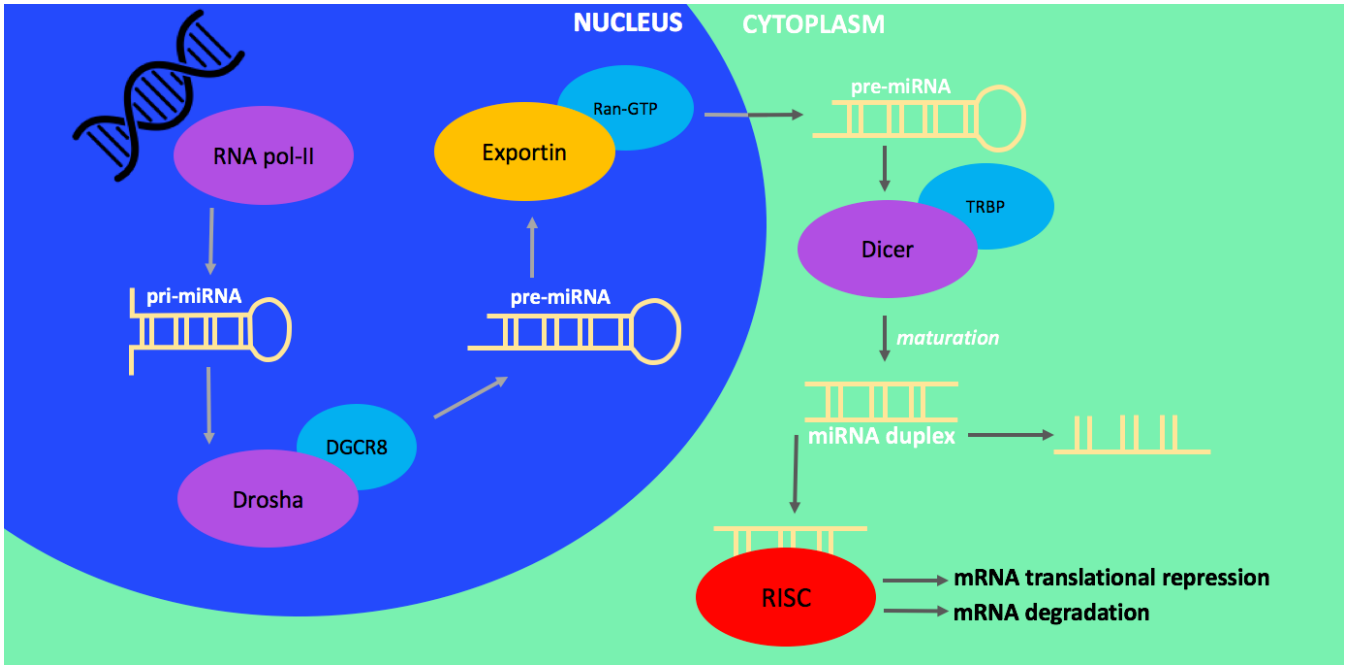

Figure 1.3: The canonical pathway of microRNA biogenesis. See text below for explanation.

Within the nucleus the pri-miRNA is cleaved by Drosha, bound by its regulatory subunit DGCR8 (DiGeorge critical region 8), to an isolated hairpin-structured precursor (pre-miRNA) approximately 60-70nt long. A two-nucleotide overhang is produced by Drosha's ribonuclease (RNase) III activity and marks the pre-miRNA for export to the cytoplasm performed by Exportin 5 associated with Ran cofactor coupled to guanosine triphosphate (GTP). Once in the cytoplasm, Exportin 5 releases the pre-miRNA when GTP is replaced by guanosine diphosphate (GDP). Dicer (another RNase), assisted by its cofactor TAR RNA binding protein (TRBP), then cleaves the pre-miRNA to produce a miRNA duplex approximately 22nt (108). The duplex then associates with Argonaute (Ago) protein where it is unwound; one strain is retained as the mature miRNA and forms an RNA-induced silencing complex (RISC) and is then capable of mRNA regulation. The two strands of the mature miRNA follow established nomenclature, -5p or -3p, dependant on whether they originate from the 5' or 3' end of the pri-miRNA loop. Often, one strand is dominant and is not annotated as -5p or -3p in the literature. However, both strands are functional in many miRNAs, and will associate with different Ago protein complexes to become active (109).

The RISC complex utilises the mature miRNA for direct target recognition using base pairing interactions with the 3'UTR of mRNA transcripts (110). As previously mentioned, miRNA-mRNA complementarity is partial and downstream regulatory mechanisms are influenced by the extent of this complementarity. A perfect match triggers degradation of the mRNA catalysed by Ago2 protein (111) whereas translational repression is the result of mismatches. In animals, the most prevalent mechanism of miRNA action is translational repression though the exact process of repression is not fully understood. A review by Tang et al. (112) outlined proposals of RISC-directed repression including: relocation or sequestration of target mRNA to processing bodies or stress granules, translational repression at initiation or post-initiation stages, mRNA decay through rapid deadenylation and protein degradation immediately following translation.

Dysregulation of miRNA levels plays a key role in disease by causing altered cell growth, apoptosis and irregular tissue differentiation. In MS, it is not clear whether miRNA dysregulation contributes to disease onset/progression or if it is a reflection of the affected cell's response to disease; it is likely both. The mechanisms that cause this dysregulation are varied (113) and include genomic sequence mutations, DNA methylation, transcription factor dysregulation, and changes in the expression of miRNA biogenesis molecules, Drosha, DGCR8 and Dicer. Expression changes in miRNA biogenesis molecules have been investigated in MS (114, 115), though their correlation with overall miRNA expression has not been fully ascertained. Magner et al. have observed that changes in Dicer expression were not correlated with miRNA expression (115), though no miRNA expression correlation analyses have been performed for Drosha or DGCR8.

MicroRNAs and Multiple Sclerosis

Analysis of miRNA expression has been conducted in many tissues in MS (Tables 1.1 and 1.2), predominantly in RRMS. As an autoimmune disease targeting the CNS, miRNA profiles in the immune system and CNS are of particular interest, and studies have been conducted on cellular tissues, including PBMCs, whole blood, T cells, B cells, and white matter (116).

Samples that are routinely acquired and processed, such as whole blood and non-cellular circulating fluids (plasma, serum and CSF), are excellent for establishing biomarkers. miRNA species are remarkably stable molecules due to their short length and minimal recognition sites for nucleases (117), and their aberrant expression may be used for diagnosis, predicting treatment response, and differentiating MS subtypes.

However, identifying the effect of dysregulation on cell activity is impossible in heterogeneous cell samples. Insight into the functional consequences of miRNA dysregulation in MS can only be resolved from analyses of individual cell subtypes, such as T and B-cells, microglia and oligodendrocytes. miRNA targets have only been experimentally validated in a few studies. Identifying the effect of dysregulated miRNAs in specific cells will provide key insight into the mechanisms of disease and guidance for the design of future MS therapies.

Table 1.1: MicroRNA observed as dysregulated in more than one MS study or with experimentally validated functional consequences. See Table 1.2 for details on sample size, miRNAs analysed and methodologies. MiRNAs dysregulated in CD4+ T-cells and NAWM have been highlighted using ϕ and θ respectively.

MicroRNA	Tissue	Direction of change in MS	Disease stage	Validated Target	Functional result
miR-15a$^{\phi}$	CD4+CD25+^{high} T-cells (118)	Up	RRMS		
	CD4+ T-cells (119)	Down	RRMS	BCL2	Decreased apoptosis.
miR-15b	Serum (120-122)	Down	RR & PPMS (120) RR, SP & PPMS (121)		
		Up after 6-months FIN-therapy	RRMS (122)		
	Whole blood (123)	Down compared to NMOSD	RRMS/CIS		
miR-16$^{\phi}$	CD4+ T-cells (119)	Down	RRMS	BCL2	Decreased apoptosis.
	CD4+ and CD8+ T-cells (124)	Up & normalised after AHSCT	RR, SP & PPMS		
miR-17-5p$^{\phi}$	CD4+ T-cells (125)	Up	RRMS	PTEN & PI3KR1	
	CD4+ T-cells (126)	Down after NTZ-therapy & up during relapse	RRMS	PTEN, BIM & TGFBR2	Reduced miR-17 decreases cell proliferation.
	Whole blood (127)	Down	RR, SP & PPMS		
miR-19b$^{\phi}$	CD4+CD25+^{high} T-cells (118)	Up	RRMS		
	B-cells (69)	Down & normalised in NTZ-treated	RRMS		
miR-20a-5p	Whole blood (127, 128)	Down	RR, SP & PPMS (127) RRMS & CIS (128)		

MicroRNA	Tissue	Direction of change in MS	Disease stage	Val. Target	Functional result
miR-21-5p	Whole blood (123)	Down compared to NMOSD	RRMS/CIS		
	PBMCs (129)	Up	RRMS		
miR-22-3p$^{\phi}$	CD4+CD25+^{high} T-cells (118)	Up	RRMS		
	Plasma (130)	Up	MS (unspecified)		
miR-26a-5p	PBMCs (131)	Up in relapse compared to remitting	RRMS – relapse and remitting states		
	PBMCs (132)	Up after 3 months IFN-β therapy in responders	RRMS - IFN-β responders and non-responders	DLG4	
	PBMCs (133)	Down after 6 months NTZ-therapy	RRMS		
miR-27a$^{\phi}$	CD4+ T-cells (134)	Up in relapse vs. remitting & HC	RRMS – relapse and remitting states		
	Serum (135)	Up in RRMS vs. SPMS	RR & SPMS		
miR-27b$^{\phi}$	Naïve CD4+ T-cells (136, 137)	Up	RR, SP & PPMS	BMI1 (136) TGFβ signalling components (137)	Inhibits Th2 differentiation. Inhibits differentiation of naïve CD4+ T-cells into T-reg.
miR-29a-3p$^{\phi}$	CD4+CD25+^{high} T-cells (118)	Up	RRMS		
	PBMCs (138)	Down after 1 month IFN-β therapy	RRMS & CIS		
miR-29b-3p$^{\phi}$	CD4+CD45RO+ T-cells (139)	Up	RR, SP & PPMS	IFN-γ	Feedback loop – IFN-γ induces miR-29b-3p expression.

MicroRNA	Tissue	Direction of change in MS	Disease stage	Validated Target	Functional result
miR-29c-3p$^{\phi\theta}$	CD4+CD25+^{high} T-cells (118)	Up	RRMS		
	PBMCs (138)	Down after 1month IFN-β therapy	RRMS & CIS		
	NAWM (140)	Down	MS (unspecified)		
miR-34a	Active & inactive WM lesion (141)	Up in active lesions	MS (unspecified)	CD47	Promotes phagocytosis of myelin by macrophages.
miR-93$^{\phi}$	CD4+CD25+^{high} T-cells (118)	Up	RRMS		
	PBMCs (142)	Up	RRMS		
miR-106b$^{\phi}$	CD4+CD25+^{high} T-cells (118)	Up	RRMS		
	B-cells (69)	Down & normalised in NTZ-treated	RRMS		
	CD4+ T-cells (126)	Up in NTZ-treated	RRMS	TGFBR2	
miR-124	Hippocampus (143)	Up in demyelinated	MS (unspecified)	AMPA receptor	Reduced memory performance.
miR-125a-5p	BEC (144)	Down	MS (unspecified)	ICAM-1	Increased monocyte migration through BBB.
	PBMCs (145)	Up	RRMS		
	Whole blood (146)	Down after NTZ-therapy	RRMS & PML		
miR-125a-3p	CSF (147)	Up & active-MS vs. RRMS	RR & SPMS	MBP, FYN, NRG1, MAP1B	Blocks maturation in OPCs impairing remyelination.

MicroRNA	Tissue	Direction of change in MS	Disease stage	Validated Target	Functional result
miR-126$^{\phi}$	CD4+ T-cells (125)	Up	RRMS		
	CD4+ T-cells (148)	Down in NTZ-treated	RRMS	POU2AFI	Regulates expression of transcription factor Spi-B.
	PBMCs (149)	Down in NTZ-treated, up in PML	RRMS		
miR-128$^{\phi}$	Naïve CD4+ T-cells (136, 137)	Up	RR, SP & PPMS	BMI1 (136)	Inhibits Th2 differentiation.
				TGFβ signalling components (137)	Inhibits differentiation of naïve CD4+ T-cells into T-reg.
miR-132	B-cells (150)	Up	RRMS	SIRT1	Increases expression of proinflammatory cytokines (TNFα and LT).
	PBMCs (133)	Up	RRMS		
miR-140-5p$^{\phi}$	CD4+ T-cells (151)	Down	RRMS	STAT1	Increased encephalitogenic Th1 differentiation.
miR-142-3p$^{\phi}$	CD4+ and CD8+ T-cells (124)	Up & normalised after AHSCT	RR, SP & PPMS		
	PBMCs (152)	Up & normalised in GA-treated	RRMS		
miR-145	Whole blood (153)	Up	RRMS		
	PBMCs (142)	Up	RRMS		
	Plasma (142, 154)	Up & RRMS vs. SPMS	RR & SPMS		
	Serum (142)	Up	RRMS		
miR-146a	PBMCs (129)	Up	RR, SP & PPMS		
	PBMCs (152)	Up & normalised in GA-treated	RRMS		
	BEC (155)	Up	MS (unspecified)	IRAK1, TRAF6, NFAT5, RhoA	Inhibits NF-κB to negatively modulate leukocyte adhesion.

MicroRNA	Tissue	Direction of change in MS	Disease stage	Validated Target	Functional result
miR-150	CSF (156)	Up in CIS-converters	CIS & MS		
miR-155$^{\phi\theta}$	Active & inactive WM lesion (141)	Up in active lesions	MS (unspecified)	CD47	Promotes phagocytosis of myelin by macrophages.
	BEC (active lesions and NAWM) (157)	Up in active lesions	RR, SP & PPMS	CLDN-2, ANXA-2, DOCK-1, SDCBP	Cell-cell complex molecules and focal adhesion molecules targeted resulting in BBB permeability.
	CD4+ and CD8+ T-cells (124)	Up & normalised after AHSCT	RR, SP & PPMS		
	NAWM (158)	Up	RR, SP & PPMS	AKR1C1 & AKR1C2	Reduced neurosteroid synthesis (including allopregnanolone).
	PBMCs (133, 152, 159)	Up & down after NTZ-therapy	RRMS		
miR-181a	Hippocampus (143)	Down in demyelinated	MS (unspecified)		
	B-cells (69)	Down	RRMS		
miR-181c	Hippocampus (143)	Down in demyelinated	MS (unspecified)		
	CSF (160)	Up	RR, SP & PPMS		
miR-191$^{\theta}$	NAWM (140)	Down	MS (unspecified)	SOX4, FZD5, BDNF, WSB1	SOX4 over-expression in oligodendrocytes prevents myelination.
	B-cells (69)	Down & normalised after 6-months NTZ-therapy	RRMS		
miR-221$^{\phi}$	CD4+CD25+^{high} T-cells (118)	Up	RRMS		
	Plasma (154)	Up in RRMS vs. ALS	RRMS & SPMS		

MicroRNA	Tissue	Direction of change in MS	Disease stage	Validated Target	Functional result
miR-223$^{\phi\theta}$	Whole blood (153)	Up	RRMS		
	CD4+CD25+^{high} T-cells (118)	Up	RRMS		
	CD4+ T-cells (161)	Up in relapse, down in remission vs. HC	RRMS		
	PBMCs (120)	Up	RRMS		
	Serum (120-122)	Down	RR & PPMS (120), RR, SP & PPMS (121), RRMS (122)		
miR-223	NAWM (140)	Up	MS (unspecified)		
miR-326$^{\phi}$	Active & inactive WM lesion (141)	Up in active lesions	MS (unspecified)	CD47	Promotes phagocytosis of myelin by macrophages.
	CD4+ T-cells (162)	Up	RRMS	Ets-1	Promotes Th-17 differentiation.
	PBMCs (152)	Up	RRMS		
	PBMCs (131)	Up in relapse compared to remitting	RRMS – relapse and remitting states		
miR-338-5p$^{\phi\theta}$	NAWM (158)	Up	RR, SP & PPMS	AKR1C1 & AKR1C2	Reduced neurosteroid synthesis (including allopregnanolone).
	CD4+CD25+^{high} T-cells (118)	Down	RRMS		
miR-340$^{\phi}$	Resting memory CD4+ CD45RO+ T-cells (136)	Up	RR, SP & PPMS	BMI1 & IL-4	Inhibits Th2 differentiation and contributes to proinflammatory Th1 response.
miR-422a	Whole blood (153)	Up	RRMS		
	Plasma (130)	Up	MS (unspecified)		
	B-cells (125)	Down	RRMS		

MicroRNA	Tissue	Direction of change in MS	Disease stage	Validated Target	Functional result
miR-497$^{\phi}$	CD4 + T-cells (125)	Up	RRMS		
	CD8+ T-cells (125)	Down	RRMS		
	B cells (125)	Up	RRMS		
miR-629-5p	CD8+ T-cells (125)	Up	RRMS		
	Whole blood (128)	Up	RRMS & CIS		
	Whole blood (146)	Down in PML onset (NTZ-therapy)	RRMS & PML		
let-7c	Plasma (154)	Up in RRMS vs. SPMS	RR & SPMS		
	Whole blood (146)	Down after NTZ- therapy	RRMS & PML		
	Serum (135)	Up	RR, SP & PPMS		
let-7d	Plasma (154)	Up in RRMS vs. HC & RRMS vs. ALS	RR & SPMS		
	PBMCs (142)	Up	RRMS		
let-7g	Hippocampus (143)	Up in demyelinated	MS (unspecified)		
	PBMCs (163)	Down	RR, SP & PPMS		

Abbreviations: AHSCT = autologous haematopoietic stem cell transplant; BEC = brain endothelial cells; CSF = cerebrospinal fluid; FIN = fingolimod; GA = glatiramer acetate; HC = healthy controls; IFN-β = interferon-beta; IFN-γ = interferon-gamma; NMOSD = neuromyelitis optica spectrum disorder; NTZ = natalizumab; OPC = oligodendrocyte precursor cell; PBMC = peripheral blood mononuclear cell; PML = progressive multifocal leukoencephalopathy; PPMS = primary progressive MS; RRMS = relapsing-remitting multiple sclerosis; SPMS = secondary progressive MS; Th = T-helper cells; T-reg = T regulatory cells; WM = white matter.

Table 1.2: Experimental details of studies recorded in Table 1.1.

Paper	Sample size and type	Methodology	Number of miRNA analysed
De Santis (118)	DC: 12 RRMS, 14 HC. VC: 10 RRMS, 10 HC	Microarray	723
Lorenzi (119)	DC: 15 RRMS, 15 HC. VC: 5 RRMS, 5 HC	qPCR	2
Ridolfi (120)	15 MS (11 remitting RRMS, 4 PPMS), 12 HC	qPCR	3
Fenoglio (121)	Italian pop – DC: 3 RRMS, 4 PPMS, 3 HC. VC: 8 RRMS, 5 PPMS, 11 HC USA pop – 15 RRMS, 13 PPMS, 30 HC	qPCR	88
Lindberg (125)	DC: 8 RRMS, 10 HC. VC: 15 RRMS, 10 HC	qPCR (TLDA)	365
Meira (126)	14 NTZ-treated RRMS, 14 untreated RRMS, 14 HC	qPCR	2
Cox (127)	59 MS (24 RRMS, 17 SPMS, 18 PPMS), 37 HC	Microarray	733
Sievers (69)	DC: 10 untreated RRMS, 10 NTZ-treated RRMS, 10 HC. VC: 30 RRMS, 7 HC	Microarray & qPCR	1059
Keller (128)	25 RRMS, 25 CIS, 25 HC	NGS, microarray & qPCR	All
Siegel (130)	4 MS, 4 HC	Microarray	>900
Honardoost (131)	20 relapsing RRMS (treatment naïve), 20 remitting RRMS (IFN-β treated), 20 HC	qPCR	2
De Felice (132)	DC: 20 IFN-β treated RRMS, 10 non-responder RRMS 3 time points (0,3,6 months). VC: 20 IFN-β treated RRMS. 3 time points (0,3,6 months)	Cloning based sequencing & qPCR	All
Guerau-de-Arellano (136)	22 MS (12 RRMS, 5 SPMS, 5 PPMS), 16 HC	qPCR (TLDA)	667

Paper	Sample size and type	Methodology	Number of miRNA analysed
Hecker (138)	DC: 4 RRMS, 2 CIS. VC: 8 RRMS, 4 CIS. 4 time points (before 1st, 2nd & 3rd IFN-β injection & 1 month after treatment)	qPCR (TLDA) & microarray	651
Junker (141)	20 MS, 10 HC	qPCR	365
Søndergaard (142)	PBMC – DC: 20 RRMS, 21 HC. VC: 12 RRMS, 20 HC Plasma – 22 RRMS, 15 HC Serum – 40 RRMS, 40 HC	Microarray (PBMCs only) & qPCR	847
Dutta (143)	18 MS (9 myelinated, 9 demyelinated hippocampus), 9 HC	qPCR	Unknown
Reijerkerk (144)	8 MS, 4 HC	Microarray & qPCR	939
Yang (145)	DC: 10 RRMS, 10 HC. VC: 40 RRMS, 40 HC. (Chinese pop)	Microarray & qPCR	754
Munoz-Culla (146)	19 RRMS (NTZ-treated) 3 time points (0,6,12 months)	qPCR (TLDA)	754
Meira (148)	12 untreated RRMS, 24 NTZ-treated RRMS, 12 HC	qPCR	1
Miyazaki (150)	19 RRMS, 19 HC	qPCR	102
Keller (153)	20 RRMS, 19 HC	Microarray	866
Gandhi (154)	DC: 10 RRMS, 9 SPMS, 9 HC. VC: 50 RRMS, 51 SPMS, 32 HC	qPCR	368
Fenoglio (129)	29 MS (16 remitting MS, 6 SPMS, 7 PPMS), 19 HC	qPCR	5
Waschbisch (152)	36 RRMS, 20 GA-treated RRMA, 18 IFN-β treated RRMS, 32HC	qPCR	5
Lopez-Ramirez (157)	6 MS (4 SPMS, 1 PPMS, 1 SP/RRMS), 6 HC	qPCR	1
Noorbakhsh (158)	16 MS (3 RRMS, 10 SPMS, 3 PPMS), 10 HC	Microarray & qPCR	847

Paper	Sample size and type	Methodology	Number of miRNA analysed
Paraboschi (159)	10 RRMS, 10 HC	Microbead-based technology	22
Haghikia (160)	53 MS (17 RRMS, 30 SPMS, 6 PPMS), 39 OND	qPCR	760
Du (162)	43 RRMS, 42 HC, 11 NMOSD	qPCR	8
Martinelli-Boneschi (163)	DC: 19 MS (7 RRMS, 6 SPMS, 6 PPMS), 14 HC VC: 10 MS (5 RRMS, 2 SPMS, 3 PPMS), 10 HC	Microarray	1145
Guerau-de-Arellano (140)	15 MS, 5 HC, mRNA qPCR on 10 samples	NanoString nCounter	800
Guan (151)	22 RRMS (4 relapse, 18 remitting), 22 HC	Affymetrix miRNA array v4 & qPCR	2578
Lecca (147)	30 MS (28 RRMS, 2 SPMS), 13 HC	qPCR	1
Fenoglio (122)	30 RRMS (FIN treated) 5 time points (0,3,6,9,12 months), 11 HC	qPCR	3
Regev (135)	DC: 26 MS (7 RRMS, 9 SPMS, 10 PPMS), 20 HC VC: 58 MS (29 RRMS, 19 SPMS, 10 PPMS), 30 HC, 74 other diseases	qPCR	652
Ahmadian-Elmi (134)	40 RRMS (20 relapse, 20 remitting)	qPCR	2
Mameli (133)	24 RRMS (NTZ treated) 2 time points (0 & 6 months), 24 HC	qPCR	4
Meira (149)	65 RRMS (21 untreated, 21 NTZ treated <24 months, 23 NTZ treated >24 months), 20 NTZ treated who developed PML	qPCR (TLDA)	377
Munoz-Culla (164)	24 RRMS (2 samples/patient – relapse vs remission), 24 HC	Affymetrix miRNA array v1.0 & qPCR	847

Paper	Sample size and type	Methodology	Number of miRNA analysed
Hosseini (161)	40 RRMS (20 relapse, 20 remitting), 12 HC	qPCR	1
Keller (123)	DC: 60 CIS/RRMS, 11 NMOSD, 43 HC VC: 19 CIS/RRMS, 18 NMOSD	NGS & qPCR	All
Arruda (124)	24 MS (5 RRMS, 18 SPMS, 1 PPMS) 3 time points (0,6, 12,24 months after AHSCT treatment), 9 HC	qPCR	3
Smith (139)	19 MS (11 RRMS, 4 SPMS, 4 PPMS), 17 HC	NanoString nCounter	1
Wu (155)	6 MS, 6 HC	qPCR	1
Bergman (156)	DC: 15 CIS, 15 MS, 27 OND VC1: 34 CIS, 43 MS, 65 OND VC2: 96 CIS, 120 MS, 214 OND	qPCR (TLDA)	754

Abbreviations: AHSCT = autologous haematopoietic stem cell transplant; CIS = clinically isolated system; DC = discovery cohort; FIN = fingolimod; GA = glatiramer acetate; HC = healthy controls; IFN-β = interferon-beta; NGS = next generation sequencing; NMOSD = neuromyelitis optica spectrum disorder; NTZ = natalizumab; OND = other neurological diseases; PML = progressive multifocal leukoencephalopathy; pop = population; PPMS = primary progressive MS; qPCR = quantitative polymerase chain reaction; RRMS = relapsing-remitting multiple sclerosis; SPMS = secondary progressive MS; TLDA = TaqMan Low Density Array; VC = validation cohort.

Here, miRNA dysregulation across published tissue types will be discussed, including effects on cellular function, the regulatory role of DMTs on miRNA expression, and potential biomarker candidates for diagnosing MS, predicting treatment responses, and differentiating disease subtypes.

MicroRNA in Central Nervous System

Limited research has been conducted on miRNA expression in tissues of the CNS, primarily because of difficulties obtaining post-mortem brain tissue samples. A study by Junker et al. (141) reported the analysis of the expression of 365 mature miRNAs in both MS lesions and control white matter. A total of 167 miRNAs were detected in all groups with data demonstrating that active and inactive MS lesions have distinct miRNA profiles. miR-155, miR-34a and miR-326 were particularly found to be up-regulated in active lesions, and CD47 was a common target for these three miRNAs. CD47 is a cell-surface protein responsible for inhibiting phagocytosis by macrophages. The consequence of the miRNAs up-regulation is reduced production of CD47, providing a permissible environment for macrophage activation and the phagocytosis of myelin. The scope of this study was limited as it looked at only a fraction of the >1800 miRNAs in the genome, and a broader analysis could highlight further candidate miRNAs involved in MS pathology. However, the identification of miR-155-5p as up-regulated in MS CNS tissue has been seen repeatedly in many studies since Junker's.

The expression of miR-155-5p appears to be highest in active lesions and reduces through chronic lesions and NAWM to a baseline low in control white matter (141, 157, 158). Furthermore, silencing of miR-155 ameliorates EAE in mice (165). miR-155 has been shown to affect the BBB to an extent that immune cells may then infiltrate the CNS. Up-regulation of miR-155 in brain endothelial cells (BEC) mediates reduced expression of cell-cell complex and focal adhesion molecules (144), making the BBB more permeable. Also, the observed up-regulation of miR-155 in the CNS of MS patients can be inducted by proinflammatory cytokines, IFN-γ and TNFα (144), further underscoring the link in MS between the central nervous and immune systems.

Other miRNAs have also been shown to exacerbate BBB breakdown. Down-regulation of miR-125a-5p in BEC results in increased expression of intercellular adhesion molecule 1 (ICAM-1), necessary for leukocyte adhesion, and permits their migration through the BBB (144). ICAM-1 expression is further enhanced by the targeting of its negative regulators by miR-155, along with VCAM-1, a similar cell adhesion molecule (166). In contrast, miR-146a over-expression in BEC negatively modulates T cell adhesion to the BBB by indirectly inhibiting VCAM1- and CCL2 (155). Interestingly, while miR-146a and miR-155 have opposite actions, anti-inflammatory and proinflammatory respectively, the expression of both is induced by proinflammatory cytokines (144, 155). In terms of exacerbating disease activity, induction of miR-155 is logical. In contrast, cytokine-mediated over-expression of miR-146a in BEC may signal a self-mediated decline in inflammation in the BBB at the conclusion of relapse.

A recent study of miRNA expression in NAWM identified a number of dysregulated miRNAs, demonstrating underlying dysregulation in the CNS of MS individuals (140). Unfortunately, details on the subtype of MS from which the samples were derived are not available, and a mix of MS subtypes make exposing stage-specific dysregulation of NAWM problematic. Nonetheless, their finding of miR-191 down-regulation and subsequent over-expression of SOX4 and BDNF (table 1.1) is very interesting. SOX4 negatively regulates myelination by oligodendrocytes (167), whereas BDNF and other genes targeted by miR-191 have known neuroprotective effects (168). Guerau-de-Arellano et al. thus came to the intriguing conclusion that NAWM is enriched in neuroprotective mechanisms, though is prone to inflammation and has reduced repair mechanisms (140). This complements the observation previously stated by Melief et al., that NAWM is alert but in an immunosuppressed state (41).

miR-125-3p is a miRNA that is enriched in the human CNS, specifically neurons and oligodendrocytes. However, its over-expression *in vitro* impairs myelination by blockading oligodendrocyte maturation (147). In the CSF of MS patients with radiologically active disease, miR-125a-3p is up-regulated, and the cellular origin of this is likely to be either neurons or oligodendrocytes undergoing damage in active MS (147). This miRNA is of particular interest as it is the opposing arm (-3p vs. -5p) of the mature miRNA duplex, miR-125a, that is down-regulated in BEC (144). Both arms of the miRNA duplex are dysregulated in MS, however in different directions.

Nonetheless, the dysregulation of both contributes to disease exacerbation; miR-125-3p by inhibiting oligodendrocyte maturation, and miR-125-5p by increasing leukocyte adhesion to the BBB (144, 147).

Dutta et al. (143) analysed post-mortem MS brains to investigate if the loss of myelin in the hippocampus has an effect on neural miRNA expression. Hippocampal demyelination reduces neural gene expression and is likely linked to memory loss in MS patients. Most significantly, the neuronal miRNA, miR-124, was found to be up-regulated in the neurons of demyelinated samples. miR-124 has target binding sites on 3'UTRs of 26 neural mRNAs. The study also analysed a mouse model of demyelinated hippocampus and found that an increase in miR-124 resulted in reduced expression of AMPA receptors and decreased memory performance; remyelination of the hippocampus reversed this effect on memory (143). Contrastingly, increased levels of miR-124 in microglia have been associated with microglial quiescence and suppression of EAE in mice (169). This highlights the diverse effects miRNAs can have on cell populations. It would appear that miR-124 expression is beneficial for MS prognosis in microglia, but detrimental when expressed more broadly in the hippocampus. It is essential therefore, that individual cell types be studied to understand the impact miRNA dysregulation has on disease aetiology and pathology.

MicroRNA in the immune system

The majority of studies on miRNAs in MS have been performed on blood derived samples as these are much more easily acquired than CNS tissue, and may be collected longitudinally. A recent study of the TGF-β-signalling pathway and miRNA expression in naïve CD4+ T-cells suggests that miRNA dysregulation is not a result of inflammation, but an inherent susceptibility factor of MS (137). However, miRNA profiles in RRMS and SPMS individuals are distinct (135, 154), indicating that while miRNA dysregulation may be a risk factor for MS, it also dynamic and shifts with changes in disease. miRNA dysregulation should therefore be considered as both contributing to disease onset and progression, and a reflection of affected tissue's response to disease.

In 2016, Munoz-Culla et al. described the “mirror pattern” of miRNA expression in relapse vs. remission of RRMS patient PBMCs (164). When observing expression of short non-coding RNAs (sncRNA including miRNA and small nucleolar RNA (snoRNA)), they found 10 sncRNAs that were dysregulated in both relapse and remission compared to HC, but in opposite directions. Of further interest, the miRNA expression profiles of each disease state were enriched for mRNA targets in different gene pathways. Relapse-miRNAs strongly target genes involved in general leukocyte metabolism, whereas miRNAs dysregulated during MS remission regulate genes involved in innate immunity (164). The aforementioned mirror effect in relapsing vs. remitting has also been observed in CD4+ T-cells. miR-233 is significantly up-regulated during relapse compared to HC, whereas it is down-regulated (not significant, p=0.07) in remission (161). miR-223 is up-regulated in many tissues: whole blood, CD4+ T-cells (relapse), PBMCs and NAWM (118, 120, 140, 153, 161); and down-regulated in serum (120-122). Furthermore, the frequency of a T/T genotype at rs1044165, a SNP in miR-223’s genomic sequence, is significantly reduced in MS patients, suggesting the polymorphism acts as a protective factor (120).

In 2009, Otaegui et al. reported differential miRNA expression in PBMCs for MS patients in relapse status, remitting status and HC. Up-regulation of miR-18b and miR-599 was indicative of relapse status, whereas up-regulation of miR-96 significantly indicated the MS patients were in remission (35). RRMS may also be distinguished from HC via miRNA expression patterns of T-regs. Specifically, miR-106b and miR-25 were down-regulated in RRMS compared to HC, and target prediction indicates genes in the TGF-β-signalling pathway may be affected by these miRNA, ultimately having an effect on T-reg differentiation and maturation (118). This is supported by the findings of Severin et al. (137).

Another study comparing relapse and remission miRNA profiles identified miR-27a (up-regulated) and miR-214 (down-regulated) as miRNAs able to distinguish relapse from remission in CD4+ T-cells (134). Up-regulation of miR-27a in serum has also been shown to differentiate RRMS from SPMS (135).

Also, miR-140 expression changes in relapsing and remitting stages of disease, negatively correlating with disease severity in PBMCs. This occurs specifically in CD4+ T-cells and non-T cells, whereas its expression remained stable in CD8+ T-

cells (151). mRNA and protein expression analyses confirmed STAT1 as a target of miR-140, and demonstrated that miRNA-associated over-expression of this gene caused increased levels of T-helper (Th)-1 differentiation (151), leading to disease exacerbation. The excessive presence of Th-1 cells is characteristic of active MS disease, and miR-29b is a key part of a feedback loop that controls the balance of Th-1 cells. miR-29b is up-regulated in CD4+ T-cells of MS patients, which represses T-bet and IFN-γ, dysregulating Th-1 bias. However, its initial up-regulation is the result of high IFN-γ (139). Persistent up-regulation of both miR-29b and IFN-γ in MS is indicative chronic inflammation.

miRNA dysregulation also has effects on other Th cells. As in Junker et al.'s study on lesions in the CNS (141), miR-326 has also been identified as being up-regulated in PBMCs of MS patients in relapse (162). Here, it targets Ets-1, a negative regulator of Th-17 cells, thus the up-regulation of miR-326 (predominantly in CD4+ T-cells) promotes differentiation of Th-17 cells. This finding was followed up with a functional study in the EAE murine model and found inhibition of miR-326 coincided with milder pathology (162).

In a study on peripheral whole blood, miR-17 and miR-20a were consistently under-expressed in RRMS, SPMS and PPMS individuals. Knock-in and knock-down experiments on these miRNAs in Jurkat cells (partially differentiated T-cell line derived from a T-cell lymphoma patient) revealed that these miRNAs targeted genes involved in translation regulation, immune response, activin A signalling regulation and vitamin B7 metabolism pathways (127). miR-17 was also identified as being dysregulated in CD4+ T-cells of RRMS patients by Lindberg et al. (125) though it was found to be up-regulated in this case. This could be due to a number of reasons: (1) small sample number, (2) analysis of different disease courses (RRMS vs. all MS subtypes) or (3) dysregulation in CD4+ T-cells may be masked in PBMCs by the expression profiles of other cell types. It is likely a combination of these three factors that resulted in contradictory findings between the studies. However, it should be noted that Lindberg et al. reported miR-497 to be over-expressed in CD4+ T-cells and B-cells whilst under-expressed in CD8+ T-cells of the same individuals compared to healthy controls (HC) (125), highlighting the critical need to focus on single cell subsets.

This is further emphasised by Søndergaard et al. (142), who analysed miRNAs in blood, plasma and serum for the purpose of identifying diagnostic biomarkers for MS. miRNA expression in PBMCs was compared between treatment naïve MS patients in clinical remission and HC. Analysis of isolated PBMC subpopulations identified antigen presenting cells and natural killer cells as the primary source of miRNA dysregulation in MS patients, though this varied between miRNAs. miR-145 was up-regulated (three-fold) in MS patients and the highest expression was seen in CD8+ T-cells, monocytes and natural killer cells. Furthermore, miR-145 expression in plasma is negatively correlated with EDSS (154). Of the 16 miRNAs analysed in plasma, only miR-145 and miR-939 were similarly dysregulated as in PBMCs (142). This suggested either that: (1) cells other than PBMCs are also releasing miRNAs, (2) PBMC cell subsets have contrasting miRNA dysregulation which is masked when looking at PBMCs as a whole, or (3) specific miRNAs are more prone to release from cells than others.

Using miRNAs as biomarkers for diagnoses of any disease is only effective if similar diseases do not exhibit dysregulation in the same miRNAs; in the case of MS, miRNAs will need to be excluded from other neurological diseases (OND) to be effective. A study compared miRNAs differentially expressed in MS whole blood to dysregulated miRNAs reported in other diseases. Of 165 miRNAs that were identified to be dysregulated by Keller et al. (153), 43 had been associated with a variety of other diseases; thus 122 are thought to be exclusively linked with MS and warrant further exploration as potential diagnostic biomarkers.

In 2014, Keller et al. (128) produced the first study in MS using next generation sequencing (NGS) for miRNA profiling in whole blood. The study employed a stringent experimental design whereby miRNAs had to be identified as dysregulated by both NGS and microarray before being further assessed with quantitative polymerase chain reaction (qPCR). Eight miRNAs were identified and three were confirmed significantly dysregulated by qPCR (miR-16-2-3p, miR-7-1-3p and miR-20a-5p). Using various methods and patient cohorts, the down-regulation of miR-20a-5p in whole blood of MS patients has been confirmed (127, 128, 153). Prediction algorithms suggest that miR-20a-5p regulates approximately 500 genes, 19 of which have been experimentally validated and many are involved in T cell regulation. This study was followed up a year later using NGS in serum and whole blood to identify

miRNAs that may be used as biomarkers to distinguish CIS/RRMS from neuromyelitis optica spectrum disorder (NMOSD). No miRNAs were significantly different between the disease groups or HC in serum, however 178 miRNAs in whole blood showed differential expression in pairwise comparisons of CIS/RRMS, NMOSD and HC (123), and should be researched further to validate them as biomarkers for differential diagnosis of NMOSD.

Non-cellular circulating miRNAs

The acquisition of samples peripheral to the CNS is much more common and less distressing for patients, and thus a more realistic approach for biomarker profiling. Identification of dysregulated miRNAs in PBMC subsets is critical to determine the mechanisms occurring in the immune system during MS pathogenesis. The impact of non-cellular circulating miRNAs on system processes is difficult to infer, as their action on specific cell types cannot be established. However, they are excellent sources for biomarker analyses. Plasma, serum and CSF samples are more easily handled in the laboratory than cell subsets, and are therefore more likely to be used in clinical practice for identifying and utilising disease biomarkers. It should be noted that longitudinal studies would exclude CSF as it is not feasible to repeatedly perform lumbar puncture to longitudinally monitor miRNA changes.

In 2013, Gandhi et al. (154) measured and compared the expression of 368 miRNAs in plasma of RRMS, SPMS and HC samples with the goal of identifying diagnostic biomarkers. A number of miRNAs were identified that distinguished RRMS vs. HC, SPMS vs. HC and RRMS vs. SPMS (Table 1). The differential expression of two miRNAs (miR-92 and let-7) distinguished RRMS from SPMS and also RRMS from ALS patients, but not SPMS from ALS; suggesting similar pathology in the neurodegenerative stage of MS (SPMS) and ALS. Differential expression of miR-92 was found in the largest number of comparisons (RRMS vs. SPMS, RRMS vs. HC and RRMS vs. ALS) and was also shown to be associated with EDSS score and disease duration. miR-92 targets CD40 pathways involved in cell cycle regulation and cell signalling and the cluster to which it belongs (miR-17-92) is involved in regulating proliferation and activation of CD4+ T-cells. Another differentially expressed miRNA is miR-145 involved in down-regulation of CTLA-4 in CD4+ T-cells; a receptor that inhibits T cell response and when mutated has been associated with autoimmune

disease. This finding is corroborated by Keller et al.'s 2014 study in whole blood (153) and by Søndergaard et al. in PBMCs (142).

A more recent study from Gandhi's group focused on identifying biomarker miRNAs in serum to differentiate between MS, HC, OND (AD and ALS) and inflammatory diseases (rheumatoid arthritis and asthma) (135). Four miRNAs distinguished between MS and OND, and a further two between MS and inflammatory diseases. An interesting outcome of this paper was the establishment of a clear definition between plasma and serum miRNA expression profiles. In plasma, miR-145 correlated strongly with EDSS (154), whereas it showed no correlation in serum where miR-199a-5p had the strongest correlation (135).

Circulating miRNAs in plasma have been analysed in a few studies. In one, authors identified 6 up-regulated and 1 down-regulated miRNAs in MS individuals (130). Microarray analysis of over 900 miRNA transcripts demonstrates a good proportion of known miRNAs however, the sample size of 4 MS patients and 4 HC was a small power study and no variation in disease stage was investigated. Two of the identified miRNAs had been identified in previous studies; miR-22 expression is increased in T-reg cells of MS patients (118) and miR-422a was found to be differential to RRMS patients compared to HC in whole blood (153). Notably miR-648 was over-expressed in MS patient plasma; as this miRNA targets the myelin-associated oligodendrocyte basic protein mRNA, reduction of protein level reduces the stability of the CNS myelin sheath (130).

To establish potential diagnostic biomarkers in CSF, Haghikia et al. (160) compared the expression profiles of miRNAs in the CSF of patients with MS, and patients with ONDs. Of the 760 miRNAs included in the panel, 50 were detectable in CSF and 3 of those (miR-922, miR-181c and miR-633) have diagnostic potential. The combined dysregulation of miR-181c and miR-633 feasibly differentiated between patients with RRMS and SPMS. All three of the miRNAs were dysregulated in MS compared to OND. Some of the ONDs were neuroinflammatory diseases that may have similar presentations to MS, supporting the potential of these miRNAs to be used as diagnostic biomarkers for MS (160). However, the sample size for OND patients was low (n=39) and diverse. A study by Bergman et al. (156) used a much larger cohort, though the OND cohorts were still not well-defined. However, 88 miRNAs were

detected in the CSF; a marked improvement on Haghikia's earlier study. miR-150 in particular stands out as its expression was able to discriminate between CIS converters and non-converters, as well as showing positive correlation with oligoclonal bands in the CSF (156).

How miRNAs end up in non-cellular fluids may be due to a number of reasons, such as apoptotic release from cells. However, extracellular vesicles, particularly exosomes, should be analysed. Exosomes are non-toxic, naturally occurring nanovesicles that are produced by a number of MS-related tissues actively produce exosomes including T- and B-cells, oligodendrocytes and astrocytes (in-depth review by Jagot and Davoust (170)). Interestingly, miRNA are often actively incorporated into exosomes by these cells, and are sufficiently small enough that they can easily cross the BBB. Future therapies may utilise exosomes for miRNA delivery to the CNS to treat MS. One study has started to explore such an option; IFN-γ-stimulated exosomes produced by dendritic cells are enriched with miR-219 and in vivo application of these exosomes in brain slide culture was sufficient to stimulate oligodendrocyte differentiation into myelinating cells (171).

MicroRNA and MS treatments

Aberrant expression of miRNAs contributes to MS pathology and thus the effect of DMTs on miRNA expression has been the key focus of numerous studies. DMTs utilise various pathways to ameliorate the progression of disease. Glatiramer acetate (GA) is a random polymer of glutamic acid, lysine, alanine, and tyrosine; it has a similar structure to myelin basic protein and is thought to act as a decoy for the immune system. Waschbisch and colleagues (152) compared the expression levels of 5 miRNAs identified in previous studies as being dysregulated in MS. The expression of the miRNAs was analysed in the PBMCs of treatment naïve RRMS subjects, GA treated RRMS, IFN-β treated RRMS, and HC. miR-142-3p and miR-146a were significantly up-regulated in the treatment naïve and IFN-β treated RRMS subjects. However, in the GA treatment group, expression of these two miRNAs was reduced to a level resembling the HC group. These miRNAs were previously identified by as being dysregulated in active white matter lesions (141) and the

reduced expression of these miRNAs in GA treated RRMS subjects warrants further research.

Interferon-beta's (IFN-β) mechanisms of action are vast and not fully understood, though it appears to inhibit trafficking of immune cells across the BBB, decreases production of proinflammatory cytokines (IL-17 and osteopontin) and increases the production of anti-inflammatory agents (IL-10) (172). A recent longitudinal study on the impact of IFN-β treatment on miRNA expression in PBMCs found that miRNA-mediated regulation plays an important role in the mechanisms of action of IFN-β in RRMS and CIS cases (138). During time-points ranging from two days to one month, Hecker et al. observed the simultaneous up-regulation of IFN-β-responsive genes and the down-regulation of miRNAs associated with apoptosis and IFN feedback loops. The miRNAs identified as being dysregulated were observed in a small discovery cohort (n=6) and validated in a moderately larger cohort (n=12). MiRNA expression screening of a larger number of cases could possibly have yielded other miRNAs also affected by IFN-β's mechanism of action. The expression of a number of miRNAs was affected by IFN-β. Interestingly, miR-193a was down-regulated following treatment, a previous study found this miRNA to be up-regulated in RRMS versus healthy HC (125) and it has also been implicated with the remission phase of RRMS (173); this supports evidence that IFN-β therapy reduces relapse rates (174). This study also supports the findings by Waschbisch et al., who found several miRNAs normalised following GA treatment (152) but were not affected by IFN-β treatment in both studies.

Natalizumab (NTZ) is an anti-α4β1 integrin antibody that restricts lymphocyte migration into the CNS, decreasing formation of lesions (175). A cross-sectional investigation into miRNA expression dynamics compared a broad panel of miRNAs in the B-cells of untreated and NTZ treated RRMS patients and HC (69). 49 miRNAs were identified as down-regulated in untreated RRMS compared to HC however, no miRNAs were found to be significantly up-regulated. When compared to untreated RRMS, 10 miRNAs were up-regulated in NTZ-treated cases six months after initiation of treatment. Of these 10, five miRNAs overlapped the miRNAs found to be dysregulated in untreated RRMS vs. HC, indicating that NTZ has a normalising effect on some miRNA expression. This effect has also been observed in CD4+ T-cells (176). MiRNA-mRNA interaction analysis identified key affected pathways as B cell

receptor, phosphatidyl-inositol-3-kinase (PI3K) and phosphatase and tensin homology (PTEN) signalling; PI3K and PTEN were also found to be targets of miR-17 by Lindberg et al. (125). Interestingly, 3 viral miRNAs from EBV were found to be down-regulated in RRMS compared to HC and two were up-regulated in NTZ treated vs. untreated RRMS (69). The implications of this finding on pathogenesis is not understood, though the high incidence of EBV-seropositivity in MS indicates that EBV-miRNAs likely play a significant role in the disease pathophysiology.

A potential side effect of NTZ treatment is the development of progressive multifocal leukoencephalopathy (PML), a virus mediated inflammation of the brain that is fatal in some cases (177). miR-10b is very lowly expressed in patients being treated with NTZ, however those that develop PML have undetectable levels of miR-10b in their PBMCs (149). This absence of expression may be used as a biomarker for monitoring patients on NTZ. Likewise, 3 miRNAs have been shown to be differentially expressed in whole blood of PML patients after 12 months on NTZ, compared to those unaffected (146). They are also candidates for monitoring PML development in patients treated with NTZ.

Fingolimod (FIN) is a modulator of sphingosine 1 phosphate (S1P) receptor (178). FIN induces down-regulation of S1P1 which is highly expressed on T- and B-cells, causing these cells to be sequestered in the lymph nodes, thus preventing migration into the CNS (179). After six months of treatment, the expression of three miRNAs in serum (miR-15b, miR-23a and miR-223) increased to levels similar to HC, and remained stable up the 12 months (the length of the study) (122). Expression of miR-150 in plasma decreases after 12 months fingolimod treatment, though it is not clear if this normalisation as a HC comparison was not performed (156). As with the aforementioned DMTs, fingolimod has a normalising effect (miR-150 not confirmed), though it would more informative to observe its effect in immune cells rather than serum and plasma.

An alternative to traditional immunosuppressive DMTs utilises a patient's own stem cells to reduce relapse and improve disability in patients with active disease (180). Autologous haematopoietic stem cell transplantation (AHSCT) is a risky procedure involving chemotherapy to eradicate the patient's white blood cells, and the re-introduction of haematopoietic stem cells to reset the immune system. A recent study analysed the effect of AHSCT on the expression of three miRNAs. miR-16, miR-142

and miR-155 were all initially up-regulated in MS CD4+ and CD8+ T-cells. Their expression normalised in both cell types 6 months after AHSCT and remained stable throughout the study's 24-month duration (124). While this finding is exciting and promising for the future of AHSCT, it should be noted that the sample cohort was a mixture of RRMS and SPMS, with active and inactive disease, and this may have skewed their baseline miRNA expression readings. An earlier study on untreated RRMS CD4+ T-cells identified miR-16 down-regulation compared to HC (119), a direct contradiction to the AHSCT study baseline.

It has been clearly demonstrated that DMTs have an effect on miRNA expression patterns. Because of this, it is important that studies aimed at elucidating the role of miRNAs in disease pathology use only samples from patients who are treatment naïve or have been free from treatment for over six months.

MicroRNA biogenesis and MS

While miRNA dysregulation is important in understanding MS and developing reliable biomarkers for diagnosis and disease activity, the mechanism of miRNA dysregulation should not be overlooked. As mentioned earlier, miRNA expression can be affected by DNA methylation. Furthermore, the molecules in the biogenesis pathway (figure 1.3) may also exhibit aberrant expression, with a knock-on effect to general miRNA expression. In RRMS Dicer is down-regulated in B-cells (181), whereas in PBMCs, Drosha, DGCR8 and Dicer are all up-regulated (114). A contradicting study in PBMCs found Dicer mRNA to be stable in RRMS, though protein was down-regulated. However, Dicer was observed to increase expression in IFN-β responders (115). As with most miRNA studies in MS, these were all carried out in RRMS patients or mixed MS subtypes, with no specific focus on SPMS.

Summary

Multiple sclerosis is a complex autoimmune disease caused by multifocal inflammatory attacks on the CNS resulting in lesional demyelination and axonal damage. Symptoms vary between patients and as disease progresses disability accumulates. Whilst there are genetic loci that confer risk of developing MS, environment also plays a crucial role. Epigenetic factors are partially heritable but also highly sensitive to environment and many studies have highlighted these factors as contributory to MS pathology.

MicroRNAs are of key interest and have the potential to play many roles in MS and its treatment. There are over 1800 miRNAs in the human genome and they are highly stable molecules, which makes them great candidates as biomarkers for diagnosing and monitoring disease progression. More importantly, they are regulators of gene expression and changes in their expression pattern have great impact on cellular pathways crucial to the pathophysiology of MS. The expression of miRNAs themselves may be affected or affecting other epigenetic mechanisms such as DNA methylation, which also has demonstrated differential presentation in MS patients.

The vast majority of studies on miRNAs in the immune system have focused on heterogeneous cell populations; analyses of miRNA expression in specific cell types (particularly CD4+ T-cells which are highly involved in disease), are essential to understand the effect of miRNA dysregulation in MS. Furthermore, SPMS has largely been ignored and either left out of studies, or analysed in conjunction with RRMS and PPMS samples. To better understand the role of the immune system in SPMS, miRNA studies need to be performed. Additionally, as SPMS patients are not treated with DMTs, expression changes key to understanding cell pathology will not be hidden by the normalising effect of most DMTs.

As with SPMS, normal appearing white matter has not been exhaustively investigated in miRNA studies, but has been shown to display pathology linked to symptomatic lesions. MiRNAs could be playing a pivotal pathological role in the NAWM and the identification, location and functional analysis of dysregulated miRNAs could yield information on MS pathology and new therapeutic strategies. Correlating these miRNAs in the NAWM to circulating body fluids will identify

potential biomarkers for monitoring disease course, as well as informing the interplay of CNS and immune system in SPMS.

Research Question and Aims

The studies included in this thesis were designed to provide answers for the following research questions:

1. Which microRNAs are dysregulated in the CD4+ T-cells of SPMS patients, and how does this affect the role of CD4+ T-cells in SPMS?
2. Are DNA methylation profiles of CD4+ T-cells different between in RRMS and SPMS, and are changes in microRNA expression caused by DNA methylation?
3. Are microRNA biogenesis molecules differentially expressed in SPMS CD4+ T-cells, and does this have an effect on microRNA expression?
4. Is DNA methylation affected by changes in microRNA expression, specifically miRNA-29b?
5. Is there differential microRNA expression in SPMS normal appearing white matter compared to controls, and how does this compare to microRNA expression patterns seen in CD4+ T-cells?

The study aims of this project are to:

1. Identify miRNAs dysregulated in SPMS CD4+ T-cells using next generation sequencing; these will be confirmed using RT-qPCR. And determine if common gene targets demonstrate associated expression changes.
2. Determine DNA methylation signature of CD4+ T-cells in SPMS and associate these with miRNA dysregulation.
3. Determine whether changes in expression of miRNA biogenesis molecules correlate with miRNA expression trends in SPMS, and compare this to a RRMS cohort.
4. Determine if levels of DNA methyltransferase enzymes correlate with miRNA-29b levels, and how this affects DNA methylation levels in CD4+ T-cells.
5. Investigate the dysregulation of microRNAs in SPMS NAWM on a series of post-mortem brain samples from control and SPMS subjects.

CHAPTER TWO – microRNA expression profile of SPMS CD4+ T-cells

Next-generation sequencing reveals broad down-regulation of microRNAs in secondary progressive multiple sclerosis CD4+ T-cells

Published in Clinical Epigenetics (IF 4.327) 27 August 2016. See appendix 1.

This chapter addresses my first research question – Is there dysregulation of miRNA expression in the CD4+ T-cells of secondary progressive MS patients?

Authors

Katherine A Sanders[1,2,3], Miles C Benton[4], Rod A Lea[4,2], Vicki E Maltby[2,3], Susan Agland[5], Nathan Griffin[2,3], Rodney J Scott[2,3,6], Lotti Tajouri[1], Jeannette Lechner-Scott[2,5,7].

Author Affiliations

1. Faculty of Health Sciences and Medicine, Bond University, Robina, Queensland, 4226, Australia.
2. Centre for Information-Based Medicine, Hunter Medical Research Institute, Newcastle, New South Wales, 2305, Australia.
3. School of Biomedical Sciences and Pharmacy, University of Newcastle, Newcastle, New South Wales, 2308, Australia.
4. Institute of Health and Biomedical Innovation, Genomics Research Centre, Brisbane, Queensland, 4059, Australia
5. Department of Neurology, Division of Medicine, John Hunter Hospital, Newcastle, New South Wales, 2305, Australia.
6. Division of Molecular Genetics, Pathology North, Newcastle, New South Wales, 2305, Australia.
7. School of Medicine and Public Health, University of Newcastle, Newcastle, New South Wales, 2308, Australia.

Abstract

Background: The immune system has a diminished role in secondary progressive MS (SPMS) compared to the relapsing-remitting disease stage. MicroRNA (miRNA) can regulate gene expression; determining their impact on immune-related cell functions, especially CD4+ T-cells, during disease progression will advance our understanding of MS pathophysiology. This study aimed to compare miRNA profiles of CD4+ T-cells from SPMS patients to healthy controls (HC) using whole miRNA transcriptome next generation sequencing (NGS).

Methods: Total RNA was extracted from CD4+ T-cells of 24 SPMS and 22 HC. miRNA expression patterns were analysed using Illumina-based small-RNA NGS in 12 SPMS and 12 HC and confirmed in all samples by qPCR.

Results: The ten most dysregulated miRNAs identified by NGS were selected for qPCR confirmation; five (miR-21-5p, miR-26b-5p, miR-29b-3p, miR-142-3p and miR-155-5p) were confirmed to be down-regulated in SPMS ($p<0.05$). SOCS6 is targeted by eight of these ten miRNAs. Consistent with this, SOCS6 expression is up-regulated in SPMS CD4+ T-cells ($p<0.05$). Previously, SOCS6 has been shown to act as a negative regulator of T-cell activation.

Conclusions: 97% of miRNA candidates identified by NGS were down-regulated in SPMS. The down-regulation of miRNAs, and increased expression of SOCS6 in SPMS CD4+ T-cells may contribute to reduced immune system activity in progressive MS.

Introduction

Multiple Sclerosis (MS) is an autoimmune disease characterized by multifocal inflammatory attacks in the central nervous system (CNS) (36). In the relapsing-remitting (RRMS) stage of the disease, CD4+ T-cells are amongst the primary infiltrators moving from the periphery, through the blood-brain barrier, and into the CNS (18). These cells then initiate an immune response that results in localized demyelination and corresponding symptoms. The later stage of MS, secondary progressive (SPMS), is characterized by compounding neurodegeneration and sustained disability; however the relevance of inflammation is unclear (32). As key regulators of gene expression, microRNA may be affecting the immune-related functions of CD4+ T-cells in SPMS and may help to elucidate their actions in SPMS.

MicroRNAs (miRNAs) are short, non-coding RNA molecules (~22bp) that regulate gene expression at the post-transcriptional stage by targeting the 3' untranslated region of target genes. Their small size and stable structure make them ideal biomarkers. miRNA expression patterns in MS have been the focus of numerous studies in recent years, many of which have concentrated on using miRNAs as biomarkers for diagnosis and prognosis (182). These studies predominantly use easily acquired (and often highly heterogeneous) samples such as whole blood, peripheral blood mononuclear cells (PBMCs), serum and plasma. Numerous dysregulated miRNAs have been identified, however which cell types are actually responsible for differing miRNA profiles and the consequences of altered miRNA expression is not clear in many studies. Furthermore, it is likely that these heterogeneous samples are masking the signal of differentially expressed miRNA in specific cell subtypes. To overcome this, we have focused on CD4+ T-cells in this study.

Next generation sequencing (NGS) allows for stringent examination of cell specific miRNA expression profiles as well as discovery of previously uncharacterized miRNAs. Here, we have used small-RNA NGS of CD4+ T-cells from SPMS patients and healthy controls (HC). The total coverage approach of NGS generates expression information on all small RNA species including all known and novel miRNAs, as well as other small RNA species (isomiRs, and snoRNAs); a clear advantage over microarray and candidate approach assays. Three previous studies in MS have used NGS to effectively identify miRNA expression profiles in the whole

blood (123, 128), serum (123) and peripheral blood mononuclear cells (PBMCs) (132) of RRMS patients. However, NGS techniques have not been used for specific cell types or in SPMS samples.

The miRNA expression profile of CD4+ T-cells, either as instigating molecules or by-products of erroneous molecular mechanisms, will provide insight into the function of these cells in SPMS. Here, we used NGS to provide a comprehensive analysis of the miRNA expression profiles of CD4+ T-cells from SPMS patients and healthy controls (HC), and confirmed these results using targeted assays.

Patients and Methods

Sample collection

Whole blood was collected at a single study centre from an initial cohort of 12 SPMS patients and 12 HC, and a replication cohort of 12 SPMS and 10 HC. All patients were diagnosed with SPMS according to the McDonald criteria (183) and demonstrated EDSS progression without evidence of relapse (8). Controls were age (±5 years) and gender matched (Table 2.1). The SPMS patient group was free of MS specific treatments for a minimum period of 6 months prior to collection.

Ethics Statement

Samples were collected at the John Hunter Hospital, and laboratory work conducted at the University of Newcastle. The Hunter New England Health Research Ethics Committee and University of Newcastle Ethics committee approved this study (05/04/13.09 and H-505-0607 respectively), and methods were carried out in accordance with institutional guidelines on human subject experiments. Written and informed consent was obtained from all patient and control subjects.

Table 2.1: Details of SPMS and healthy control individuals.

	Next-generation sequencing		Replication cohort	
	SPMS	HC	SPMS	HC
Number	12	12	12	10
Female	9	9	8	5
Age in yrs (mean ±SD)	60.2 ±8.3	61.3 ±9.5	61.4.0 ±6.5	60.1 ±5.9
EDSS (mean ±SD)	6.9 ±0.9	NA	5.9 ±1.0	NA
Active SPMS	3	NA	4	NA
Disease duration in yrs (mean ±SD)	25.6 ±11.1	NA	18.3 ±6.5	NA
Progression duration (mean ±SD)	10.8 ±8.1	NA	8.9 ±6.2	NA

EDSS = expanded disability status scale, SD = standard deviation, NA = not applicable.

Blood sample processing

PBMCs were isolated from 45mL of heparinised whole blood by density gradient centrifugation on lymphoprep (Axis-Shield PoC AS, Norway). CD4+ T-cells were enriched from the PBMCs using EasySep magnetic negative selection according to manufacturer's protocol (StemCell Technologies, Canada). The purity of the CD4+ selection was assessed by flow cytometry using a FITC conjugated anti-CD4 antibody (anti-human CD4 antibody, clone OTK4, FITC, catalogue# 60016FI, StemCell Technologies, Canada) on a BD FACSCanto II flow cytometer, then analysed using FACSDiva software (BD Biosciences, USA) at the Analytical

Biomolecular Research Facility of the University of Newcastle. All samples met a minimum purity threshold of >90%.

RNA isolation

Total RNA was isolated from the CD4+ T-cells using the miRNeasy Mini kit (Qiagen, USA) following the manufacturer's instructions. The quality of the RNA was assessed using the RNA 6000 Nano kit on a 2100 Bioanalyzer (Agilent Technologies, USA); a RNA integrity number (RIN) greater than 8 was deemed suitable for sequencing and RT-qPCR. Purity was measured on an Epoch spectrophotometer (BioTek, USA) and concentration was measured using the high sensitivity RNA kit on Qubit 2.0 Fluorometer (Life Technologies, Thermo Fisher Scientific, USA).

miRNA sequencing and analysis

A cohort of 12 SPMS and 12 HC samples was run through NGS at the Diamantina Institute, University of Queensland, Brisbane, Australia. Samples were individually barcoded and then sequenced in two multiplexed pools each containing 12 samples. The sequencing libraries were prepared from 1µg total RNA, using the TruSeq Small RNA preparation kit (Illumina, USA), and sequenced using the 50bp fragment protocol on the HiSeq 2500 platform. The sequencing generated 4-9 million reads per sample, more than sufficient for expression and discovery applications. The sample sequencing reads were demultiplexed using the CASAVA 1.8 software package (Illumina, USA). The Illumina adapter sequences were trimmed from the fastq files using Trimmomatic (184). All reads were aligned and counted against miRBase 21 (104).

RT-qPCR

Mature miRNA TaqMan assays (Applied Biosystems, Thermo Fisher Scientific, USA) were used for reverse transcription qPCR (RT-qPCR) to determine expression of the ten most differentially expressed miRNAs in the initial NGS cohort as well as a replication cohort of 12 SPMS and 10 HC (assay IDs in miRNA numerical order: 000397, 000399, 000407, 000408, 000409, 000413, 002223, 000464, 002623,

000524). The small RNA RNU44 (ref: 001094) was used as an endogenous control. RNU44 has previously been demonstrated to be a stable control in CD4+ T –cells (125) and its stability has been shown in our 47 samples (mean ±standard deviation Ct value of 23.58 ±0.63). RNU44 was used for normalization using the ΔCt method. The relative expression ($2^{-\Delta Ct}$) of all samples (24 SPMS and 22 HC) was calculated.

Statistical analysis

The two-sample Kolmogorov-Smirnov test (K-S test) was used to test whether differences in expression level was statistically significant between the case and control group as implemented in R. The K-S test was chosen (over the F test comparison of means) because of the non-normality of the expression level distributions among miRNAs. Our statistical significance threshold allowing for multiple testing correction was determined using the False Discovery Rate (FDR) procedure of Benjamini-Hochberg (185). Based on the number of miRNA elements, this threshold was set at 1.2×10^{-4}. We also considered a relaxed (or nominal) significance threshold of 0.05. In addition to using statistical significance thresholds for miRNA selection we also included a count threshold of >800 to exclude miRNAs that were very lowly expressed and unlikely to be replicated with the less-sensitive RT-qPCR (see appendix 2). The K-S test was also used to determine significant differential miRNA and *SOCS6* expression from the RT-qPCR relative expression data.

Correlation to patient characteristics

The Pearson correlation coefficient was calculated using RT-qPCR data for MS samples (n=24) and patient characteristics: EDSS, age, disease duration and progression duration. A correlation coefficient (*r* value) >±0.5 was considered strong, ±-0.3-0.49 moderate, and <±0.29 weak.

Gene target prediction

miRSystem integrates seven different target gene prediction algorithms and contains experimentally validated data on miRNA:mRNA interactions (106). This integration

system was used to identify genes that may be targeted by more than one of our identified dysregulated miRNAs.

Analysis of SOCS6 expression

500ng of total RNA was reverse transcribed using high-capacity cDNA reverse transcription kits (Applied Biosystems, Thermo Fisher Scientific, USA) in 21 SPMS and 21 HC samples. qPCR was performed using an exon-spanning TaqMan probe for SOCS6 (ref: Hs00377781_m1). Expression of SOCS6 was determined as relative expression to the housekeeping genes *GAPDH* (ref: 4326317E) and β-actin (ref: 4326215E) using a ViiA 7 (Applied Biosystems, Thermo Fisher Scientific, USA).

Results

We used NGS to establish miRNA expression profiles in CD4+ T-cells from a cohort of 12 SPMS and 12 HC samples. RT-qPCR was then employed to validate differences in miRNA expression in the NGS cohort as well as a second cohort of 12 SPMS and 10 HC samples (total 24 SPMS and 22 HC).

NGS

Whilst we did not observe any statistically significant miRNAs at the FDR correct threshold, which probably reflects the modest sample size, we did observe 42 miRNAs at the nominal significance threshold (97% of these were down-regulated). Of these 42 miRNAs, only 10 met our secondary criteria of having a read count >800: miR-21-5p (p=0.031), miR-23a-3p (p=0.007), miR-26b-5p (p=0.031), miR-27a-3p (p=0.031), miR-27b-3p (p=0.031), miR-29b-3p (p=0.007), miR-30e-5p (p=0.031), miR-142-3p (p=0.031), miR-155-5p (p=0.031) and miR-221-3p (p=0.031). Each of these miRNAs were found to be down-regulated in SPMS as summarized in Figure 2.1, and were forwarded for replication testing in an independent cohort.

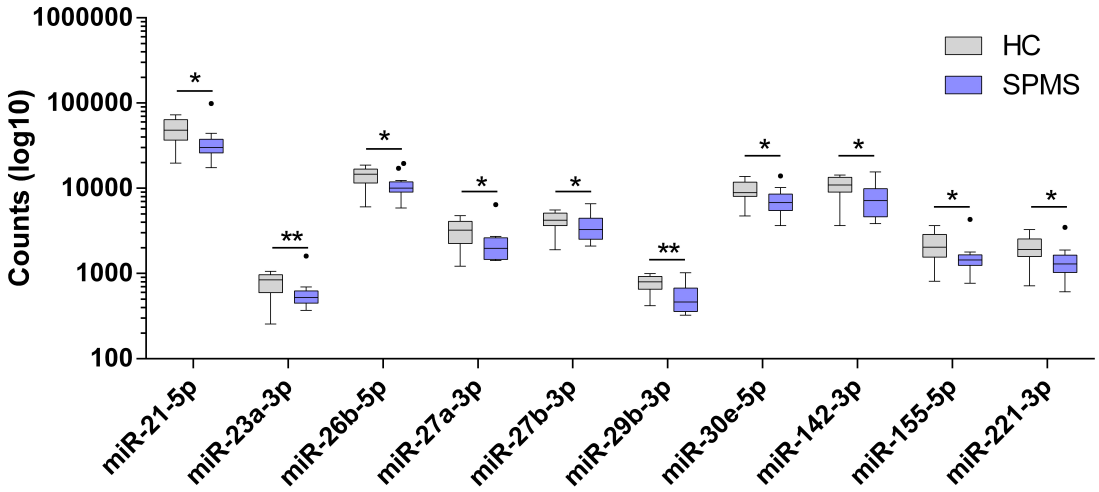

Figure 2.1: Tukey boxplot demonstrating the ten most significantly dysregulated microRNA identified using NGS. Data is presented as log10 of the read count and clearly exhibits the down-regulation of miRNAs in SPMS (purple) compared to HC (grey). Whiskers represent data within 1.5 interquartile range (IQR) of the upper and lower quartile. Data points outside of the 1.5 IQR are represented by black dots. * $p<0.05$, ** $p<0.01$.

RT-qPCR

To confirm our NGS findings, the top ten most dysregulated miRNAs were selected for further analysis in 24 SPMS and 22 HC samples using RT-qPCR (including the 12 SPMS and 12 HC samples that underwent NGS analysis). Of these ten miRNAs, RT-qPCR confirmed significant down-regulation of miR-21-5p (p=0.0048), miR-26b-5p (p=0.007) miR-29b-3p (p=0.00001), miR-142-3p (p=0.05) and miR-155-5p (p=0.001) in SPMS CD4+ T-cells (figure 2.2). These five miRNAs were confirmed in the original NGS cohort, the replication cohort, and the combined cohort. This provides statistically significant evidence of replication indicating these five miRNAs are very unlikely to be false positives. A trend of down-regulation of miRNA in SPMS samples was still observed across all ten miRNAs.

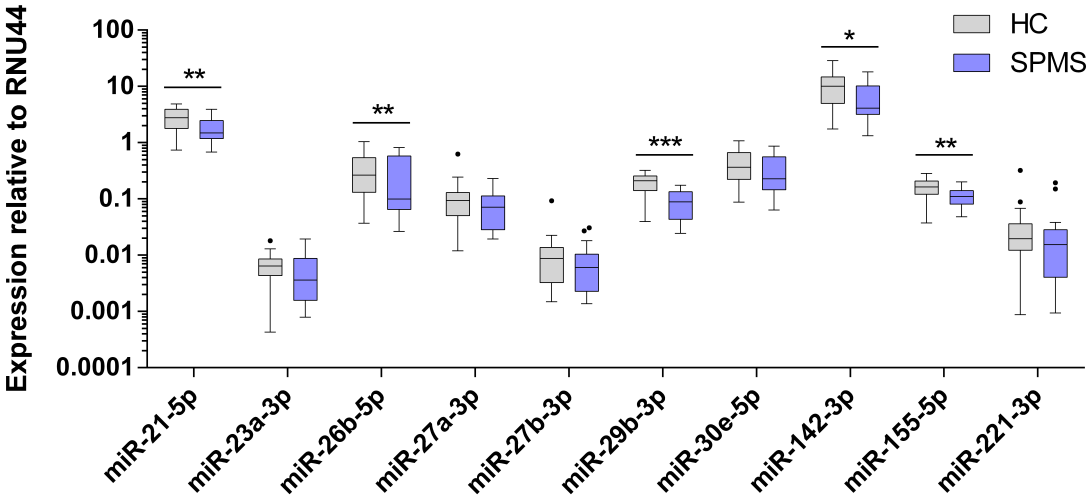

Figure 2.2: Tukey boxplot of top ten miRNAs expression (relative to RNU44) using RT-qPCR. Significant down-regulation of miR-21-5p, miR-29b-3p, miR-142-3p and miR-155-5p in SPMS was confirmed. Whiskers represent data within 1.5 interquartile range (IQR) of the upper and lower quartile. Data points outside of the 1.5 IQR are represented by black dots. * p<0.05, ** p<0.01, *** p<0.001.

Comparison of methods

Concordance of differential expression can vary between quantitation methods (186). To determine the magnitude of fold-change in SPMS vs. HC we compared qPCR and NGS results and found no change in the degree of decreased expression between NGS and RT-qPCR methods in the miRNAs confirmed by RT-qPCR (figure 2.3).

Correlation to patient characteristics

No strong correlations between miRNA expression and patient characteristics were identified (table 2.2). However, moderate positive correlation between EDSS, and miR-21-5p, miR-26b-5p and miR-29b-3p was seen. Further positive correlation was also found between disease duration and miR-21-5p and miR-155-5p. All miRNAs demonstrated weak correlation to patient age and progression duration.

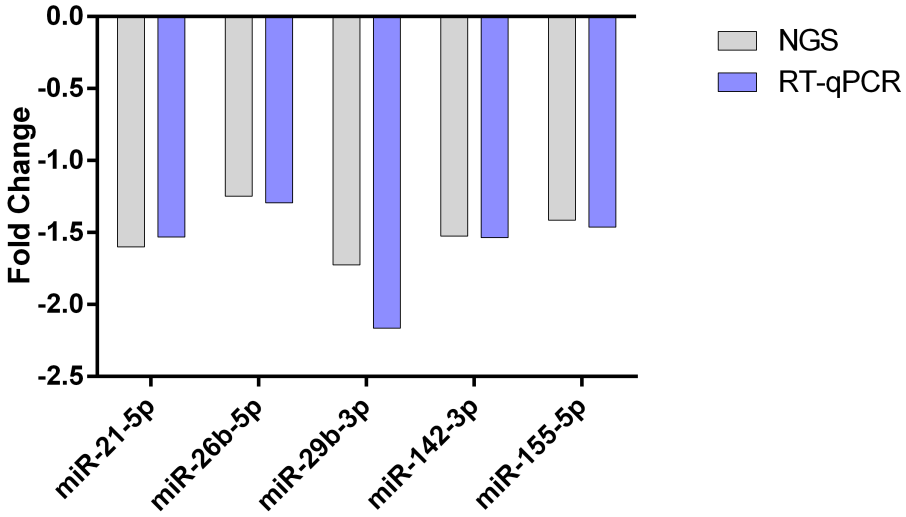

Figure 2.3: Comparison of miRNA fold-change between NGS and RT-qPCR. Magnitude of change is consistent between NGS and RT-qPCR methods.

Table 2.2: Correlation coefficients calculated from RT-qPCR data against patient characteristics.

	miR-21-5p	miR-26b-5p	miR-29b-3p	miR-142-3p	miR-155-5p
EDSS	0.34	**0.42**	**0.41**	0.28	0.26
Age (HC)	0.22	0.17	0.31	0.21	-0.08
Age (SPMS)	-0.07	-0.17	-0.17	-0.30	-0.01
Disease duration	**0.49**	0.15	0.23	-0.08	**0.49**
Progression duration	0.12	0.12	0.11	-0.07	0.17

Correlation of miRNA expression and age of HC has also been calculated as a reference point for age of patients. Moderate correlations are in bold text.

Target prediction

miRNA fold change was <2 in all miRNAs. It is therefore unlikely that any one particular miRNA is causing a great effect on gene expression. It is more likely to be a combination of multiple miRNAs targeting a few specific genes. Furthermore, as RT-qPCR is a less sensitive methodology than NGS, and the trend of down-

regulation is still seen (though not significant) in the other miRNAs, all ten miRNAs were cross-analysed potential gene targets. miRSystem was used to identify genes that have multiple target genes in common, both in the five confirmed miRNAs and all ten miRNAs identified by NGS. One gene, bromodomain and WD repeat domain containing 1 (*BRWD1*), is targeted by all five confirmed miRNAs. No genes are targeted by all ten miRNAs however; eight genes are targeted by eight of the miRNAs (table 2.3).

Table 2.3: Genes identified by miRSystem targeted by eight of the ten microRNAs. Verified targeting miRNAs are identified with a "V".

	miR-21-5p	miR-23a-3p	miR-26b-5p	miR-27a-3p	miR-27b-3p	miR-29b-3p	miR-30e-5p	miR-142-3p	miR-155-5p	miR-221-3p
ACVR2B	V	V	V	V	V	V			V	V
ZBTB41	V	V		V	V	V	V	V	V	
BRWD1	V	V	V			V	V	V	V	V
CAMTA1	V	V		V	V	V	V		V	V
CFL2	V	V		V	V	V	V	V	V	
SOCS6	V	V	V	V	V		V	V	V	
MIER3		V	V	V	V	V	V		V	V
KLF12	V	V	V	V	V	V	V			V

These genes are involved in transmembrane ligand binding, regulation of actin filaments, or are transcription factors. However, only one gene is specifically linked to immune cell functioning, *SOCS6* (suppressor of cytokine signalling 6). This gene has previously been reported to negatively regulate T-cell activation by promoting ubiquitin-dependent proteolysis (187) and was thus selected for further investigated.

SOCS6 expression

Gene expression analysis using RT-qPCR was conducted to determine whether *SOCS6* is up-regulated in SPMS CD4+ T-cells in direct negative correlation to the miRNA expression (Figure 2.4). Both the preliminary and validation cohorts were

analysed and *SOCS6* expression is increased in SPMS compared to HC. Normalisation against *GAPDH* and β-actin generated the same results (data for β-actin not shown).

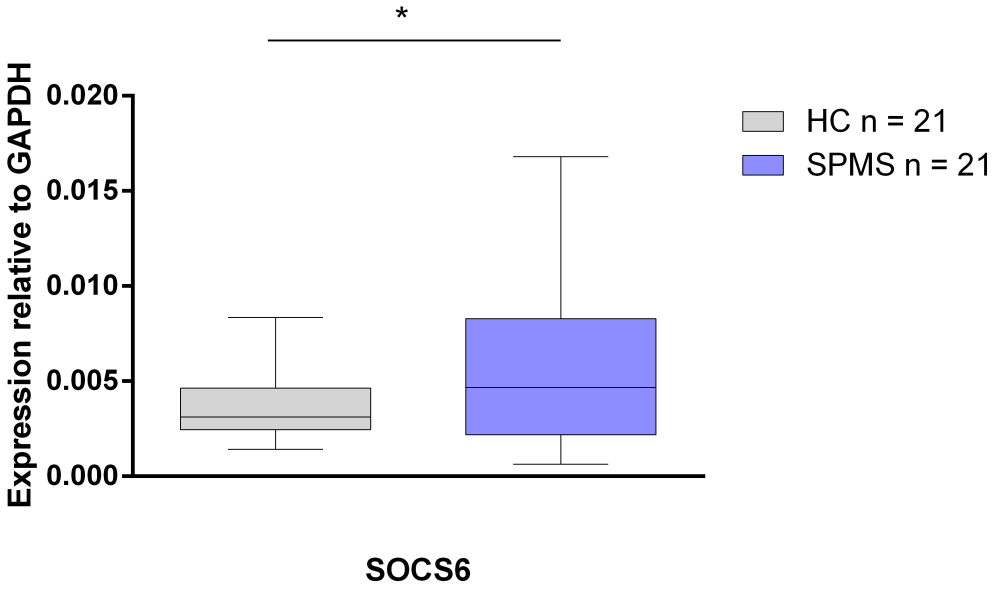

Figure 2.4: Expression of *SOCS6* relative to *GAPDH*. Up-regulation of *SOCS6* in SPMS is significant though widely distributed (* p=0.042).

Discussion

This is the first study in MS to utilize NGS for miRNA expression profiling in the CD4+ T-cells of SPMS patients. We found 42 miRNAs that are dysregulated in the CD4+ T-cells of SPMS patients as compared to controls; 97% of which were down-regulated. TaqMan assays confirmed five of these miRNAs (miR-21-5p, miR-26b-5p, miR-29b-3p, miR-142-3p and miR-155-5p) to be down-regulated in SPMS. Each of these miRNAs (excluding miR-26b) has been reported on previously in MS though not necessarily in SPMS or CD4+ T-cells. Lindberg *et al.* (125) identified seven miRNAs dysregulated in the CD4+ T-cells from RRMS patients, but did not identify dysregulation in any of the five miRNA in this study. Thus, down-regulation of these miRNAs may be exclusive to SPMS.

Here, we report a decrease in miR-155-5p expression in MS; this is the first study to identify this. miR-155-5p has a major proinflammatory role in MS and has been shown to be up-regulated in a number of tissues. Studies of post-mortem brain tissue

find a gradient of miR-155-5p expression that peaks in active lesions (141) and associated neurovascular units (157), and decreases through chronic lesions and normal appearing white matter to a low baseline in healthy control white matter (157, 158). This increased expression of miR-155 has been associated with suppression of: *CD47* in active lesions that creates a permissive environment for myelin phagocytosis (141); focal adhesion and cell-cell complex molecules in the blood brain barrier, thus increasing permeability (157) and; *AKR1C1* and *AKR1C2*, essential for biosynthesis of allopregnanolone (a neuroprotective steroid) (158).

Interestingly, a study of miR-155 in the EAE mouse model found that miR-155 expression in CD4+ T-cells increases during EAE and that miR-155$^{-/-}$ mice had an attenuation of EAE (165). Specifically, Th17 cells lacking miR-155-5p are unable to cause EAE (188). miR-155-5p is required for normal immune function (189) and together, these studies confirm the significant role that miR-155-5p over-expression plays in the inflammatory process of MS. In contrast, our finding of miR-155-5p down-regulation may be exclusive to SPMS patients and/or CD4+ T-cells, and is consistent with SPMS as a non-inflammatory mediated disease.

In PBMCs, miR-155-5p is up-regulated in RRMS (152, 159). Waschbisch et al. compared miR-155 expression in PBMCs of 74 RRMS patients against 32 controls and identified at baseline up-regulation of miR-155-5p and miR-142-3p. Glatiramer acetate (GA) treatment resulted in normalized expression of miR-142-3p. However, in our study, all patients had been treatment free for >6 months prior to collection and thus GA cannot be attributed as the cause of miR-142-3p down-regulation in our patient cohort.

A recent study on autologous haematopoietic stem cell transplant (AHSCT) also found co-dysregulation of miR-155-5p and miR-142-3p (124). Contrary to our results, Arruda et al. found these miRNAs to be up-regulated in MS patient CD4+ T-cells before treatment (cohort was 75% SPMS). However, we reason that there are differences in the immune activity of the patient cohorts. AHSCT is most effective in active MS disease and the European Bone Marrow Transplant Register recommended that only SPMS patients with some inflammatory activity and gadolinium-enhancing (Gd+) lesions be considered for AHSCT (190). Six of the 19 SPMS patients enrolled in the Arruda et al. study presented with gadolinium-enhancing lesions in the year approaching the treatment indicating inflammatory

activity. Further, the average disease duration in the Arruda et al. study was 8.1 years, as opposed to 25.6 (primary cohort) or 18.6 (replication cohort) years in our study. While the AHSCT study also utilized TaqMan microRNA assays, our data is corroborated further by NGS expression analysis, which is a more sensitive measure of expression changes.

In a study of potential biomarkers in Alzheimer's disease (AD), miR-26b-5p was shown to be down-regulated in the serum and CSF of AD patients when compared to patients with inflammatory neurological diseases (191) supporting the predominantly neurodegenerative pathology of SPMS.

Previously, miR-29b-3p is reported as being up-regulated in memory CD4+ T-cells in all MS subtypes however, the SPMS sample group was very small (n=4) (139) compared to our cohort (n=24). This study also identified a feedback loop where miR-29b-3p targets IFN-γ which induces miR-29b-3p expression (139). The noted reduction of IFN- γ in peripheral blood of SPMS patients compared to RRMS (192) may contribute to our observed reduction of miR-29b-3p in SPMS patients.

Over-expression of miR-29b in systemic lupus erythematosus (SLE) has been linked to hypomethylation of DNA in CD4+ T-cells (193). While there are currently no studies on DNA methylation in SPMS, it would be interesting to see if the down-regulation of miR-29b that we have identified here in CD4+ T-cells is associated with genome-wide hypermethylation in SPMS.

Increased miR-21-5p promotes differentiation of Th17 cells in the EAE mouse model and miR-21-5p knock-out mice have a defective Th17 differentiation pathway, resulting in resistance to EAE (194). Fenoglio et al. found increased miR-21-5p expression in RRMS (active relapse phase) PMBCs compared to controls, though no difference in SPMS. Again, this may be contributed to the relatively small sample size (n=6) (129). As with our other significantly dysregulated miRNAs, miR-21-5p has a demonstrated mechanism of increasing T-cell activity.

Also of interest, we previously reported miR-20a-5p down-regulation in the whole blood of all MS subtypes (195). This miRNA was one of the 42 dysregulated miRNAs identified by NGS and is significantly down-regulated in SPMS compared to HC. However, it narrowly missed the 800 read cut-off for qPCR confirmation. miR-20a-5p is also predicted to target *SOCS6*.

All ten miRNAs showed down-regulation in RT-qPCR, however the difference was statistically significant in only five. Recently, molecules responsible for microRNA biogenesis (Drosha, Dicer and DGCR8) were found to be over-expressed in the PBMCs of RRMS compared to healthy controls (114). It would be interesting to see if this is still the case in SPMS or if a down-regulation of the machinery may be the cause of the observed reduction of miRNA expression observed in this study.

Eight of the top ten dysregulated miRNA were predicted to target *SOCS6* by MirSystem. Consistent with this, increased expression of *SOCS6* in the SPMS cohort is in direct negative correlation with the miRNA expression profiles, strongly indicating a mRNA:miRNA relationship. To our knowledge, this is the first study to identify *SOCS6* as a gene of interest in MS. It is a highly conserved gene with very low expression levels in healthy thymus and brain tissues and is down-regulated in gastric, colorectal and pancreatic cancers (196-199). In colorectal cancer, methylation changes have been ruled out as the mechanism of down-regulation (198), therefore this down-regulation may be due to altered miRNA expression. MiR-424-5p is responsible for the down-regulation of *SOCS6* in pancreatic cancer (199) however we found no differences in miR-424-5p expression between SPMS and HC in this study.

The function of *SOCS6* as a negative regulator of T-cell activation (187) and its observed over-expression in SPMS CD4+ T-cells, supports the notion of reduced immune activity in SPMS. Very little is known about *SOCS6* and mores studies are required to determine if it may be a novel therapeutic target.

This is the first study to use NGS miRNA profiling to assess miRNA expression in the CD4+ T-cells of SPMS patients. Future studies should focus on using the same technique in treatment naïve RRMS patients to determine if this is a SPMS exclusive trend and remove the confounding factor of treatment effects. Furthermore, miRNA expression profiles of other cell subtypes should be investigated, as whole blood analysis is likely masking significant changes in individual cell subsets. Ideally, all of our patients would have had inactive SPMS, however as SPMS is a difficult disease stage to define and collect we have included some active SPMS patients in this study. In this study, we chose to focus on CD4+ T-cells as they are traditionally thought to be the main cell infiltrates. Our previous studies also show that CD4+ T-cells exhibit significant changes in methylation profiles in RRMS (98, 99).

Conclusions

Here we have shown a general down-regulation of miRNAs in CD4+ T-cells compared to HC, with five miRNAs confirmed as significant in two independent assays. This indicates that miRNA expression may be over-normalising in SPMS CD4+ T-cells. *SOCS6* is a predicted target of the majority of these miRNAs and, consistent with this, we found *SOCS6* to be up-regulated in this cohort. These are novel findings that point towards a diminished role for CD4+ T-cells in SPMS, and adds further evidence of SPMS as a neurodegenerative disease stage, not an inflammation-driven one.

Acknowledgements

This study was supported by the John Hunter Hospital Charitable Trust and the Bloomfield Group Foundation. KAS, VEM and RAL are supported by fellowships from Multiple Sclerosis Research Australia. KAS is also funded by the Trish MS Research Foundation postgraduate scholarship. VEM is supported by a post-doctoral fellowship from the Canadian Institute of Health Research.

We would like to thank the MS patients and clinical team at the John Hunter Hospital MS clinic who participated in this study. We also acknowledge the Analytical Biomolecular Research Facility at the University of Newcastle for flow cytometry support and the Diamantina Institute at the University of Queensland for NGS services.

Author contributions

KAS, MCB and RAL wrote the main manuscript text. KAS, VEM, and NG performed experiments. KAS and SA collected samples. MCB and RAL analysed NGS data. RJS, LT and JLS supervised the study. All authors reviewed the manuscript.

CHAPTER THREE – DNA methylation profile of SPMS CD4+ T-cells

Methylation at the MHC locus is associated with MS progression independently of *HLA-DRB1*

This chapter addresses my second research question: Are DNA methylation profiles of CD4+ T-cells different between in RRMS and SPMS, and are changes in microRNA expression caused by DNA methylation?

Abstract

Background: Multiple sclerosis (MS) is characterised by inflammatory attacks of the central nervous system that initially are followed by recovery. In the secondary progressive stage the periods of recovery cease, leading to relentless accumulation of disability due to ongoing demyelination and neurodegeneration. DNA methylation is an epigenetic modification that is involved in gene expression. In a previous study, we found that there are DNA methylation changes at *HLA-DRB1* in relapsing-remitting MS (RRMS) patients compared to controls in CD4+ but not CD8+ T-cells. This study aimed to confirm these findings in an MS cohort free of any treatment and to compare the global DNA methylation profiles of CD4+ T-cells in secondary progressive (SPMS) and RRMS patients.

Methods: Total DNA was extracted from the CD4+ T-cells of 27 female RRMS and 25 matched healthy controls and 23 female SPMS and 19 matched healthy control subjects. DNA was bisulfite converted and hybridised to Illumina 450K arrays. Beta values were analysed using a multi-CpG penalised regression approach (GLMNet) to identify MS-associated CpGs.

Results: We were able to confirm our previous data that demonstrated a differentially methylated region at the *HLA-DRB1* locus in RRMS patients. In addition, we identified a striking differential signal at *RNF39* in RRMS patients, a gene previously reported to be associated with MS. Surprisingly, we found the majority of associated sites are unique to their respective patient subgroup, with only 16 overlapping differentially methylated sites in RRMS and SPMS. Also surprisingly, the majority of

these sites were contained within the *RNF39* DMR and not the *HLA-DRB1* DMR. Globally, we find RRMS patients to have equal hypo- and hypermethylation compared to healthy controls compared to a striking global hypermethylation in SPMS patients (75%) compared to healthy controls.

Conclusions: Our findings provide the first global comparison of DNA methylation profiles in RRMS and SPMS patients. We find a substantial difference between the two disease subgroups in CD4+ T-cells, and larger studies are warranted to further understand how this contributes to MS pathophysiology.

Introduction

MS is an autoimmune disease characterized by lymphocyte mediated inflammation causing demyelination and axonal degeneration. In the RRMS phase of disease, lymphocytes move from the periphery into the CNS, where they initiate an immune response that results in demyelination and corresponding symptoms (relapse). This is followed by a phase of recovery and repair (remission). Approximately 60% of patients will progress from RRMS to SPMS (32), which is characterised by increasing disability (measured by EDSS) in the absence of relapses (8). This stage is thought to be more neurodegenerative in nature and the role of inflammation is less clear.

MS aetiology is assumed to be a combination of genetic predisposition and environmental exposures. Despite several large genome-wide association studies (GWAS), there remains a large proportion of unexplained heritability in terms of MS risk (80, 200). Epigenetics can influence the genome in the absence of DNA sequence changes. Environmental exposures such as smoking and sunlight exposure have been demonstrated to modify epigenetic mechanisms, providing a plausible link between environmental factors and disease (49, 201). One such epigenetic mechanism is DNA methylation, which is the addition of a methyl group to CpG dinucleotides. We, and others, have used genome-wide DNA methylation technologies to assess differentially methylated regions (DMRs) of CD4+ and CD8+ T-cells in RRMS patients compared to healthy controls (94, 98, 99, 101). We found a striking methylation signal located on chromosome 6p21 with a peak signal at HLA-DRB1, in relapsing-remitting patients compared to healthy controls, that was only

present in CD4+ T-cells (98). There are no studies to date that provide a comparison between the methylation profiles of RRMS and SPMS patients.
Furthermore, DNA methylation is capable of regulating other epigenetic mechanisms. In diseases other than MS, microRNA (miRNA) expression is affected by DNA methylation in miRNA promoter regions (113). Previously, we reported broad down-regulation of miRNA in CD4+ T-cells (202) but the mechanism behind this remains unclear. DNA hypermethylation in promotor regions may be a contributing factor to this miRNA dysregulation.

In this study, we performed a genome-wide DNA methylation study of CD4+ T-cells from RRMS, SPMS patients and healthy controls to (1) replicate our initial results in RRMS in a group of patients who were not on any immunomodulatory therapy, (2) determine if the methylation signal we found in CD4+ T-cells is unique to RRMS patients, or ubiquitous across all MS patients, and (3) determine if there are unique methylation changes specific to SPMS, and whether these may affect expression of miRNAs. Identification of epigenetic loci associated with the different stages of disease could provide potential targets for new therapies and help explain the transition from RRMS to SPMS.

Patients and Methods

Sample collection

Whole blood was collected from 25 female RRMS patients and 27 age-matched female healthy donors, and 23 female SPMS patients and 19 age-matched female controls (Table 3.1). All patients were diagnosed with MS according to the McDonald criteria (183). SPMS patients were defined as those who demonstrated EDSS progression without evidence of relapse in the 24 months prior to collection (8). RRMS patients were treatment naïve (18 patients) or had not taken immunomodulatory or steroid treatment for a minimum of 3 months (9 patients). SPMS patients had not taken immunomodulatory or steroid treatment for a minimum of 6 months. Healthy control samples were collected from volunteers off the Hunter Medical Research Institute Register.

Table 3.1: Characteristics of patients and controls

	RRMS HC	RRMS	SPMS HC	SPMS
Total	27	25	19	23
Age in yrs (mean ±SD)	38.2 ± 11.1	38.6 ± 12.7	57.6 ± 12.1	58.4 ± 9.4
EDSS (mean ±SD)	n/a	2.1 ± 1.5	n/a	6.6 ± 1.3
Disease duration in yrs (mean ±SD)	n/a	7.6 ± 11.4	n/a	25 ± 11.0

EDSS = Expanded Disability Status Score

Ethics statement

The Hunter New England Health Research Ethics Committee and the University of Newcastle Ethics committee approved this study (05/04/13.09 and H-505-0607 respectively), and methods were carried out in accordance with institutional guidelines on human subject experiments. Written and informed consent was obtained from all patient and control subjects.

Blood sample processing and DNA methylation arrays

PBMCs were isolated from whole blood by density gradient centrifugation using Lymphoprep (Axis-Shield PoC AS, Norway) following standard laboratory procedures. Total CD4+ T-cells were extracted from the PBMC population using EasySep negative magnetic separation according to the manufacturers' instructions (StemCell Technologies, Canada). After isolation, cell purity was assessed by flow cytometry. Cells were stained with a FITC-conjugated CD4 antibody (60016F1 StemCell Technologies) and collected on a BD FACSCanto II flow cytometer, then analysed using FACSDiva software (BD Biosciences). All samples met the minimum purity cut-off of 90%. DNA was extracted with the Qiagen microDNA extraction kit (Qiagen, USA) and bisulfite converted using the MethylEasy Xceed kit according to the manufacturers' instructions. Converted DNA was then applied to the Illumina Infinium Human450K Beadchip arrays (service provided by Diamantina, Queensland).

Data analysis

Data was analysed as previously described. An in-house data analysis pipeline that used a combination of R/Bioconductor and custom scripts was designed. Illumina 450k raw intensity data (idat files) were parsed into the Bioconductor MINFI package (203). Methylation data was background-corrected and control-normalised according to MINFI routines (204). Data was cleaned by removing (failed) CpG probes for which the intensity of both the methylated and unmethylated probes was <1000 units across all samples. A threshold of 1000 units was selected based on the profile of the available negative control probes. Y chromosome probes were filtered out. All probe sequences were mapped to the human genome (buildHg19) using BOWTIE (205) to identify potential hybridisation anomalies. In total 33457 CpG probes were identified to align to the human genome multiple times and were filtered out of subsequent analysis.

Measures of methylation level (β values) were produced for each probe and ranged from 0 [completely unmethylated] to 1 [completely methylated]. Data was corrected for HLA-DRB1 genotype, and as differential methylation has been seen in CD4+ T-cells and not in CD8 or CD19 (unpublished data), it can be said that HLA is not influencing results. Likewise, differences in RRMS vs. SPMS are not due to HLA genotype as the same distribution is seen in both groups. To identify DMRs associated with MS subtypes in this female cohort a penalised ridge-regression mixed with lasso in an elastic-net framework was used as implemented via the R package *glmnet* (206). Briefly, *glmnet* fits a generalized linear model via penalized maximum likelihood. The regularization path is computed for the lasso or elastic-net penalty at a grid of values for the regularization parameter lambda λ. The elastic-net penalty is controlled by α, and bridges the gap between lasso (α=1, the default) and ridge α=0. The tuning parameter (α=1) controls the overall strength of the penalty. The ridge penalty shrinks the coefficients of correlated predictors towards each other while the lasso tends to pick one of them and discard the others. The elastic-net penalty mixes these two; if predictors are correlated in groups, an α=0 tends to select the groups in or out together. In our testing, cross-validation suggested that a λ of 425 was appropriate, so this was used to fit the final model for identification of DMRs. In order to 'rank' the sites we defined the absolute range for each CpG site, that is

the absolute value of the largest observed beta minus the smallest observed beta for a given CpG site.

Statistical analyses

Given the relatively modest sample size, this study was underpowered to detect significant differentially methylated positions (DMP) at the methylome-wide level and thus we used a series of prioritisation steps to identify the most robust loci. Specifically, a DMP was defined as containing CpGs **i)** that yielded a $p<0.05$ ie. nominally associated with MS and **ii)** that yielded a Δmeth of ±10% ie. a relatively large differential methylation. Subsequently, a DMR was defined as a DMP **iii)** that had ≥2 adjacent CpGs within 1000 bp physical distance and **iv)** whereby adjacent CpGs yielded a Δmeth in the same direction ie. all 3 CpGs in the DMR were consistently hypo- or hyper- methylated.

Results

We recruited 25 RRMS patients and 27 age-matched healthy donors, and 23 female SPMS patients and 19 age-matched female controls. Clinical characteristics are shown in Table 3.1.

Methylation profiles in RRMS

The methylation profiles of RRMS patient CD4+ T-cells were analysed using Illumina Infinium Human450K Beadchip arrays, and compared against controls. CD4+ T-cells from RRMS patients have 275 significantly deregulated CpGs across 153 genes and 80 locations with no gene association compared to age-matched controls. Of the 275 CpGs, 49% (n=134) were hypermethylated and 51% (n=141) were hypomethylated (Figure 3.1). Table 3.2 shows the top 10% (27 total) of CpGs which are differentially methylated, (for full list see Appendix 3, table A3.1). Within the 275 sites, 14% are located within the MHC region. Nine of these CpG sites that were identified in our previous work and five of these are located in the *HLA-DRB1* gene (98). The percent change at the *HLA-DRB1* locations is slightly lower for each CpG site in this study than our previous study; however, they all are dysregulated in the same direction

(primary hypomethylation). In addition to the previously identified sites, we also identified 3 new CpGs within the *HLA-DRB1* cluster. All except one are located within the same 400bp region. We also observed hypermethylated regions at *HLA-DRB5* and *HLA-DQB1* that were identified in our previous study (table A3.1) (98). At the *HLA-DRB5* region we identified one previously identified probe plus an additional 2 sites. We did not see any change in methylation at the CpG sites in *HLA-DRB6* previously identified, but did find two new hypermethylated sites (Table 3.2 and Table A3.1).

In addition to the cluster of HLA associated CpGs, there was another cluster within the MHC locus at *RNF39* (Ring Finger Protein 39). We observed 11 hypermethylated CpGs in the top-ranked differentially methylated probes, which map to *RNF39* and are tightly clustered within a 312bp region. This region spans the boundary between intron 3 and exon 4, and spreads into exon 4. Also within the MHC region, there is a smaller cluster of 3 CpGs within a 45bp span at the transcription start site (TSS) of *HCG4P6* (table A3.2).

To identify additional regions of potential interest that were not within the MHC locus, we considered DMRs as regions where genes had 2 or more differentially methylated CpG sites that were less than 500bp apart. Using this criterion, we identified 3 additional DMRs (table A3.3). *C21orf56* has 4 hypomethylated CpG sites within 153bp, *ERICH1* has 4 CpGs in a 122bp region, and *PM20D1* has 6 CpGs in 163bp (table A3.3). One of the probes within *C21orf56* was identified in our previous cohort; however, the other two DMRs are unique to this study.

None of the other major MS genes outside the HLA identified in the GWAS by the IMSGC (80) (i.e. *CD58, THADA, EOMES, MLANA, IL2RA, STAT3*) revealed any significantly CpG site changes as judged by the assay used for this study.

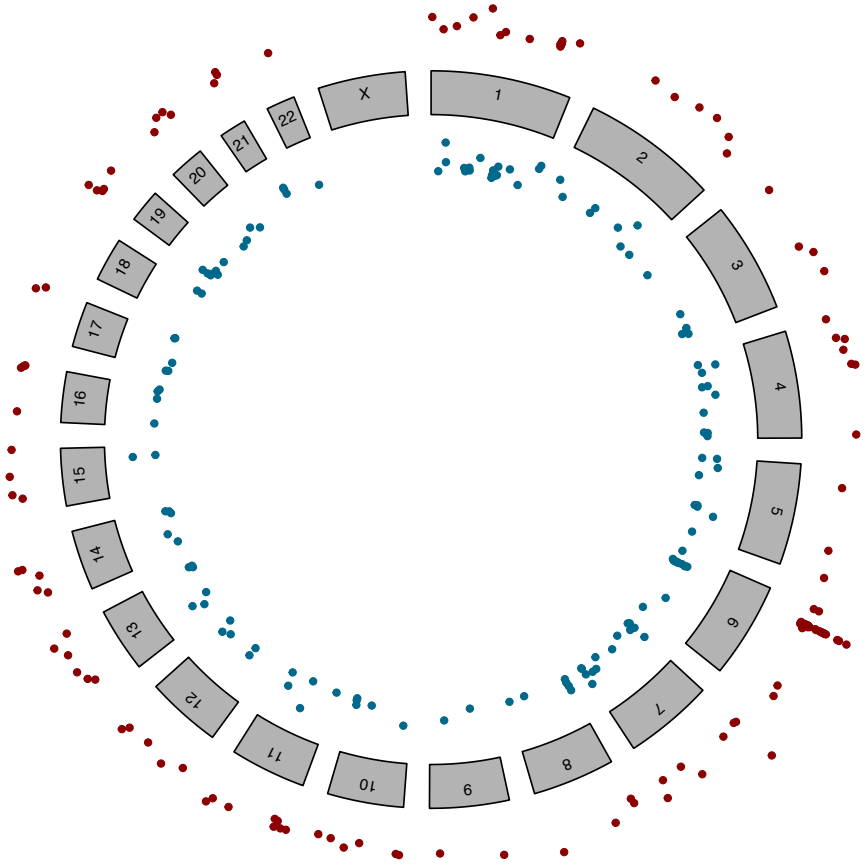

Figure 3.1: A genome-wide differential methylation plot of RRMS CD4+ T-cells. Data points outside the circle (red) represent increased methylation in RRMS patients compared to healthy controls (i.e. Δ_{meth}), whereas Data points inside the circle (blue) represent decreased methylation in the RRMS group.

Table 3.2: Top 10% of differentially methylated CpGs in RRMS patient CD4+ T-cells.

Probe ID	Chr	Position	Gene	Median (case)	Median (control)	Δ_{meth}	Adj *p* value	p_{FDR}	Feature
cg23403836	7	1616229	KIAA1908	0.750865	0.435553	0.315312	1.60E-05	0.00284	Body
cg20536971	13	100989375	PCCA	0.639244	0.345777	0.293467	0.00178	0.01576	Body
cg22071943	5	1225434	SLC6A18	0.368136	0.643653	-0.27552	0.002769	0.01755	TSS200
cg15602423	6	32552095	HLA-DRB1	0.387082	0.658822	-0.27174	0.00434	0.01844	Body
cg03398919	2	173118470		0.474625	0.73943	-0.26481	0.004671	0.01844	
cg07844442	10	129144269	DOCK1	0.465688	0.728887	-0.2632	0.013719	0.02760	Body
cg08822897	11	64258103		0.284157	0.533063	-0.24891	0.000367	0.01349	
cg20374173	10	14227415	FRMD4A	0.339618	0.587672	-0.24805	0.001926	0.01576	Body
cg08912652	11	130779479	SNX19	0.851534	0.6036	0.247934	0.003191	0.01755	Body
cg10415021	11	110890228		0.486528	0.731505	-0.24498	0.00319	0.01755	
cg05248234	17	79495519	FSCN2	0.261872	0.492531	-0.23066	0.015893	0.02909	1stExon; 5'UTR
cg16706502	14	31927974	C14orf126	0.597671	0.367749	0.229923	0.008531	0.02385	TSS1500
cg22802014	1	31732891	SNRNP40	0.675691	0.902554	-0.22686	0.000434	0.01349	3'UTR
cg19774683	6	32522400	HLA-DRB6	0.576704	0.355419	0.221285	0.039277	0.04526	Body
cg06052372	16	83967808		0.550688	0.766873	-0.21619	0.012049	0.02733	
cg16999994	11	1001560	AP2A2	0.453497	0.238958	0.214539	0.015443	0.02909	Body
cg13232075	1	204556835		0.42867	0.215897	0.212773	0.016589	0.02925	
cg08136432	16	88902276	GALNS	0.645258	0.857102	-0.21184	0.015855	0.02909	Body
cg03706056	21	37437565	SETD4	0.531861	0.32023	0.211631	0.014348	0.02808	TSS1500
cg07909498	4	79627477		0.486084	0.280086	0.205998	0.001949	0.01576	
cg13423887	**6**	**32632694**	**HLA-DQB1**	**0.294241**	**0.49987**	**-0.20563**	**0.004161**	**0.01844**	**Body**
cg01341801	**6**	**32489203**	**HLA-DRB5**	**0.454757**	**0.249419**	**0.205338**	**0.040802**	**0.04535**	**Body**
cg14645244	6	32552205	HLA-DRB1	0.317864	0.521037	-0.20317	0.017405	0.02991	Body
cg23128510	2	175922785		0.860042	0.657146	0.202896	0.001749	0.01576	
cg02100397	19	646890		0.446869	0.648013	-0.20114	0.009409	0.02385	
cg05875700	8	638208	ERICH1	0.120484	0.319176	-0.19869	0.004548	0.01844	Body
cg18662228	2	236867804	AGAP1	0.422887	0.621416	-0.19853	0.035895	0.04330	Body

Bold font indicates common probes between this study and our previous work (98).

Methylation profiles in SPMS patients

The methylation profiles of SPMS patient CD4+ T-cells were analysed using Illumina Infinium Human450K Beadchip arrays, and compared against controls. CD4+ T-cells from SPMS patients had 243 significantly deregulated CpGs spanning 145 genes, and 77 probes that map to locations without gene association (Figure 3.2). Of the 243 CpGs, 75% (183) were hypermethylated and 25% (60) were hypomethylated.

Table 3.3 shows the top 10% of differentially methylation sites, the full list of differentially methylated sites that met a significance threshold of $p<0.05$ is shown in Appendix 3, table A3.4. Surprisingly, none of the HLA regions identified in RRMS patients were also identified in SPMS patients. However, there were 2 single CpG sites within the top ranked probes that map to HLA genes – a unique site at *HLA-DRB1* (cg15820961), and one at *HLA-DQA1* (cg24969496). There were no probes located within any of the non-MHC variants identified in the GWAS studies by the IMSGC (80).

When filtered for DMRs that contained at least 2 probes within 500bp of each other, there were 7 DMRs (Table A3.5). Intriguingly, the largest DMR maps to the MHC locus at *RNF39*. At *RNF39* in SPMS patients, we find 8 CpGs within a 72bp span, 7 of which are shared sites between SPMS and RRMS patients. However, all of these sites are hypomethylated, as opposed to the hypermethylation seen in the RRMS cohort. We also find a smaller DMR at the transcriptional start site of *DUSP22* that contains 3 probes within a 420bp region. There are 5 additional small DMRs outside the MHC locus at *POU6F2, PARD6G, SLC17A9* and *APOL2*. Similar to RRMS patients, none of the other major MS genes outside the MHC identified in the GWAS by the IMSGC (80) revealed any significantly CpG site changes as judged by the assay used for this study.

As DNA methylation can affect the expression of miRNAs, as well as mRNAs, differentially methylated CpGs were cross-examined for their potential effect on miRNA TSS. Using miRStart (207), a database of miRNA transcriptional start sites, the location of differentially methylated CpGs in SPMS CD4+ T-cells (tables 3.2 and A3.4) were cross compared with known miRNA TSS. There was no overlap in genomic location of CpGs identified in table 3.3 and miRNA TSS.

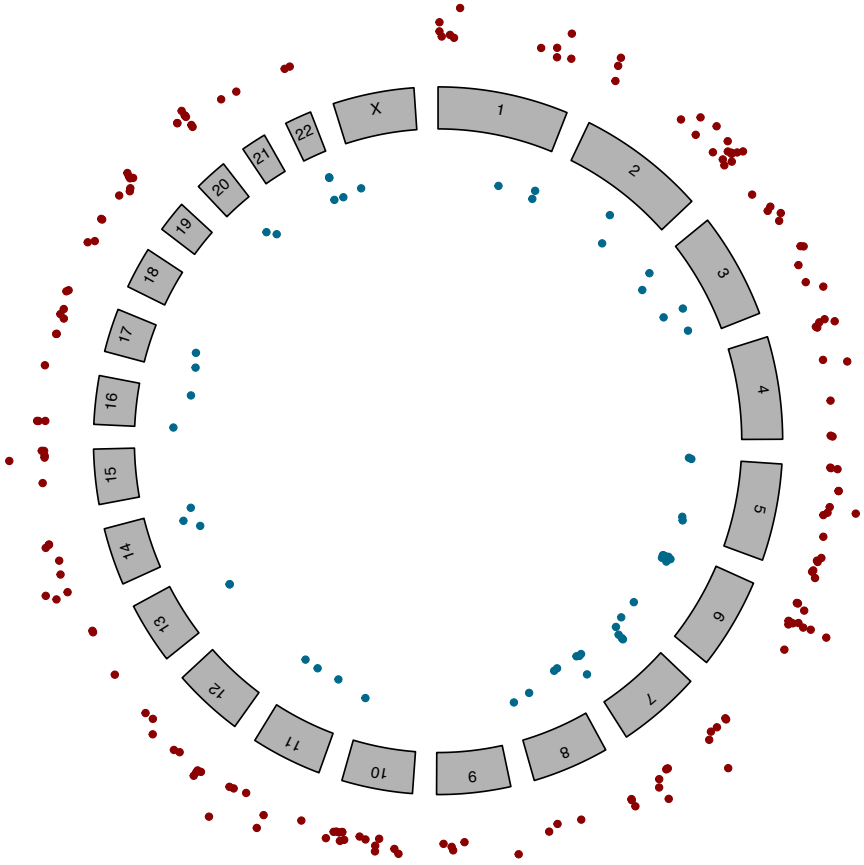

Figure 3.2: A genome-wide differential methylation plot of SPMS CD4+ T-cells. Data points outside the circle (red) represent increased methylation in SPMS patients compared to healthy controls (i.e. Δ_{meth}), whereas data points inside the circle (blue) represent decreased methylation in the RRMS group.

Table 3.3: Top 10% of differentially methylated CpGs in SPMS patient CD4+ T-cells.

Probe ID	Chr	Position	Gene	Median (case)	Median (control)	Δ_{meth}	Adj *P* value	P_{FDR}	Feature
cg17666981	6	28878192	TRIM27	0.91827	0.80185	0.116422	0.00013	0.01258	Body
cg04913265	11	133939627	JAM3	0.64597	0.51509	0.130878	0.00015	0.01258	Body
cg21901928	7	55139847	EGFR	0.80165	0.66480	0.136848	0.00016	0.01258	Body
cg04579183	15	88119834	NCRNA00052	0.81117	0.46961	0.341567	0.00020	0.01258	TSS1500
cg11553311	5	66541588		0.55113	0.38735	0.163781	0.00041	0.01579	
cg06182923	1	33985406	CSMD2	0.72875	0.61344	0.115305	0.00051	0.01579	Body
cg16706502	14	31927974	C14orf126	0.48565	0.10314	0.382514	0.00063	0.01579	TSS1500
cg04750100	2	136595281	LCT	0.34751	0.44905	-0.10153	0.00066	0.01579	TSS1500
cg10543947	22	36635882	APOL2	0.07416	0.20949	-0.13532	0.00068	0.01579	TSS200; 1stExon; 5'UTR
cg16121206	22	36636055	APOL2	0.39490	0.51881	-0.12399	0.00074	0.01579	TSS200; TSS1500
cg20802616	1	211590292	C1orf97	0.53618	0.42629	0.10989	0.00081	0.01579	Body
cg05792312	11	61781116		0.62427	0.30122	0.323044	0.00082	0.01579	
cg14170201	7	155191709		0.89102	0.65896	0.23206	0.00084	0.01579	
cg07733481	3	122694286	SEMA5B	0.09248	0.20363	-0.11114	0.00091	0.01579	5'UTR
cg25377865	4	72669944		0.74934	0.64726	0.102076	0.00107	0.01711	
cg24867279	6	28853021		0.55999	0.44089	0.119097	0.00119	0.01711	
cg23596425	2	1494263	TPO	0.84194	0.71555	0.126387	0.00123	0.01711	Body
cg24305906	2	241352106		0.85492	0.71616	0.138752	0.00126	0.01711	
cg08610773	2	184896169		0.88075	0.77837	0.102381	0.00149	0.01818	
cg04245305	3	195940754		0.95732	0.7168	0.240529	0.00161	0.01818	
cg01406776	4	8386748	ACOX3	0.86822	0.65601	0.212212	0.00163	0.01818	Body
cg09756125	7	158250978	PTPRN2	0.51451	0.74159	-0.22708	0.00171	0.01818	Body
cg07093060	3	174092757		0.47112	0.68013	-0.20901	0.00172	0.01818	

Comparison between MS subtypes

To determine which CpGs sites were common to MS patients versus those which are unique to each of the MS subtypes, we did a pairwise comparison of the full list of deregulated probes (275 RRMS and 243 SPMS CpG probes). Surprisingly, there are only 16 probes that are shared between the two patient subgroups, only 4 of which show change in the same direction (Table A3.4). Interestingly, 7 of these are the *RNF39* CpG sites; however, they are dysregulated in opposite directions.

Discussion

Our study is the first to compare the genome-wide methylation levels in CD4+ T-cells of RRMS and SPMS patients. Our most striking result is the lack of shared CpGs between RRMS and SPMS patients. When comparing the two patient subgroups, we found RRMS patients show equal hypo- and hyper methylation (51% and 49% respectively) compared to a tendency towards hypermethylation (75%) in SPMS patients. This translated to only 16 overlapping CpGs between RRMS and SPMS patients, suggesting that RRMS and SPMS patients have unique CD4+ T-cell methylation profiles. Surprisingly, although we confirmed 5 of the CpGs in *HLA-DRB1*, from our previous study (98) in RRMS patients, we saw only one CpG at this site in SPMS patients. This was not one of the sites identified in either of our studies. In addition, we have identified a new DMR in the MS associated gene, *RNF39* in both RRMS and SPMS patients. Interestingly, while this DMR is hypermethylated in RRMS patients, it is hypomethylated in SPMS patients. Taken together, our data suggest that DNA methylation is dynamic and may change with disease course.

One consideration for the lack of shared CpGs between RRMS and SPMS could be confounding effects due to treatment over time. The effects of immunomodulatory therapy on methylation in MS patients is unknown, although there is some evidence that immunomodulatory therapy used for other diseases, such as multiple myeloma, can alter the expression of DNA methyltransferases (208). Given that the majority of SPMS patients would have been given treatment at some stage during their disease, it is possible this could cause lasting methylation changes. Future studies would benefit from following patients longitudinally during various treatments to determine the effect over time on epigenetic profiles. DNA methylation changes with chronological age (91) although we find it unlikely that this is a confounding factor in our results as each cohort was compared to a separate age- and gender-matched cohort to correct for effects of aging. It is therefore possible that hypermethylation is a hallmark of disease progression; however, larger scales studies will be required to confirm this. At present, the underlying cause of this hypermethylation in SPMS is unknown. In CD4+ T-cells of systemic lupus erythematosus (SLE) patients, the up-regulation of miR-29b results in under-expression of its target genes (*DNMT3a* and *DNMT3b*), causing global hypomethylation in these cells (193). As miR-29b was one of our previously reported down-regulated miRNAs in SPMS CD4+ T-cells (202), it

will be worth analysing expression of these DNA methyltransferase genes to determine if the hypermethylation observed here is a consequence of miRNA expression changes. There were no differentially methylated CpGs in miRNA promoters, indicating that DNA methylation does not affect miRNA expression in CD4+ T-cells; further analysis will indicate whether miRNA expression instead affects DNA methylation.

In our previous study, we found a tight cluster of 8 hypomethylated CpGs in *HLA-DRB1* (98). In the current study, we were able to confirm 5 of these CpG sites, plus an additional 3 CpG sites clustered within the same 358bp region. These sites were only present in RRMS, although a single site in a distant region of HLA-DRB1 was identified in SPMS patients. Although there is a lower effect size in the new study, the dysregulation is occurring in the same direction (primarily hypomethylation). This is a region heavily populated by SNPs, though the absence of this signal in the SPMS cohort provides support for its independence from the *HLA-DRB1*1501* genotype. The frequency of the *HLA-DRB1*1501* allele does not change between the RRMS and SPMS cohorts (data not shown), but the methylation signal at this location does. Additionally, we assessed the global methylation levels in CD8+ T-cells, in the cohort from the Graves et al. (9) study and found no change in *HLA-DRB1* methylation signal in this cell type. This is further support for the SNP-independent nature of this signal.

This is the first evidence of differential methylation in *RNF39* being associated with MS, and the hypermethylation of this locus in early stage of disease may represent a major effect epigenetics locus for MS. However, its use as a biomarker would be impractical due to the time-consuming nature of analysing a single DMR in an isolated cell subtype. The biological relevance of this locus can only be speculated at this point; however, it resides within the gene body and spans an intron/exon boundary so it is plausible that hypermethylation is involved in aberrant expression of alternately spliced transcripts or a regulatory element for nearby genes. Interestingly, one of the sites identified in the RRMS cohort (cg10568066) was also identified in a recent study which investigated the role methylation of CpG sites and ageing (209). *RNF39* is a poorly characterized gene. In rats, *RNF39* encodes a protein that plays a role in the early phase of synaptic plasticity (210). In humans, SNP rs9393989 has been previously associated with MS (211). However, this SNP is located greater than

30kb upstream of the DMR in intron 3 so it is unlikely that it is contributing to the differential methylation signal.

RNF39 is also associated with other autoimmune conditions, such as Bechet's disease, a chronic relapsing inflammatory disease (212). This study found a SNP near *RNF39* associated with the disease, although the functional consequences of this are not yet unknown. In addition, hypermethylation of 11 CpGs sites within *RNF39* was seen in the naïve CD4+ T-cells of patients with SLE who had a history of discoid rash (213). Interestingly, 8 of these sites are the same sites we have identified in this study (cg10568066, cg12633154, cg13401893, cg10930308, cg03343571, cg13185413, cg09279736, cg00947782) and have similar Δ_{METH} values to our RRMS cohort ($mean_{RRMS}$ = 0.13; $mean_{SLE}$ = 0.16) (213). Future studies on RNF39 in MS should investigate differential gene expression within MS disease stages and then potentially explore the function of this gene within MS pathophysiology.

It is also interesting to note that although there is an overrepresentation of probes located within the MHC region in the top ranked probes in RRMS patients, this is not the case in SPMS patients. This may be reflective of the diminishing role of systemic inflammation in the progressive stages of disease (32). The largest DMR found in SPMS patients is also *RNF39*, but in SPMS patients this locus is hypomethylated rather than hypermethylated.

This is the first study to compare genome-wide differences in the methylation profiles of CD4+ T-cells of RRMS and SPMS patients. Our findings confirm our previous results at the MS risk locus *HLA-DRB1* but suggest that changes in methylation at this locus are specific to the early stages of disease. We also demonstrated dysregulation of methylation in a new MHC locus, *RNF39.* In RRMS patients we find this to be hypermethylated, but hypomethylated in SPMS patients. Taken together our results underline the fact that methylation is a dynamic process and highlight the importance of the MHC locus in MS.

CHAPTER FOUR – microRNA biogenesis, miR-29b, and DNA methylation

Interplay of microRNA biogenesis, miR-29b and DNA methylation in MS CD4+ T-cells

This chapter addresses my third and fourth research questions – Are microRNA biogenesis molecules differentially expressed in SPMS CD4+ T-cells, and does this have an effect on microRNA expression? And, is DNA methylation affected by changes in microRNA expression, specifically miRNA-29b?

Abstract

Background: The production of microRNAs (miRNA) involves processing by a number of molecules including the RNase III enzymes, Drosha and Dicer, plus Drosha's regulatory subunit, DGCR8. In secondary progressive multiple sclerosis (SPMS), miRNAs are broadly down-regulated in CD4+ T-cells. This study aims to determine whether changes in expression of miRNA biogenesis molecules could be contributing to the wide scale down-regulation of miRNAs in SPMS, whether this is the same in relapsing-remitting MS (RRMS), and if this may result in DNA hypermethylation by miRNA-mediated differential expression of DNA methyltransferases.

Methods: Total RNA was extracted from 22 RRMS and 21 SPMS patients and 22 and 21 healthy controls (HC) age and gender-matched to the RRMS and SPMS cohorts respectively. RT-qPCR was used to measure expression of *DROSHA, DGCR8, DICER* and Drosha's transcription factor, *C-MYC.*

Results: *DROSHA* and *DGCR8* were down-regulated in both RRMS and SPMS CD4+ T-cells. Down-regulation was greater in the SPMS cohort. There were no changes in expression of *DICER* or *C-MYC*.

Conclusions: The change in expression of miRNA biogenesis molecules correlates with the broad down-regulation of miRNAs in SPMS CD4+ T-cells including miR-29b.

This may facilitate increased expression of *DNMT3b*, resulting in previously reported hypermethylation in these cells. The impact in RRMS remains unclear.

Introduction

Multiple Sclerosis (MS) is a neuroinflammatory disease of the central nervous system (CNS) characterized by lymphocyte-mediated attack causing demyelination and axonal degeneration. The underlying cause of MS remains unclear, but risk of developing MS is influenced by a combination of genetic and environmental factors. Epigenetic mechanisms can impact gene expression without changes to the DNA sequences. Importantly, these differences can be modified by environmental factors. Epigenetics is emerging as an important concept in MS susceptibility and disease progression.

One epigenetic mechanism of regulation is microRNA (miRNA) mediated transcriptional silencing. miRNA are small non-coding RNAs that regulate gene expression by binding to the 3'untranslated region of mRNAs. Canonically (Figure 1.3), their production pathway commences in the cell nucleus, where miRNA genes are transcribed by RNA polymerase II, producing a primary miRNA (pri-miRNA) structure (107). The pri-miRNA is cleaved by Drosha, bound by its regulatory subunit DGCR8 (DiGeorge critical region 8), to stem-loop structure (pre-miRNA), approximately 60-70nt long (214). A 2nt overhang is produced by Drosha's RNase III activity and marks the pre-miRNA for export to the cytoplasm performed by Exportin 5 associated with Ran cofactor coupled to GTP. Once in the cytoplasm, Exportin 5 releases the pre-miRNA when GTP is replaced by GDP. Dicer (another RNase) then cleaves the pre-miRNA to produce a miRNA duplex approximately 22nt (108). The duplex then associates with Argonaute (Ago) proteins where it is unwound; one strain is retained as the mature miRNA and forms an RNA-induced silencing complex (RISC) and is then capable of mRNA regulation.

miRNA expression patterns in MS have been the focus of numerous studies in recent years (182) but few studies have focused on the molecules responsible for miRNA biogenesis: Drosha, DGCR8, and Dicer. Last year, Jafari et al. (114) found that these three molecules were up-regulated in RRMS patients' peripheral blood mononuclear cells compared to healthy controls. Furthermore, levels of *DICER* inversely correlate

with disability (expanded disability status scale, EDSS), and expression increases with treatment with interferon β, demonstrating a positive effect (lower EDSS) from treatment (115).

Previously, we have shown that 97% of dysregulated miRNA in SPMS CD4+ T-cells are down-regulated (202). In that study, miR-29b was significantly down-regulated in the SPMS samples. This miRNA targets the mRNAs of DNA methyltransferases; *DNMT3a* and *DNMT3b* directly, and *DNMT1* via *SP1* (215-217). DNA methyltransferases catalyse the addition of a methylation group to CpG dinucleotides. We, and others, have previously assessed the DNA methylation levels in CD4+ and CD8+ T-cells and CD19+ B-cells in relapsing-remitting MS patients (RRMS) and found the most significant changes in the methylation profiles of CD4+ T-cells (94, 98, 99, 101) (Graves et al, unpublished). In a follow-up study, we compared methylation in the CD4+ T-cells of RRMS and SPMS patients and found distinct differences between the two disease stages (Chapter Three). Most notably, we notice slight overall hypomethylation in RRMS patients (51%) but overall hypermethylation in SPMS patients (75%).

This study aims to determine whether down-regulation of miRNA biogenesis molecules in CD4+ T-cells is the underlying cause of miRNA down-regulation in SPMS, and compare this to RRMS. We also sought to determine if levels of DNA methyltransferase enzymes correlated with miRNA-29b levels, and if this may be the underlying cause of hypermethylation observed in Chapter Three.

Dysregulation of miRNA levels plays a key role in disease by causing altered cell growth and activity, apoptosis and irregular tissue differentiation (detailed review (218)). In MS, it is not clear whether miRNA dysregulation contributes to disease onset/progression or if it is a reflection of the affected cell's response to disease; it is likely both. Identifying the underlying cause of miRNA dysregulation will further our understanding of MS.

Patients and methods

Sample collection

Whole blood was collected at the John Hunter Hospital from 22 RRMS and 21 SPMS female patients, plus 22 healthy controls (HC) age and gender-matched to the RRMS cohort, and 21 HC matched to the SPMS cohort (Table 4.1). All patients were diagnosed with MS according to the McDonald criteria (183), and SPMS when they had demonstrated EDSS progression without evidence of relapse. The RRMS cohort was treatment naïve and the SPMS cohort was free of MS specific treatments for a minimum period of 6 months prior to collection. We also sought to determine if levels of DNA methyltransferase enzymes correlated with miRNA-29b levels.

Table 4.1: Details of RRMS and SPMS patients and their matched healthy control cohorts.

	RRMS	HC (RRMS matched)	SPMS	HC (SPMS matched
Number	22	22	21	21
Age in yrs (mean ±SD)	38.8 ±10.7	38.2 ±10.5	59.6 ±10.6	58.8 ±10.1
EDSS (mean ±SD)	2.4 ±1.4	NA	6.8 ±1.0	NA
Disease duration in yrs (mean ±SD)	5.2 ±6.1	NA	27.8 ±14.7	NA
Progression duration (mean ±SD)	NA	NA	9.4 ±4.6	NA

EDSS = expanded disability status scale, SD = standard deviation, NA = not applicable.

Ethics statement

The Hunter New England Health Research Ethics Committee, University of Newcastle Ethics committee and Bond University Human Research Ethics Committee approved this study (05/04/13.09, H-505-0607 and RO1382 respectively),

and methods were carried out in accordance with institutional guidelines on human subject experiments. Written and informed consent was obtained from all patient and control subjects.

Blood sample processing

PBMCs were isolated from 45mL of heparinised whole blood by density gradient centrifugation on lymphoprep (Axis-Shield PoC AS, Norway). CD4+ T-cells were enriched from the PBMCs using EasySep magnetic negative selection according to manufacturer's protocol (StemCell Technologies, Canada). The purity of the CD4+ selection was assessed by flow cytometry using a FITC conjugated anti-CD4 antibody (anti-human CD4 antibody, clone OTK4, FITC, catalogue# 60016FI, StemCell Technologies, Canada) on a BD FACSCanto II flow cytometer, then analysed using FACSDiva software (BD Biosciences, USA) at the Analytical Biomolecular Research Facility of the University of Newcastle. All samples met a minimum purity threshold of >90%.

RNA isolation

Total RNA was isolated from the CD4+ T-cells using the miRNeasy Mini kit (Qiagen, USA) following the manufacturer's instructions. The quality of the RNA was assessed using the RNA 6000 Nano kit on a 2100 Bioanalyzer (Agilent Technologies, USA); all samples had a minimum RNA integrity number (RIN) greater than 8. Purity was measured on an Epoch spectrophotometer (BioTek, USA) and concentration was measured using the high sensitivity RNA kit on Qubit 2.0 Fluorometer (Life Technologies, Thermo Fisher Scientific, USA).

RT-qPCR

500ng of total RNA was reverse transcribed using high-capacity cDNA reverse transcription kits (Applied Biosystems, Thermo Fisher Scientific, USA). Initially qPCR was performed using previously published primer sets (114) (Table 4.2) and SYBR green (KAPA SYBR FAST qPCR kit, KAPA Biosystems, USA). However, the DGCR8 primer set produced more than one product therefore an exon-spanning TaqMan

probe (ref: Hs00256062) was used intead. Exon-spanning TaqMan probes for *C-MYC* (ref: Hs00153408*) DNMT1* (ref: Hs0094875)*, DNMT3a* (ref: Hs01027166)*, DNMT3b* (ref: Hs00171876) and *SP1* (ref: Hs00916521) were also used. Expression of these genes was determined relative to the housekeeping genes *GAPDH* (ref: 4326317E) and β-actin (ref: 4326215E) using a ViiA 7 Real-Time PCR system (Applied Biosystems, Thermo Fisher Scientific, USA).

miR-29b RT-qPCR

10ng total RNA was reverse transcribed using the TaqMan MicroRNA Reverse Transcription Kit (Applied Biosystems, Thermo Fisher Scientific, USA). A mature miRNA TaqMan assay (Applied Biosystems, Thermo Fisher Scientific, USA) was used to determine expression of miR-29b (assay ID: 000413) with RNU44 (ref: 001094) as an endogenous control.

Table 4.2: Primers used by Jafari et al. (2015) for qPCR. The *DROSHA* and *DICER* primers were used in this study; *DGCR8* was excluded as it had multiple products.

Target	Sequence	Amplicon size (bp)
DROSHA F	5'-CATGTCACAGAATGTCGTTCCA-3'	115
DROSHA R	5'-GGGTGAAGCAGCCTCAGATTT-3'	115
DICER F	5'-TTAACCTTTTGGTGTTTGATGAGTGT-3'	94
DICER R	5'-GGACATGATGGACAATTTTCACA-3'	94
DGCR8 F	5'-GCAAGATGCACCCACAAAGA-3'	93
DGCR8 R	5'-TTGAGGACACGCTGCATGTAC-3'	93

bp = base pairs, F = forward primer, R = reverse primer.

Statistical analysis

The two-sample Kolmogorov-Smirnov test (K-S test) was used to test whether differences in relative expression was statistically significant between the RRMS and SPMS groups and the respective control groups.

Results

miRNA biogenesis machinery

We recruited 22 RRMS patients and 22 age matched controls and 21 SPMS patients and 21 age matched controls. Due to the substantial age difference between the two patient groups (see table 4.1), we assessed each patient subgroup to a separate control cohort to control for age effects. To determine if down-regulation of miRNA biogenesis machinery could be the cause of overall down regulation of miRNA in MS patients seen in our previous study (202) we measured the levels of the miRNA processing machinery (*DROSHA, DGCR8* and *DICER*). We initially performed RT-qPCR using previously published primers from Jafari *et al* 2015 and found that *DROSHA* was significantly down-regulated in RRMS and SPMS (figure 1 A-B) compared to HC (p_{RRMS}=0.010 and p_{SPMS}=0.018). There was no significant change in expression of either or *DGCR8* or *DICER* in either patient group (Dicer: p_{RRMS}=0.53; p_{SPMS}=0.20) (data not shown and figure 4.1). However, upon assessment of the PCR products, we found that the primers designed for *DGCR8* amplification resulted in two products 200 bp apart (data not shown). To determine if this was confounding the results, we used Taqman probes which span exon boundaries to *DGCR8*. Using this new primer/probe set, we found *DGCR8* to be significantly down-regulated in both patient groups (p_{RRMS}=0.028; p_{SPMS}=0.028) (figure 4.1 E-F).

miRNA-29b

We have previously reported down-regulation of miR-29b in SPMS CD4+ T-cells (202). To confirm these results in this cohort, we used RT-qPCR to assess changes in miR-29b (Figure 4.2). We find in this cohort that miR-29b is significantly downregulated in SPMS patients compared to controls (p=0.034), however, we do not observe any change in miR-29b expression in RRMS compared to controls (p=0.85).

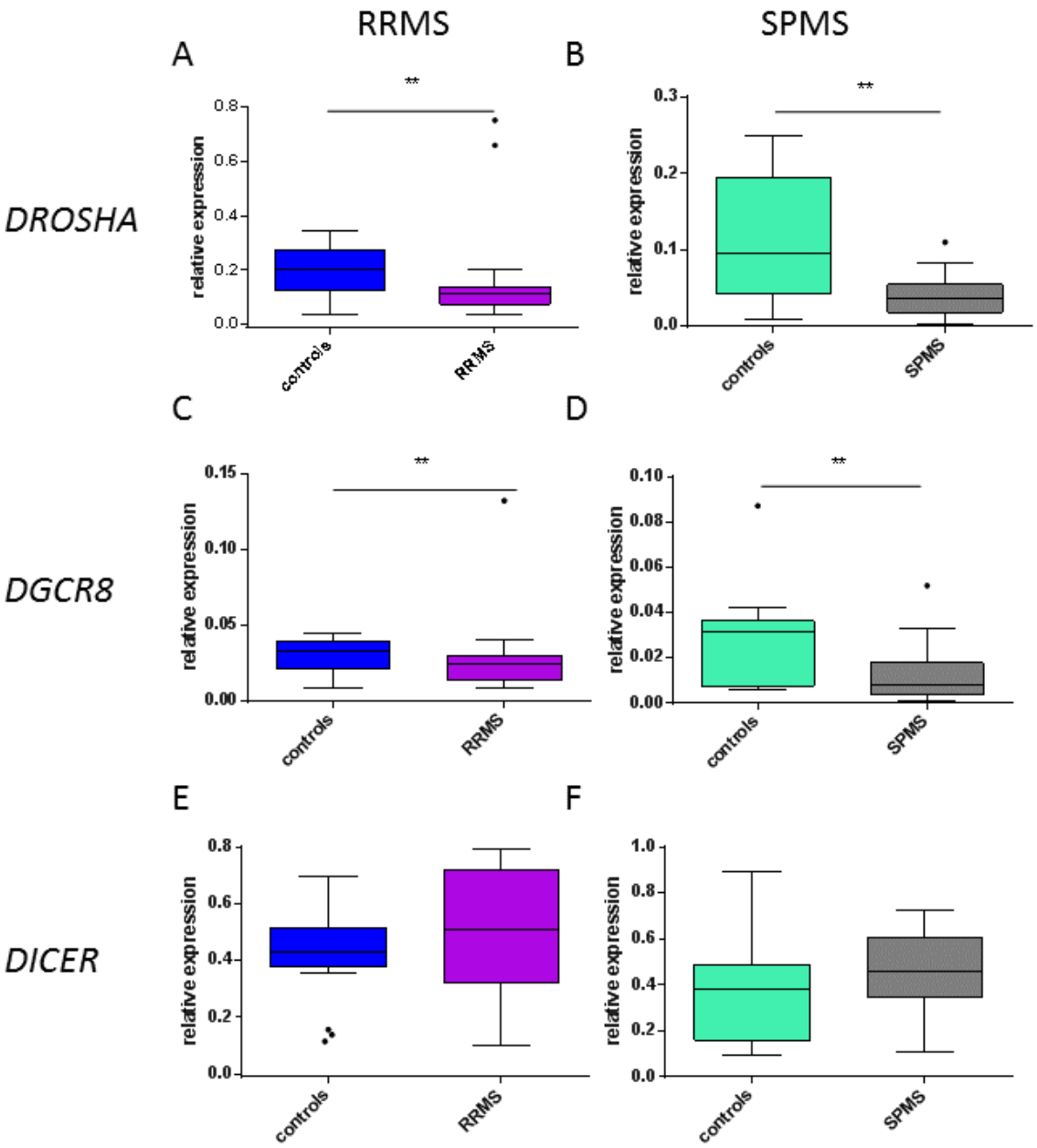

Figure 4.1: Tukey boxplots of expression relative to *GAPDH* of *DROSHA, DGCR8*, and *DICER* in HC (blue) compared to RRMS (pink) (A,C,E), and HC (green) compared to SPMS (grey) (B,D,F). Whiskers represent data within 1.5 interquartile range (IQR) of the upper and lower quartile. Data points outside of the 1.5 IQR are represented by black dots. ** $p<0.01$.

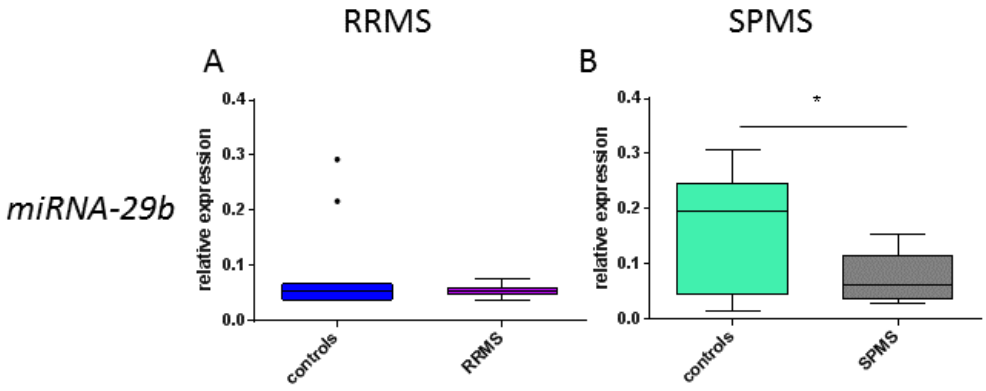

Figure 4.2: Tukey boxplot of miR-29b-3p expression relative to *RNU44* in (A) HC (blue) and RRMS (pink), and (B) HC (green) and SPMS (grey). Whiskers represent data within 1.5 IQR of the upper and lower quartile. Data points outside of the 1.5 IQR are represented by black dots. *$p<0.05$.

DNA methyltransferase enzymes

miR-29b has been shown to directly target *DNMT3a* and *DNMT3*b and indirectly target *DNMT1* in acute myeloid leukaemia and lung cancer (215, 216). The aberrant expression of miR-29b in these two cancers resulted in global changes in DNA methylation. To assess whether miR-29b could be responsible for the 75% hypomethylation we have previously seen in SPMS patients, but not RRMS, we investigated the relative expression levels of the three DNA methyltransferases *DNMT1*, *DNMT3a* and *DNMT3*b.

As shown in Figure 4.3, *DNMT1* is downregulated in RRMS patients compared to HC ($p=0.028$), but there is no change in SPMS patients ($p=0.18$). Previously published data demonstrated that *DNMT1* is targeted indirectly by miR-29b through the transcription factor *SP1 (216).* Therefore, we investigated the levels of *SP1* in both RRMS and SPMS patients. Consistent with the downregulation of *DNMT1* in RRMS patients, we find *SP1* to be significantly downregulated in RRMS patients compared to healthy controls ($p=0.028$). Interestingly, we also find significant downregulation of *SP1* in SPMS patients compared to healthy controls.

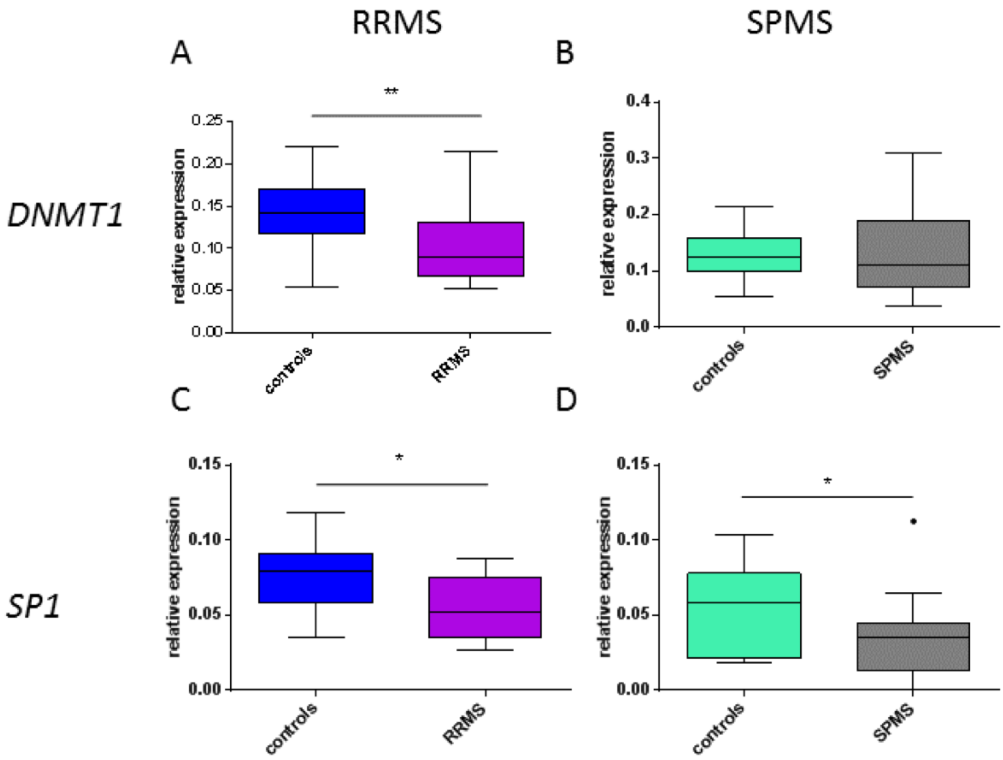

Figure 4.3: Tukey boxplot of expression relative to *GAPDH* of *DNMT1* in (A) HC (blue) and RRMS (pink), and (B) HC (green) and SPMS (grey); and *SP1* (C) HC (blue) and RRMS (pink), and (D) HC (green) and SPMS (grey). Whiskers represent data within 1.5 IQR of the upper and lower quartile. Data points outside of the 1.5 IQR are represented by black dots. *p<0.05, **p<0.01.

To investigate the expression of *DNMT3a* and *DNMT3b* (figure 4.4), we used RT-qPCR to assess levels of these transcripts. We find no change in *DNMT3a* in SPMS compared to their respective control groups (p=0.86) but a slight downregulation of *DNMT3a* in RRMS (p=0.03). There was no change in relative expression of *DNMT3b* in RRMS patients (p=0.79) but a significant upregulation of *DNMT3b* in SPMS patients (p=0.0024).

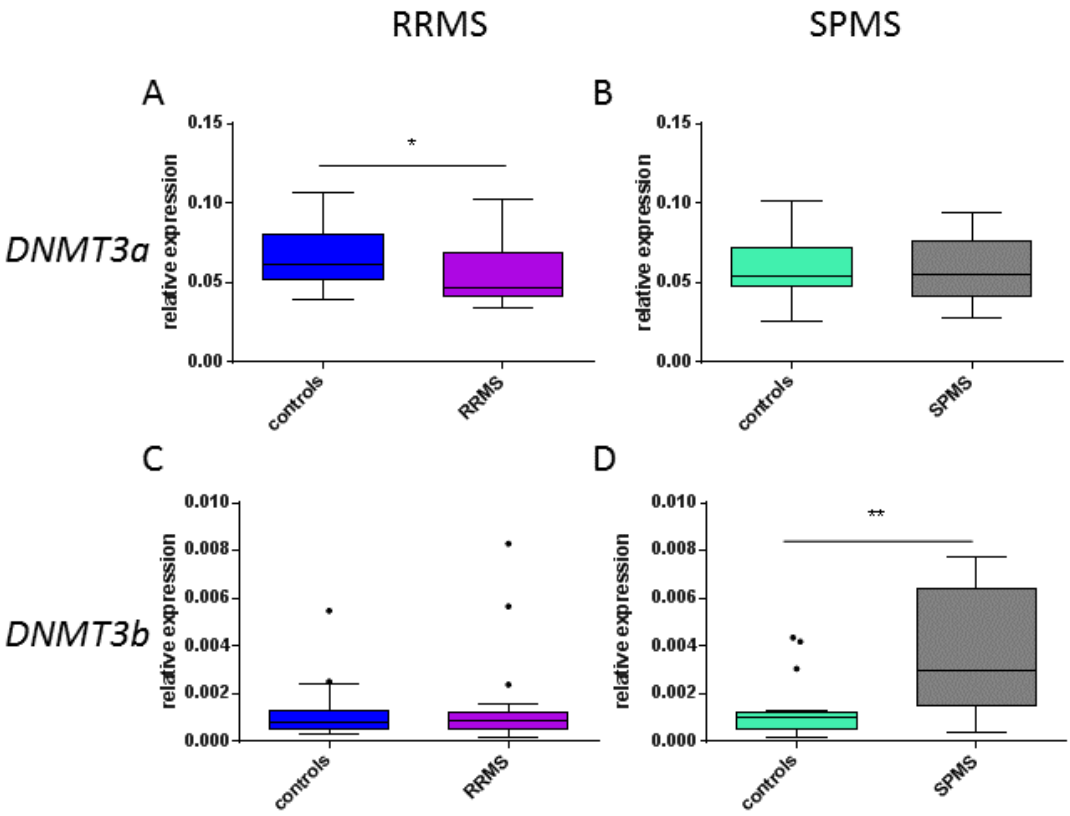

Figure 4.4: Tukey boxplot of *DNMT3a* expression relative to *GAPDH* in (A) HC (blue) and RRMS (pink), and (B) HC (green) and SPMS (grey); and *DNMT3b* (C) HC (blue) and RRMS (pink), and (D) HC (green) and SPMS (grey). Whiskers represent data within 1.5 IQR of the upper and lower quartile. Data points outside of the 1.5 IQR are represented by black dots. $^{**}p<0.01$.

Discussion

In this study, we characterized the expression of the miRNA biogenesis machinery and DNA methyltransferases in MS patients and healthy controls. Our data show that *DROSHA* and *DGCR8* are significantly down regulated in both RRMS and SPMS patients compared to healthy controls, but *DICER* is not affected. This is consistent with our published data on SPMS patients, where we demonstrated an overall decrease in miRNA expression. One of the most significantly down regulated miRNA in that study was miR-29b, which targets the DNA methyltransferases *DNMT1*, *DNMT3a* and *DNMT3b*. Consistent with this, we were able to show a subsequent increase in *DNMT3b* expression in SPMS patients. This is the first study

to compare the levels of miRNA biogenesis machinery in different disease states of MS.

A recent study by Jafari and colleagues evaluated the expression miRNA biogenesis machinery and found *DROSHA, DICER* and *DGCR8* all to be upregulated in RRMS patients (114). We initially used the primers from this study in our study, however, we found that the *DGCR8* primers were sub-optimal; therefore, we chose to use TaqMan probes. Additionally, Jafari et al. used *RPL38* as a housekeeping gene, as opposed to our study, which used *GAPDH* or *β-actin*. *RPL38* expression is decreased in some MS patients and is therefore an unreliable housekeeping gene (219). Finally, we used CD4+ T-cells in our study compared to PBMCs which were used in the Jafari study. It is possible that the miRNA biogenesis machinery is significantly upregulated in one of the other cell types compared to CD4+ T-cells, which would mask the subtle differences we find in our study. In fact, a study of $CD19^{+}$ B-cells in MS patients demonstrated that *DICER* transcript and protein levels are decreased in patients compared to controls (181). This correlated with increased expression of the co-stimulatory molecules CD80 and CD86 (181).

The initial stage in post-transcriptional processing, is pri-miRNA cleavage by Drosha, bound by its regulatory subunit DGCR8, (called the microprocessor complex) to the stem-loop structure (pre-miRNA) (214). Consistent with this, we see decrease of both of these transcripts in both disease stages. After export to the cytoplasm the RNase, Dicer, cleaves the pre-miRNA to produce the mature miRNA duplex approximately 22nt (108). We did not find any change in *DICER* in either disease stage, however, there are several factors that contribute to *DICER* expression (220), so it is likely regulated in a different manner than *DROSHA* and *DGCR8*.

Based on our findings, we propose that in SPMS patients, decreased biogenesis molecules (specifically the microprocessor complex) results in a global decrease in miRNA, including miR-29b, resulting in increased *DNMT3b*, and overall hypermethylation in SPMS patients (Figure 4.5). At this time, we can only speculate as to how this process starts, however, the transcription factor c-myc is known to modulate miRNA processing via regulation of Drosha (221). Additionally, *C-MYC* expression was affected in a squamous cell carcinoma cell line by vitamin D exposure (205), a known environmental risk factor of MS (52). We investigated *C-MYC* in our patient groups, but found no significant changes in expression (Appendix

4). It is possible that other undetermined factors, such as DNA methylation, may affect *DROSHA* and *DGCR8*.

In RRMS patients, the results are less clear. While *DROSHA* and *DGCR8* expression are both decreased in these patients, the levels of miR-29b are unchanged. *DNMT3a* and *DNMT3b* remain unchanged but levels of *DNMT1* and its transcription factor, *SP1,* decrease. While this may explain the slight decrease in global methylation we have seen in RRMS patients, it suggests that the DNA methyltransferase enzymes are regulated by mechanisms other than or in additional to miRNA.

This is the first study to investigate the levels of miRNA biogenesis machinery in the CD4+ T-cells of RRMS and SPMS patients. We propose a mechanism where the miRNA microprocessor complex (Drosha-DGCR8) is downregulated by an unknown mechanism. This potentially leads to a cascade of events, resulting in global hypermethylation in SPMS patients. Future studies should focus on elucidating the mechanism by which Drosha and DGCR8 are downregulated in progressive patients, and confirming differential expression at the protein level.

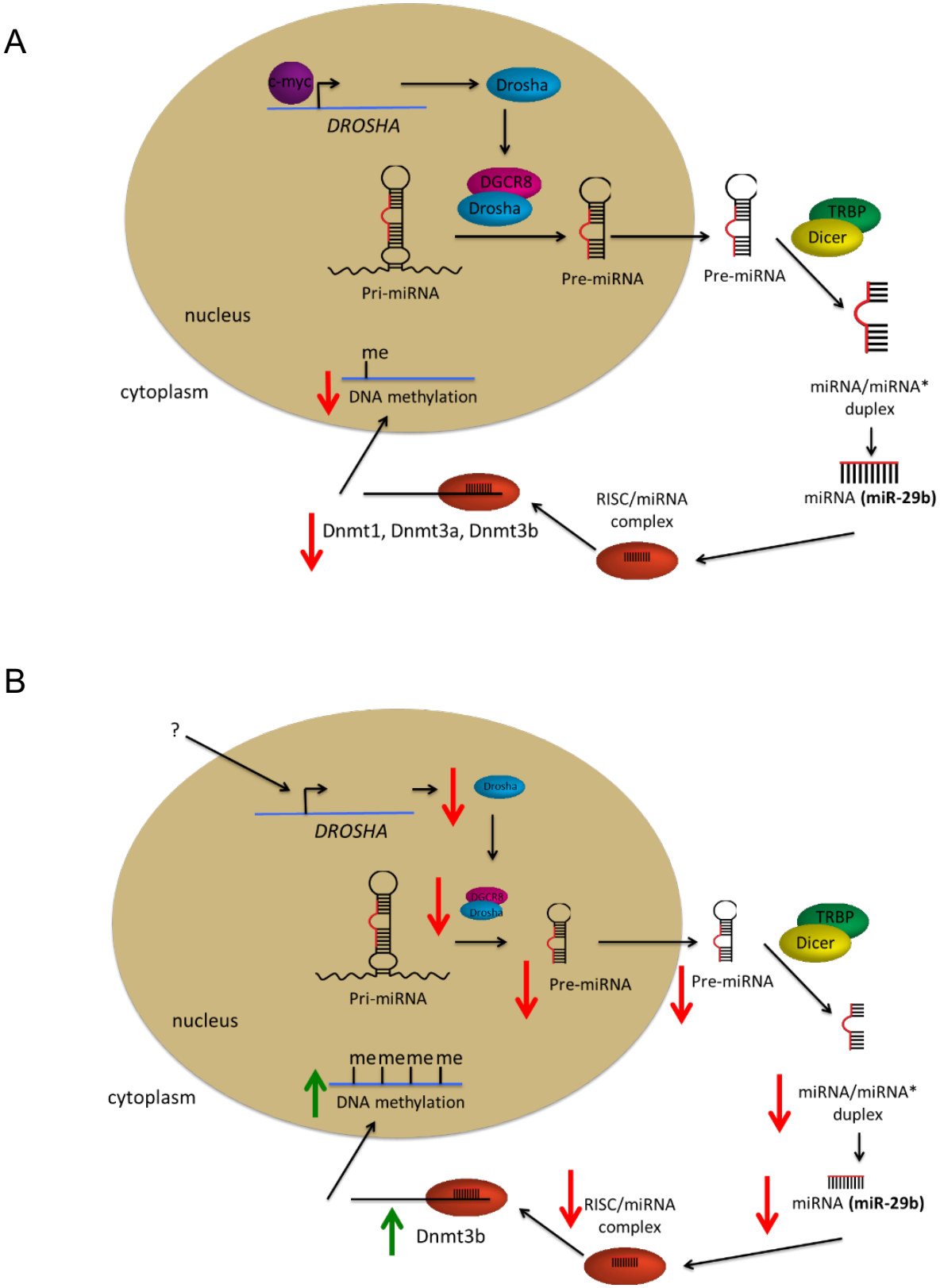

Figure 4.5: Schematic representation of miRNA biogenesis (specific to miR-29b) in (A) controls and (B) SPMS patients.

CHAPTER FIVE – microRNA expression profile of SPMS NAWM

microRNA expression profile of SPMS normal appearing white matter

This chapter addresses my fifth research question – is there differential microRNA expression in SPMS normal appearing white matter compared to controls, and how does this compare to microRNA expression patterns seen in CD4+ T-cells?

Abstract

Background: In MS, the normal appearing white matter (NAWM) is the site of pathology initiation. Previous studies have identified differences between NAWM in MS patients and control WM indicating NAWM is in an alerted, though immunosuppressed state. Previous studies have analysed miRNA expression in NAWM across MS disease subtypes; this is the first study to analyse miRNA expression in solely secondary progressive MS (SPMS) NAWM.

Methods: Using NanoString nCounter technology, the expression of 800 miRNAs was analysed in formalin-fixed, paraffin-embedded (FFPE) brain tissue samples (10 SPMS NAWM and 10 control white matter). Differential expression was confirmed using RT-qPCR with mature miRNA TaqMan probes in 13 SPMS and 10 control samples.

Results: Three miRNAs were confirmed to be down-regulated in SPMS NAWM compared to controls, miR-29b-3p, miR-219-5p and miR-451a. miR-29b-3p has also been confirmed down-regulated in SPMS CD4+ T-cells. There is no other overlap in miRNA dysregulation between NAWM and peripheral CD4+ T-cells.

Conclusions: These three miRNAs target genes in focal adhesion and adherens junction pathways, crucial to blood-brain barrier functioning. As well as playing a crucial role in oligodendrocyte maturation. Their dysregulation in NAWM likely contributes to priming the region for development of MS pathology.

Introduction

The normal appearing white matter (NAWM) in MS is the site where pathology initiates prior to development of symptomatic lesions. Light microscopic analysis shows its morphology is no different to healthy brains. However, diffusion tensor imaging (43) and molecular analyses, including gene expression (222) and DNA methylation (100) studies, demonstrate that there are differences that likely contribute to future development of lesions. In particular, Melief et al. (41) found that microglia in the NAWM region of the MS brain are in an alerted though immunosuppressed state.

The role of miRNAs in regulating gene expression makes them key molecules of interest in tissues associated with disease. The majority of studies on miRNA in the MS brain have focused on lesions, where differentially expressed miRNAs have been associated with phagocytosis promotion, Th17 differentiation, impaired neurosteroid synthesis and decreased memory performance (141, 143, 158, 162). Recently, a study on miRNA expression in periventricular NAWM was conducted (140), however the subtypes of MS from which the samples were derived are not disclosed.

As in previous chapters, samples from SPMS donors have been used here. This allows comparison of miRNA expression profiles with those of CD4+ T-cells of patients with the same disease subtype. The brain tissue samples used in this study are from archived banks, and some have been stored for up to 12 years. mRNA and DNA are susceptible to significant degradation over such a period of time, and amplification of gene transcripts is highly heterogeneous amongst samples (223). However, miRNA integrity is remarkably robust over many years of storage (224) and is comparable with frozen tissue for sensitivity, with only minor reductions in amplification (223). As such, this study focuses on results of miRNA expression only, and will hypothesise on the effects on gene expression using target prediction and pathway analysis software.

In this study, miRNA expression profiles of NAWM from SPMS patients are compared to controls. NanoString nCounter technology profiles the expression of 800 miRNAs using unique fluorescent-coded probes which can be counted in a sample using microscopy; thus removing the need to amplify the sample. Advantages of this methodology include highly accurate quantification of miRNA species and low total

RNA input (225); both essential features when working with valuable samples such as post-mortem FFPE brain tissue. The results of this investigation will reveal whether NAWM of SPMS patients differs in miRNA expression from normal control brain, and how this compares both to similar studies and CD4+ T-cells from the same MS subtype.

Materials and Methods

Samples

Post-mortem FFPE brain tissue sections were obtained from the UK Multiple Sclerosis Tissue Bank (MS and control samples) and the Multiple Sclerosis Research Australia brain bank (MS samples only). Each section was pre-cut by the respective tissue banks to a thickness of 5μm. The majority of MS samples came from SPMS donors, and control samples from individuals who passed from non-inflammatory and non-neurodegenerative illnesses. Due to the limited availability of tissues, the sample characteristics (table 5.1) are quite varied between SPMS and control samples. Among the control samples, the gender ratio was 1:4 female to male, which is not representative of MS epidemiology (1). Furthermore, we received three primary progressive MS (PPMS) samples; these were included in the experiments, however all analysis presented here is from SPMS samples only. Any cases where significance was rescinded by addition of the PPMS samples is noted.

Ethics Statement

Prior to death, patients gave their consent for using their brain tissues for research purposes according to local ethical guidelines. MS was diagnosed according to the McDonald criteria (183). Cases were excluded if the post-mortem interval exceeded 48 hours, and if gender and type of MS was unknown. Ethics approval was also obtained from Hunter New England Health (HNE 09/04/15/5.13), the University of Newcastle, Australia (UoN H-2009-0365), and Bond University (RO1382).

Table 5.1: Details of the SPMS and control brain tissue samples.

	SPMS		Controls
	NanoString nCounter	**qPCR**	**nCounter & qPCR**
Number	10	13 (9 same as nCounter)	10
Age in years (mean ±SD)	63.0 ±9.4	63.2 ±7.8	74.1 ±16.5
Female	7	8	2
PMI in hours (mean ±SD)	18.2 ±6.8	22.1 ±17.3	20.0 ±14.1
Brain region	PFC (n=3), TEMP (n=5), other (n=2)	PFC (n=4), TEMP (n=5), other (n=4)	PFC (n=6), TEMP (n=2), other (n=2)

Abbreviations: PMI – post-mortem interval, SD – standard deviation, PFC – prefrontal cortex, TEMP – temporal lobe, other brain regions – parietal, superior frontal gyrus, Brodmann areas 9 and 11.

Histology

One section from each SPMS sample was stained with Luxol Fast Blue - Periodic Acid-Schiff (LFB-PAS). LFB is a myelin-specific stain, and PAS was used to identify myelin by-products. The protocol for LFB-PAS staining and the criteria for identifying pathological regions can be found in Appendix 5. In the LFB-PAS stained MS sections, 27 regions of NAWM, 74 chronic lesions, 58 remyelinated areas and 1 active lesion were identified. Due to the constraints of RNA yield outlined below, sample acquisition was limited to NAWM regions (figure 5.1 A-B), specifically samples with clearly defined NAWM with an area >25mm^2.

Trouble-shooting tissue dissection

Laser capture microdissection: miRNA extraction was attempted from areas of NAWM, chronic lesions and remyelinated areas. Due to the small size of these areas, laser capture microdissection (LCM) using a PALM MicroBeam (Carl Zeiss Microscopy) was utilised. LCM uses a navigated laser to dissect around an area of

tissue to be collected, and with a series of defocused ultraviolet (UV) laser bursts, catapults pieces of tissue into a microfuge tube cap containing 10µl of buffer. The surface tension of the buffer provides an adherent surface to collect the sample.

LCM is very time consuming, 1 sample per day. Furthermore, as it is a UV laser, long exposure to the radiation may degrade the miRNA as it is captured. Samples collected using purely LCM continually produced low RNA yields (<50ng).

Collection buffer: Two collection buffers were trialled with LCM to identify which captured the most material and was most compatible with miRNA extraction. Xylene (100%) and PKD buffer (Qiagen, USA) produced comparable RNA yields. PKD buffer was selected over xylene to streamline the collection process; PKD buffer is used in the first step of the miRNeasy FFPE tissue extraction kit (Qiagen, USA) protocol. In contrast, tissue collected with xylene must be extricated from the xylene using centrifugation and evaporation prior to RNA extraction.

miRNA extraction kits: Initially, total RNA was extracted using Qiagen's miRNeasy FFPE tissue kit, and RNA yields from LCM were very low. To determine if this low yield was a consequence of the extraction kit, six samples were extracted using Quick-RNA MiniPrep (Zymo Research, USA). No significant difference in RNA yield was detected between the extraction methods and thus experiments were continued with the Qiagen kits and its proprietary PKD buffer.

Region of collection: Areas of NAWM, chronic lesions and remyelinated lesions were collected with LCM, and RNA extracted. This was done to determine whether it was feasible to compare miRNAs in NAWM and pathological areas of the tissue sections. Areas of pathology yielded very low RNA quantities (<50ng). LFB-PAS staining shows few cells in chronic lesions, and remyelinated regions have reduced populations of oligodendrocytes compared to NAWM. This reduced cellularity in pathological regions is the likely cause of low RNA yields. Thus, NAWM remained the sole focus of this study.

To overcome these issues, the method of tissue dissection and RNA extraction was adjusted to that described below.

NAWM acquisition

Sections for RNA extraction were deparaffinised using sequential absolute ethanol and xylene washes. Areas of NAWM were delineated using navigated laser microdissection (PALM MicroBeam, Carl Zeiss Microscopy) (226) and the tissue areas removed (figure 5.1 C-D) using the MesoDissection system (AvanSci Bio, USA) or scalpel. PKD buffer (Qiagen, USA) from the RNA extraction kit was used as the lifting agent. 3-5 consecutive sections were pooled for RNA extraction. The number of sections used depended on the size of the NAWM area.

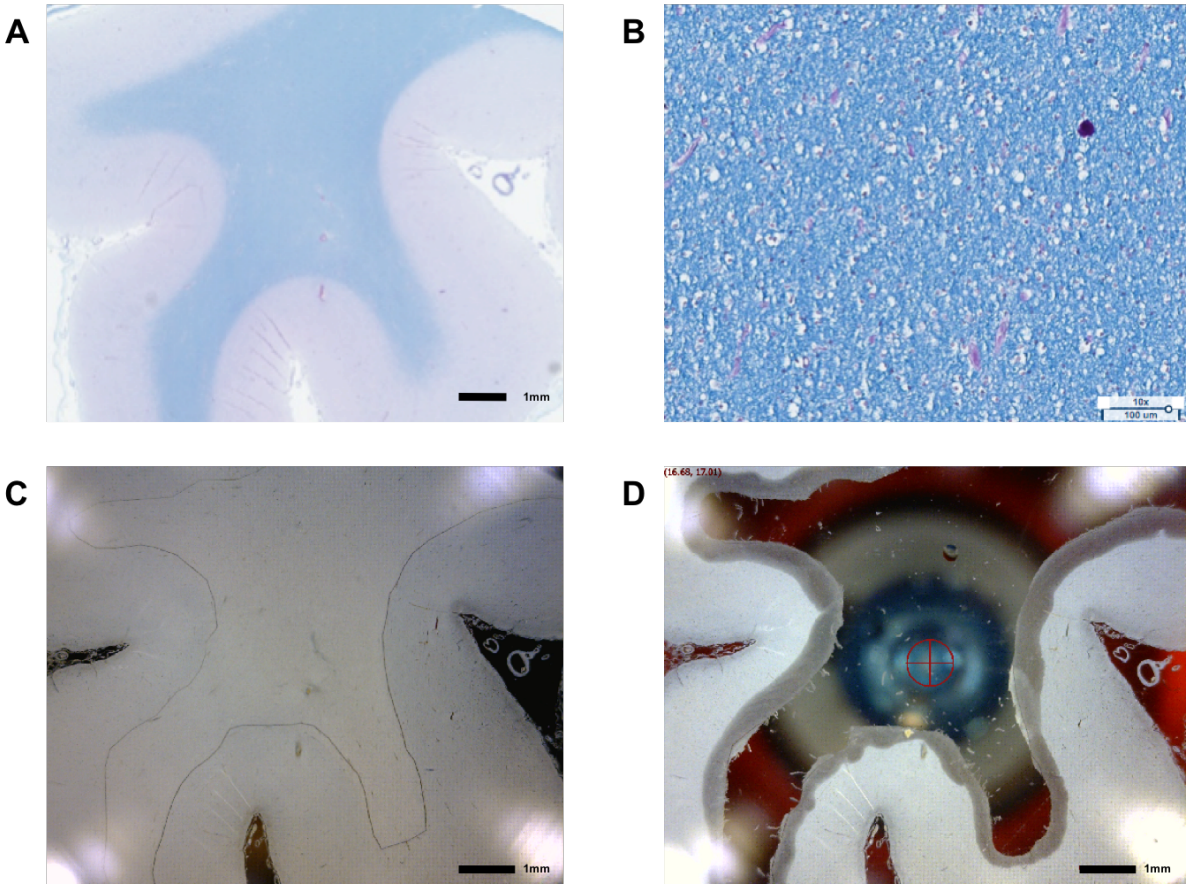

Figure 5.1: Images showing sample staining, characterisation and tissue extraction. (A) Macroscopic view of section stained with LFB-PAS. The NAWM can be easily identified by its consistent blue colour in the centre of the slide. It is surrounded by purple-stained grey matter. (B) 200x magnification of NAWM in the same section. The myelin is consistent and densely packed; the defining feature of NAWM. (C) Unstained, consecutive section. The NAWM outline has been scored using laser microdissection. (D) The same section following NAWM sample removal using the MesoDissection system.

RNA extraction and concentration

MicroRNA was extracted from the tissue using miRNeasy FFPE tissue extraction kit (Qiagen, USA). The concentration and purity of the extracted RNA was measured on a Qubit 2.0 Fluorometer (Life Technologies, USA) and an Epoch Micro-Volume Spectrophotometer System (BioTek, USA) respectively. A value of >1.8 on the optical density 260/280 ratio was considered suitable purity for downstream gene expression experiments (227). Further quality control (QC) of the RNA's integrity would normally be tested on a Bioanalyzer (Agilent, USA), however determination of the RNA integrity number depends on 18S and 28S ribosomal RNA subunit ratio which is not indicative of miRNA quality, thus Bioanalyzer QC was not deemed appropriate for these samples and down-stream experiments.

Total RNA for downstream nCounter (NanoString, USA) analysis was concentrated to 33ng/µl using RNAstable tube kit (Biomatrica, USA) and vacuum centrifugation at ambient temperature.

NanoString nCounter

The expression of 800 miRNAs was analysed using nCounter Human v2 miRNA expression assay (NanoString, USA) following manufacturer's guidelines. Briefly, 100ng of purified total RNA was added to the sample preparation reaction in 3µl. miRNAs were annealed to a bridging code and ligated with a miRNA specific tag sequence. Un-ligated tags were removed with enzymatic purification. Samples were hybridised overnight at 65°C to probe pairs. These pairs include a capture probe with 3' biotin molecule for attachment to the nCounter cartridge, and a reporter probe comprising four fluorescent colours in six positions at its 5' end. The sequence of colours on the reporter probe allows the identity of specific miRNAs to be resolved during data collection.

After 24 hours, sample reactions were loaded onto the nCounter Prep Station for automated, post-hybridisation removal of excess probes and immobilisation to the cartridge. The cartridge was then loaded onto the Digital Analyzer where reporter probe counts were tabulated into a CSV file. All samples passed QC against six positive and six negative miRNA assay controls, and were normalised against the geometric mean of the top 100 miRNA counts.

The nCounter's limit of detection is ~10 copies/cell, and has a reproducibility rate greater than RT-qPCR (225, 228). Therefore, as with my NGS study in Chapter Two, selection criteria were established to determine which of the miRNAs the nCounter identified as differentially expressed, would be selected for confirmation with RT-qPCR. These criteria comprised: miRNA exhibits >1.8-fold difference between SPMS and control samples, >100 copies of the miRNA must have been detected in at least one of the sample cohorts, and a mature miRNA TaqMan probe (Applied Biosystems, USA) must be commercially available.

RT-qPCR

Differential expression of the seven miRNAs identified using the nCounter system were validated using RT-qPCR (224). 10ng of total RNA per miRNA target was reverse transcribed using TaqMan MicroRNA Reverse Transcription Kit (Applied Biosystems, Thermo Fisher Scientific, USA). Mature miRNA TaqMan assays were used to determine expression of hsa-let-7c (ref: 000379), hsa-miR-29b-3p (ref: 000413), hsa-miR-219-5p (ref: 000522), hsa-miR-320e (ref: 243005), miR-451a (ref: 001141), hsa-miR-630 (ref: 001563), hsa-miR-664-3p (ref: 002897) with hsa-miR-26b (ref: 000407) as an endogenous control, using a ViiA 7 Real-Time PCR system (Applied Biosystems, Thermo Fisher Scientific, USA). RNU6B (ref: 001093) was considered as an alternative endogenous control, however it failed to amplify in some samples. This was likely because of its larger amplicon size compared to miR-26b (42bp vs. 21bp respectively) being inherently incompatible with the degraded nature of the FFPE samples.

Comparison with CD4+ T-cells of differentially expressed miRNA

The overall aim of this thesis is to compare the miRNA profiles of blood and brain tissue in MS patients. The miRNAs identified as significantly different in CD4+ T-cells were analysed in the MS NAWM tissue. However, due to substantial limitations on RNA quantity, a reduced number of samples were analysed. Mature miRNA TaqMan assays were used to determine expression of hsa-miR-21-5p (ref: 000397) (9 SPMS, 9 control), hsa-miR-142-3p (ref: 000464) (9 SPMS, 7 control) and hsa-miR-155-5p (ref: 002623) (3 SPMS, 3 control) with hsa-miR-26b as an endogenous control.

Statistical analysis

A *t*-test was initially performed on the nCounter data using NanoString's software, nSolver. However, due to the wide distribution of the data sets between SPMS and HC groups, a non-parametric, two-sample Kolmogorov-Smirnov test (K-S test) was used to compare cumulative distributions, and determine significant differences in expression of each miRNA for both nCounter and RT-qPCR data. Our statistical significance threshold allowing for multiple testing correction was determined using the FDR procedure of Benjamini-Hochberg (185). The significance threshold was set at $p<0.05$.

Gene target prediction and pathway analysis

miRSystem integrates seven different target gene prediction algorithms and contains experimentally validated data on miRNA:mRNA interactions (106). This integration system was used to identify genes that may be targeted by more than one of our identified dysregulated miRNAs.

miRPath v3 from DNA Intelligent Analysis (DIANA) (230) combines gene targets from TarBase v7 (231) to determine KEGG pathways that may be affected by miRNA expression changes. Using this software, pathways with targets of more than one of the key miRNAs were identified.

Results

NanoString nCounter

miRNA from the white matter of 10 SPMS and 10 control subjects was profiled using the NanoString nCounter system. Of the 800 miRNAs examined, 57 showed significantly different expression, and seven met the cut-off criteria (see methods section) to be further analysed with RT-qPCR. Let-7c ($p=0.003$), miR-320e ($p=0.003$), and miR-630 ($p=0.015$) were up-regulated in SPMS NAWM compared to controls, whereas miR-29b-3p ($p=0.05$), miR-219-5p ($p=0.015$), miR-451a ($p=0.003$) and miR-664-3p ($p=0.015$) are down-regulated in SPMS NAWM tissue (figure 5.2).

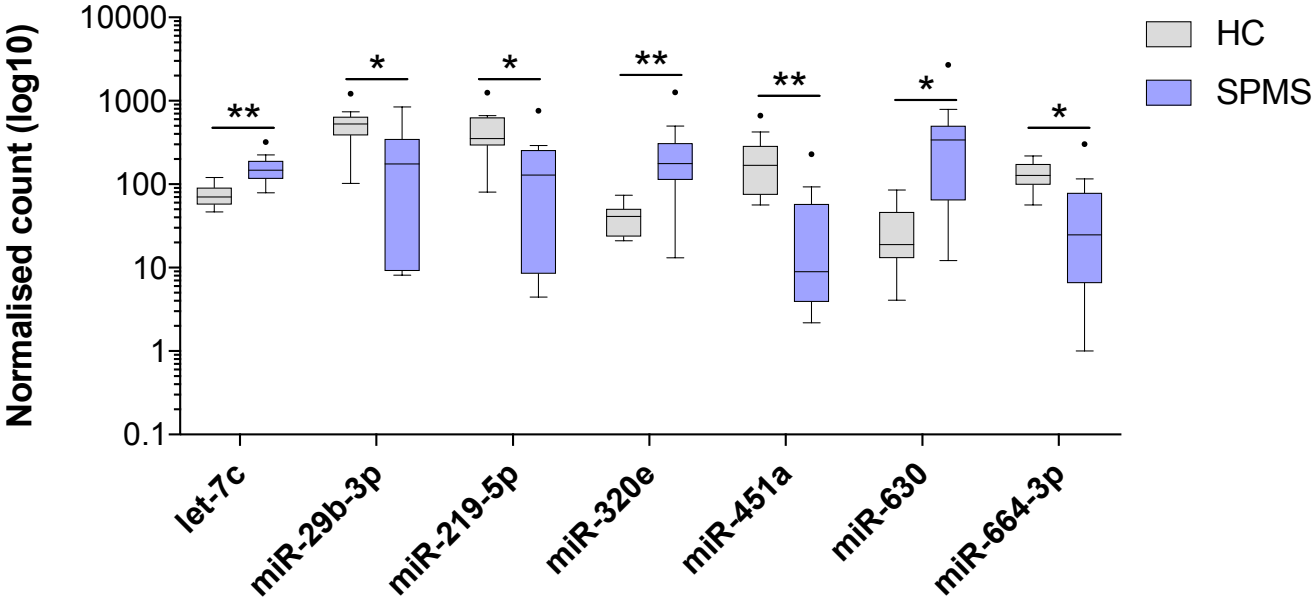

Figure 5.2: Tukey box plot of the top 7 differentially expressed miRNAs in SPMS NAWM identified using NanoString nCounter system. Whiskers represent data within 1.5 interquartile range (IQR) of the upper and lower quartile. Data points outside of the 1.5 IQR are represented by black dots. * p<0.05, ** p<0.01.

Despite miR-26b being differentially expressed in SPMS CD4+ T-cells (Chapter Two), it demonstrated consistent expression within SPMS and control white matter samples in the NanoString dataset (p=0.84) adding assurance to its use as an endogenous control for RT-qPCR.

RT-qPCR

The expression of the seven miRNAs identified using NanoString nCounter were re-analysed with RT-qPCR in the same 20 samples, plus a further three SPMS samples (10 control and 13 SPMS). All seven of the miRNAs demonstrated differences in expression in the same direction indicated by the nCounter data, however only three reached statistical significance (figure 5.3). miR-29b-3p (p=0.017), miR-219-5p (p=0.009) and miR-451a (p=0.002) were confirmed as down-regulated in SPMS NAWM compared to controls.

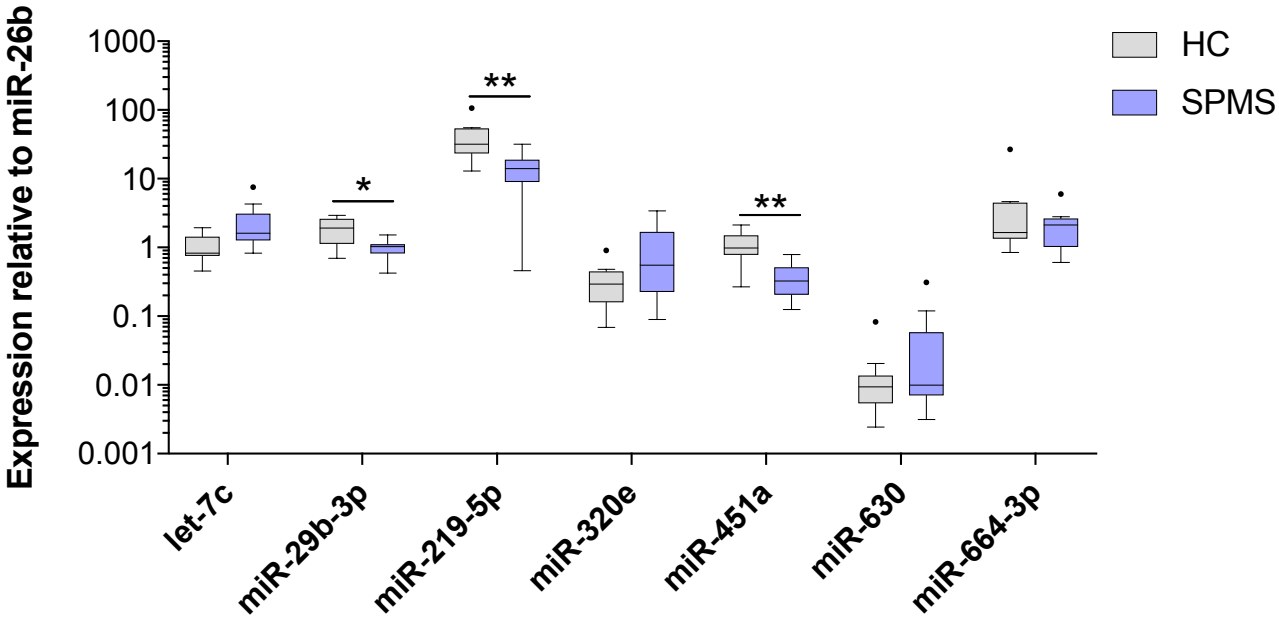

Figure 5.3: Tukey box plot demonstrating RT-qPCR data of the top 7 differentially expressed miRNAs in SPMS NAWM. miR-29b-3p, miR-219-5p and miR-451a were confirmed to be significantly down-regulated in SPMS NAWM compared to control white matter. Whiskers represent data within 1.5 IQR of the upper and lower quartile. Data points outside of the 1.5 IQR are represented by black dots. * p<0.05, ** p<0.01.

Gene targets and pathway analysis

miRSystem identified no common gene target of the three miRNAs confirmed with RT-qPCR, however 59 genes are targeted by combinations of two out of the three miRNAs. When looking at gene targets for all seven miRNAs identified by nCounter, Ataxin-1 (*ATXN1*) is targeted by four, however, the direction of change amongst these miRNAs is inconsistent (two up-regulated and two down-regulated, with similar fold-changes) indicating that collectively these miRNAs probably are not having an effect on expression of *ATXN1*.

KEGG pathway analysis using DIANA identified a number of pathways targeted by both miR-29b-3p and miR-451a (table 5.2). Many are related to cancer, however focal adhesion (both miRNAs target *AKT1* and *BCL2*) and adherens junction are particularly interesting due to their strong links with blood-brain barrier (BBB) function. No targets for miR-219-5p were identified with TarBase v7.

Table 5.2: KEGG pathways containing genes targeted by both miR-29b-3p and miR-451a. Significance threshold set at $p<0.0001$.

KEGG pathway	*p* value	No. of genes
Colorectal cancer (hsa05210)	2.702e-08	22
Viral carcinogenesis (hsa05203)	1.529e-07	32
Endometrial cancer (hsa05213)	5.116e-06	17
Amoebiasis (hsa05146)	6.517e-06	22
Hepatitis B (hsa05161)	5.293e-05	29
Focal adhesion (hsa04510)	8.590e-05	42
Adherens junction (hsa04520)	8.733e-05	15
Glioma (hsa05214)	8.733e-05	16
Pathways in cancer (hsa05200)	9.768e-05	60

Comparison with CD4+ T-cell miRNA

In Chapter Two, five miRNAs were confirmed to be dysregulated in the CD4+ T-cells of SPMS patients: miR-21-5p, miR-26b-5p miR-29b-3p, miR-142-3p and miR-155-5p. Of these five miRNAs, miR-29b-3p was the only one to be confirmed as down-regulated in both SPMS NAWM and CD4+ T-cells (Figures 2.2 and 4.3). In this study, miR-26b-5p has been selected as the endogenous control based on advice from TaqMan application notes (229). Interestingly, miR-155-5p failed to be detected by nCounter and RT-qPCR, and neither miR-21-5p (p=0.36) nor miR-142-3p (p=0.23) showed significant expression changes in SPMS NAWM (figure 5.4).

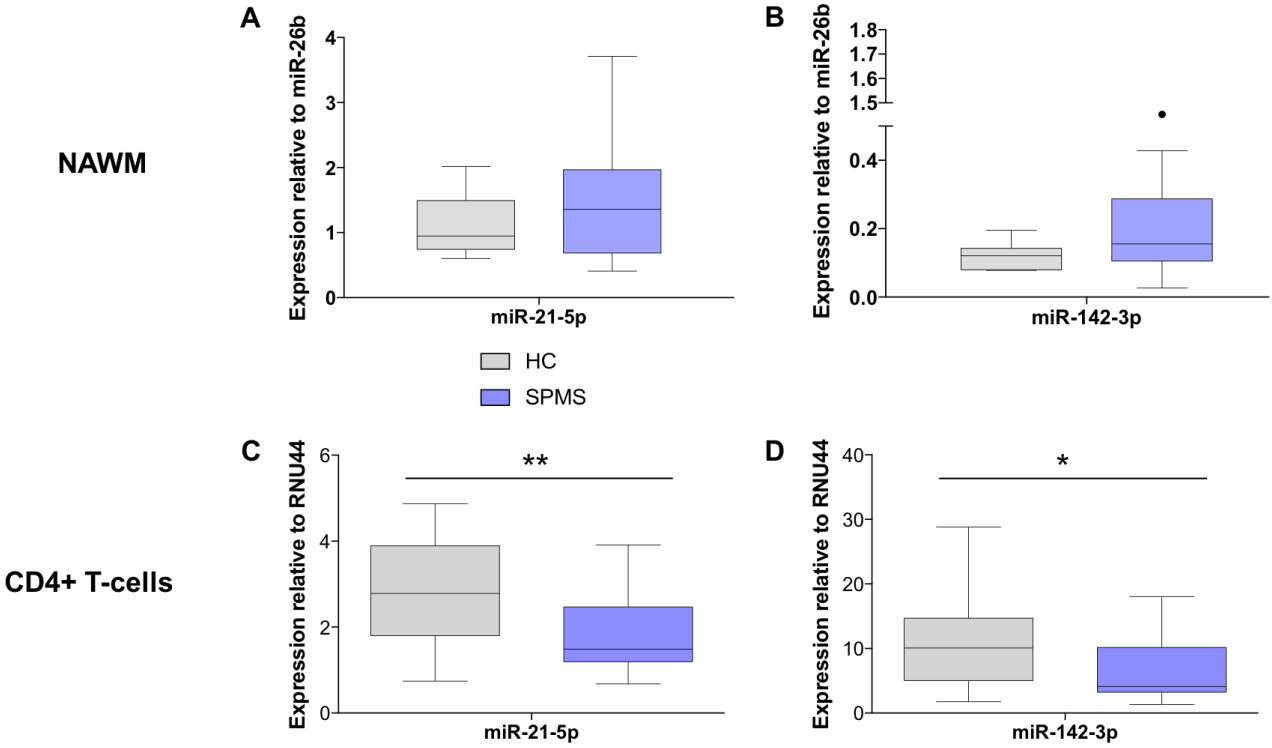

Figure 5.4: Comparison of miR-21-5p and miR-142-3p expression profiles in NAWM (A,B) and CD4+ T-cells (C,D) of SPMS individuals using RT-qPCR. Whiskers represent data within 1.5 IQR of the upper and lower quartile. Data points outside of the 1.5 IQR are represented by black dots. * $p<0.05$, ** $p<0.01$.

Discussion

Here we have performed a comprehensive analysis of miRNA expression in the NAWM of SPMS individuals using NanoString nCounter technology. Three miRNAs (miR-29b-3p, miR-219-5p and miR-451a) were found to be significantly down-regulated in SPMS samples compared to controls. Comparisons to other studies in NAWM, and possible implications of dysregulation of these miRNAs will be discussed here. However, studies on NAWM in the experimental autoimmune encephalomyelitis (EAE) model will not be discussed, as chemical induction of disease likely cannot provide an accurate representation of NAWM.

Two previous studies have profiled miRNA expression in MS NAWM. Guerau-de-Arellano (140) used NanoString nCounter to compare undefined-MS subtype, periventricular NAWM with half the number of control samples (n=5) that we have

used here. It is unclear whether their samples were fresh-frozen or FFPE, and how it was established that the regions analysed were pathology free. While there is no overlap in identified miRNAs with this study, another member of the mature miR-29 family (miR-29c) was significantly down-regulated in their MS samples, and miRSystem found miR-29b-3p and miR-29c-3p to have ~95% of their targets in common with each other. In Noorbakhsh et al.'s (158) study, they found up-regulation of miR-219-5p in MS NAWM; directly contradicting our finding of miR-219-5p down-regulation. However, both of these previous studies were limited by low sample numbers and using undefined MS samples. Without knowing more details about the types of samples used, it is unreasonable to directly compare our findings.

miR-29b-3p and its role in methylation has been previously established in CD4+ T-cells in Chapter Three and by Qin et al. (193). Here, it is down-regulated in SPMS NAWM, just as we have seen in SPMS CD4+ T-cells. If miR-29b's effect on methylation is replicated in the brain as we saw in CD4+ T-cells, it can be expected that differentially methylated regions in NAWM will preferentially demonstrate hypermethylation. A recent study on methylation patterns in MS NAWM showed that of 539 DMRs, 59% were hypermethylated (100), indicating that miR-29b may be affecting methylation in NAWM, but not to the extent that it does in CD4+ T-cells.

Previously, miR-451a was identified as differentially expressed in SPMS CD4+ T-cells, though this could not be confirmed with RT-qPCR (Appendix 2). Here, common target and pathway analysis identified two genes in the focal adhesion pathway targeted by both miR-451a and miR-29b-3p. These were serine/threonine kinase (*AKT1*), a mediator of neuronal survival via oligodendrocytes (232), and apoptosis regulator BCL2 (*BCL2*). 15 genes in the adherens junction pathway are also targeted by either miR-29b-3p or miR-451a. Proper functioning of both of these pathways is essential to normal BBB function, and disruption of protein expression in these pathways has been linked to BBB disruption in MS (157, 233). miRNA-mediated changes may be affecting the efficacy of these pathways in NAWM, either priming the region for macrophage infiltration, or mounting a defence against autoimmune attack. Without miRNA interaction and gene expression studies however, we are unable to hypothesise which of these scenarios may be reality.

The role of miR-219-5p in oligodendrocyte differentiation and precursor cell (OPC) maturation is particularly interesting. miR-219 is enriched in normal white matter,

particularly in oligodendrocytes (234). A study on topographical cues and gene silencing with miRNAs, found that electrospun microfibres incorporated with miR-219 were effective in driving OPC differentiation and oligodendrocyte maturation, and then remyelination (235). In this study, we identified down-regulation of miR-219-5p in SPMS NAWM, indicating a diminished influence on oligodendrocyte remyelination activity. This is supported by Juncker et al.'s (141) study which found miR-219-5p down-regulated in inactive MS lesions compared to normal brain. It would appear that regions of the MS brain with inactive disease (NAWM and inactive lesions) have reduced miR-219-5p expression, which in turn reduces oligodendrocyte presence or activity, ultimately perpetuating pathology.

Of the miRNAs dysregulated in this study only one, miR-29b-3p, has overlapping results with SPMS CD4+ T-cells. Both miR-21-5p and miR-142-3p were analysed to determine if they too were down-regulated in NAWM, however we find that they show a trend of up-regulation, though not significantly. A limitation of this study was the small quantity of RNA available for RT-qPCR, and the sample number for these miRNAs was reduced. This may have resulted in lost significance, however as these miRNAs were up-regulated in NAWM, it is unlikely that a few more samples would have changed the expression pattern to that seen in CD4+ T-cells.

Another limitation was the absence of miR-155-5p expression data. In many studies, miR-155-5p has been of key interest and is up-regulated in MS samples. Its expression appears to be highest in active lesions and reduces through chronic lesions and NAWM to a baseline low in control white matter (141, 157, 158). Using both NanoString nCounter and RT-qPCR, miR-155-5p was undetected in our samples. The reason for this is unknown; it may be that it is not present in these samples, our samples may reflect severely "burned out" MS, or that both methods *independently* failed to amplify it.

This is the first study to profile miRNA expression in SPMS NAWM. Three miRNAs were identified to be down-regulated compared to control white matter. These miRNAs play crucial roles in maintaining BBB integrity, oligodendrocyte function and methylation. Future studies will work on identifying the specific cell types in which this dysregulation occurs using *in situ* hybridisation to further our understanding of the impact this dysregulation has in the SPMS brain.

Acknowledgements

This study was funded by Multiple Sclerosis Research Australia (MSRA) and the John Hunter Hospital Charitable trust. KA Sanders was supported by a postgraduate scholarship from the MSRA and Trish MS Research Foundation. Samples were gratefully received from the UK Multiple Sclerosis Tissue Bank and MSRA Brain Bank. This study would not have been possible without the assistance of Associate Professor Michael Barnett and his colleagues, Dr Linda Ly and Dr Twishi Gulati at the Brain and Mind Research Institute, University of Sydney. Their help and training in analysing pathology in the MS brain sections was essential for correct identification of NAWM regions for RNA extraction. Ms Rebecca Seeto, with the aid of a MSRA vacation scholarship, assisted with histological staining and hands-on bench work. Dr Moira Graves was responsible for sample acquisition from the UK and preliminary H&E staining of slides.

CHAPTER SIX – DISCUSSION

This project has explored microRNA (miRNA) expression and the cause of dysregulation in CD4+ T-cells of secondary progressive (SPMS) patients, and used this information to guide an exploratory miRNA-profiling study in the normal appearing white matter (NAWM) of SPMS brain tissue donors.

miRNA expression in CD4+ T-cells

A key initial finding that inspired following chapters was the observation of broad down-regulation of miRNAs in CD4+ T-cells of SPMS patients. The literature review of miRNA dysregulation in MS (Chapter One), demonstrated the dynamic up- and down-regulation of miRNAs seen in MS-associated tissues. The study in Chapter Two bucked that trend, and showed that 97% of all miRNAs that demonstrated dysregulation were under-expressed compared to controls (202). NGS was used for initial expression profiling, which has the advantage over other methodologies in that all miRNAs present in a sample are identified, as such, the statement of “broad down-regulation” is valid. However, the cause of this down-regulation had to be established, and changes in DNA methylation and expression of miRNA biogenesis molecules was explored.

While DNA methylation was predominantly hypermethylated in SPMS CD4+ T-cells compared to controls, none of the differentially methylated CpGs were within miRNA transcription start sites (TSS). Therefore, it is unlikely that this is the underlying cause for miRNA down-regulation in SPMS. However, following the lead of Jafari et al. (114), expression of miRNA biogenesis molecules was analysed, and significant down-regulation of *DROSHA* and *DGCR8*, the nuclear molecules responsible for cleaving the pri-miRNA structure from the pre-miRNA, was found. In the absence of this RNase and its cofactor, miRNAs cannot be manufactured; the down-regulation these two molecules is thus a significant contributor to broad miRNA down-regulation seen in SPMS CD4+ T-cells. The instigator of *DROSHA* and *DGCR8* down-regulation however remains unclear; there were no differentially methylated regions

near their TSSs, and so a mechanism other than methylation must be affecting their expression.

One hypothesis for this was that an external factor, such as vitamin D, might target *C-MYC,* the transcription factor of *DROSHA*, resulting in a decrease in *DROSHA*'s expression. This theory was attractive because of the strong relationship between *C-MYC* expression and vitamin D (205), a well-studied environmental MS risk factor (52). *C-MYC*'s expression in SPMS was found to be stable (appendix 4), however without measuring vitamin D serum levels of study participants, it cannot be concluded that *C-MYC* is causing down-regulation of *DROSHA* or if there is another cause independent of its transcription factor. This warrants further investigation.

Methylation and miRNAs

While DNA methylation changes aren't in miRNA TSSs and have thus been ruled out as the cause for miRNA down-regulation here, there was still a very interesting finding; RRMS and SPMS DNA methylation profiles in CD4+ T-cells are distinct. RRMS CD4+ T-cells demonstrated nearly equal proportions of hypo- and hypermethylation (51% and 49% respectively). In contrast, SPMS strongly geared towards hypermethylation; 75% of differentially methylated CpGs were hypermethylated compared to age and gender matched controls.

In a study of DNA methylation in SLE CD4+ T-cells, over-expression of miR-29b was found to cause hypomethylation (193). miR-29b directly targets the 3' UTR of *DNMT3a* and *DNMT3b*, DNA methyltransferases responsible for producing *de novo* methylation sites. In Chapter Two, miR-29b is found to be significantly down-regulated in CD4+ T-cells. To determine its possible effect on DNA methylation, the expression of miR-29b and the DNMTs were analysed in a female-only cohort (Chapter Four) with significant sample crossover with the DNA methylation SPMS cohort (Chapter Three). miR-29b was re-confirmed to be down-regulated in SPMS CD4+ T-cells, and associated up-regulation of *DNMT3b* was observed.

A chain of events leading to DNA hypermethylation in SPMS CD4+ T-cells thus presents itself. miRNA biogenesis molecules, *DROSHA* and *DGCR8* are down-regulated (mechanism unknown), causing broad down-regulation of miRNAs. One of

these miRNAs (miR-29b) is significantly reduced, and its target (*DNMT3b*) becomes over-expressed. This leads to *de novo* methylation, ultimately manifesting as DNA hypermethylation in these cells. A result of this would be transcriptional silencing, reducing the activity of CD4+ T-cells in SPMS.

Reduced CD4+ T-cell activity

The role of the immune system in SPMS is poorly understood, though it is predominantly thought that this disease stage is driven by neurodegeneration, rather than inflammation. The findings presented within this thesis support that postulation by demonstrating a series of changes within CD4+ T-cells that hinder their activity. Eight of the ten most dysregulated miRNAs identified using NGS have a common target, suppressor of cytokine signalling 6 (*SOCS6*). The expression of *SOCS6* is negatively correlated to the expression of these miRNAs, i.e. *SOCS6* is up-regulated in SPMS CD4+T-cells (Chapter Two). *SOCS6* is a negatively regulator of T cell activation (187); thus, its up-regulation seen here indicates that it will act to prevent T cell activation, reducing immune system activity in SPMS.

Another consequence of broad miRNA down-regulation was the reduction in miR-29b leading to DNA hypermethylation and transcriptional silencing. The dominance of hypermethylated regions in SPMS compared to the inflammatory-driven RRMS disease stage, indicates that there is a genome-wide push towards reducing cell activity in SPMS.

Furthermore, one of the most highly expressed miRNAs in MS studies, miR-155, was down-regulated in these cells. miR-155 can be classed as an inflammatory miRNA as its expression may be activated by proinflammatory cytokines and it acts to disrupt the BBB (144). Also, its absence in EAE ameliorates disease (165). Its down-regulation in SPMS may have the effect of reducing its inflammatory activity with respect to the BBB and CD4+ T-cell disruption and migration across the barrier.

Each of these changes is a cause or consequence of disease progression. The effect of ageing can be excluded as a contributing factor in these changes as all parameters were compared to age- and gender-matched controls. Altogether, these factors limit the activity of CD4+ T-cells in the SPMS disease stage, and supports the

hypothesis that disability accumulation in SPMS is caused more by neurodegeneration than systemic inflammation.

NAWM in SPMS

Unlike SPMS CD4+ T-cells, the miRNA expression profiles of NAWM tissue exhibited both up- and down-regulation of miRNA. This analysis was performed using the NanoString nCounter system, a non-amplification based method of detecting expression nuances. Using RT-qPCR, three miRNAs were confirmed to be down-regulated in these SPMS NAWM samples compared to controls. The predicted role of these miRNAs includes maintenance of BBB integrity, and oligodendrocyte maturation and activity. Potential alterations to the activity of these pathways corroborates other works on miRNA in the CNS, specifically lesions and BECs (141, 157, 234), and demonstrates a common thread between classically disease-active tissues and NAWM, which is normal in appearance only.

Of the three dysregulated miRNAs, only one (miR-29b) overlapped with our findings in CD4+ T-cells. Methylation profiling of NAWM was not performed in this study, however previous works by Huynh et al. (100) found a moderate lean (59%) towards hypermethylated DMRs in NAWM tissue. This indicates that miR-29b might also be having an effect on methylation in NAWM, but it cannot be ascertained without performing simultaneous methylation and miR-29b expression profiling in a larger sample cohort.

Correlation of miRNA expression between CD4+ T-cells and NAWM in SPMS samples was investigated. Comparison of the three NAWM miRNAs (miR-29b, miR-219 and miR-451a) to CD4+ T-cell NGS data established significant down-regulation of miR-29b was common between both data sets, and was able to be corroborated with RT-qPCR in both instances. Further, NGS showed miR-451a was up-regulated in CD4+ T-cells; the only miRNA in these samples to demonstrate change in that direction. However, expression of this miRNA was very low (<45 copies/sample), and attempts to confirm this dysregulation with RT-qPCR failed; even demonstrating significant *down*-regulation in the replication cohort. The third candidate, miR-219, was stably expressed in CD4+ T-cells.

Using RT-qPCR, the other miRNAs dysregulated in CD4+ T-cells (Chapter One) were analysed in NAWM. miR-26b was stably expressed, and miR-21 and miR-142 demonstrated slight up-regulation, though this was not significant. miR-155-5p was not detected in NAWM by either NanoString nCounter or RT-qPCR indicating that this miRNA may be severely down-regulated/not expressed in these samples, however methodological or sample error cannot be excluded.

The common down-regulation of miR-29b in NAWM and CD4+ T-cells in SPMS is interesting and the cause remains unknown. Up-regulation of a specific miRNA in a tissue may be the result of unrelated cells over-expressing it, and then either apoptosing or releasing exosomes containing that miRNA into a circulating body fluid where they may present as over-expression in another tissue (236). However, down-regulation of miRNAs is not transmissible in this way, and cannot account for the decreased expression of miR-29b. It may also be coincidence that miR-29b is dysregulated in the same direction in these tissues.

Limitations and future directions

The priority of future investigation should be to establish causal relationships between *DROSHA, DGCR8,* microRNAs (both general and miR-29b), and *DNMT3b* within CD4+ T-cells. Following this, functional characterisation should be performed to determine the effect that these factors have on CD4+ T-cells and how that contributes to progressive MS; with the aim of exploiting these differences for therapeutic gain.

MiRNAs are regulators of gene expression though there are molecules that add a further level of regulation by regulating expression of miRNAs themselves. Circular miRNA sponges were reported in Nature in February 2013 (237) and the existence of numerous circular RNAs (circRNAs) has been demonstrated, including a circRNA sponge for miR-7 with over 70 binding sites for the single miRNA (237). This has obvious implications for the clarification of miRNA dysregulation. For miRNAs found to be under-expressed, miRNA expression may be normal but the expression of as-of-yet unidentified circRNAs is dysregulated. miRNA has a demonstrated impact on MS pathophysiology, and circRNAs may be a further confounding factor in understanding this disease. Unfortunately, due to the relatively recent observation of

circRNA sponges, it was not possible to detect their presence in the study samples, though this would be an exceptional addition to future miRNA-profiling projects. Indeed, if they can be incorporated into exosomes, then they could be cause for simultaneous down-regulation of miR-29b in NAWM and CD4+ T-cells observed here.

Considering Munoz-Culla's paper on sex-differences in miRNA expression in RRMS (164), it would be beneficial to repeat experiments from Chapters Two and Five in larger cohorts with female and male samples analysed separately. Their study highlighted the existence of a mirror pattern of miRNA expression in relapse and remission disease state, however only 80% of miRNAs dysregulated in a mixed-gender cohort were also confirmed in female-only analyses. Thus, differences in miRNA expression seen in CD4+ T-cells and NAWM here, may not be representative of male or female patients in isolation.

Differential gene expression data reported within this thesis was not established at the protein level, and therefore caution must be exercised when interpreting the functional consequences of differential gene expression within MS. A clear future research direction from this thesis' findings would be to investigate the protein expression levels of these same genes, and following confirmation/refutation of differences, proceed with functional studies.

The quantity and quality of RNA and DNA within our NAWM samples severely limited the molecular parameters that could be examined. Fragmentation of these molecules prevented profiling of large fragments including mRNA and DNA. Indeed, the short non-coding RNA RNU6B was unreliable as an endogenous control despite its short, 42bp length. Thus, miRNA expression profiling was the only metric measured in this study. However, the absence of gene expression examination does not greatly hinder the conclusions reached regarding affected pathways, as analysis of differentially expressed miRNAs has been found to be more informative than differentially expressed genes regarding the identification of affected pathways (238). This is because multiple miRNAs often target groups of genes within a pathway together, whereas analysis of gene expression is more likely to be confounded by genes exhibiting spurious or random dysregulation.

Future studies of miRNA in NAWM would benefit from including DNA methylation profiling to explore the relationship of miR-29b and differential methylation. Furthermore, as has been clearly demonstrated here and in other literature, the profile of individual cell subsets can be masked, and often contradicted, when observed amongst a heterogeneous cell population such as whole blood, or in this case NAWM. Unfortunately, in the samples used here, the quantity of material required to consider oligodendrocytes, astrocytes, etc. in isolation was not available. However, future studies should endeavour to isolate these cell types and profile them independently to provide a clearer picture of miRNA expression dynamics in the SPMS CNS.

Conclusion

This thesis demonstrates the convergence of several factors, led by changes in miRNA expression, to reduce activity of CD4+ T-cells in SPMS. Broad down-regulation of miRNAs was identified in these cells, a novel observation in MS miRNA studies, caused by decreased expression of miRNA biogenesis molecules. This resulted in: up-regulation of *SOCS6*, negatively regulating T cell activation; and *de novo* hypermethylation driven by miR-29b-associated up-regulation of *DNMT3b*. Each of these findings points towards CD4+ T-cells having a diminished role in SPMS disease activity, and therefore are less responsive to current approved therapies. Additionally, analysis of miRNA expression in NAWM further demonstrates that this tissue is only “normal” in its appearance, and dysregulated miRNAs here may act to prevent oligodendrocyte maturation and thus hinder remyelination efforts. This suggests that neurodegenerative mechanisms are fully operational in NAWM during SPMS. In conclusion, we are closer to understanding the mechanisms of disease progression in MS; miRNA down-regulation prompts CD4+ T-cells to take a backseat in this disease stage, and neurodegeneration assisted by miRNA dysregulation, is primed to occur in normal appearing brain tissue. Consequently, future research on treatments should move away from immunosuppression, and focus more on remyelination in this stage of disease.

APPENDIX ONE

The main text of Chapter Two was published in Clinical Epigenetics, in 2016 (DOI 10.1186/s13148-016-0253-y). Clinical Epigenetics is an open access journal and all articles are distributed under the terms of the Creative Commons Attribution 4.0 International License. (CC BY 4.0) This license permits unrestricted use, distribution and reproduction provided appropriate credit is attributed to authors. Full details of the licence can be found at http://creativecommons.org/licenses/by/4.0.

The following pages contain the published format of the article, Next-generation sequencing reveals broad down-regulation of microRNAs in secondary progressive multiple sclerosis CD4+ T-cells.

Sanders et al. Clinical Epigenetics (2016) 8:87
DOI 10.1186/s13148-016-0253-y

Clinical Epigenetics

RESEARCH Open Access

Next-generation sequencing reveals broad down-regulation of microRNAs in secondary progressive multiple sclerosis CD4+ T cells

Katherine A. Sanders[1,2,3], Miles C. Benton[4], Rod A. Lea[4,2], Vicki E. Maltby[2,3], Susan Agland[5], Nathan Griffin[2,3], Rodney J. Scott[2,3,6], Lotti Tajouri[1] and Jeannette Lechner-Scott[2,5,7*]

Abstract

Background: Immunoactivation is less evident in secondary progressive MS (SPMS) compared to relapsing-remitting disease. MicroRNA (miRNA) expression is integral to the regulation of gene expression; determining their impact on immune-related cell functions, especially CD4+ T cells, during disease progression will advance our understanding of MS pathophysiology. This study aimed to compare miRNA profiles of CD4+ T cells from SPMS patients to healthy controls (HC) using whole miRNA transcriptome next-generation sequencing (NGS). Total RNA was extracted from CD4 + T cells and miRNA expression patterns analyzed using Illumina-based small-RNA NGS in 12 SPMS and 12 HC samples. Results were validated in a further cohort of 12 SPMS and 10 HC by reverse transcription quantitative polymerase chain reaction (RT-qPCR).

Results: The ten most dysregulated miRNAs identified by NGS were selected for qPCR confirmation; five (miR-21-5p, miR-26b-5p, miR-29b-3p, miR-142-3p, and miR-155-5p) were confirmed to be down-regulated in SPMS ($p < 0.05$). *SOCS6* is targeted by eight of these ten miRNAs. Consistent with this, *SOCS6* expression is up-regulated in SPMS CD4+ T cells ($p < 0.05$). This is of particular interest as *SOCS6* has previously been shown to act as a negative regulator of T cell activation.

Conclusions: Ninety-seven percent of miRNA candidates identified by NGS were down-regulated in SPMS. The down-regulation of miRNAs and increased expression of *SOCS6* in SPMS CD4+ T cells may contribute to reduced immune system activity in progressive MS.

Keywords: Multiple sclerosis, Secondary progressive, MicroRNAs, Immunology, CD4+ T cells, Next-generation sequencing

Abbreviations: AD, Alzheimer's disease; AHSCT, Autologous hematopoietic stem cell transplant; CNS, Central nervous system; DNA, Deoxyribonucleic acid; EAE, Experimental autoimmune encephalitis; EDSS, Expanded disability status scale; FDR, False discovery rate; GA, Glatiramer acetate; HC, Healthy controls; K-S test, Kolmogorov-Smirnov test; miRNA, MicroRNA; MS, Multiple sclerosis; NGS, Next-generation sequencing; PBMC, Peripheral blood mononuclear cells; RNA, Ribonucleic acid; RRMS, Relapsing remitting MS; RT-qPCR, Reverse transcription quantitative polymerase chain reaction; SD, Standard deviation; *SOCS6*, Suppressor of cytokine signaling 6; SPMS, Secondary progressive MS

* Correspondence: Jeannette.lechner-scott@hnehealth.nsw.gov.au
[2]Centre for Information-Based Medicine, Hunter Medical Research Institute, Newcastle, New South Wales 2305, Australia
[5]Department of Neurology, Division of Medicine, John Hunter Hospital, Locked Bag 1, Hunter Region Mail Centre, Newcastle NSW 2310, Australia
Full list of author information is available at the end of the article

Background

Multiple sclerosis (MS) is an autoimmune disease characterized by multifocal inflammatory attacks in the CNS [1]. In the relapsing-remitting (RRMS) stage of the disease, CD4+ T cells are among the primary infiltrators moving from the periphery, through the blood-brain barrier, and into the CNS [2]. These cells then initiate an immune response that results in localized demyelination and corresponding symptoms. The later stage of MS, secondary progressive (SPMS), is characterized by compounding neurodegeneration and increasing disability; however, the relevance of inflammation is unclear [3]. As key regulators of gene expression, microRNAs (miRNAs) may be affecting the immune-related functions of CD4+ T cells in SPMS and may help to elucidate the actions of these cells in SPMS.

MiRNAs are short, non-coding RNA molecules (~22 bp) that regulate gene expression at the posttranscriptional stage by targeting the 3′ untranslated region of target genes. Their small size and stable structure make them ideal biomarkers. In recent years, miRNA expression patterns in MS have been the focus of numerous studies, many of which have concentrated on using miRNAs as biomarkers for diagnosis and prognosis [4]. These studies predominantly use easily acquired (and often highly heterogeneous) samples such as whole blood, peripheral blood mononuclear cells (PBMCs), serum, and plasma. Numerous dysregulated miRNAs have been identified, however which cell types are actually responsible for differing miRNA profiles, and the consequences of altered miRNA expression is not clear in many studies. Furthermore, it is likely that these heterogeneous samples are masking the signal of differentially expressed miRNA in specific cell subtypes. To overcome this, we have focused on CD4+ T cells in this study on SPMS.

Next-generation sequencing (NGS) allows for stringent examination of cell-specific miRNA expression profiles as well as discovery of previously uncharacterized miRNAs. Here, we have used small-RNA NGS analysis of CD4+ T cells from SPMS patients and healthy controls (HC). The total coverage approach of NGS generates expression information on all small RNA species including all known and novel miRNAs, as well as other small RNA species (isomiRs and snoRNAs)—a clear advantage over microarray and candidate approach assays. Three previous studies in MS have used NGS to effectively identify miRNA expression profiles in the whole blood [5, 6], serum [6], and PBMCs [7] from RRMS patients. However, NGS techniques have not been used for specific cell types or in SPMS samples.

The miRNA expression profile of CD4+ T cells, either as instigating molecules or by-products of erroneous molecular mechanisms, will provide insight into the function of these cells in SPMS. Here, we used NGS to provide a comprehensive analysis of the miRNA expression profiles of CD4+ T cells from SPMS patients and healthy controls (HC) and confirmed these results using targeted expression assays.

Methods

Sample collection

Whole blood was collected at a single study center from an initial cohort of 12 SPMS patients and 12 HC and a replication cohort of 12 SPMS and 10 HC. All patients were diagnosed with SPMS according to the McDonald criteria [8] and demonstrated EDSS progression without evidence of relapse in the 24 months prior to collection. Controls were age (±5 years) and gender matched (Table 1). The SPMS patient group was free of MS-specific treatments for a minimum period of 6 months prior to collection. Samples were collected at the John Hunter Hospital, and laboratory work was conducted at the Hunter Medical Research Institute, Newcastle.

Blood sample processing

PBMCs were isolated from 45 mL of heparinized whole blood by density gradient centrifugation on lymphoprep (Axis-Shield PoC AS, Norway). CD4+ T cells were enriched from the PBMCs using EasySep magnetic negative selection according to the manufacturer's protocol (StemCell Technologies, Canada). The purity of the CD4

Table 1 Details of SPMS and healthy control individuals

	Next generation sequencing		Replication cohort	
	SPMS	HC	SPMS	HC
Number	12	12	12	10
Female	9	9	8	5
Age in years (mean ± SD)	60.2 ± 8.3	61.3 ± 9.5	61.4.0 ± 6.5	60.1 ± 5.9
EDSS (mean ± SD)	6.9 ± 0.9	NA	5.9 ± 1.0	NA
Active SPMS	3	NA	4	NA
Disease duration in years (mean ± SD)	25.6 ± 11.1	NA	18.3 ± 6.5	NA
Progression duration (mean ± SD)	10.8 ± 8.1	NA	8.9 ± 6.2	NA

EDSS expanded disability status scale, *SD* standard deviation, *NA* not applicable

+ selection was assessed by flow cytometry using a FITC-conjugated anti-CD4 antibody (anti-human CD4 antibody, clone OTK4, FITC, catalog# 60016FI, StemCell Technologies, Canada) on a BD FACSCanto II flow cytometer and then analyzed using FACSDiva software (BD Biosciences, USA) at the Analytical Biomolecular Research Facility of the University of Newcastle. All samples met a minimum purity threshold of >90 %.

RNA isolation

Total RNA was isolated from the CD4+ T cells using the miRNeasy Mini kit (Qiagen, USA) following the manufacturer's instructions. The quality of the RNA was assessed using the RNA 6000 Nano kit on a 2100 Bioanalyzer (Agilent Technologies, USA); a RNA integrity number greater than 8 was deemed suitable for sequencing and reverse transcription quantitative polymerase chain reaction (RT-qPCR). Purity was measured on an Epoch spectrophotometer (BioTek, USA), and concentration was measured using the high-sensitivity RNA kit on Qubit 2.0 Fluorometer (Life Technologies, Thermo Fisher Scientific, USA).

miRNA sequencing and analysis

A cohort of 12 SPMS and 12 HC samples was run through NGS at the Diamantina Institute, University of Queensland, Brisbane, Australia. Samples were individually barcoded and then sequenced in two multiplexed pools each containing 12 samples. The sequencing libraries were prepared from 1-μg total RNA, using the TruSeq small RNA preparation kit (Illumina, USA) and sequenced using the 50-bp fragment protocol on the HiSeq 2500 platform. The sequencing generated four to nine million reads per sample, more than sufficient for expression and discovery applications. The sample sequencing reads were demultiplexed using the CASAVA 1.8 software package (Illumina, USA). The Illumina adapter sequences were trimmed from the fastq files using Trimmomatic [9]. All reads were aligned and counted against miRBase 21 [10].

RT-qPCR

Mature miRNA TaqMan assays (Applied Biosystems, Thermo Fisher Scientific, USA) were used to determine expression of the ten most differentially expressed miRNAs in the initial NGS cohort as well as a replication cohort of 12 SPMS and 10 HC (assay IDs in miRNA numerical order: 000397, 000399, 000407, 000408, 000409, 000413, 002223, 000464, 002623, 000524). The small RNA RNU44 (ref: 001094) was used as an endogenous control. RNU44 has previously been demonstrated to be a stable control in CD4+ T cells [11], and its stability has been shown in our 47 samples (mean ± standard deviation Ct value of 23.58 ± 0.63). RNU44 was used for normalization using the ΔCt method. The relative expression ($2^{-\Delta Ct}$) of all samples (24 SPMS and 22 HC) was calculated.

Statistical analysis

The two-sample Kolmogorov-Smirnov test (K-S test) was used to test whether differences in expression levels were statistically significant between the case and control groups as implemented in R. The K-S test was chosen (over the *F* test comparison of means) because of the non-normality of the expression level distributions among miRNAs. Our statistical significance threshold allowing for multiple testing correction was determined using the False Discovery Rate (FDR) procedure of Benjamini-Hochberg [12]. Based on the number of miRNA elements, this threshold was set at 1.2×10^{-4}. We also considered a relaxed (or nominal) significance threshold of 0.05. In addition to using statistical significance thresholds for miRNA selection, we also included a count threshold of >800 to exclude miRNAs that had very low expression levels and were unlikely to be replicated with the less-sensitive RT-qPCR. The K-S test was also used to determine significant differential miRNA and *SOCS6* expression from the RT-qPCR relative expression data.

Correlation to patient characteristics

The Pearson correlation coefficient was calculated using RT-qPCR data for MS samples ($n = 24$) and patient characteristics: EDSS, age, disease duration, and progression duration. A correlation coefficient (r value) >±0.5 was considered strong, ±0.3–0.49 moderate, and <±0.29 weak.

Gene target prediction

miRSystem integrates seven different target gene prediction algorithms and contains experimentally validated data on miRNA:mRNA interactions [13]. This integration system was used to identify genes that may be targeted by more than one of our identified dysregulated miRNAs.

Analysis of SOCS6 expression

Five hundred nanograms of total RNA was reverse transcribed using high-capacity cDNA reverse transcription kits (Applied Biosystems, Thermo Fisher Scientific, USA) in 21 SPMS and 21 HC samples. qPCR was performed using an exon-spanning TaqMan probe for *SOCS6* (ref: Hs00377781_m1). Expression of *SOCS6* was determined as relative expression to the housekeeping genes *GAPDH* (ref: 4326317E) and *β-actin* (ref: 4326215E) using a ViiA 7 (Applied Biosystems, Thermo Fisher Scientific, USA).

Results

We used NGS to establish miRNA expression profiles in CD4+ T cells from a cohort of 12 SPMS and 12 HC samples. RT-qPCR was then employed to validate differences in miRNA expression in the NGS cohort as well as a replication cohort of 12 SPMS and 10 HC samples (total 24 SPMS and 22 HC).

NGS

We observed three statistically significant miRNAs (miR-451a, miR-1246, and miR-144-5p) at the FDR-corrected threshold (Additional file 1: Figure S1), which probably reflects the modest sample size. These miRNAs were very lowly expressed (<100 reads per sample), and we were unable to confirm this dysregulation with RT-qPCR. We also observed 42 miRNAs at the nominal significance threshold (97 % of these were down-regulated). Of these 42 miRNAs, only 10 met our secondary criteria of having a read count >800: miR-21-5p ($p = 0.031$), miR-23a-3p ($p = 0.007$), miR-26b-5p ($p = 0.031$), miR-27a-3p ($p = 0.031$), miR-27b-3p ($p = 0.031$), miR-29b-3p ($p = 0.007$), miR-30e-5p ($p = 0.031$), miR-142-3p ($p = 0.031$), miR-155-5p ($p = 0.031$), and miR-221-3p ($p = 0.031$). Each of these miRNAs was found to be down-regulated in SPMS as summarized in Fig. 1 and was forwarded for replication testing in an independent cohort.

RT-qPCR

To confirm our NGS findings, the top ten most dysregulated miRNAs were selected for further analysis in 24 SPMS and 22 HC samples using RT-qPCR (including the 12 SPMS and 12 HC samples that underwent NGS analysis). Of these ten miRNAs, RT-qPCR confirmed significant down-regulation of miR-21-5p ($p = 0.0048$), miR-26b-5p ($p = 0.007$) miR-29b-3p ($p = 0.00001$), miR-142-3p ($p = 0.05$), and miR-155-5p ($p = 0.001$) in SPMS CD4+ T cells (Fig. 2). These five miRNAs were confirmed in the original NGS cohort, the replication cohort, and the combined cohort. This provides statistically significant evidence of replication, indicating that these five miRNAs are very unlikely to be false positives. A trend of down-regulation of miRNA in SPMS samples was still observed across all ten miRNAs.

Comparison of methods

Concordance of differential expression can vary between quantitation methods [14]. To determine the magnitude of fold-change in SPMS vs. HC, we compared RT-qPCR and NGS results and found no change in the degree of decreased expression between NGS and RT-qPCR methods in the miRNAs confirmed by RT-qPCR (Fig. 3).

Correlation to patient characteristics

No strong correlations between miRNA expression and patient characteristics were identified (Table 2). However, moderate positive correlation between EDSS and miR-21-5p, miR-26b-5p, and miR-29b-3p was seen. Further positive correlation was also found between disease duration and miR-21-5p and miR-155-5p. All miRNAs demonstrated weak correlation to patient age and progression duration.

Correlation of miRNA expression and age of HC has also been calculated as a reference point for age of patients. Moderate correlations are in bold text.

Target prediction

miRNA fold-change was <2 for all miRNAs. It is therefore unlikely that any one particular miRNA is causing a significant effect on gene expression alone. It is more likely to be a combination of multiple miRNAs targeting a few specific genes. Furthermore, as RT-qPCR is a less-sensitive methodology than NGS, and the trend of down-regulation is still observed (though not significant) in the other miRNAs, all ten miRNAs were cross-analyzed for potential gene targets. miRSystem was used

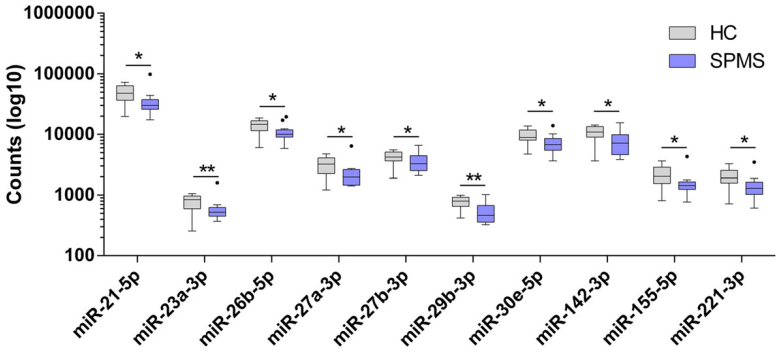

Fig. 1 Tukey boxplot demonstrating the ten most significantly dysregulated microRNAs identified using NGS. Data is presented as log10 of the read count and clearly exhibits the down-regulation of miRNAs in SPMS (*purple*) compared to HC (*gray*). *Whiskers* represent data within 1.5 interquartile range (IQR) of the upper and lower quartile. Data points outside of the 1.5 IQR are represented by black dots. *$p < 0.05$, **$p < 0.01$

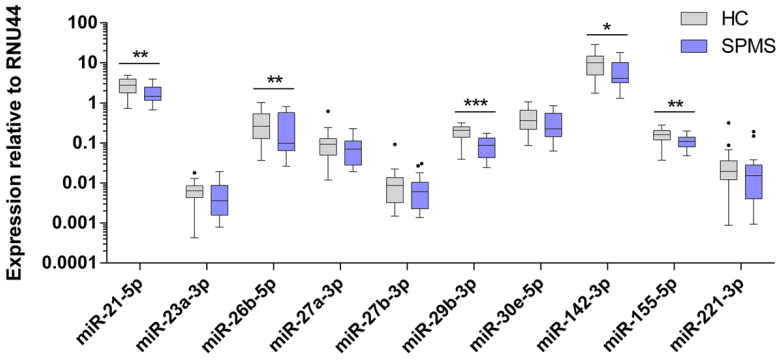

Fig. 2 Tukey boxplot of top ten miRNAs expression (relative to RNU44) using RT-qPCR. Significant down-regulation of miR-21-5p, miR-26b-3p, miR-29b-3p, miR-142-3p, and miR-155-5p in SPMS was confirmed. *Whiskers* represent data within 1.5 interquartile range (IQR) of the upper and lower quartile. Data points outside of the 1.5 IQR are represented by black dots. $p < 0.05$, $^{**}p < 0.01$, $^{***}p < 0.001$

to identify genes that have multiple target genes in common, both in the five confirmed miRNAs and all ten miRNAs identified by NGS. One gene, bromodomain and WD repeat domain containing 1 (*BRWD1*), is targeted by all five confirmed miRNAs. No genes are targeted by all ten miRNAs; however, eight genes are targeted by eight of the miRNAs (Table 3).

These genes are involved in transmembrane ligand binding, regulation of actin filaments, or are transcription factors. However, only one gene is specifically linked to immune cell function, *SOCS6* (suppressor of cytokine signaling 6). This gene has previously been reported to negatively regulate T cell activation by promoting ubiquitin-dependent proteolysis [15] and was consequently selected for further investigated.

SOCS6 expression

Gene expression analysis using RT-qPCR was conducted to determine whether *SOCS6* is up-regulated in SPMS CD4+ T cells in direct negative correlation to the miRNA expression (Fig. 4). Both the preliminary and validation cohorts were analyzed, and *SOCS6* expression is increased in SPMS compared to HC. Normalization against *GAPDH* and *β-actin* generated the same results (data for β-actin not shown).

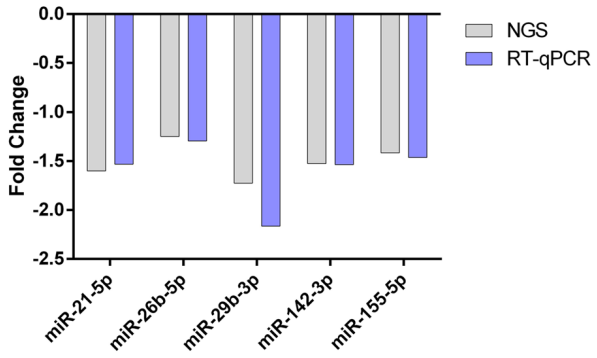

Fig. 3 Comparison of miRNA fold-change between NGS and RT-qPCR. Magnitude of change is consistent between NGS and RT-qPCR methods

Discussion

This is the first study in MS to utilize NGS for miRNA expression profiling in the CD4+ T cells of SPMS patients. We found 42 miRNAs that are dysregulated in the CD4+ T cells of SPMS patients as compared to controls: 97 % of which were down-regulated. TaqMan assays confirmed five of these miRNAs (miR-21-5p, miR-26b-5p, miR-29b-3p, miR-142-3p, and miR-155-5p) to be down-regulated in SPMS. Each of these miRNAs (excluding miR-26b) has been reported on previously in MS though not necessarily in SPMS or CD4+ T cells. Lindberg et al. [11] identified seven miRNAs dysregulated in CD4+ T cells from RRMS patients but did not identify dysregulation in any of the five miRNA in this study. Thus, down-regulation of these miRNAs may be exclusive to SPMS.

Here, we report a decrease in miR-155-5p expression in MS. miR-155-5p has a pro-inflammatory role in MS and is up-regulated in a number of tissues. Studies of postmortem brain tissue find a gradient of miR-155-5p expression that peaks in active lesions [16] and associated neurovascular units [17] and decreases through chronic lesions and normal appearing white matter to a low baseline in healthy control (non-MS) white matter [17, 18]. This increased expression of miR-155 has been associated with the suppression of *CD47* in active lesions that creates a permissive environment for myelin phagocytosis [16]; focal adhesion and cell-cell complex molecules in the blood-brain barrier, thus increasing permeability [17] and; *AKR1C1* and *AKR1C2*, essential for biosynthesis of allopregnanolone (a neuroprotective steroid) [18].

Interestingly, a study of miR-155 in the EAE mouse model found that miR-155 expression in CD4+ T cells

Table 2 Correlation coefficients calculated from RT-qPCR data against patient characteristics

	miR-21-5p	miR-26b-5p	miR-29b-3p	miR-142-3p	miR-155-5p
EDSS	0.34	0.42	0.41	0.28	0.26
Age (HC)	0.22	0.17	0.31	0.21	−0.08
Age (SPMS)	−0.07	−0.17	−0.17	−0.30	−0.01
Disease duration	0.49	0.15	0.23	−0.08	0.49
Progression duration	0.12	0.12	0.11	−0.07	0.17

increases during EAE and that miR-155$^{-/-}$ mice had an attenuation of EAE [19]. Specifically, Th17 cells lacking miR-155-5p are unable to cause EAE [20]. miR-155-5p is required for normal immune function [21], and together, these studies confirm that the significant role miR-155-5p over-expression plays in the inflammatory process of MS. In contrast, our finding of miR-155-5p down-regulation may be exclusive to SPMS patients and/or CD4+ T cells and is consistent with SPMS as a non-inflammatory mediated disease.

miR-155-5p and miR-142-3p have been identified as dysregulated in RRMS PBMCs [22], and a recent study on autologous hematopoietic stem cell transplant (AHSCT) also found co-dysregulation of miR-155-5p and miR-142-3p [23]. Contrary to our results, Arruda et al. found these miRNAs to be up-regulated in MS patient CD4+ T cells before treatment (cohort was 75 % SPMS). However, AHSCT is most effective in active MS disease, and six of the 19 SPMS patients enrolled in the Arruda et al. study presented with gadolinium-enhancing lesions in the year approaching the treatment indicating inflammatory activity. Further, the average disease duration in the Arruda et al. study was 8.1 years, as opposed to 25.6 (primary cohort) or 18.6 (replication cohort) years in our study. Our data is corroborated further by NGS expression analysis, which is a more sensitive measure of expression changes.

In a study of potential biomarkers in Alzheimer's disease (AD), miR-26b-5p was shown to be down-regulated in the serum and CSF of AD patients when compared to patients with inflammatory neurological diseases [24], supporting the predominantly neurodegenerative pathology of SPMS. Over-expression of miR-29b insystemic lupus erythematosus (SLE) has been linked to hypomethylation of DNA in CD4+ T cells [25]. While there are currently no studies on DNA methylation in SPMS, it would be interesting to see if the down-regulation of miR-29b that we have identified here in CD4+ T cells is associated with genome-wide hypermethylation in SPMS.

Increased miR-21-5p promotes differentiation of Th17 cells in the EAE mouse model, and miR-21-5p knock-out mice are resistant to EAE [26]. Fenoglio et al. found increased miR-21-5p expression in RRMS (active relapse phase) PMBCs compared to controls, though no difference in SPMS. Again, this may be attributed to the relatively small sample size ($n = 6$) [27].

Also of interest, we previously reported miR-20a-5p down-regulation in the whole blood of all MS subtypes [28]. This miRNA was one of the 42 dysregulated miRNAs identified by NGS and is significantly down-regulated in SPMS compared to HC. However, it narrowly missed the 800 read cut-off for qPCR confirmation. miR-20a-5p is also predicted to target *SOCS6*.

Eight of the top ten dysregulated miRNAs were predicted to target *SOCS6* using MirSystem. Consistent with this, increased expression of *SOCS6* in the SPMS cohort is in direct negative correlation with the miRNA expression profiles, strongly indicating a mRNA:miRNA

Table 3 Genes identified by miRSystem targeted by eight of the ten microRNAs

	miR-21-5p	miR-23a-3p	miR-26b-5p	miR-27a-3p	miR-27b-3p	miR-29b-3p	miR-30e-5p	miR-142-3p	miR-155-5p	miR-221-3p
ACVR2B	V	V	V	V	V	V			V	V
ZBTB41	V	V		V	V	V	V	V	V	
BRWD1	V	V	V			V	V	V	V	V
CAMTA1	V	V		V	V	V	V		V	V
CFL2	V	V		V	V	V	V	V	V	
SOCS6	V	V	V	V	V		V	V	V	
MIER3		V	V	V	V	V	V		V	V
KLF12	V	V	V	V	V	V	V			V

Verified targeting miRNAs are identified with a "V"

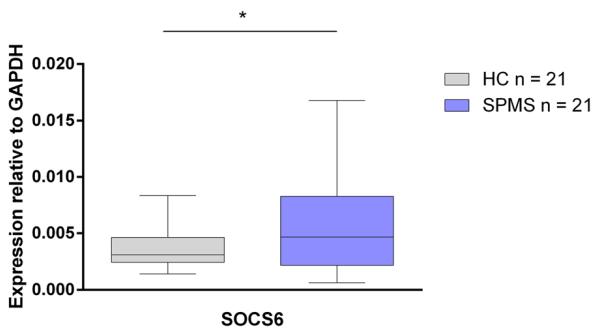

Fig. 4 Expression of *SOCS6* relative to *GAPDH*. Up-regulation of *SOCS6* in SPMS is significant though widely distributed (*$p = 0.042$)

relationship. To our knowledge, this is the first study to identify *SOCS6* as a gene of interest in MS. It is a highly conserved gene with very low expression levels in healthy thymus and brain tissues and is down-regulated in gastric, colorectal, and pancreatic cancers [29–32]. In colorectal cancer, methylation changes have been ruled out as the mechanism of down-regulation [31]; therefore, down-regulation may be due to altered miRNA expression. MiR-424-5p is responsible for the down-regulation of *SOCS6* in pancreatic cancer [32]; however, we found no differences in miR-424-5p expression between SPMS and HC in this study.

The function of *SOCS6* as a negative regulator of T cell activation [15] and its observed over-expression in SPMS CD4+ T cells supports the notion of reduced immune activity in SPMS. Very little is known about *SOCS6*, and more studies are required to determine if it may be a novel therapeutic target.

This is the first study to use NGS miRNA profiling to assess miRNA expression in the CD4+ T cells of SPMS patients. Future studies should focus on using the same technique in treatment naïve RRMS patients to determine if this is a SPMS exclusive trend and remove the confounding factor of treatment effects. Furthermore, miRNA expression profiles of other cell subtypes should be investigated, as whole blood analysis is likely masking significant changes in individual cell subsets. Ideally, all of our patients would have had inactive SPMS; however, as SPMS is a difficult disease stage to define and collect, we have included some active SPMS patients in this study. In this study, we chose to focus on CD4+ T cells as they are thought to be the main cell infiltrates. Our previous studies also show that CD4+ T cells exhibit significant changes in methylation profiles in RRMS [33, 34].

Conclusions

Here, we have shown a general down-regulation of miRNAs in CD4+ T cells compared to HC, with five miRNAs confirmed as significant in two independent assays. This indicates that miRNA expression may be over-normalizing in SPMS CD4+ T cells. *SOCS6* is a predicted target of the majority of these miRNAs and, consistent with this, we found *SOCS6* to be up-regulated in this cohort. These are novel findings that point towards a diminished role for CD4+ T cells in SPMS and add further evidence for SPMS being a neurodegenerative disease stage, not an inflammation-driven one.

Additional file

Additional file 1: Figure S1. Volcano plot of differentially expressed miRNAs identified with NGS. The FDR-corrected significance threshold is demarked with a green line at $p < 1.2 \times 10^{-4}$. Three miRNAs were identified at the threshold. Mean read counts were low in all three miRNAs: miR-451a (SPMS mean = 76.3, HC mean = 18.9), miR-1246 (SPMS mean = 94.9, HC mean = 51.9), and miR-144-5p (SPMS mean = 15.1, HC mean = 5.5). Differential expression could not be replicated with RT-qPCR. (PNG 57 kb)

Acknowledgements
We would like to thank the MS patients and clinical team at the John Hunter Hospital MS clinic who participated in this study. We also acknowledge the Analytical Biomolecular Research Facility at the University of Newcastle for the flow cytometry support and the Diamantina Institute at the University of Queensland for the NGS services.

Funding
This study was supported by the John Hunter Hospital Charitable Trust and the Bloomfield Group Foundation. KAS, VEM, and RAL are supported by fellowships from Multiple Sclerosis Research Australia. KAS is also funded by the Trish MS Research Foundation postgraduate scholarship. VEM is supported by a postdoctoral fellowship from the Canadian Institutes of Health Research.

Availability of data and material
Data available on request and subject to ethics committee approval.

Authors' contributions
KAS, MCB, and RAL wrote the main manuscript text. KAS, VEM, SA, and NG performed the experiments. MCB and RAL analyzed the NGS data. RJS, LT, and JLS supervised the study. All authors reviewed the manuscript. All authors read and approved the final manuscript.

Competing interests
JL-S receives non-direct funding as well as honoraria for presentations and membership on advisory boards from Genzyme, Biogen, Bayer Health Care, Merck, Teva, and Novartis, Australia.
The authors, KAS, MCB, RAL, VEM, SA, NG, RJS, and LT, declare that they have no competing interests.

Consent for publication
Not applicable.

Ethics approval and consent to participate
The Hunter New England Health Research Ethics Committee and University of Newcastle Ethics committee approved this study (05/04/13.09 and H-505-0607, respectively), and methods were carried out in accordance with institutional guidelines on human subject experiments. Written and informed consent was obtained from all patient and control subjects.

Author details
[1]Faculty of Health Sciences and Medicine, Bond University, Robina, Queensland 4226, Australia. [2]Centre for Information-Based Medicine, Hunter Medical Research Institute, Newcastle, New South Wales 2305, Australia. [3]School of Biomedical Sciences and Pharmacy, University of Newcastle, Newcastle, New South Wales 2308, Australia. [4]Institute of Health and Biomedical Innovation, Genomics Research Centre, Brisbane, Queensland 4059, Australia. [5]Department of Neurology, Division of Medicine, John Hunter

Hospital, Locked Bag 1, Hunter Region Mail Centre, Newcastle NSW 2310, Australia. [6]Division of Molecular Genetics, Pathology North, Newcastle, New South Wales 2305, Australia. [7]School of Medicine and Public Health, University of Newcastle, Newcastle, New South Wales 2308, Australia.

Received: 29 June 2016 Accepted: 9 August 2016
Published online: 27 August 2016

References

1. Compston A, Coles A. Multiple sclerosis. Lancet. 2008;372:1502–17.
2. Broux B, Stinissen P, Hellings N. Which immune cells matter? The immunopathogenesis of multiple sclerosis. Crit Rev Immunol. 2013;33:283–306.
3. Segal BM. Stage-specific immune dysregulation in multiple sclerosis. J Interferon Cytokine Res. 2014;34:633–40.
4. Raphael I, Webb J, Stuve O, Haskins W, Forsthuber T. Body fluid biomarkers in multiple sclerosis: how far we have come and how they could affect the clinic now and in the future. Expert Rev Clin Immunol. 2015;11:69–91.
5. Keller A, Leidinger P, Steinmeyer F, Stahler C, Franke A, Hemmrich-Stanisak G, Kappel A, Wright I, Dorr J, Paul F, et al. Comprehensive analysis of microRNA profiles in multiple sclerosis including next-generation sequencing. Mult Scler. 2013;20:295–303.
6. Keller A, Leidinger P, Meese E, Haas J, Backes C, Rasche L, Behrens JR, Pfuhl C, Wakonig K, Giess RM, et al. Next-generation sequencing identifies altered whole blood microRNAs in neuromyelitis optica spectrum disorder which may permit discrimination from multiple sclerosis. J Neuroinflammation. 2015;12:196.
7. De Felice B, Mondola P, Sasso A, Orefice G, Bresciamorra V, Vacca G, Biffali E, Borra M, Pannone R. Small non-coding RNA signature in multiple sclerosis patients after treatment with interferon-beta. BMC Med Genomics. 2014;7:26.
8. Polman CH, Reingold SC, Banwell B, Clanet M, Cohen JA, Filippi M, Fujihara K, Havrdova E, Hutchinson M, Kappos L, et al. Diagnostic criteria for multiple sclerosis: 2010 revisions to the McDonald criteria. Ann Neurol. 2011;69:292–302.
9. Bolger AM, Lohse M, Usadel B. Trimmomatic: a flexible trimmer for Illumina sequence data. Bioinformatics. 2014;30:2114–20.
10. Kozomara A, Griffiths-Jones S. miRBase: annotating high confidence microRNAs using deep sequencing data. Nucleic Acids Res. 2014;42:D68–73.
11. Lindberg RL, Hoffmann F, Mehling M, Kuhle J, Kappos L. Altered expression of miR-17-5p in CD4+ lymphocytes of relapsing-remitting multiple sclerosis patients. Eur J Immunol. 2010;40:888–98.
12. Benjamini Y, Hochberg Y. Controlling the false discovery rate: a practical and powerful approach to multiple testing. J R Stat Soc Ser B Methodol. 1995;57:289–300.
13. Lu T-P, Lee C-Y, Tsai M-H, Chiu Y-C, Hsiao CK, Lai L-C, Chuang EY. miRSystem: an integrated system for characterizing enriched functions and pathways of microRNA targets. PLoS ONE. 2012;7:e42390.
14. Mestdagh P, Hartmann N, Baeriswyl L, Andreasen D, Bernard N, Chen C, Cheo D, D'Andrade P, DeMayo M, Dennis L, et al. Evaluation of quantitative miRNA expression platforms in the microRNA quality control (miRQC) study. Nat Methods. 2014;11:809–15.
15. Choi YB, Son M, Park M, Shin J, Yun Y. SOCS-6 negatively regulates T cell activation through targeting p56lck to proteasomal degradation. J Biol Chem. 2010;285:7271–80.
16. Junker A, Krumbholz M, Eisele S, Mohan H, Augstein F, Bittner R, Lassmann H, Wekerle H, Hohlfeld R, Meinl E. MicroRNA profiling of multiple sclerosis lesions identifies modulators of the regulatory protein CD47. Brain. 2009;132:3342–52.
17. Lopez-Ramirez MA, Wu D, Pryce G, Simpson JE, Reijerkerk A, King-Robson J, Kay O, de Vries HE, Hirst MC, Sharrack B, et al. MicroRNA-155 negatively affects blood-brain barrier function during neuroinflammation. FASEB J. 2014;28(6):2551–65.
18. Noorbakhsh F, Ellestad KK, Maingat F, Warren KG, Han MH, Steinman L, Baker GB, Power C. Impaired neurosteroid synthesis in multiple sclerosis. Brain. 2011;134:2703–21.
19. Murugaiyan G, Beynon V, Mittal A, Joller N, Weiner HL. Silencing microRNA-155 ameliorates experimental autoimmune encephalomyelitis. J Immunol. 2011;187:2213–21.
20. Hu R, Huffaker TB, Kagele DA, Runtsch MC, Bake E, Chaudhuri AA, Round JL, O'Connell RM. MicroRNA-155 confers encephalogenic potential to Th17 cells by promoting effector gene expression. J Immunol. 2013;190:5972–80.
21. Rodriguez A, Vigorito E, Clare S, Warren MV, Couttet P, Soond DR, van Dongen S, Grocock RJ, Das PP, Miska EA, et al. Requirement of bic/microRNA-155 for normal immune function. Science. 2007;316:608–11.
22. Waschbisch A, Atiya M, Linker RA, Potapov S, Schwab S, Derfuss T. Glatiramer acetate treatment normalizes deregulated microRNA expression in relapsing remitting multiple sclerosis. PLoS One. 2011;6:e24604.
23. Arruda LC, Lorenzi JC, Sousa AP, Zanette DL, Palma PV, Panepucci RA, Brum DS, Barreira AA, Covas DT, Simoes BP, et al. Autologous hematopoietic SCT normalizes miR-16, -155 and -142-3p expression in multiple sclerosis patients. Bone Marrow Transplant. 2015;50:380–9.
24. Galimberti D, Villa C, Fenoglio C, Serpente M, Ghezzi L, Cioffi SM, Arighi A, Fumagalli G, Scarpini E. Circulating miRNAs as potential biomarkers in Alzheimer's disease. J Alzheimers Dis. 2014;42:1261–7.
25. Qin H, Zhu X, Liang J, Wu J, Yang Y, Wang S, Shi W, Xu J. MicroRNA-29b contributes to DNA hypomethylation of CD4+ T cells in systemic lupus erythematosus by indirectly targeting DNA methyltransferase 1. J Dermatol Sci. 2013;69:61–7.
26. Murugaiyan G, da Cunha AP, Ajay AK, Joller N, Garo LP, Kumaradevan S, Yosef N, Vaidya VS, Weiner HL. MicroRNA-21 promotes Th17 differentiation and mediates experimental autoimmune encephalomyelitis. J Clin Invest. 2015;125:1069–80.
27. Fenoglio C, Cantoni C, De Riz M, Ridolfi E, Cortini F, Serpente M, Villa C, Comi C, Monaco F, Mellesi L, et al. Expression and genetic analysis of miRNAs involved in CD4+ cell activation in patients with multiple sclerosis. Neurosci Lett. 2011;504:9–12.
28. Cox MB, Cairns MJ, Gandhi KS, Carroll AP, Moscovis S, Stewart GJ, Broadley S, Scott RJ, Booth DR, Lechner-Scott J. Consortium ANMSG: MicroRNAs miR-17 and miR-20a inhibit T cell activation genes and are under-expressed in MS whole blood. PLoS One. 2010;5:e12132.
29. Lai RH, Wang MJ, Yang SH, Chen JY. Genomic organization and functional characterization of the promoter for the human suppressor of cytokine signaling 6 gene. Gene. 2009;448:64–73.
30. Lai RH, Hsiao YW, Wang MJ, Lin HY, Wu CW, Chi CW, Li AF, Jou YS, Chen JY. SOCS6, down-regulated in gastric cancer, inhibits cell proliferation and colony formation. Cancer Lett. 2010;288:75–85.
31. Letellier E, Schmitz M, Baig K, Beaume N, Schwartz C, Frasquilho S, Antunes L, Marcon N, Nazarov PV, Vallar L, et al. Identification of SOCS2 and SOCS6 as biomarkers in human colorectal cancer. Br J Cancer. 2014;111:726–35.
32. Wu K, Hu G, He X, Zhou P, Li J, He B, Sun W. MicroRNA-424-5p suppresses the expression of SOCS6 in pancreatic cancer. Pathol Oncol Res. 2013;19:739–48.
33. Graves M, Benton M, Lea R, Boyle M, Tajouri L, Macartney-Coxson D, Scott R, Lechner-Scott J. Methylation differences at the HLA-DRB1 locus in CD4+ T-Cells are associated with multiple sclerosis. Mult Scler. 2014;20:1033–41.
34. Maltby VE, Graves MC, Lea RA, Benton MC, Sanders KA, Tajouri L, Scott RJ, Lechner-Scott J. Genome-wide DNA methylation profiling of CD8+ T cells shows a distinct epigenetic signature to CD4+ T cells in multiple sclerosis patients. Clin Epigenetics. 2015;7:118.

APPENDIX TWO

In Chapter Two, the decision was made to validate miRNAs that had a NGS read count of >800 with RT-qPCR. In this appendix, I will present the initial data that was used to set this threshold.

Identification of differentially expressed miRNAs with NGS

The statistical significance threshold allowing for multiple testing correction was determined using the False Discovery Rate (FDR) procedure of Benjamini-Hochberg (185). Based on the number of miRNA elements, this threshold was set at 1.2×10^{-4}. As can be seen in Figure A2.1, only three miRNAs were found to meet this threshold. Therefore, a relaxed significance threshold of 0.05 was also considered.

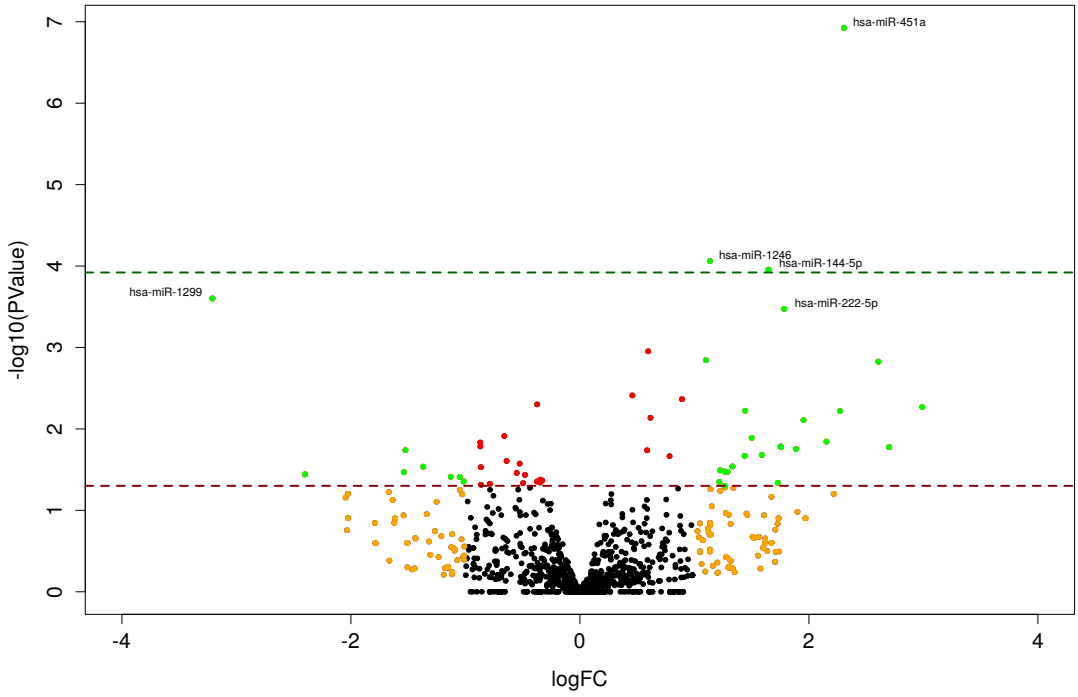

Figure A2.1: Volcano plot of differentially expressed miRNAs identified with NGS. The significance threshold is demarked with a green line at $p<1.2x10^{-4}$.

The top five identified by NGS (Figure A2.2) were selected for validation with RT-qPCR.

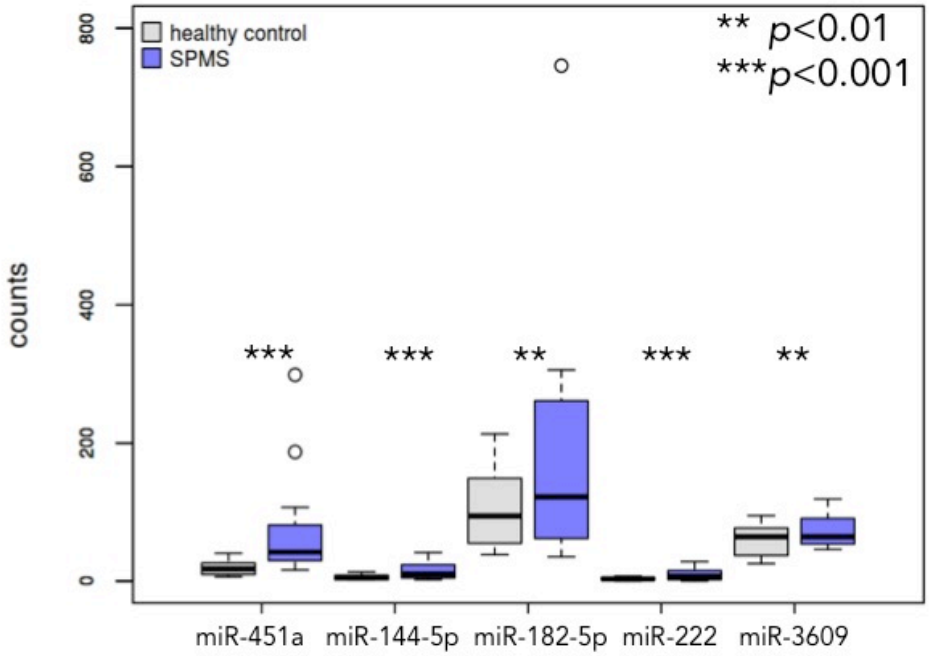

Figure A2.2: Five most dysregulated miRNAs identified in SPMS by NGS (with standard error bars). Box plot showing the distribution of read counts across the miRNAs. The outlier at miR-182-5p is 746 reads. * $p<0.05$, ** $p<0.01$, *** $p<0.001$.

RT-qPCR validation

At the time of validation, there was no TaqMan probe for miR-1246 on the market. The two remaining miRNAs below the threshold, miR-451a and miR-144-5p, were validated with RT-qPCR, as well as a further three miRNAs with significant (Table A2.1).

Table A2.1: Significantly different miRNAs, mean NGS read count, and TaqMan ID.

miRNA	*P* value	SPMS mean	HC mean	Assay ID
miR-451a	1.19E-07	76.3	18.9	001141
miR-144-5p	0.00011	15.1	5.5	002148
miR-222-5p	0.00033	9.7	3.2	002097
miR-3609	0.00111	73.0	59.1	466233_mat
miR-182-5p	0.00143	190.6	103.1	002334

Each miRNA was analysed with RT-qPCR in 11 SPMS and 12 HC samples (the RNA from one of the SPMS samples was exhausted by NGS analysis). miR-451a was the only miRNA to replicate the significant difference observed by NGS (Figure A2.3).

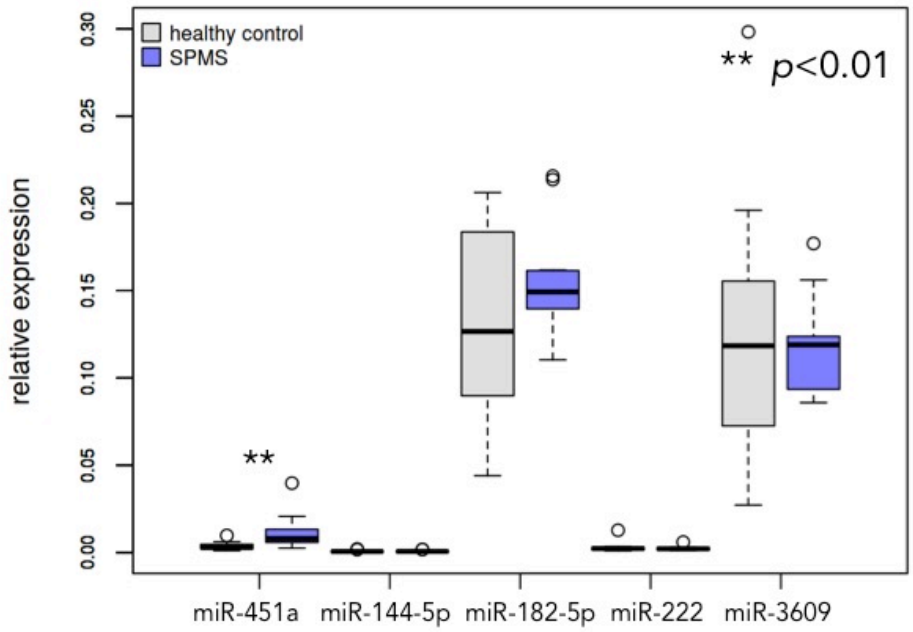

Figure A2.3: RT-qPCR results of the five most dysregulated miRNAs identified by NGS. Expression relative to RNU44. Only miR-451a is significantly different. ** $p<0.01$.

A further cohort of 12 SPMS and 10 HC was collected to determine if the results of miR-451a dysregulation in the CD4+ T-cells of SPMS could be replicated. The outcome was $p=0.002$, however, the direction of change was reversed (data not

shown). When both cohorts were combined, SPMS was still shown to be up-regulated, however without significance.

This result highlights the volatility of differential expression in targets that are expressed at low quantities. NGS is a more sensitive technique than RT-qPCR, however to confirm results, expression of miRNAs must be high enough for accurate detection by RT-qPCR (186). In this study (Chapter Two), we set a read count threshold of >800 reads to increase the likelihood of confirming dysregulated miRNAs; half of our selected miRNAs were verified subsequently verifed. This is a substantial improvement on our initial miRNA selection shown in this appendix.

APPENDIX THREE

Additional data tables for Chapter Three, listing all sites of differential methylation in RRMS and SPMS samples.

Table A3.1: All differentially methylated RRMS probes

Probe ID	Chr	Position	Gene	Median (case)	Median (control)	Δ_{meth}	Adj *P* value	P_{FDR}	Feature
cg22802014	1	31732891	SNRNP40	0.675691	0.9025544	0.226863	0.00043379	0.01349928	3'UTR
cg13232075	1	204556835		0.42867	0.2158971	0.212773	0.016589302	0.02925311	
cg26354017	1	205819088	PM20D1	0.598945	0.410684	0.188261	0.01409406	0.02788393	1stExon
cg17178900	1	205818956	PM20D1	0.646248	0.4698254	0.176423	0.013796407	0.0276007	Body
cg14159672	1	205819179	PM20D1	0.616326	0.4436191	0.172707	0.017227167	0.02991532	1stExon
cg14893161	1	205819251	PM20D1	0.497891	0.3284282	0.169463	0.008958083	0.02385308	5'UTR;1stExon
cg10759817	1	92101219	HSP90B3P	0.746079	0.5770942	0.168985	0.000691305	0.01349928	Body
cg11965913	1	205819406	PM20D1	0.466796	0.3025438	0.164252	0.024620965	0.03518624	TSS200
cg24503407	1	205819492	PM20D1	0.560205	0.4035858	0.156619	0.014934774	0.02888959	TSS1500
cg15600437	1	17309539	MFAP2	0.584121	0.7395363	0.155416	0.049651594	0.0498328	TSS1500
cg03526459	1	146549940		0.334275	0.488696	0.154421	0.029448057	0.03893373	
cg11733135	1	81878937		0.691877	0.8432839	0.151407	0.034438784	0.04266066	
cg26824678	1	19777949	CAPZB	0.723739	0.5762676	0.147471	0.042979316	0.04616919	Body
cg24853868	1	146555624		0.33628	0.4827652	0.146485	0.012223783	0.02733567	
cg16060930	1	117487269	PTGFRN	0.794897	0.6562882	0.138609	0.021352909	0.03299767	Body
cg02487331	1	146550467		0.337817	0.4739996	0.136182	0.04962751	0.0498328	
cg09226051	1	247611502	NLRP3	0.513351	0.6480892	0.134739	0.000627387	0.01349928	Body
cg09476440	1	109693377	KIAA1324	0.723577	0.5908203	0.132757	0.045201623	0.04762623	Body
cg26034147	1	40359924		0.907444	0.7772675	0.130177	0.021506643	0.03304093	
cg13064658	1	212003989	LPGAT1	0.146288	0.2734523	0.127164	0.047417682	0.0486562	5'UTR;1stExon
ch.1.230734885R	1	232668262		0.229938	0.1045985	0.125339	0.004810853	0.0184486	
cg03954786	1	156218113	PAQR6	0.623975	0.5069909	0.116984	0.029728269	0.03911614	TSS1500
cg11680857	1	152635200	LCE2D	0.678225	0.7931205	0.114896	0.030685671	0.03966728	TSS1500
cg01533966	1	90363165	LRRC8D	0.617605	0.7303915	0.112787	0.016187833	0.02909578	5'UTR
cg23961843	1	183623675	RGL1;APOBEC4	0.555658	0.6674704	0.111813	0.005133492	0.0184486	5'UTR;TSS1500

cg05750824	1	64786354		0.625354	0.5136841	0.11167	0.003900629	0.0184486	
cg11734019	1	156258991	TMEM79	0.827758	0.9369172	0.109159	0.005435173	0.0184486	Body
cg03847896	1	112154295		0.725538	0.8346475	0.109109	0.002473373	0.01729845	
cg03737629	1	78343253	FAM73A	0.70336	0.8081955	0.104835	0.019325419	0.03126171	3'UTR
cg13111532	1	1886543	KIAA1751	0.700034	0.5955732	0.104461	0.005148969	0.0184486	3'UTR
cg00124902	1	34645109	C1orf94	0.307761	0.4121305	0.10437	0.009282805	0.02385308	Body;5'UTR
cg24928141	1	92154087	TGFBR3	0.822321	0.9265897	0.104268	0.026602678	0.03657868	Body
cg22729008	1	245581518	KIF26B	0.608356	0.7122467	0.103891	0.001076896	0.01349928	Body
cg15602298	1	157670825	FCRL3	0.688728	0.7905508	0.101822	0.02415317	0.03495854	TSS200
cg07844442	10	129144269	DOCK1	0.465688	0.728887	0.263199	0.013719484	0.0276007	Body
cg20374173	10	14227415	FRMD4A	0.339618	0.5876724	0.248054	0.00192587	0.01576607	Body
cg14368220	10	88024553	MIR346;GRID1	0.523063	0.3444181	0.178645	0.012888037	0.0276007	TSS200;Body
cg05818501	10	1451648	ADARB2	0.624073	0.4863054	0.137767	0.013779848	0.0276007	Body
cg07506153	10	131665884	EBF3	0.849761	0.7262866	0.123475	0.045389875	0.04764205	Body
cg17686260	10	131412764	MGMT	0.736152	0.8591174	0.122965	0.045677968	0.04776213	Body
cg16871435	10	65682643		0.571437	0.4509912	0.120446	0.048720828	0.0495028	
ch.10.6667087F	10	6627081		0.201843	0.0856604	0.116183	0.016102692	0.02909578	
cg11963436	10	93567261	TNKS2	0.421508	0.5361234	0.114615	0.023574769	0.03448437	Body
cg06749524	10	111152929		0.636387	0.5255409	0.110846	0.039532404	0.04526519	
cg16255663	10	131350999	MGMT	0.786541	0.8955565	0.109016	0.031567164	0.04027247	Body
cg08822897	11	64258103		0.284157	0.5330633	0.248906	0.000366993	0.01349928	
cg08912652	11	130779479	SNX19	0.851534	0.6035999	0.247934	0.003191097	0.01755103	Body
cg10415021	11	110890228		0.486528	0.7315048	0.244976	0.003190267	0.01755103	
cg16999994	11	1001560	AP2A2	0.453497	0.2389582	0.214539	0.015443339	0.02909578	Body
cg27049594	11	124439146	OR8A1	0.702716	0.5144453	0.18827	0.00888529	0.02385308	TSS1500
cg10528424	11	1858572	SYT8	0.515347	0.683099	0.167752	0.037348548	0.04427091	Body
cg08849813	11	17825098	SERGEF	0.818926	0.6647311	0.154195	0.040697202	0.04535861	Body
cg26155681	11	20384377	HTATIP2	0.204587	0.076961	0.127626	0.011812851	0.02730792	TSS1500

cg11820026	11	117696743	FXYD2	0.466212	0.5827476	0.116535	0.033705763	0.0421322	Body;TSS1500
cg10470368	11	64146517		0.713807	0.8274771	0.11367	0.047249041	0.0486562	
cg09233619	11	23421870		0.79124	0.6833519	0.107888	0.04818827	0.0492631	
ch.11.96117892F	11	96612684		0.171835	0.0690581	0.102777	0.009319399	0.02385308	
cg05279513	11	9880619	SBF2	0.368282	0.2664416	0.101841	0.013784607	0.0276007	Body
cg23432430	12	125538377		0.688214	0.885203	0.196989	0.003950116	0.0184486	
cg08922148	12	120156140	CIT	0.946986	0.7632092	0.183777	0.005242721	0.0184486	Body
cg19353052	12	113516445	DTX1	0.717358	0.5367952	0.180563	0.016056516	0.02909578	Body
cg05929129	12	132698423	GALNT9	0.637537	0.8180473	0.18051	0.040151024	0.04535861	Body
cg22543924	12	9065171		0.748225	0.567864	0.180361	0.039662413	0.04526519	
cg16749614	12	43203955		0.363636	0.5267235	0.163087	0.005081544	0.0184486	
cg26864661	12	76661181		0.329825	0.1789349	0.15089	0.024519194	0.03518624	
cg18675623	12	108165306		0.774635	0.9189088	0.144274	0.007974389	0.02317632	
cg12050434	12	43030949		0.478141	0.5882205	0.11008	0.025451687	0.03571028	
cg15876417	12	40014132	ABCD2	0.311083	0.2104378	0.100646	0.006819605	0.02155622	TSS1500
cg20536971	13	100989375	PCCA	0.639244	0.3457767	0.293467	0.00178004	0.01576607	Body
cg12195446	13	110424497	IRS2	0.602628	0.7640382	0.16141	0.044592222	0.04730496	Body
cg16151959	13	42704154	DGKH	0.597791	0.7570254	0.159234	0.031941558	0.04047893	Body
cg23209353	13	21728944	SKA3	0.748578	0.9055555	0.156977	0.007335443	0.02216755	3'UTR
cg00587941	13	114741241		0.775566	0.9197742	0.144208	0.042582922	0.04616919	
cg05918715	13	26622819	SHISA2	0.624138	0.4839725	0.140166	0.036421154	0.04335852	Body
cg21117559	13	33750464	STARD13	0.598822	0.7271982	0.128377	0.001312928	0.01349928	5'UTR;Body
cg08861434	13	112062652		0.811541	0.6949501	0.116591	0.038072259	0.04475967	
cg17602481	13	114890515	RASA3	0.425003	0.5350984	0.110095	0.022587514	0.03357603	Body
cg24492140	13	34392781	RFC3	0.347627	0.2429989	0.104628	0.013036336	0.0276007	Body
ch.13.80513820F	13	81615819		0.231031	0.1267289	0.104302	0.00708215	0.02173612	
ch.13.721274R	13	51955414	INTS6	0.183218	0.083083	0.100135	0.005568123	0.0184486	Body
cg16706502	14	31927974	C14orf126	0.597671	0.3677487	0.229923	0.008531065	0.02385308	TSS1500

cg23489384	14	21199099		0.431048	0.6273493	0.196302	0.027078348	0.03704749	
cg19555075	14	96038687		0.486176	0.646259	0.160083	0.035452879	0.04313957	
cg09849871	14	90794949	C14orf102	0.590174	0.7229734	0.1328	0.044724688	0.04730496	5'UTR;Body
cg05057827	14	98670848		0.535752	0.6684415	0.132689	0.01828521	0.03029176	
cg21123519	14	69095679		0.528684	0.3981703	0.130513	0.001257521	0.01349928	
cg26419287	14	52482697	NID2	0.81378	0.6968667	0.116913	0.028720062	0.03852691	Body
cg02299497	14	69095570		0.512602	0.3987508	0.113851	0.002516138	0.01729845	
cg15874048	14	45369753	C14orf28	0.776834	0.8838401	0.107007	0.008090642	0.02317632	Body
cg10193711	14	22917797		0.286659	0.1811468	0.105512	0.041879099	0.04606701	
cg22688471	15	79788143		0.434047	0.6017523	0.167706	0.000441644	0.01349928	
cg26261358	15	24043142		0.439735	0.303435	0.1363	0.042666802	0.04616919	
cg18258571	15	31589348		0.796013	0.6773533	0.11866	0.007679102	0.02270702	
cg16580742	15	81491460	IL16	0.660663	0.7639649	0.103302	0.015903548	0.02909578	5'UTR
cg22724998	15	60288082		0.730351	0.628135	0.102216	0.006922507	0.02163283	
cg27370471	15	101932559	PCSK6	0.341079	0.2390524	0.102027	0.0122265	0.02733567	Body
cg06052372	16	83967808		0.550688	0.7668728	0.216185	0.012048532	0.02733567	
cg08136432	16	88902276	GALNS	0.645258	0.857102	0.211844	0.015854896	0.02909578	Body
cg06520095	16	66458043		0.461162	0.6356145	0.174452	0.013384386	0.0276007	
cg03940883	16	14380714		0.522861	0.3633758	0.159485	0.027537276	0.03730419	
cg04963199	16	87868947	SLC7A5	0.76144	0.6093043	0.152135	0.044041231	0.04711273	Body
cg09351263	16	85864047		0.358325	0.20894	0.149385	0.030472362	0.03966728	
cg08072101	16	7855274		0.577858	0.699078	0.12122	0.013091957	0.0276007	
cg03444934	16	83171314	CDH13	0.637991	0.5213834	0.116607	0.021667375	0.03310293	Body
cg26764761	16	87682142	JPH3	0.822179	0.7076038	0.114575	0.039668768	0.04526519	Body
cg05248234	17	79495519	FSCN2	0.261872	0.4925312	0.230659	0.015892741	0.02909578	1stExon;5'UTR
cg26536949	17	57053		0.599729	0.7673243	0.167595	0.022438678	0.03353607	
cg17225604	17	22193895		0.626322	0.7815582	0.155236	0.04718926	0.0486562	
cg15189015	17	72707255	RAB37;CD300LF	0.311868	0.190029	0.121839	0.00644531	0.02061	Body

cg01978703	17	973713	ABR	0.639712	0.7612032	0.121491	0.035058278	0.0430403	Body
cg07073561	17	79615824		0.419376	0.304418	0.114958	0.030724114	0.03966728	
cg21997403	17	80436296	NARF	0.794696	0.9057571	0.111061	0.018113968	0.03018995	Body
cg00348031	18	77236278	NFATC1	0.575922	0.7665373	0.190615	0.031487177	0.04027247	Body
cg21848624	18	77219388	NFATC1	0.700386	0.8837675	0.183382	0.011916185	0.02730792	Body
cg02100397	19	646890		0.446869	0.6480127	0.201144	0.009409183	0.02385308	
cg06688803	19	45457306	CLPTM1	0.595637	0.7879626	0.192326	0.025131932	0.03544247	TSS1500
cg18624102	19	39523840	FBXO27	0.594034	0.4025173	0.191516	0.013778059	0.0276007	TSS1500
cg02872767	19	1525453	PLK5P	0.67122	0.8520397	0.18082	0.018108722	0.03018995	Body
cg06684911	19	1792217	ATP8B3	0.804177	0.647139	0.157038	0.01736245	0.02991532	Body
cg06417478	19	12876846	HOOK2	0.299338	0.4543382	0.155	0.047326404	0.0486562	Body
cg15793258	19	4638503	TNFAIP8L1	0.695698	0.8382843	0.142586	0.016382074	0.02925311	TSS1500
cg04515524	19	17489148	PLVAP	0.048768	0.1661439	0.117376	0.023245425	0.03432775	TSS1500
cg03159252	19	639161	FGF22	0.698331	0.8120778	0.113746	0.00355935	0.01812632	TSS1500
cg15765251	19	888814	MED16	0.83004	0.7199737	0.110066	0.003341693	0.01801893	Body
cg17713488	19	10077935	COL5A3	0.64599	0.5361738	0.109816	0.040905216	0.04535861	Body
cg03162251	19	6230240	MLLT1	0.91844	0.8179302	0.100509	0.041335932	0.04565213	Body
cg03398919	2	173118470		0.474625	0.7394302	0.264806	0.004671297	0.0184486	
cg23128510	2	175922785		0.860042	0.6571458	0.202896	0.001749153	0.01576607	
cg18662228	2	236867804	AGAP1	0.422887	0.6214159	0.198528	0.035894928	0.04330606	Body;Body
cg18109430	2	26700908	OTOF	0.455952	0.6410422	0.18509	0.013250986	0.0276007	5'UTR;1stExon
cg17600943	2	207803547	CPO	0.530004	0.6897406	0.159736	0.038411938	0.04475967	TSS1500
cg15176306	2	224813276		0.825838	0.6763457	0.149492	0.042928436	0.04616919	
cg07227024	2	202163482	ALS2CR12	0.131089	0.278768	0.147679	0.000475902	0.01349928	Body
cg06292076	2	105464104		0.36969	0.2521428	0.117547	0.008409699	0.02384193	
cg19052272	2	3704530	ALLC	0.739728	0.8551447	0.115416	0.00133052	0.01349928	TSS1500
cg04021592	2	145280784		0.471238	0.3596413	0.111597	0.002902851	0.01755103	
cg17375248	2	66811157		0.347265	0.2406005	0.106665	0.004949084	0.0184486	

cg16781264	2	101087575	NMS	0.170287	0.2740618	0.103775	0.011871476	0.02730792	Body
cg10481584	2	104708897		0.652542	0.7535819	0.10104	0.003726548	0.0184486	
cg18757817	2	208572165		0.778124	0.6778044	0.10032	0.004511609	0.0184486	
cg00704664	20	60500578	CDH4	0.345943	0.5201933	0.17425	0.025603849	0.03574141	Body
cg11979743	20	814510	FAM110A	0.056549	0.2171236	0.160575	0.049933172	0.04993317	1stExon;5'UTR
cg16310958	20	25281332	ABHD12	0.881089	0.734672	0.146418	0.029395652	0.03893373	Body;3'UTR
cg22181382	20	16559406		0.737036	0.8609042	0.123868	0.03228775	0.04072996	
cg13877999	20	42194607	SGK2	0.832059	0.7171075	0.114952	0.00545094	0.0184486	5'UTR;TSS200
cg25155022	20	42285962		0.141135	0.2439266	0.102792	0.00873656	0.02385308	
cg10463299	20	54987330	CASS4	0.246572	0.144518	0.102054	0.005117605	0.0184486	5'UTR;1stExon
cg07135405	20	62573077	UCKL1;MIR1914	0.669006	0.5670104	0.101996	0.017805707	0.03016535	Body;TSS200
cg03706056	21	37437565	SETD4	0.531861	0.3202301	0.211631	0.014347968	0.02808617	TSS1500
cg05200811	21	47581042		0.60568	0.7461273	0.140447	0.001374472	0.01349928	
cg11766577	21	47581405	C21orf56	0.658041	0.7862002	0.128159	0.001007457	0.01349928	Body
cg10296238	**21**	**47605174**	**C21orf56**	**0.426374**	**0.3058234**	**0.120551**	**0.005318879**	**0.0184486**	**TSS1500**
cg07747299	21	47604052	C21orf56	0.293361	0.1868764	0.106484	0.003174026	0.01755103	5'UTR
cg13126279	21	47581558	C21orf56	0.684086	0.7874304	0.103344	0.002959042	0.01755103	Body
cg13306870	22	39527583	CBX7	0.480372	0.2822077	0.198164	0.009185058	0.02385308	3'UTR
cg11942221	22	29686496	EWSR1	0.789882	0.8933278	0.103446	0.008822572	0.02385308	3'UTR;Body
cg08977311	3	168308798	C3orf50	0.301847	0.4850454	0.183199	0.009869976	0.02401985	Body
cg20979384	3	22422855		0.752234	0.5764904	0.175744	0.009810956	0.02401985	
cg25692928	3	139724110	CLSTN2	0.416727	0.2501755	0.166552	0.003989108	0.0184486	Body
cg22542451	3	182883005		0.708108	0.8613532	0.153246	0.010537683	0.02541985	
cg26845082	3	13555664		0.14589	0.289814	0.143924	0.03163219	0.04027247	
cg19996396	3	121946297	CASR	0.83526	0.7166261	0.118634	0.023998369	0.03491826	5'UTR
cg15116298	3	176070137		0.714921	0.8239822	0.109061	0.013040165	0.0276007	
cg03865648	3	173113856		0.365423	0.2594162	0.106007	0.003008476	0.01755103	
cg13143743	3	177570694		0.557152	0.6626737	0.105521	0.030109502	0.03942911	

cg06821582	3	133115942	TMEM108	0.642777	0.7465181	0.103741	0.00919548	0.02385308	3'UTR
cg07909498	4	79627477		0.486084	0.2800855	0.205998	0.001949259	0.01576607	
cg08669168	4	53757661	SCFD2	0.835372	0.6463968	0.188975	0.008062758	0.02317632	Body
cg04277055	4	185749877		0.77836	0.937318	0.158958	0.015022586	0.02888959	
cg07952421	4	69435601	UGT2B15	0.702727	0.8546197	0.151893	0.016130477	0.02909578	TSS1500
cg08395784	4	708242	PCGF3	0.886842	0.7529529	0.133889	0.040320094	0.04535861	5'UTR
cg26398228	4	33062845		0.700324	0.5668501	0.133474	0.017376575	0.02991532	
cg12486486	4	69179905	YTHDC1	0.649333	0.7736884	0.124356	0.006065826	0.01962473	Body
cg17858192	4	16077807	PROM1	0.119375	0.2420208	0.122646	0.013286271	0.0276007	5'UTR;TSS200
cg08343347	4	36076000	ARAP2	0.674576	0.7965573	0.121981	0.009490741	0.02385308	Body
cg20419181	4	38063874	TBC1D1	0.226535	0.1087169	0.117818	0.004324672	0.0184486	Body
cg01218619	4	25090298		0.131097	0.2462354	0.115139	0.000880088	0.01349928	
cg23057687	4	91760659	TMSL3;FAM190A	0.775173	0.8900736	0.1149	0.00226485	0.01639036	TSS1500;Body
cg11459852	4	176983371		0.611287	0.7149338	0.103646	0.027445628	0.03730419	
cg09976051	4	178362394	AGA	0.516853	0.6201499	0.103296	0.014400547	0.02808617	Body
cg20311846	4	77356250	SHROOM3	0.504259	0.40202	0.102239	0.003549557	0.01812632	TSS200
cg05791544	4	129697855		0.680316	0.7817073	0.101391	0.023342866	0.03432775	
ch.4.3427878R	4	186088653	KIAA1430	0.5876	0.4872309	0.100369	0.004810046	0.0184486	Body
cg22071943	5	1225434	SLC6A18	0.368136	0.6436527	0.275517	0.002768542	0.01755103	TSS200
cg13972557	5	116075820		0.41291	0.5923241	0.179414	0.035368203	0.04313957	
cg20381404	5	34008215	AMACR	0.270747	0.1127238	0.158023	0.034135756	0.04247662	5'UTR;1stExon
cg09101062	5	43487508	C5orf34	0.629164	0.7841494	0.154986	0.046098005	0.04801876	Body
cg06611487	5	115284110		0.428588	0.5766908	0.148103	0.02135849	0.03299767	
cg07021532	5	178322737	ZFP2	0.51678	0.3795244	0.137256	0.019769955	0.03166502	TSS200
cg00631759	5	178549790	ADAMTS2	0.693457	0.823285	0.129828	0.013850533	0.0276007	Body
cg17386240	**5**	**135384080**	**TGFBI**	**0.750006**	**0.6253156**	**0.124691**	**0.04233129**	**0.04616919**	**Body**
cg24861747	5	1228214	SLC6A18	0.38044	0.498622	0.118182	0.034955787	0.0430403	Body
cg23404351	5	21751337	CDH12	0.618356	0.727346	0.10899	0.002190382	0.01639036	3'UTR

cg23208285	5	131879579	IL5	0.463846	0.5711815	0.107335	0.00113185	0.01349928	TSS1500
cg16362014	5	118321556	DTWD2	0.831087	0.9335787	0.102492	0.020127963	0.03183873	Body
cg15602423	6	32552095	HLA-DRB1	0.387082	0.658822	0.27174	0.004339504	0.0184486	Body
cg19774683	6	32522400	HLA-DRB6	0.576704	0.355419	0.221285	0.039276661	0.04526519	Body
cg13423887	**6**	**32632694**	**HLA-DQB1**	**0.294241**	**0.4998702**	**0.205629**	**0.004160722**	**0.0184486**	**Body**
cg01341801	**6**	**32489203**	**HLA-DRB5**	**0.454757**	**0.2494189**	**0.205338**	**0.040802068**	**0.04535861**	**Body**
cg14645244	6	32552205	HLA-DRB1	0.317864	0.5210373	0.203174	0.017405278	0.02991532	Body
cg15982117	**6**	**32552106**	**HLA-DRB1**	**0.491871**	**0.6840959**	**0.192224**	**0.01980503**	**0.03166502**	**Body**
cg09949906	6	32552350	HLA-DRB1	0.50703	0.6988308	0.191801	0.028860633	0.03852754	Body
cg10568066	6	30039442	RNF39	0.559707	0.3719741	0.187733	2.07E-05	0.00284003	Body;Body
cg09139047	**6**	**32552042**	**HLA-DRB1**	**0.575764**	**0.7543663**	**0.178602**	**0.02807999**	**0.03785293**	**Body**
cg12633154	6	30039435	RNF39	0.476967	0.3096604	0.167306	7.72E-05	0.00531071	Body
cg08578320	**6**	**32552039**	**HLA-DRB1**	**0.588386**	**0.7542884**	**0.165903**	**0.013641217**	**0.0276007**	**Body**
cg25644740	6	29894152	HCG4P6	0.612309	0.4482485	0.16406	0.018615396	0.0306541	TSS1500
cg13401893	6	30039432	RNF39	0.508331	0.3499875	0.158344	5.96E-05	0.00531071	Body
cg26566189	6	31096127	PSORS1C1	0.26758	0.1107795	0.156801	0.007113638	0.02173612	5'UTR
cg11082635	6	166856074	RPS6KA2	0.559012	0.7146204	0.155608	0.044200307	0.04711273	Body
cg01502466	6	29898751		0.619984	0.7718625	0.151879	0.048782754	0.0495028	
cg04520169	6	29894195	HCG4P6	0.524282	0.3766725	0.14761	0.009649986	0.02390762	TSS1500
cg17129519	6	30618299	C6orf136	0.944813	0.7976128	0.1472	0.002252759	0.01639036	Body
cg10632894	**6**	**32552453**	**HLA-DRB1**	**0.680863**	**0.8247369**	**0.143874**	**0.038349852**	**0.04475967**	**Body**
cg07382347	6	30039408	RNF39	0.294639	0.1527094	0.141929	0.000675493	0.01349928	Body
ch.6.2893423F	6	150056792	NUP43	0.346538	0.2055566	0.140981	0.002749507	0.01755103	Body
cg00101728	6	2953027	SERPINB6	0.683052	0.5434986	0.139553	0.013641541	0.0276007	Body
cg26981746	6	32490012	HLA-DRB5	0.632837	0.5007592	0.132078	0.03619832	0.04330606	Body
cg05082466	6	2953123	SERPINB6	0.748285	0.617495	0.13079	0.005338464	0.0184486	Body
cg12015991	6	32490043	HLA-DRB5	0.777577	0.6491037	0.128473	0.022145049	0.03346093	Body
cg00689685	6	32139812	AGPAT1	0.855609	0.729527	0.126082	0.033262206	0.04176761	5'UTR

cg10930308	6	30039476	RNF39	0.317058	0.1925099	0.124548	0.000844306	0.01349928	Body
cg03343571	6	30039175	RNF39	0.333766	0.212244	0.121522	0.000565339	0.01349928	Body
cg00807871	6	37617124	MDGA1	0.530052	0.4092444	0.120808	0.020145232	0.03183873	Body
cg13185413	6	30039202	RNF39	0.325802	0.2064434	0.119358	0.001239273	0.01349928	Body
cg17416722	**6**	**32554385**	**HLA-DRB1**	**0.27086**	**0.1522284**	**0.118632**	**0.035962454**	**0.04330606**	**Body**
cg23237314	6	29894197	HCG4P6	0.491808	0.3743178	0.11749	0.011159773	0.02668642	TSS1500
cg14494781	6	2615341		0.747282	0.8646492	0.117367	0.019087815	0.0311596	
cg09279736	6	30039403	RNF39	0.403957	0.2868337	0.117124	0.000450969	0.01349928	Body
cg13838276	6	118158769		0.350411	0.4638685	0.113458	0.004597123	0.0184486	
cg19178509	6	30850581	DDR1	0.447425	0.3385171	0.108908	0.026587704	0.03657868	TSS1500
cg00947782	6	30039142	RNF39	0.209929	0.1017924	0.108137	0.000978311	0.01349928	Body
cg06764333	6	133564466	EYA4	0.189686	0.0821493	0.107537	0.004498488	0.0184486	5'UTR
cg16078649	6	30039466	RNF39	0.450735	0.3456927	0.105042	0.000632921	0.01349928	Body
cg01360627	6	31544931	TNF	0.360477	0.4640847	0.103608	0.002891433	0.01755103	Body
cg08491487	6	30039130	RNF39	0.180668	0.077568	0.1031	0.002686581	0.01755103	Body
cg09637172	6	31545252	TNF	0.555132	0.6581686	0.103036	0.007638552	0.02270702	Body
cg04627110	6	29635507	MOG	0.784873	0.6833891	0.101484	0.040490044	0.04535861	3'UTR;Body
cg19383211	6	32527588	HLA-DRB6	0.823525	0.7226065	0.100918	0.009541233	0.02385308	Body
cg23403836	7	1616229	KIAA1908	0.750865	0.4355525	0.315312	1.60E-05	0.00284003	Body
cg13211008	7	158541253	ESYT2	0.197682	0.3921768	0.194495	0.017879828	0.03016535	Body
cg07846874	7	11568529	THSD7A	0.589262	0.776991	0.187729	0.015589787	0.02909578	Body
cg22953237	7	31425682		0.697235	0.5135543	0.183681	0.016594491	0.02925311	
cg09281805	7	4751840	FOXK1	0.722338	0.5407225	0.181615	0.024694342	0.03518624	Body
cg27468880	7	965995	ADAP1	0.75221	0.9269222	0.174712	0.038245078	0.04475967	Body
cg13279926	7	157464161	PTPRN2	0.688199	0.8381708	0.149972	0.000908014	0.01349928	Body
cg07249765	7	4244643	SDK1	0.737384	0.8765873	0.139203	0.049487898	0.0498328	Body
cg05917273	7	116200522	CAV1	0.591951	0.7247149	0.132764	0.024869568	0.03525325	3'UTR
cg21823080	7	148096241	CNTNAP2	0.497508	0.3699064	0.127601	0.036219616	0.04330606	Body

cg08355157	7	158809128	LOC154822	0.476048	0.6012454	0.125197	0.020692036	0.03251606	Body
cg19665696	7	949154	ADAP1	0.252647	0.3680813	0.115434	0.011829421	0.02730792	Body
cg06096382	7	43151725	HECW1	0.611506	0.7252477	0.113742	0.038769732	0.04498598	TSS1500
cg04130408	7	73703236	CLIP2	0.499443	0.6114619	0.112019	0.011679302	0.02730792	TSS1500
cg25612754	7	948567	ADAP1	0.241761	0.3479876	0.106227	0.00132084	0.01349928	Body
cg23144994	7	141431499	FLJ40852	0.655606	0.7597921	0.104187	0.004297515	0.0184486	Body
cg09506675	7	112727914	GPR85	0.603872	0.5003716	0.103501	0.040284083	0.04535861	TSS1500;TSS200
cg00981661	7	130984525	MKLN1	0.610023	0.7134876	0.103465	0.004487339	0.0184486	Body
cg19590115	7	157632890	PTPRN2	0.811536	0.9149834	0.103447	0.005563624	0.0184486	Body
cg03453431	7	157225567		0.327601	0.2248833	0.102718	0.001869502	0.01576607	
cg12581298	7	1080836	C7orf50	0.856163	0.7534656	0.102698	0.020991344	0.03279897	Body
cg01827933	7	93960063		0.401166	0.2986182	0.102547	0.001616886	0.01533254	
cg05875700	8	638208	ERICH1	0.120484	0.3191762	0.198692	0.004547501	0.0184486	Body
cg01053087	8	637909	ERICH1	0.163553	0.3298633	0.16631	0.002127504	0.01639036	Body
cg22029879	8	1790861	ARHGEF10	0.811315	0.6783574	0.132957	0.04291427	0.04616919	5'UTR
cg20601736	8	652315	ERICH1	0.885785	0.7551862	0.130599	0.016011637	0.02909578	Body
cg12641240	8	638330	ERICH1	0.068507	0.1937307	0.125224	0.017514624	0.02991628	Body
cg08682625	8	128470793	LOC727677	0.443527	0.3212344	0.122293	0.000960086	0.01349928	Body
cg04554929	8	105342491		0.321258	0.440364	0.119106	0.022002308	0.03342892	
cg04687040	8	142427117		0.565232	0.6839672	0.118735	0.019148992	0.0311596	
cg19128026	8	1792615	ARHGEF10	0.750262	0.8583527	0.108091	0.008858247	0.02385308	Body
cg05023707	8	39845127	IDO2	0.911901	0.8059079	0.105993	0.003481524	0.01812632	Body
cg21234082	9	124363848	DAB2IP	0.718972	0.5899272	0.129045	0.022310569	0.03352681	Body
cg10384133	9	45733081		0.509316	0.636885	0.127569	0.026563786	0.03657868	
ch.9.25704165R	9	25714165		0.207643	0.0999138	0.10773	0.006062024	0.01962473	
cg13990129	9	108311111	FSD1L	0.751863	0.854377	0.102514	0.005248116	0.0184486	3'UTR

Bold font indicates probes which are common between this study and our previous work (98).

Table A3.2: RRMS DMRs within the MHC locus

Probe ID	Chr	Position	Gene	Median (case)	Median (control)	Δ_{meth}	Adj. *p* value	p_{FDR}	Feature
cg00101728	6	2953027	SERPINB6	0.543499	0.683052	0.139553	0.013642	0.027601	Body
cg05082466	6	2953123	SERPINB6	0.617495	0.748285	0.13079	0.005338	0.018449	Body
cg25644740	6	29894152	HCG4P6	0.448248	0.612309	0.16406	0.018615	0.030654	TSS1500
cg04520169	6	29894195	HCG4P6	0.376672	0.524282	0.14761	0.00965	0.023908	TSS1500
cg23237314	6	29894197	HCG4P6	0.374318	0.491808	0.11749	0.01116	0.026686	TSS1500
cg15602423	6	32552095	HLA-DRB1	0.658822	0.387082	-0.27174	0.00434	0.018449	Body
cg14645244	6	32552205	HLA-DRB1	0.521037	0.317864	-0.20317	0.017405	0.029915	Body
cg15982117	**6**	**32552106**	**HLA-DRB1**	**0.684096**	**0.491871**	**-0.19222**	**0.019805**	**0.031665**	**Body**
cg09949906	6	32552350	HLA-DRB1	0.698831	0.50703	-0.1918	0.028861	0.038528	Body
cg09139047	6	32552042	HLA-DRB1	0.754366	0.575764	-0.1786	0.02808	0.037853	Body
cg08578320	6	32552039	HLA-DRB1	0.754288	0.588386	-0.1659	0.013641	0.027601	Body
cg10632894	6	32552453	HLA-DRB1	0.824737	0.680863	-0.14387	0.03835	0.04476	Body
cg17416722	6	32554385	HLA-DRB1	0.152228	0.27086	0.118632	0.035962	0.043306	Body
cg01341801	6	32489203	HLA-DRB5	0.249419	0.454757	0.205338	0.040802	0.045359	Body
cg26981746	6	32490012	HLA-DRB5	0.500759	0.632837	0.132078	0.036198	0.043306	Body
cg12015991	6	32490043	HLA-DRB5	0.649104	0.777577	0.128473	0.022145	0.033461	Body
cg19774683	6	32522400	HLA-DRB6	0.355419	0.576704	0.221285	0.039277	0.045265	Body
cg19383211	6	32527588	HLA-DRB6	0.722607	0.823525	0.100918	0.009541	0.023853	Body
cg10568066	6	30039442	RNF39	0.371974	0.559707	0.187733	2.07E-05	0.00284	Body
cg12633154	6	30039435	RNF39	0.30966	0.476967	0.167306	7.72E-05	0.005311	Body
cg13401893	6	30039432	RNF39	0.349987	0.508331	0.158344	5.96E-05	0.005311	Body
cg07382347	6	30039408	RNF39	0.152709	0.294639	0.141929	0.000675	0.013499	Body
cg10930308	6	30039476	RNF39	0.19251	0.317058	0.124548	0.000844	0.013499	Body
cg03343571	6	30039175	RNF39	0.212244	0.333766	0.121522	0.000565	0.013499	Body
cg13185413	6	30039202	RNF39	0.206443	0.325802	0.119358	0.001239	0.013499	Body

cg09279736	6	30039403	RNF39	0.286834	0.403957	0.117124	0.000451	0.013499	Body
cg00947782	6	30039142	RNF39	0.101792	0.209929	0.108137	0.000978	0.013499	Body
cg16078649	6	30039466	RNF39	0.345693	0.450735	0.105042	0.000633	0.013499	Body
cg08491487	6	30039130	RNF39	0.077568	0.180668	0.1031	0.002687	0.017551	Body

Bold font indicates probes which are common between this study and our previous work (98).

Table A3.3: RRMS DMRs outside the MHC locus

Probe ID	**Chr**	**Position**	**Gene**	**Median (case)**	**Median (control)**	**Δ_{meth}**	**Adj. *p* value**	**p_{FDR}**	**Feature**
cg11766577	21	47581405	C21orf56	0.7862	0.658041	-0.12816	0.001007	0.013499	Body
cg10296238	21	47605174	C21orf56	0.305823	0.426374	0.120551	0.005319	0.018449	TSS1500
cg07747299	21	47604052	C21orf56	0.186876	0.293361	0.106484	0.003174	0.017551	5'UTR
cg13126279	21	47581558	C21orf56	0.78743	0.684086	-0.10334	0.002959	0.017551	Body
cg05875700	8	638208	ERICH1	0.319176	0.120484	-0.19869	0.004548	0.018449	Body
cg01053087	8	637909	ERICH1	0.329863	0.163553	-0.16631	0.002128	0.01639	Body
cg20601736	8	652315	ERICH1	0.755186	0.885785	0.130599	0.016012	0.029096	Body
cg12641240	8	638330	ERICH1	0.193731	0.068507	-0.12522	0.017515	0.029916	Body
cg26354017	1	2.06E+08	PM20D1	0.410684	0.598945	0.188261	0.014094	0.027884	1stExon
cg17178900	1	2.06E+08	PM20D1	0.469825	0.646248	0.176423	0.013796	0.027601	Body
cg14159672	1	2.06E+08	PM20D1	0.443619	0.616326	0.172707	0.017227	0.029915	1stExon
cg11965913	1	2.06E+08	PM20D1	0.302544	0.466796	0.164252	0.024621	0.035186	TSS200
cg24503407	1	2.06E+08	PM20D1	0.403586	0.560205	0.156619	0.014935	0.02889	TSS1500
cg14893161	1	2.06E+08	PM20D1	0.328428	0.497891	0.169463	0.008958	0.023853	5'UTR;1stExon

Table A3.4: All differentially methylated SPMS probes

Probe ID	Chr	Position	Gene	Median (case)	Median (control)	Δ_{meth}	Adj *p* value	P_{FDR}	Feature
cg06182923	1	33985406	CSMD2	0.613448	0.728753	0.115305	0.000512	0.015791	Body
cg20802616	1	211590292	C1orf97	0.426296	0.536186	0.10989	0.000818	0.015791	Body
cg07584620	1	2265881	MORN1	0.579576	0.82636	0.246784	0.003764	0.022817	Body
cg04798314	1	246668601	SMYD3	0.760551	0.492173	-0.26838	0.00745	0.027175	Body
cg15385476	1	196112818		0.681472	0.802111	0.120639	0.01076	0.03144	
cg05392448	1	2266933	MORN1	0.668357	0.809182	0.140825	0.015164	0.034438	Body
cg14669863	1	155247706	HCN3	0.168098	0.048754	-0.11934	0.021975	0.039487	Body
cg05376227	1	171111193	FMO6P	0.610546	0.720282	0.109736	0.023138	0.040449	Body
cg16675581	1	19637256	AKR7A2;PQLC2	0.64618	0.791704	0.145524	0.026244	0.042515	Body;TSS1500
cg03961283	1	223566761	C1orf65	0.217803	0.318535	0.100732	0.027373	0.042902	5'UTR;1stExon
cg25771854	1	247420421	VN1R5	0.836948	0.725852	-0.1111	0.029601	0.04386	1stExon
cg13928473	1	6063654		0.321326	0.512242	0.190916	0.035688	0.046343	
cg17753661	1	26441637	PDIK1L	0.812072	0.916511	0.10444	0.04249	0.048096	Body
cg20821187	1	200452917		0.53509	0.646455	0.111365	0.048929	0.049693	
cg04750100	2	136595281	LCT	0.449045	0.347519	-0.10153	0.000668	0.015791	TSS1500
cg23596425	2	1494263	TPO	0.715555	0.841943	0.126387	0.001234	0.017112	Body
cg24305906	2	241352106		0.716169	0.854922	0.138752	0.001268	0.017112	
cg08610773	2	184896169		0.778373	0.880754	0.102381	0.001495	0.018181	
cg17455348	2	213406960		0.390888	0.596972	0.206084	0.00225	0.019771	
cg20325573	2	236234204		0.653175	0.757113	0.103938	0.002563	0.020762	
cg20862283	2	156838956		0.564822	0.666258	0.101436	0.002656	0.020816	
cg05373263	2	3063115		0.723954	0.833038	0.109084	0.004048	0.022817	
cg03489016	2	230124603	PID1	0.709549	0.833569	0.12402	0.004874	0.0252	Body
cg15837943	2	231734413	ITM2C	0.411754	0.669383	0.257629	0.005362	0.025548	Body
cg03028786	2	224897425	SERPINE2	0.638894	0.785711	0.146818	0.006365	0.026666	5'UTR;TSS1500;Body

cg18663897	2	240900096	NDUFA10	0.585099	0.795998	0.210899	0.01179	0.03144	3'UTR
cg01290856	2	134324896	NCKAP5	0.718362	0.873496	0.155134	0.023336	0.040505	5'UTR
cg22836174	2	228231970	TM4SF20	0.608463	0.814805	0.206342	0.027691	0.042902	Body
cg10224537	2	168673805	B3GALT1	0.678081	0.817123	0.139043	0.03421	0.046044	TSS1500
cg14448393	2	164471195	FIGN	0.699979	0.593757	-0.10622	0.035243	0.046044	Body
cg18757817	2	208572165		0.613568	0.721836	0.108268	0.040246	0.047246	
cg14973360	2	9800511		0.847607	0.953549	0.105942	0.042563	0.048096	
cg18662228	2	236867804	AGAP1	0.310465	0.55812	0.247655	0.045914	0.049368	Body
cg07733481	3	122694286	SEMA5B	0.203631	0.092489	-0.11114	0.00091	0.015791	5'UTR
cg04245305	3	195940754		0.7168	0.957329	0.240529	0.001616	0.018181	
cg07093060	3	174092757		0.680138	0.471123	-0.20901	0.001721	0.018181	
cg27423959	3	126945870		0.287779	0.456109	0.16833	0.002074	0.01938	
cg15001930	3	124306820	KALRN	0.578064	0.769411	0.191348	0.003052	0.022817	Body
cg05674046	3	64211994	PRICKLE2	0.803021	0.909884	0.106862	0.003421	0.022817	TSS1500
cg04814784	3	10182561	VHL	0.582548	0.286998	-0.29555	0.003486	0.022817	TSS1500
cg24524379	3	46600244	LRRC2	0.234935	0.338452	0.103517	0.007604	0.027175	5'UTR
cg06051312	3	73045440	PPP4R2	0.824415	0.935549	0.111135	0.007899	0.027818	TSS1500
cg04156077	3	149421196	WWTR1	0.557934	0.745576	0.187642	0.014555	0.034195	TSS200
cg11108991	3	178984910	KCNMB3	0.570648	0.677315	0.106668	0.014777	0.034199	TSS200
cg05126514	3	49697458	BSN	0.394914	0.520379	0.125465	0.015634	0.034566	Body
cg10666341	3	119348585	PLA1A	0.856089	0.660493	-0.1956	0.021421	0.039487	3'UTR
cg20187719	3	13691967	LOC285375	0.143143	0.366947	0.223804	0.02786	0.042902	TSS1500
cg19726630	3	32400704	CMTM8	0.166092	0.050292	-0.1158	0.043851	0.048598	Body
cg25377865	4	72669944		0.647265	0.749341	0.102076	0.001077	0.017112	
cg01406776	4	8386748	ACOX3	0.656012	0.868224	0.212212	0.001633	0.018181	Body
cg03271827	4	726053	PCGF3	0.437336	0.628997	0.191662	0.006236	0.026666	5'UTR
cg01503299	4	2963264	NOP14	0.588444	0.692817	0.104373	0.01625	0.035256	Body
cg03640465	4	10042842	SLC2A9	0.438843	0.688466	0.249623	0.028802	0.043203	TSS1500

cg24794857	4	187113578	CYP4V2	0.228094	0.33663	0.108536	0.03058	0.044754	Body
cg16301894	4	129389744		0.584892	0.703459	0.118567	0.031364	0.044833	
cg27251155	4	8155589	ABLIM2	0.820801	0.922974	0.102173	0.034918	0.046044	Body
cg04118610	4	62707027	LPHN3	0.561343	0.67866	0.117316	0.041099	0.047479	Body
cg04277055	4	185749877		0.806784	0.940016	0.133232	0.042915	0.048096	
cg11553311	5	66541588		0.387355	0.551136	0.163781	0.000411	0.015791	
cg11791078	5	36273196	RANBP3L	0.516162	0.749421	0.233259	0.006939	0.027047	Body
cg09819502	5	36242508	C5orf33	0.076951	0.33556	0.258609	0.007012	0.027047	TSS1500
cg00268547	5	2179563		0.643432	0.748968	0.105536	0.011371	0.03144	
cg01231141	5	178692691	ADAMTS2	0.453387	0.557818	0.104431	0.01223	0.03144	Body
cg09146088	5	145305089		0.536783	0.792077	0.255295	0.012237	0.03144	
cg24844518	5	156811669	CYFIP2	0.822607	0.55309	-0.26952	0.018005	0.037033	Body
cg07601741	5	153160425	GRIA1	0.570811	0.680244	0.109433	0.018329	0.037033	Body
cg06422277	5	63458646		0.699619	0.841201	0.141582	0.020188	0.038994	
cg18236584	5	151476553		0.627348	0.760146	0.132798	0.021834	0.039487	
cg25673075	5	111963982		0.46002	0.664048	0.204028	0.021997	0.039487	
cg13653328	5	148520669	ABLIM3	0.72607	0.494983	-0.23109	0.022751	0.040062	TSS1500
cg17534070	5	168195355	SLIT3;MIR218-2	0.652943	0.779386	0.126443	0.024362	0.041424	Body;TSS200
cg04480106	5	72934606	RGNEF	0.701768	0.81463	0.112861	0.024889	0.041424	5'UTR
cg00546757	5	170845058		0.547751	0.742788	0.195037	0.027243	0.042902	
cg18803147	5	2743124		0.617812	0.505722	-0.11209	0.028445	0.043009	
cg12562822	5	1219873	SLC6A19	0.244169	0.40093	0.156761	0.034624	0.046044	Body
cg09434603	5	499552	SLC9A3	0.708705	0.819674	0.110969	0.039592	0.047225	Body
cg13913990	5	172970	PLEKHG4B	0.774701	0.577771	-0.19693	0.043999	0.048598	Body
cg24805360	5	77930038	LHFPL2	0.38465	0.546793	0.162143	0.048235	0.049457	5'UTR
cg17666981	6	28878192	TRIM27	0.80185	0.918272	0.116422	0.000132	0.012583	Body
cg24867279	6	28853021		0.440899	0.559996	0.119097	0.00119	0.017112	
cg13872627	6	31238036	HLA-C	0.467414	0.619214	0.1518	0.003559	0.022817	Body

cg03115532	6	28185726	LOC222699	0.653625	0.822196	0.168571	0.009168	0.028934	Body
cg23069046	6	6543402	LOC285780	0.684474	0.789554	0.10508	0.009168	0.028934	Body
cg25716013	6	75954053	COX7A2	0.603378	0.707249	0.103871	0.009335	0.029081	TSS1500
cg13185413	6	30039202	RNF39	0.406628	0.277418	-0.12921	0.011261	0.03144	Body
cg13604933	6	40145993		0.850344	0.651854	-0.19849	0.01739	0.036478	
cg20866694	6	27181670		0.414254	0.292546	-0.12171	0.017875	0.037033	
cg24969496	6	32606845	HLA-DQA1	0.522875	0.738345	0.21547	0.02038	0.038994	Body
cg06249604	6	30039206	RNF39	0.266341	0.160964	-0.10538	0.026962	0.042877	Body
cg00947782	6	30039142	RNF39	0.255623	0.148406	-0.10722	0.030244	0.044541	Body
cg10930308	6	30039476	RNF39	0.373728	0.263968	-0.10976	0.032706	0.04594	Body
cg14782559	6	33131893	COL11A2	0.587449	0.758851	0.171401	0.034454	0.046044	Body
cg14926196	6	37616482	MDGA1	0.374123	0.502335	0.128212	0.03798	0.047033	Body
cg03343571	6	30039175	RNF39	0.37883	0.277639	-0.10119	0.038325	0.047033	Body
cg15383120	6	291909	DUSP22	0.355595	0.485997	0.130402	0.038696	0.047033	TSS200
cg12633154	6	30039435	RNF39	0.550688	0.435403	-0.11529	0.041129	0.047479	Body
cg15820961	6	32558459	HLA-DRB1	0.741706	0.863241	0.121535	0.04313	0.048096	TSS1500
cg11235426	6	292522	DUSP22	0.323171	0.432058	0.108887	0.044658	0.048663	1stExon;5'UTR
cg02379549	6	36887307	C6orf89	0.896679	0.777463	-0.11922	0.045231	0.049067	Body
cg07365741	6	170478434		0.613454	0.456203	-0.15725	0.04713	0.049385	
cg13401893	6	30039432	RNF39	0.577691	0.469281	-0.10841	0.047292	0.049385	Body
cg08491487	6	30039130	RNF39	0.225518	0.124175	-0.10134	0.047621	0.049385	Body
cg18110333	6	292329	DUSP22	0.336236	0.480119	0.143883	0.047942	0.049385	1stExon;5'UTR
cg15744124	6	32306089	C6orf10	0.695888	0.828451	0.132563	0.049399	0.049693	Body
cg21901928	7	55139847	EGFR	0.664807	0.801655	0.136848	0.000164	0.012583	Body
cg14170201	7	155191709		0.658967	0.891026	0.23206	0.000847	0.015791	
cg09756125	7	158250978	PTPRN2	0.741593	0.514513	-0.22708	0.001714	0.018181	Body
cg18850127	7	39170497	POU6F2	0.679178	0.501934	-0.17724	0.003236	0.022817	Body
cg20302533	7	39170763	POU6F2	0.684205	0.531256	-0.15295	0.004059	0.022817	Body

cg00859877	7	158246263	PTPRN2	0.592679	0.85617	0.263491	0.006854	0.027047	Body
cg15212455	7	39170539	POU6F2	0.778134	0.66443	-0.1137	0.008333	0.028434	Body
cg19195077	7	47778880		0.456591	0.620059	0.163468	0.017125	0.036478	
cg05541356	7	150903922		0.326318	0.479816	0.153498	0.020339	0.038994	
cg23549902	7	5184155		0.37424	0.478793	0.104553	0.024727	0.041424	
cg22109827	7	30727326		0.735974	0.466243	-0.26973	0.027936	0.042902	
cg25709790	7	24742552	DFNA5	0.599622	0.780914	0.181292	0.030771	0.044754	Body
cg09281805	7	4751840	FOXK1	0.533396	0.751872	0.218476	0.031125	0.044754	Body
cg00867835	7	149484985	SSPO	0.653832	0.533157	-0.12067	0.035159	0.046044	Body
cg19389973	7	36692197	AOAH	0.482959	0.690356	0.207397	0.037756	0.047033	Body
cg16618979	7	143108841		0.917679	0.724636	-0.19304	0.038731	0.047033	
cg16576544	7	129410227	MIR182	0.757646	0.85802	0.100374	0.038778	0.047033	Body
cg09546755	7	132424008		0.648499	0.762903	0.114404	0.039678	0.047225	
cg20026367	7	130875551	MKLN1	0.762934	0.872693	0.109759	0.040034	0.047225	Body
cg10900271	7	156157852		0.819961	0.56028	-0.25968	0.044336	0.048663	
cg22535849	7	4118583	SDK1	0.792579	0.609142	-0.18344	0.045817	0.049368	Body
cg01760090	8	1365659		0.45751	0.586951	0.129442	0.004064	0.022817	
cg04123498	8	142283564		0.8625	0.545042	-0.31746	0.004106	0.022817	
cg13070650	8	99490901	STK3	0.85201	0.749864	-0.10215	0.007584	0.027175	Body
cg19128026	8	1792615	ARHGEF10	0.752932	0.855117	0.102184	0.012027	0.03144	Body
cg02490460	8	1365502		0.593412	0.702811	0.109399	0.014333	0.034147	
cg19787013	8	145737513	RECQL4	0.456545	0.692351	0.235805	0.021576	0.039487	Body
cg21512324	8	89718417		0.675024	0.794211	0.119187	0.024498	0.041424	
cg09019154	8	19616280		0.507047	0.310656	-0.19639	0.037667	0.047033	
cg26077133	8	10049871	MSRA	0.644693	0.430444	-0.21425	0.043147	0.048096	Body
cg17531142	8	128940078	PVT1	0.646113	0.768895	0.122782	0.049693	0.049693	Body
cg13876960	9	9998791	PTPRD	0.488714	0.603157	0.114443	0.002375	0.019901	5'UTR
cg13890969	9	113804367		0.616747	0.732108	0.115361	0.01384	0.03397	

cg14451627	9	115987035	SLC31A1	0.813929	0.923608	0.109678	0.024693	0.041424	5'UTR
cg21177183	9	129281647		0.759673	0.882018	0.122345	0.043091	0.048096	
cg14117219	9	94476689		0.073225	0.182177	0.108952	0.049571	0.049693	
cg08751451	10	53287690	PRKG1	0.585886	0.706745	0.120859	0.005619	0.026257	Body
cg15393936	10	15354631	FAM171A1	0.689283	0.843025	0.153742	0.006213	0.026666	Body
cg13754569	10	134956778		0.718748	0.908916	0.190168	0.007598	0.027175	
cg24668570	10	134973778	KNDC1	0.292176	0.109391	-0.18278	0.00889	0.028934	TSS200
cg14609104	10	111989324	MXI1	0.73054	0.911835	0.181295	0.008992	0.028934	Body
cg19301501	10	22768167		0.770547	0.87322	0.102673	0.012372	0.03144	
cg11005552	10	105648138	OBFC1	0.340865	0.442656	0.101791	0.012421	0.03144	Body
cg23479191	10	54338992		0.594593	0.701234	0.10664	0.013518	0.03352	
cg20245361	10	71725755		0.725305	0.860217	0.134912	0.028072	0.042902	
cg01512466	10	125624685	CPXM2	0.724984	0.855813	0.130829	0.028496	0.043009	Body
cg14964115	10	116634877	FAM160B1	0.451246	0.602083	0.150837	0.032999	0.046044	Body
cg23698271	10	121346762	TIAL1	0.599016	0.783631	0.184615	0.033739	0.046044	Body
cg18621672	10	82112873	DYDC1	0.278917	0.45743	0.178513	0.037615	0.047033	5'UTR
cg00817464	10	111662876	XPNPEP1	0.516173	0.726959	0.210786	0.039688	0.047225	Body
cg24051234	10	111912029		0.71876	0.865647	0.146887	0.041227	0.047479	
cg27057480	10	49659559	ARHGAP22	0.228219	0.358829	0.13061	0.047562	0.049385	Body
cg04913265	11	133939627	JAM3	0.515099	0.645977	0.130878	0.00015	0.012583	Body
cg05792312	11	61781116		0.301228	0.624272	0.323044	0.000822	0.015791	
cg06394820	11	60608291	CCDC86	0.565686	0.776733	0.211047	0.006273	0.026666	TSS1500
cg08912652	11	130779479	SNX19	0.701171	0.87019	0.169019	0.022262	0.039487	Body
cg10662047	11	123472546	GRAMD1B	0.527266	0.791022	0.263756	0.025832	0.042413	Body
cg14512156	11	660597	DEAF1	0.712934	0.859028	0.146094	0.031615	0.044927	Body
cg26864826	11	33760479		0.491878	0.245368	-0.24651	0.03384	0.046044	
cg19680693	11	94111807	GPR83	0.495187	0.320769	-0.17442	0.038505	0.047033	3'UTR
cg19471911	11	102079985	YAP1	0.396051	0.613639	0.217588	0.039951	0.047225	Body

cg17187785	11	132107476	NTM	0.914946	0.743543	-0.1714	0.047884	0.049385	Body
cg10578777	12	7781093		0.728872	0.905711	0.17684	0.003724	0.022817	
cg11748730	12	99815844	ANKS1B	0.384339	0.484957	0.100618	0.006528	0.026887	Body
cg14906510	12	7781169		0.805048	0.910312	0.105263	0.007351	0.027175	
cg25828445	12	7781288		0.75044	0.892315	0.141876	0.010161	0.030863	
cg05565442	12	58011856		0.300373	0.556137	0.255764	0.011112	0.03144	
cg08762603	12	2031417		0.651426	0.755396	0.103971	0.011647	0.03144	
cg25198316	12	48598048	OR10AD1	0.753209	0.91442	0.161211	0.015647	0.034566	TSS1500
cg08693745	12	132286231		0.576389	0.719436	0.143047	0.029051	0.043309	
cg14912045	12	117184799	RNFT2	0.734524	0.841404	0.106879	0.038098	0.047033	Body
cg18446441	13	32480222	EEF1DP3	0.760913	0.874419	0.113506	0.026134	0.042515	Body
cg24702069	13	109352806	MYO16	0.150338	0.270571	0.120233	0.046485	0.049385	Body
cg26813483	13	111980537	C13orf16	0.181445	0.314982	0.133537	0.047721	0.049385	Body
cg23881368	13	47472343	HTR2A	0.681471	0.560657	-0.12081	0.047759	0.049385	TSS1500
cg24320398	13	47472158	HTR2A	0.786896	0.627135	-0.15976	0.049284	0.049693	TSS1500
cg16706502	14	31927974	C14orf126	0.10314	0.485653	0.382514	0.000633	0.015791	TSS1500
cg05122082	14	20710905	OR11H4	0.724618	0.840612	0.115994	0.002072	0.01938	TSS200
cg22824376	14	77648248	TMEM63C	0.240042	0.119732	-0.12031	0.003903	0.022817	5'UTR
cg14293999	14	101840368		0.461624	0.77028	0.308656	0.004815	0.0252	
cg16147201	14	105041159		0.534088	0.750436	0.216347	0.00841	0.028434	
cg13528570	14	105708343	BRF1	0.698573	0.878507	0.179933	0.008912	0.028934	Body;5'UTR
cg11186706	14	54815745		0.67984	0.86824	0.1884	0.013491	0.03352	
cg24976563	14	24587638	DCAF11	0.704412	0.934959	0.230547	0.01495	0.034273	Body
cg14218851	14	103018726		0.610948	0.460758	-0.15019	0.0209	0.039487	
cg21193926	14	76443578	TGFB3	0.195675	0.418231	0.222556	0.02204	0.039487	Body
cg23022053	14	52733243	PTGDR	0.893364	0.699746	-0.19362	0.041012	0.047479	TSS1500
cg04579183	15	88119834	NCRNA00052	0.469611	0.811179	0.341567	0.000207	0.012583	TSS1500
cg21557108	15	50410962	ATP8B4	0.237793	0.35237	0.114577	0.018359	0.037033	5'UTR

cg23009094	15	101862689	PCSK6	0.768406	0.892074	0.123668	0.022203	0.039487	Body
cg21829038	15	101593831	LRRK1	0.742025	0.925927	0.183902	0.033253	0.046044	Body
cg27018984	15	90796557	TTLL13	0.755236	0.896252	0.141017	0.034676	0.046044	Body
cg03478313	15	93655850		0.744629	0.893277	0.148648	0.035854	0.046343	
cg27634195	16	1440421		0.637084	0.509941	-0.12714	0.004754	0.0252	
cg06394109	16	1152511		0.550503	0.774634	0.224131	0.009752	0.029997	
cg04004158	16	1152474		0.724891	0.826409	0.101518	0.012162	0.03144	
cg05185784	16	90016020	DEF8	0.572342	0.688635	0.116293	0.012321	0.03144	5'UTR;Body
cg07869343	16	1797050	MAPK8IP3	0.793063	0.91519	0.122128	0.038904	0.047033	Body
cg00645020	16	84693148	KLHL36	0.666618	0.535202	-0.13142	0.047963	0.049385	Body
cg01401135	17	76522783	DNAH17	0.83475	0.954378	0.119628	0.014011	0.034046	Body
cg07973125	17	54858770		0.928315	0.6821	-0.24622	0.017413	0.036478	
cg02159489	17	79459563		0.678078	0.85289	0.174812	0.018593	0.037033	
cg14957731	17	39165697	KRTAP3-1	0.614446	0.732681	0.118235	0.019068	0.03767	TSS1500
cg20663042	17	6734940	TEKT1	0.144001	0.247326	0.103325	0.02454	0.041424	5'UTR
cg00901687	17	48585270	MYCBPAP	0.621566	0.741851	0.120286	0.025301	0.041824	TSS1500
cg25988106	17	7258481	TMEM95	0.499592	0.722502	0.222911	0.026996	0.042877	TSS200
cg08102564	17	19620263	SLC47A2	0.563148	0.446589	-0.11656	0.035135	0.046044	TSS1500
cg23633026	17	34067305	RASL10B	0.594436	0.735079	0.140643	0.042865	0.048096	Body
cg13590055	18	77917647	LOC100130522;PARD6G	0.273641	0.377314	0.103673	0.011909	0.03144	Body;3'UTR
cg20094343	18	34917603	BRUNOL4	0.263903	0.438243	0.17434	0.011962	0.03144	Body
cg19815565	18	77917615	LOC100130522;PARD6G	0.250322	0.353988	0.103665	0.014232	0.034147	Body;3'UTR
cg07258983	18	42255459		0.69047	0.848518	0.158048	0.030974	0.044754	
cg05900567	19	37466940		0.442992	0.676886	0.233893	0.005067	0.025265	
cg10771931	19	34972145	WTIP	0.718033	0.89071	0.172677	0.008425	0.028434	TSS1500
cg16253115	19	33781998		0.831872	0.941227	0.109354	0.011671	0.03144	
cg18437039	19	1444202		0.458154	0.582318	0.124164	0.015896	0.034799	
cg08835041	19	37461278		0.755358	0.876124	0.120767	0.016656	0.035818	

cg26562263	19	21863715		0.229641	0.345673	0.116031	0.034378	0.046044	
cg04515524	19	17489148	PLVAP	0.048071	0.178275	0.130204	0.044595	0.048663	TSS1500
cg11495604	20	62053198	KCNQ2	0.79919	0.98268	0.18349	0.002278	0.019771	Body
cg17811452	20	44007674	TP53TG5;SYS1-DBNDD2	0.52683	0.294003	-0.23283	0.004131	0.022817	TSS1500;Body
cg12099423	20	61590751	SLC17A9	0.259185	0.375558	0.116373	0.005095	0.025265	Body
cg17221813	20	61590823	SLC17A9	0.388501	0.524941	0.136441	0.005229	0.025412	Body
cg09595245	20	44649233	SLC12A5	0.830374	0.930548	0.100174	0.005821	0.026666	TSS1500
cg19223824	20	44682963	SLC12A5	0.635471	0.871532	0.236061	0.006051	0.026666	Body
cg19142181	20	61591066	SLC17A9	0.366628	0.538726	0.172098	0.006707	0.027047	Body
cg12751644	20	60527061		0.64485	0.529829	-0.11502	0.014635	0.034195	
cg00704664	20	60500578	CDH4	0.268554	0.483874	0.215321	0.032512	0.045933	Body
cg18819889	20	60119597	CDH4	0.728146	0.874762	0.146617	0.048598	0.049619	Body
cg04985582	21	15645988	ABCC13	0.437947	0.555831	0.117885	0.020097	0.038994	TSS200
cg00607912	21	43240355	PRDM15	0.846525	0.965583	0.119058	0.026566	0.042751	Body
cg10543947	22	36635882	APOL2	0.209491	0.074167	-0.13532	0.000684	0.015791	TSS200;1stExon;5'UTR
cg16121206	22	36636055	APOL2	0.518891	0.394903	-0.12399	0.000745	0.015791	TSS200;TSS1500
cg02018040	22	27152963		0.761077	0.547243	-0.21383	0.018497	0.037033	
cg01234546	22	50723473	PLXNB2	0.806808	0.565704	-0.2411	0.022203	0.039487	Body
cg19470385	22	46446562	C22orf26	0.753671	0.856455	0.102784	0.037526	0.047033	3'UTR
cg09219182	22	37255542	NCF4	0.535842	0.754528	0.218686	0.037891	0.047033	TSS1500
cg23887839	NA	NA	NA	0.655725	0.360589	-0.29514	0.001886	0.019093	NA
cg24139837	X	3730151		0.261992	0.080879	-0.18111	0.015309	0.034445	

Table A3.5: SPMS DMRs within the MHC

Probe ID	Chr	Position	Gene	Median (case)	Median (control)	Δ_{meth}	Adj. *p* value	P_{FDR}	Feature
cg13185413	6	30039202	RNF39	0.40662837	0.2774177	-0.12921067	0.011260733	0.031440175	Body
cg06249604	6	30039206	RNF39	0.266340697	0.160964176	-0.105376521	0.026962202	0.042876543	Body
cg00947782	6	30039142	RNF39	0.255622964	0.148405783	-0.107217181	0.030243898	0.044541014	Body
cg10930308	6	30039476	RNF39	0.373728199	0.263967562	-0.109760637	0.03270644	0.045940259	Body
cg03343571	6	30039175	RNF39	0.378829882	0.277638722	-0.10119116	0.038325094	0.047033022	Body
cg12633154	6	30039435	RNF39	0.550688103	0.435403086	-0.115285017	0.041129289	0.047479204	Body
cg13401893	6	30039432	RNF39	0.577691457	0.469281157	-0.1084103	0.047291604	0.049385389	Body
cg08491487	6	30039130	RNF39	0.225517557	0.124174938	-0.101342619	0.04762052	0.049385389	Body
cg15383120	6	291909	DUSP22	0.35559474	0.485996596	0.130401856	0.038696026	0.047033022	TSS200
cg11235426	6	292522	DUSP22	0.323171335	0.432058198	0.108886863	0.044657615	0.048662783	1stExon;5'UTR
cg18110333	6	292329	DUSP22	0.336235687	0.480119023	0.143883336	0.047941744	0.049385389	1stExon;5'UTR
cg18850127	7	39170497	POU6F2	0.679178294	0.501934444	-0.17724385	0.003236295	0.022816897	Body
cg20302533	7	39170763	POU6F2	0.684204571	0.531256436	-0.152948135	0.004058751	0.022816897	Body
cg15212455	7	39170539	POU6F2	0.778133703	0.664430196	-0.113703507	0.008332628	0.028433856	Body
cg23881368	13	47472343	HTR2A	0.681470902	0.560657426	-0.120813476	0.047759105	0.049385389	TSS1500
cg24320398	13	47472158	HTR2A	0.786896069	0.627134741	-0.159761328	0.049283649	0.049692891	TSS1500
cg13590055	18	77917647	LOC100130522;PARD6G	0.273640951	0.377314174	0.103673223	0.011909407	0.031440175	Body;3'UTR
cg19815565	18	77917615	LOC100130522;PARD6G	0.250322353	0.353987748	0.103665395	0.014231871	0.034147073	Body;3'UTR
cg12099423	20	61590751	SLC17A9	0.259185276	0.37555796	0.116372684	0.005094544	0.025264782	Body
cg17221813	20	61590823	SLC17A9	0.388500876	0.524941381	0.136440505	0.005228754	0.025411747	Body
cg19142181	20	61591066	SLC17A9	0.366627625	0.538725837	0.172098212	0.006707346	0.027047422	Body
cg10543947	22	36635882	APOL2	0.209491257	0.074166907	-0.13532435	0.000684484	0.015791453	TSS200;1stExon;5'UTR
cg16121206	22	36636055	APOL2	0.5188908	0.394902851	-0.123987949	0.000745084	0.015791453	TSS200;TSS1500

APPENDIX FOUR

C-MYC is *DROSHA*'s transcription factor, and we therefore performed RT-qPCR to determine whether it is a contributing factor in the down-regulation of *DROSHA* that we reported. Figure A4.1 demonstrates that there was no significant difference in expression of *C-MYC* between MS patients and their respective HCs.

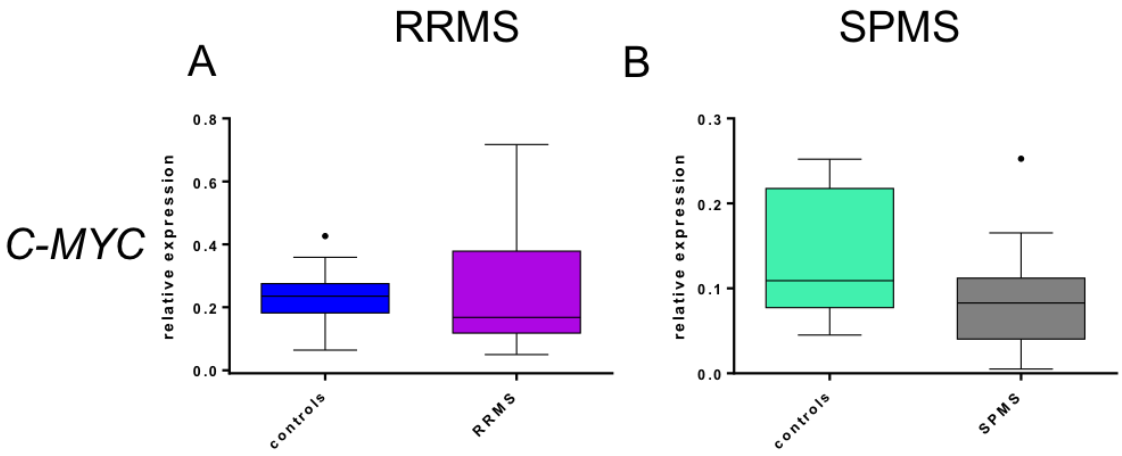

Figure A4.1 Tukey boxplot of expression relative to *GAPDH* of *C-MYC* in (A) HC (blue) and RRMS (pink), and (B) HC (green) and SPMS (grey). Whiskers represent data within 1.5 interquartile range (IQR) of the upper and lower quartile. Data points outside of the 1.5 IQR are represented by black dots.

APPENDIX FIVE

Luxol Fast Blue - Periodic Acid-Schiff staining **and** Pathology Criteria

Equipment

Plate at 58°C

Oven at 60°C

Cover slips

Reagents

Acetic acid (10%)

Acid alcohol

Scott blue solution

dH_2O

DPX (mounting fluid)

EtOH (70, 95 and 100%)

Haematoxylin

Lithium carbonate

Luxol fast blue

Periodic acid

Schiff's reagent

Xylene

Preparation of stains

1% Periodic Acid – Store at 4°C

Periodic acid (Sigma P7578-25G)	1g
dH_2O	100ml

0.1% Luxol Fast Blue – Store at room temperature for 12 months (re-usable)

Luxol Fast Blue	0.1g
95% EtOH	100ml
10% Acetic acid	0.5ml

Saturated Lithium Carbonate

Lithium carbonate	1g
dH_2O	100ml

Protocol

Provided by Brain and Mind Research Institute, Sydney

Approximate time to complete – 5 hours

1. Bring Schiff's reagent to room temperature.
2. De-wax sections at 58°C for 20 min.
3. Deparaffinise sections:
    a. 2x Xylene 5 min
    b. 2x 100% EtOH 5 min
    c. 95% EtoH 5 min
    d. 70% EtOH 5 min
    e. 2x dH_2O 5 min
4. Place sections in 1% periodic acid solution for 10 min.
5. Wash sections in:
    a. Running tap water for 4 min
    b. dH_2O for 1 min
6. Pipette Schiff's reagent onto sections and sit for 30 min.
7. Wash sections in running tap water for 10 min.
8. Set oven to 60°C.
9. Wash sections in:
    a. 70% EtOH for 1 min
    b. 95% EtOH for 1 min
10. Stain sections with 0.1% LFB at 60°C for 2 hours.
11. Cool slides in tap water for 5 min.
12. Differentiate sections in lithium carbonate (1/3 tap water and 2/3 saturated solution of lithium carbonate) (2-3 dips).
13. Place sections in tap water for 5 min.
14. Counter stain with Haematoxylin:
    a. Place slides in haematoxylin for 30 secs
    b. Wash in running tap water for 1 min
    c. Dip 2 times in acid alcohol
    d. Wash in running tap water for 1 min
    e. Scott blue solution 2 min

15. Dehydrate sections:
    a. 70% EtOH 3 min
    b. 95% EtOH 3 min
    c. 2x 100% EtOH 5 min

d. Xylene 6 min
e. Xylene 3 min

16. Mount coverslip (DPX or appropriate substitute)

Criteria for identifying MS related pathology

Normal appearing white matter: Consistent myelin coverage (LFB positive) with oligodendrocytes exhibiting normal pathology, parallel to the axons.

Active Lesion: LFB positive material (i.e. phagocytosed myelin) seen clustered within macrophages.

Recently active lesion: Presence of macrophages containing PAS positive material. Indicative of myelin phagocytosed a while ago; the macrophages are no longer actively attacking the myelin.

Chronic lesion: Absence of LFB positive material. Astrocytes can be clearly seen.

Remyelinated lesion: Patchy areas of myelin and few oligodendrocytes. No evidence of macrophage activity.

REFERENCES

1. Koch-Henriksen N, Sorensen PS. The changing demographic pattern of multiple sclerosis epidemiology. Lancet neurology. 2010;9(5):520-32.
2. Kalincik T, Vivek V, Jokubaitis V, Lechner-Scott J, Trojano M, Izquierdo G, et al. Sex as a determinant of relapse incidence and progressive course of multiple sclerosis. Brain. 2013.
3. Ebers GC, Bulman DE, Sadovnick AD, Paty DW, Warren S, Hader W, et al. A population-based study of multiple sclerosis in twins. N Engl J Med. 1986;315(26):1638-42.
4. Willer CJ, Dyment DA, Risch NJ, Sadovnick AD, Ebers GC, Canadian Collaborative Study G. Twin concordance and sibling recurrence rates in multiple sclerosis. Proc Natl Acad Sci U S A. 2003;100(22):12877-82.
5. Koch M, Uyttenboogaart M, van Harten A, De Keyser J. Factors associated with the risk of secondary progression in multiple sclerosis. Mult Scler. 2008;14(6):799-803.
6. Scalfari A, Neuhaus A, Daumer M, Muraro PA, Ebers GC. Onset of secondary progressive phase and long-term evolution of multiple sclerosis. J Neurol Neurosurg Psychiatry. 2013.
7. Tutuncu M, Tang J, Zeid NA, Kale N, Crusan DJ, Atkinson EJ, et al. Onset of progressive phase is an age-dependent clinical milestone in multiple sclerosis. Mult Scler. 2013;19(2):188-98.
8. Lorscheider J, Buzzard K, Jokubaitis V, Spelman T, Havrdova E, Horakova D, et al. Defining secondary progressive multiple sclerosis. Brain. 2016;139(Pt 9):2395-405.
9. Trapp BD, Nave KA. Multiple sclerosis: an immune or neurodegenerative disorder? Annual review of neuroscience. 2008;31:247-69.
10. D'Amico E, Patti F, Zanghi A, Zappia M. A Personalized Approach in Progressive Multiple Sclerosis: The Current Status of Disease Modifying Therapies (DMTs) and Future Perspectives. Int J Mol Sci. 2016;17(10).
11. McDonnell GV, Hawkins SA. Primary progressive multiple sclerosis: increasing clarity but many unanswered questions. Journal of the neurological sciences. 2002;199(1-2):1-15.
12. Cottrell DA, Kremenchutzky M, Rice GP, Koopman WJ, Hader W, Baskerville J, et al. The natural history of multiple sclerosis: a geographically based study. 5. The clinical features and natural history of primary progressive multiple sclerosis. Brain. 1999;122 (Pt 4):625-39.
13. Thompson A. Overview of primary progressive multiple sclerosis (PPMS): similarities and differences from other forms of MS, diagnostic criteria, pros and cons of progressive diagnosis. Mult Scler. 2004;10 Suppl 1:S2-7.
14. Miller DH, Weinshenker BG, Filippi M, Banwell BL, Cohen JA, Freedman MS, et al. Differential diagnosis of suspected multiple sclerosis: a consensus approach. Mult Scler. 2008;14(9):1157-74.
15. McDonald WI, Compston A, Edan G, Goodkin D, Hartung HP, Lublin FD, et al. Recommended diagnostic criteria for multiple sclerosis: guidelines from the International Panel on the diagnosis of multiple sclerosis. Ann Neurol. 2001;50(1):121-7.
16. Polman CH, Reingold SC, Edan G, Filippi M, Hartung HP, Kappos L, et al. Diagnostic criteria for multiple sclerosis: 2005 revisions to the "McDonald Criteria". Ann Neurol. 2005;58(6):840-6.
17. Kurtzke JF. Rating neurologic impairment in multiple sclerosis: an expanded disability status scale (EDSS). Neurology. 1983;33(11):1444-52.

18. Broux B, Stinissen P, Hellings N. Which immune cells matter? The immunopathogenesis of multiple sclerosis. Critical reviews in immunology. 2013;33(4):283-306.
19. Neuwelt EA, Bauer B, Fahlke C, Fricker G, Iadecola C, Janigro D, et al. Engaging neuroscience to advance translational research in brain barrier biology. Nature reviews Neuroscience. 2011;12(3):169-82.
20. Engelhardt B, Ransohoff RM. The ins and outs of T-lymphocyte trafficking to the CNS: anatomical sites and molecular mechanisms. Trends in immunology. 2005;26(9):485-95.
21. Ransohoff RM, Kivisakk P, Kidd G. Three or more routes for leukocyte migration into the central nervous system. Nature reviews Immunology. 2003;3(7):569-81.
22. Man S, Ubogu EE, Ransohoff RM. Inflammatory cell migration into the central nervous system: a few new twists on an old tale. Brain pathology. 2007;17(2):243-50.
23. Louveau A, Smirnov I, Keyes TJ, Eccles JD, Rouhani SJ, Peske JD, et al. Structural and functional features of central nervous system lymphatic vessels. Nature. 2015;523(7560):337-41.
24. Abbott NJ, Ronnback L, Hansson E. Astrocyte-endothelial interactions at the blood-brain barrier. Nature reviews Neuroscience. 2006;7(1):41-53.
25. Miljkovic D, Timotijevic G, Mostarica Stojkovic M. Astrocytes in the tempest of multiple sclerosis. FEBS letters. 2011;585(23):3781-8.
26. Larochelle C, Alvarez JI, Prat A. How do immune cells overcome the blood-brain barrier in multiple sclerosis? FEBS letters. 2011;585(23):3770-80.
27. Ludowyk PA, Willenborg DO, Parish CR. Selective localisation of neuro-specific T lymphocytes in the central nervous system. J Neuroimmunol. 1992;37(3):237-50.
28. Lassmann H, Bruck W, Lucchinetti CF. The immunopathology of multiple sclerosis: an overview. Brain pathology. 2007;17(2):210-8.
29. Holman DW, Klein RS, Ransohoff RM. The blood-brain barrier, chemokines and multiple sclerosis. Biochimica et biophysica acta. 2011;1812(2):220-30.
30. Biernacki K, Prat A, Blain M, Antel JP. Regulation of cellular and molecular trafficking across human brain endothelial cells by Th1- and Th2-polarized lymphocytes. J Neuropathol Exp Neurol. 2004;63(3):223-32.
31. Chitnis T. The role of CD4 T cells in the pathogenesis of multiple sclerosis. Int Rev Neurobiol. 2007;79:43-72.
32. Segal BM. Stage-specific immune dysregulation in multiple sclerosis. Journal of interferon & cytokine research : the official journal of the International Society for Interferon and Cytokine Research. 2014;34(8):633-40.
33. Kuhlmann T, Lingfeld G, Bitsch A, Schuchardt J, Bruck W. Acute axonal damage in multiple sclerosis is most extensive in early disease stages and decreases over time. Brain. 2002;125(Pt 10):2202-12.
34. Bjartmar C, Wujek JR, Trapp BD. Axonal loss in the pathology of MS: consequences for understanding the progressive phase of the disease. Journal of the neurological sciences. 2003;206(2):165-71.
35. Williams A, Piaton G, Aigrot MS, Belhadi A, Theaudin M, Petermann F, et al. Semaphorin 3A and 3F: key players in myelin repair in multiple sclerosis? Brain. 2007;130(Pt 10):2554-65.
36. Compston A, Coles A. Multiple sclerosis. Lancet. 2008;372(9648):1502-17.
37. Brownell B, Hughes JT. The distribution of plaques in the cerebrum in multiple sclerosis. J Neurol Neurosurg Psychiatry. 1962;25:315-20.

38. Lassmann H, Bruck W, Lucchinetti C. Heterogeneity of multiple sclerosis pathogenesis: implications for diagnosis and therapy. Trends Mol Med. 2001;7(3):115-21.
39. Gay D, Esiri M. Blood-brain barrier damage in acute multiple sclerosis plaques. An immunocytological study. Brain. 1991;114 (Pt 1B):557-72.
40. Barkhof F, Bruck W, De Groot CJ, Bergers E, Hulshof S, Geurts J, et al. Remyelinated lesions in multiple sclerosis: magnetic resonance image appearance. Arch Neurol. 2003;60(8):1073-81.
41. Melief J, Schuurman KG, van de Garde MD, Smolders J, van Eijk M, Hamann J, et al. Microglia in normal appearing white matter of multiple sclerosis are alerted but immunosuppressed. Glia. 2013;61(11):1848-61.
42. Recks MS, Stormanns ER, Bader J, Arnhold S, Addicks K, Kuerten S. Early axonal damage and progressive myelin pathology define the kinetics of CNS histopathology in a mouse model of multiple sclerosis. Clin Immunol. 2013;149(1):32-45.
43. Ge Y, Law M, Grossman RI. Applications of diffusion tensor MR imaging in multiple sclerosis. Ann N Y Acad Sci. 2005;1064:202-19.
44. Schmierer K, Wheeler-Kingshott CA, Boulby PA, Scaravilli F, Altmann DR, Barker GJ, et al. Diffusion tensor imaging of post mortem multiple sclerosis brain. NeuroImage. 2007;35(2):467-77.
45. Rovaris M, Agosta F, Pagani E, Filippi M. Diffusion tensor MR imaging. Neuroimaging clinics of North America. 2009;19(1):37-43.
46. Genova HM, DeLuca J, Chiaravalloti N, Wylie G. The relationship between executive functioning, processing speed, and white matter integrity in multiple sclerosis. Journal of clinical and experimental neuropsychology. 2013;35(6):631-41.
47. Jaenisch R, Bird A. Epigenetic regulation of gene expression: how the genome integrates intrinsic and environmental signals. Nature genetics. 2003;33 Suppl:245-54.
48. Skinner MK, Manikkam M, Guerrero-Bosagna C. Epigenetic transgenerational actions of environmental factors in disease etiology. Trends in endocrinology and metabolism: TEM. 2010;21(4):214-22.
49. Wan ES, Qiu W, Baccarelli A, Carey VJ, Bacherman H, Rennard SI, et al. Cigarette smoking behaviors and time since quitting are associated with differential DNA methylation across the human genome. Hum Mol Genet. 2012;21(13):3073-82.
50. Zhou Y, Simpson S, Jr., Holloway AF, Charlesworth J, van der Mei I, Taylor BV. The potential role of epigenetic modifications in the heritability of multiple sclerosis. Mult Scler. 2014;20(2):135-40.
51. Simpson S, Jr., Blizzard L, Otahal P, Van der Mei I, Taylor B. Latitude is significantly associated with the prevalence of multiple sclerosis: a meta-analysis. J Neurol Neurosurg Psychiatry. 2011;82(10):1132-41.
52. Munger KL, Levin LI, Hollis BW, Howard NS, Ascherio A. Serum 25-hydroxyvitamin D levels and risk of multiple sclerosis. JAMA : the journal of the American Medical Association. 2006;296(23):2832-8.
53. Pereira F, Barbachano A, Singh PK, Campbell MJ, Munoz A, Larriba MJ. Vitamin D has wide regulatory effects on histone demethylase genes. Cell Cycle. 2012;11(6):1081-9.
54. Smolders J, Menheere P, Kessels A, Damoiseaux J, Hupperts R. Association of vitamin D metabolite levels with relapse rate and disability in multiple sclerosis. Mult Scler. 2008;14(9):1220-4.

55. Simpson S, Jr., Taylor B, Blizzard L, Ponsonby AL, Pittas F, Tremlett H, et al. Higher 25-hydroxyvitamin D is associated with lower relapse risk in multiple sclerosis. Ann Neurol. 2010;68(2):193-203.
56. Hart PH, Gorman S, Finlay-Jones JJ. Modulation of the immune system by UV radiation: more than just the effects of vitamin D? Nature reviews Immunology. 2011;11(9):584-96.
57. Hernán MA, Olek MJ, Ascherio A. Cigarette smoking and incidence of multiple sclerosis. American journal of epidemiology. 2001;154(1):69-74.
58. Hou L, Wang D, Baccarelli A. Environmental chemicals and microRNAs. Mutation research. 2011;714(1-2):105-12.
59. Marczylo EL, Amoako AA, Konje JC, Gant TW, Marczylo TH. Smoking induces differential miRNA expression in human spermatozoa: a potential transgenerational epigenetic concern? Epigenetics : official journal of the DNA Methylation Society. 2012;7(5):432-9.
60. Banerjee A, Luettich K. MicroRNAs as potential biomarkers of smoking-related diseases. Biomarkers in medicine. 2012;6(5):671-84.
61. Ito K, Lim S, Caramori G, Chung KF, Barnes PJ, Adcock IM. Cigarette smoking reduces histone deacetylase 2 expression, enhances cytokine expression, and inhibits glucocorticoid actions in alveolar macrophages. FASEB journal : official publication of the Federation of American Societies for Experimental Biology. 2001;15(6):1110-2.
62. Chen D, Fang L, Li H, Tang MS, Jin C. Cigarette smoke component acrolein modulates chromatin assembly by inhibiting histone acetylation. J Biol Chem. 2013;288(30):21678-87.
63. Yang SR, Chida AS, Bauter MR, Shafiq N, Seweryniak K, Maggirwar SB, et al. Cigarette smoke induces proinflammatory cytokine release by activation of NF-kappaB and posttranslational modifications of histone deacetylase in macrophages. American journal of physiology Lung cellular and molecular physiology. 2006;291(1):L46-57.
64. Ascherio A, Munger KL. Environmental risk factors for multiple sclerosis. Part I: the role of infection. Ann Neurol. 2007;61(4):288-99.
65. Handel AE, Williamson AJ, Disanto G, Handunnetthi L, Giovannoni G, Ramagopalan SV. An updated meta-analysis of risk of multiple sclerosis following infectious mononucleosis. PLoS One. 2010;5(9).
66. Niller HH, Wolf H, Minarovits J. Epigenetic dysregulation of the host cell genome in Epstein-Barr virus-associated neoplasia. Seminars in cancer biology. 2009;19(3):158-64.
67. Godshalk SE, Bhaduri-McIntosh S, Slack FJ. Epstein-Barr virus-mediated dysregulation of human microRNA expression. Cell Cycle. 2008;7(22):3595-600.
68. Pfeffer S, Zavolan M, Grasser FA, Chien M, Russo JJ, Ju J, et al. Identification of virus-encoded microRNAs. Science. 2004;304(5671):734-6.
69. Sievers C, Meira M, Hoffmann F, Fontoura P, Kappos L, Lindberg RL. Altered microRNA expression in B lymphocytes in multiple sclerosis: towards a better understanding of treatment effects. Clin Immunol. 2012;144(1):70-9.
70. Kleinewietfeld M, Manzel A, Titze J, Kvakan H, Yosef N, Linker RA, et al. Sodium chloride drives autoimmune disease by the induction of pathogenic TH17 cells. Nature. 2013;496(7446):518-22.
71. Farez MF, Fiol MP, Gaitan MI, Quintana FJ, Correale J. Sodium intake is associated with increased disease activity in multiple sclerosis. J Neurol Neurosurg Psychiatry. 2015;86(1):26-31.

72. Wang YJ, Li R, Yan JW, Wan YN, Tao JH, Chen B, et al. The epidemiology of alcohol consumption and multiple sclerosis: a review. Neurol Sci. 2015;36(2):189-96.
73. Langer-Gould A, Brara SM, Beaber BE, Koebnick C. Childhood obesity and risk of pediatric multiple sclerosis and clinically isolated syndrome. Neurology. 2013;80(6):548-52.
74. Munger KL, Bentzen J, Laursen B, Stenager E, Koch-Henriksen N, Sorensen TI, et al. Childhood body mass index and multiple sclerosis risk: a long-term cohort study. Mult Scler. 2013;19(10):1323-9.
75. Patsopoulos NA, Barcellos LF, Hintzen RQ, Schaefer C, van Duijn CM, Noble JA, et al. Fine-mapping the genetic association of the major histocompatibility complex in multiple sclerosis: HLA and non-HLA effects. PLoS Genet. 2013;9(11):e1003926.
76. McElroy JP, Oksenberg JR. Multiple sclerosis genetics 2010. Neurologic clinics. 2011;29(2):219-31.
77. Chao MJ, Herrera BM, Ramagopalan SV, Deluca G, Handunetthi L, Orton SM, et al. Parent-of-origin effects at the major histocompatibility complex in multiple sclerosis. Hum Mol Genet. 2010;19(18):3679-89.
78. Van der Walt A, Stankovich J, Bahlo M, Taylor BV, Van der Mei IA, Foote SJ, et al. Heterogeneity at the HLA-DRB1 allelic variation locus does not influence multiple sclerosis disease severity, brain atrophy or cognition. Mult Scler. 2011;17(3):344-52.
79. Balnyte R, Rastenyte D, Vaitkus A, Mickeviciene D, Skrodeniene E, Vitkauskiene A, et al. The importance of HLA DRB1 gene allele to clinical features and disability in patients with multiple sclerosis in Lithuania. BMC neurology. 2013;13:77.
80. International Multiple Sclerosis Genetics C, Beecham AH, Patsopoulos NA, Xifara DK, Davis MF, Kemppinen A, et al. Analysis of immune-related loci identifies 48 new susceptibility variants for multiple sclerosis. Nature genetics. 2013;45(11):1353-60.
81. International Multiple Sclerosis Genetics C, Hafler DA, Compston A, Sawcer S, Lander ES, Daly MJ, et al. Risk alleles for multiple sclerosis identified by a genomewide study. N Engl J Med. 2007;357(9):851-62.
82. De Jager PL, Jia X, Wang J, de Bakker PI, Ottoboni L, Aggarwal NT, et al. Meta-analysis of genome scans and replication identify CD6, IRF8 and TNFRSF1A as new multiple sclerosis susceptibility loci. Nature genetics. 2009;41(7):776-82.
83. International Multiple Sclerosis Genetics C, Wellcome Trust Case Control C, Sawcer S, Hellenthal G, Pirinen M, Spencer CC, et al. Genetic risk and a primary role for cell-mediated immune mechanisms in multiple sclerosis. Nature. 2011;476(7359):214-9.
84. Patsopoulos NA, Bayer Pharma MSGWG, Steering Committees of Studies Evaluating I-b, a CCRA, Consortium AN, GeneMsa, et al. Genome-wide meta-analysis identifies novel multiple sclerosis susceptibility loci. Ann Neurol. 2011;70(6):897-912.
85. Yan J, Greer JM. NF-kappa B, a potential therapeutic target for the treatment of multiple sclerosis. CNS & neurological disorders drug targets. 2008;7(6):536-57.
86. Goris A, Pauwels I, Gustavsen MW, van Son B, Hilven K, Bos SD, et al. Genetic variants are major determinants of CSF antibody levels in multiple sclerosis. Brain. 2015;138(Pt 3):632-43.
87. Munoz-Culla M, Irizar H, Otaegui D. The genetics of multiple sclerosis: review of current and emerging candidates. Appl Clin Genet. 2013;6:63-73.
88. Disanto G, Sandve GK, Berlanga-Taylor AJ, Morahan JM, Dobson R, Giovannoni G, et al. Genomic regions associated with multiple sclerosis are active in B cells. PLoS One. 2012;7(3):e32281.

89. Klose RJ, Bird AP. Genomic DNA methylation: the mark and its mediators. Trends Biochem Sci. 2006;31(2):89-97.
90. Okano M, Bell DW, Haber DA, Li E. DNA methyltransferases Dnmt3a and Dnmt3b are essential for de novo methylation and mammalian development. Cell. 1999;99(3):247-57.
91. Horvath S. DNA methylation age of human tissues and cell types. Genome biology. 2013;14(10):R115.
92. Lim U, Song MA. Dietary and lifestyle factors of DNA methylation. Methods Mol Biol. 2012;863:359-76.
93. Sokratous M, Dardiotis E, Tsouris Z, Bellou E, Michalopoulou A, Siokas V, et al. Deciphering the role of DNA methylation in multiple sclerosis: emerging issues. Auto Immun Highlights. 2016;7(1):12.
94. Baranzini SE, Mudge J, van Velkinburgh JC, Khankhanian P, Khrebtukova I, Miller NA, et al. Genome, epigenome and RNA sequences of monozygotic twins discordant for multiple sclerosis. Nature. 2010;464(7293):1351-6.
95. Liggett T, Melnikov A, Tilwalli S, Yi Q, Chen H, Replogle C, et al. Methylation patterns of cell-free plasma DNA in relapsing-remitting multiple sclerosis. Journal of the neurological sciences. 2010;290(1-2):16-21.
96. Kumagai C, Kalman B, Middleton FA, Vyshkina T, Massa PT. Increased promoter methylation of the immune regulatory gene SHP-1 in leukocytes of multiple sclerosis subjects. J Neuroimmunol. 2012;246(1-2):51-7.
97. Calabrese R, Zampieri M, Mechelli R, Annibali V, Guastafierro T, Ciccarone F, et al. Methylation-dependent PAD2 upregulation in multiple sclerosis peripheral blood. Mult Scler. 2012;18(3):299-304.
98. Graves M, Benton M, Lea R, Boyle M, Tajouri L, Macartney-Coxson D, et al. Methylation differences at the HLA-DRB1 locus in CD4+ T-Cells are associated with multiple sclerosis. Mult Scler. 2014;20(8):1033-41.
99. Maltby VE, Graves MC, Lea RA, Benton MC, Sanders KA, Tajouri L, et al. Genome-wide DNA methylation profiling of CD8+ T cells shows a distinct epigenetic signature to CD4+ T cells in multiple sclerosis patients. Clinical epigenetics. 2015;7:118.
100. Huynh JL, Garg P, Thin TH, Yoo S, Dutta R, Trapp BD, et al. Epigenome-wide differences in pathology-free regions of multiple sclerosis-affected brains. Nature neuroscience. 2014;17(1):121-30.
101. Bos SD, Page CM, Andreassen BK, Elboudwarej E, Gustavsen MW, Briggs F, et al. Genome-wide DNA methylation profiles indicate CD8+ T cell hypermethylation in multiple sclerosis. PLoS One. 2015;10(3):e0117403.
102. Han L, Witmer PD, Casey E, Valle D, Sukumar S. DNA methylation regulates MicroRNA expression. Cancer Biol Ther. 2007;6(8):1284-8.
103. Sinkkonen L, Hugenschmidt T, Berninger P, Gaidatzis D, Mohn F, Artus-Revel CG, et al. MicroRNAs control de novo DNA methylation through regulation of transcriptional repressors in mouse embryonic stem cells. Nat Struct Mol Biol. 2008;15(3):259-67.
104. Kozomara A, Griffiths-Jones S. miRBase: annotating high confidence microRNAs using deep sequencing data. Nucleic acids research. 2014;42(Database issue):D68-73.
105. Lewis BP, Burge CB, Bartel DP. Conserved seed pairing, often flanked by adenosines, indicates that thousands of human genes are microRNA targets. Cell. 2005;120(1):15-20.
106. Lu T-P, Lee C-Y, Tsai M-H, Chiu Y-C, Hsiao CK, Lai L-C, et al. miRSystem: An Integrated System for Characterizing Enriched Functions and Pathways of MicroRNA Targets. PLos ONE. 2012;7(8):e42390.

107. Cullen BR. Transcription and processing of human microRNA precursors. Molecular cell. 2004;16(6):861-5.
108. Graves P, Zeng Y. Biogenesis of mammalian microRNAs: a global view. Genomics, proteomics & bioinformatics. 2012;10(5):239-45.
109. Czech B, Hannon GJ. Small RNA sorting: matchmaking for Argonautes. Nature reviews Genetics. 2011;12(1):19-31.
110. Bartel DP. MicroRNAs: target recognition and regulatory functions. Cell. 2009;136(2):215-33.
111. Liu J, Carmell MA, Rivas FV, Marsden CG, Thomson JM, Song JJ, et al. Argonaute2 is the catalytic engine of mammalian RNAi. Science. 2004;305(5689):1437-41.
112. Tang G, Tang X, Mendu V, Tang X, Jia X, Chen QJ, et al. The art of microRNA: various strategies leading to gene silencing via an ancient pathway. Biochimica et biophysica acta. 2008;1779(11):655-62.
113. Croce CM. Causes and consequences of microRNA dysregulation in cancer. Nature reviews Genetics. 2009;10(10):704-14.
114. Jafari N, Shaghaghi H, Mahmoodi D, Shirzad Z, Alibeiki F, Bohlooli S, et al. Overexpression of microRNA biogenesis machinery: Drosha, DGCR8 and Dicer in multiple sclerosis patients. Journal of clinical neuroscience : official journal of the Neurosurgical Society of Australasia. 2015;22(1):200-3.
115. Magner WJ, Weinstock-Guttman B, Rho M, Hojnacki D, Ghazi R, Ramanathan M, et al. Dicer and microRNA expression in multiple sclerosis and response to interferon therapy. J Neuroimmunol. 2016;292:68-78.
116. Jin XF, Wu N, Wang L, Li J. Circulating MicroRNAs: A Novel Class of Potential Biomarkers for Diagnosing and Prognosing Central Nervous System Diseases. Cell Mol Neurobiol. 2013.
117. Krol J, Loedige I, Filipowicz W. The widespread regulation of microRNA biogenesis, function and decay. Nature reviews Genetics. 2010;11(9):597-610.
118. De Santis G, Ferracin M, Biondani A, Caniatti L, Rosaria Tola M, Castellazzi M, et al. Altered miRNA expression in T regulatory cells in course of multiple sclerosis. J Neuroimmunol. 2010;226(1-2):165-71.
119. Lorenzi JC, Brum DG, Zanette DL, de Paula Alves Souza A, Barbuzano FG, Dos Santos AC, et al. miR-15a and 16-1 are downregulated in CD4+ T cells of multiple sclerosis relapsing patients. Int J Neurosci. 2012;122(8):466-71.
120. Ridolfi E, Fenoglio C, Cantoni C, Calvi A, De Riz M, Pietroboni A, et al. Expression and Genetic Analysis of MicroRNAs Involved in Multiple Sclerosis. Int J Mol Sci. 2013;14(3):4375-84.
121. Fenoglio C, Ridolfi E, Cantoni C, De Riz M, Bonsi R, Serpente M, et al. Decreased circulating miRNA levels in patients with primary progressive multiple sclerosis. Mult Scler. 2013;19(14):1938-42.
122. Fenoglio C, De Riz M, Pietroboni AM, Calvi A, Serpente M, Cioffi SM, et al. Effect of fingolimod treatment on circulating miR-15b, miR23a and miR-223 levels in patients with multiple sclerosis. J Neuroimmunol. 2016;299:81-3.
123. Keller A, Leidinger P, Meese E, Haas J, Backes C, Rasche L, et al. Next-generation sequencing identifies altered whole blood microRNAs in neuromyelitis optica spectrum disorder which may permit discrimination from multiple sclerosis. Journal of neuroinflammation. 2015;12(1):196.

124. Arruda LC, Lorenzi JC, Sousa AP, Zanette DL, Palma PV, Panepucci RA, et al. Autologous hematopoietic SCT normalizes miR-16, -155 and -142-3p expression in multiple sclerosis patients. Bone Marrow Transplant. 2015;50(3):380-9.
125. Lindberg RL, Hoffmann F, Mehling M, Kuhle J, Kappos L. Altered expression of miR-17-5p in CD4+ lymphocytes of relapsing-remitting multiple sclerosis patients. Eur J Immunol. 2010;40(3):888-98.
126. Meira M, Sievers C, Hoffmann F, Rasenack M, Kuhle J, Derfuss T, et al. Unraveling natalizumab effects on deregulated miR-17 expression in CD4+ T cells of patients with relapsing-remitting multiple sclerosis. Journal of immunology research. 2014;2014:897249.
127. Cox MB, Cairns MJ, Gandhi KS, Carroll AP, Moscovis S, Stewart GJ, et al. MicroRNAs miR-17 and miR-20a inhibit T cell activation genes and are under-expressed in MS whole blood. PLoS One. 2010;5(8):e12132.
128. Keller A, Leidinger P, Steinmeyer F, Stahler C, Franke A, Hemmrich-Stanisak G, et al. Comprehensive analysis of microRNA profiles in multiple sclerosis including next-generation sequencing. Mult Scler. 2014;20(3):295-303.
129. Fenoglio C, Cantoni C, De Riz M, Ridolfi E, Cortini F, Serpente M, et al. Expression and genetic analysis of miRNAs involved in CD4+ cell activation in patients with multiple sclerosis. Neurosci Lett. 2011;504(1):9-12.
130. Siegel SR, Mackenzie J, Chaplin G, Jablonski NG, Griffiths L. Circulating microRNAs involved in multiple sclerosis. Mol Biol Rep. 2012;39(5):6219-25.
131. Honardoost MA, Kiani-Esfahani A, Ghaedi K, Etemadifar M, Salehi M. miR-326 and miR-26a, two potential markers for diagnosis of relapse and remission phases in patient with relapsing-remitting multiple sclerosis. Gene. 2014;544(2):128-33.
132. De Felice B, Mondola P, Sasso A, Orefice G, Bresciamorra V, Vacca G, et al. Small non-coding RNA signature in multiple sclerosis patients after treatment with interferon-beta. BMC medical genomics. 2014;7:26.
133. Mameli G, Arru G, Caggiu E, Niegowska M, Leoni S, Madeddu G, et al. Natalizumab Therapy Modulates miR-155, miR-26a and Proinflammatory Cytokine Expression in MS Patients. PLoS One. 2016;11(6):e0157153.
134. Ahmadian-Elmi M, Bidmeshki Pour A, Naghavian R, Ghaedi K, Tanhaei S, Izadi T, et al. miR-27a and miR-214 exert opposite regulatory roles in Th17 differentiation via mediating different signaling pathways in peripheral blood CD4+ T lymphocytes of patients with relapsing-remitting multiple sclerosis. Immunogenetics. 2016;68(1):43-54.
135. Regev K, Paul A, Healy B, von Glenn F, Diaz-Cruz C, Gholipour T, et al. Comprehensive evaluation of serum microRNAs as biomarkers in multiple sclerosis. Neurol Neuroimmunol Neuroinflamm. 2016;3(5):e267.
136. Guerau-de-Arellano M, Smith KM, Godlewski J, Liu Y, Winger R, Lawler SE, et al. Micro-RNA dysregulation in multiple sclerosis favours pro-inflammatory T-cell-mediated autoimmunity. Brain. 2011;134(Pt 12):3578-89.
137. Severin ME, Lee PW, Liu Y, Selhorst AJ, Gormley MG, Pei W, et al. MicroRNAs targeting TGFbeta signalling underlie the regulatory T cell defect in multiple sclerosis. Brain. 2016;139(Pt 6):1747-61.
138. Hecker M, Thamilarasan M, Koczan D, Schroder I, Flechtner K, Freiesleben S, et al. MicroRNA Expression Changes during Interferon-Beta Treatment in the Peripheral Blood of Multiple Sclerosis Patients. Int J Mol Sci. 2013;14(8):16087-110.

139. Smith KM, Guerau-de-Arellano M, Costinean S, Williams JL, Bottoni A, Mavrikis Cox G, et al. miR-29ab1 deficiency identifies a negative feedback loop controlling Th1 bias that is dysregulated in multiple sclerosis. J Immunol. 2012;189(4):1567-76.
140. Guerau-de-Arellano M, Liu Y, Meisen WH, Pitt D, Racke MK, Lovett-Racke AE. Analysis of miRNA in Normal Appearing White Matter to Identify Altered CNS Pathways in Multiple Sclerosis. J Autoimmune Disord. 2015;1(1).
141. Junker A, Krumbholz M, Eisele S, Mohan H, Augstein F, Bittner R, et al. MicroRNA profiling of multiple sclerosis lesions identifies modulators of the regulatory protein CD47. Brain. 2009;132(Pt 12):3342-52.
142. Søndergaard HB, Hesse D, Krakauer M, Sorensen PS, Sellebjerg F. Differential microRNA expression in blood in multiple sclerosis. Mult Scler. 2013.
143. Dutta R, Chomyk AM, Chang A, Ribaudo MV, Deckard SA, Doud MK, et al. Hippocampal demyelination and memory dysfunction are associated with increased levels of the neuronal microRNA miR-124 and reduced AMPA receptors. Ann Neurol. 2013.
144. Reijerkerk A, Lopez-Ramirez MA, van Het Hof B, Drexhage JA, Kamphuis WW, Kooij G, et al. MicroRNAs Regulate Human Brain Endothelial Cell-Barrier Function in Inflammation: Implications for Multiple Sclerosis. J Neurosci. 2013;33(16):6857-63.
145. Yang D, Wang WZ, Zhang XM, Yue H, Li B, Lin L, et al. MicroRNA Expression Aberration in Chinese Patients with Relapsing Remitting Multiple Sclerosis. Journal of molecular neuroscience : MN. 2013.
146. Munoz-Culla M, Irizar H, Castillo-Trivino T, Saenz-Cuesta M, Sepulveda L, Lopetegi I, et al. Blood miRNA expression pattern is a possible risk marker for natalizumab-associated progressive multifocal leukoencephalopathy in multiple sclerosis patients. Mult Scler. 2014.
147. Lecca D, Marangon D, Coppolino GT, Mendez AM, Finardi A, Costa GD, et al. MiR-125a-3p timely inhibits oligodendroglial maturation and is pathologically up-regulated in human multiple sclerosis. Sci Rep. 2016;6:34503.
148. Meira M, Sievers C, Hoffmann F, Derfuss T, Kuhle J, Kappos L, et al. MiR-126: a novel route for natalizumab action? Mult Scler. 2014.
149. Meira M, Sievers C, Hoffmann F, Haghikia A, Rasenack M, Decard BF, et al. Natalizumab-induced POU2AF1/Spi-B upregulation: A possible route for PML development. Neurol Neuroimmunol Neuroinflamm. 2016;3(3):e223.
150. Miyazaki Y, Li R, Rezk A, Misirliyan H, Moore C, Farooqi N, et al. A novel microRNA-132-surtuin-1 axis underlies aberrant B-cell cytokine regulation in patients with relapsing-remitting multiple sclerosis. PLoS One. 2014;9(8):e105421.
151. Guan H, Singh UP, Rao R, Mrelashvili D, Sen S, Hao H, et al. Inverse correlation of expression of microRNA-140-5p with progression of multiple sclerosis and differentiation of encephalitogenic T helper type 1 cells. Immunology. 2016;147(4):488-98.
152. Waschbisch A, Atiya M, Linker RA, Potapov S, Schwab S, Derfuss T. Glatiramer acetate treatment normalizes deregulated microRNA expression in relapsing remitting multiple sclerosis. PLoS One. 2011;6(9):e24604.
153. Keller A, Leidinger P, Lange J, Borries A, Schroers H, Scheffler M, et al. Multiple sclerosis: microRNA expression profiles accurately differentiate patients with relapsing-remitting disease from healthy controls. PLoS One. 2009;4(10):e7440.
154. Gandhi R, Healy B, Gholipour T, Egorova S, Musallam A, Shuja M, et al. Circulating microRNAs as biomarkers for disease staging in multiple sclerosis. Ann Neurol. 2013.

155. Wu D, Cerutti C, Lopez-Ramirez MA, Pryce G, King-Robson J, Simpson JE, et al. Brain endothelial miR-146a negatively modulates T-cell adhesion through repressing multiple targets to inhibit NF-kappaB activation. J Cereb Blood Flow Metab. 2015;35(3):412-23.
156. Bergman P, James T, Kular L, Ruhrmann S, Kramarova T, Kvist A, et al. Next-generation sequencing identifies microRNAs that associate with pathogenic autoimmune neuroinflammation in rats. Journal of immunology. 2013;190(8):4066-75.
157. Lopez-Ramirez MA, Wu D, Pryce G, Simpson JE, Reijerkerk A, King-Robson J, et al. MicroRNA-155 negatively affects blood-brain barrier function during neuroinflammation. FASEB journal : official publication of the Federation of American Societies for Experimental Biology. 2014.
158. Noorbakhsh F, Ellestad KK, Maingat F, Warren KG, Han MH, Steinman L, et al. Impaired neurosteroid synthesis in multiple sclerosis. Brain. 2011;134(9):2703-21.
159. Paraboschi EM, Solda G, Gemmati D, Orioli E, Zeri G, Benedetti MD, et al. Genetic association and altered gene expression of mir-155 in multiple sclerosis patients. Int J Mol Sci. 2011;12(12):8695-712.
160. Haghikia A, Hellwig K, Baraniskin A, Holzmann A, Decard BF, Thum T, et al. Regulated microRNAs in the CSF of patients with multiple sclerosis: a case-control study. Neurology. 2012;79(22):2166-70.
161. Hosseini A, Ghaedi K, Tanhaei S, Ganjalikhani-Hakemi M, Teimuri S, Etemadifar M, et al. Upregulation of CD4+T-Cell Derived MiR-223 in The Relapsing Phase of Multiple Sclerosis Patients. Cell J. 2016;18(3):371-80.
162. Du C, Liu C, Kang J, Zhao G, Ye Z, Huang S, et al. MicroRNA miR-326 regulates TH-17 differentiation and is associated with the pathogenesis of multiple sclerosis. Nat Immunol. 2009;10(12):1252-9.
163. Martinelli-Boneschi F, Fenoglio C, Brambilla P, Sorosina M, Giacalone G, Esposito F, et al. MicroRNA and mRNA expression profile screening in multiple sclerosis patients to unravel novel pathogenic steps and identify potential biomarkers. Neurosci Lett. 2012;508(1):4-8.
164. Munoz-Culla M, Irizar H, Saenz-Cuesta M, Castillo-Trivino T, Osorio-Querejeta I, Sepulveda L, et al. SncRNA (microRNA & snoRNA) opposite expression pattern found in multiple sclerosis relapse and remission is sex dependent. Sci Rep. 2016;6:20126.
165. Murugaiyan G, Beynon V, Mittal A, Joller N, Weiner HL. Silencing microRNA-155 ameliorates experimental autoimmune encephalomyelitis. J Immunol. 2011;187(5):2213-21.
166. Cerutti C, Soblechero-Martin P, Wu D, Lopez-Ramirez MA, de Vries H, Sharrack B, et al. MicroRNA-155 contributes to shear-resistant leukocyte adhesion to human brain endothelium in vitro. Fluids Barriers CNS. 2016;13(1):8.
167. Potzner MR, Griffel C, Lutjen-Drecoll E, Bosl MR, Wegner M, Sock E. Prolonged Sox4 expression in oligodendrocytes interferes with normal myelination in the central nervous system. Mol Cell Biol. 2007;27(15):5316-26.
168. Luhder F, Gold R, Flugel A, Linker RA. Brain-derived neurotrophic factor in neuroimmunology: lessons learned from multiple sclerosis patients and experimental autoimmune encephalomyelitis models. Arch Immunol Ther Exp (Warsz). 2013;61(2):95-105.
169. Ponomarev ED, Veremeyko T, Barteneva N, Krichevsky AM, Weiner HL. MicroRNA-124 promotes microglia quiescence and suppresses EAE by deactivating macrophages via the C/EBP-alpha-PU.1 pathway. Nat Med. 2011;17(1):64-70.
170. Jagot F, Davoust N. Is It worth Considering Circulating microRNAs in Multiple Sclerosis? Frontiers in immunology. 2016;7:129.

171. Pusic AD, Pusic KM, Kraig RP, editors. IFNγ Stimulated dendritic cell exosomes as a therapeutic for remyelination. Society for Neuroscience; 2013 9-13 Nov; San Diego, California.
172. Mahurkar S, Suppiah V, O'Doherty C. Pharmacogenomics of interferon beta and glatiramer acetate response: A review of the literature. Autoimmunity reviews. 2013.
173. Otaegui D, Baranzini SE, Armananzas R, Calvo B, Munoz-Culla M, Khankhanian P, et al. Differential micro RNA expression in PBMC from multiple sclerosis patients. PLoS One. 2009;4(7):e6309.
174. Jacobs LD, Cookfair DL, Rudick RA, Herndon RM, Richert JR, Salazar AM, et al. Intramuscular interferon beta-1a for disease progression in relapsing multiple sclerosis. The Multiple Sclerosis Collaborative Research Group (MSCRG). Ann Neurol. 1996;39(3):285-94.
175. Polman CH, O'Connor PW, Havrdova E, Hutchinson M, Kappos L, Miller DH, et al. A randomized, placebo-controlled trial of natalizumab for relapsing multiple sclerosis. N Engl J Med. 2006;354(9):899-910.
176. Ingwersen J, Menge T, Wingerath B, Kaya D, Graf J, Prozorovski T, et al. Natalizumab restores aberrant miRNA expression profile in multiple sclerosis and reveals a critical role for miR-20b. Ann Clin Transl Neurol. 2015;2(1):43-55.
177. D'Amico E, Zanghi A, Leone C, Tumani H, Patti F. Treatment-Related Progressive Multifocal Leukoencephalopathy in Multiple Sclerosis: A Comprehensive Review of Current Evidence and Future Needs. Drug Saf. 2016;39(12):1163-74.
178. Brinkmann V, Davis MD, Heise CE, Albert R, Cottens S, Hof R, et al. The immune modulator FTY720 targets sphingosine 1-phosphate receptors. J Biol Chem. 2002;277(24):21453-7.
179. Chun J, Hartung HP. Mechanism of action of oral fingolimod (FTY720) in multiple sclerosis. Clin Neuropharmacol. 2010;33(2):91-101.
180. Atkins HL, Bowman M, Allan D, Anstee G, Arnold DL, Bar-Or A, et al. Immunoablation and autologous haemopoietic stem-cell transplantation for aggressive multiple sclerosis: a multicentre single-group phase 2 trial. Lancet. 2016;388(10044):576-85.
181. Aung LL, Balashov KE. Decreased Dicer expression is linked to increased expression of co-stimulatory molecule CD80 on B cells in multiple sclerosis. Mult Scler. 2015;21(9):1131-8.
182. Raphael I, Webb J, Stuve O, Haskins W, Forsthuber T. Body fluid biomarkers in multiple sclerosis: how far we have come and how they could affect the clinic now and in the future. Expert review of clinical immunology. 2015;11(1):69-91.
183. Polman CH, Reingold SC, Banwell B, Clanet M, Cohen JA, Filippi M, et al. Diagnostic criteria for multiple sclerosis: 2010 revisions to the McDonald criteria. Ann Neurol. 2011;69(2):292-302.
184. Bolger AM, Lohse M, Usadel B. Trimmomatic: a flexible trimmer for Illumina sequence data. Bioinformatics. 2014;30(15):2114-20.
185. Benjamini Y, Hochberg Y. Controlling the False Discovery Rate: A Practical and Powerful Approach to Multiple Testing. Journal of the Royal Statistical Society Series B (methodological). 1995;57(1):289-300.
186. Mestdagh P, Hartmann N, Baeriswyl L, Andreasen D, Bernard N, Chen C, et al. Evaluation of quantitative miRNA expression platforms in the microRNA quality control (miRQC) study. Nature methods. 2014;11(8):809-15.
187. Choi YB, Son M, Park M, Shin J, Yun Y. SOCS-6 negatively regulates T cell activation through targeting p56lck to proteasomal degradation. J Biol Chem. 2010;285(10):7271-80.

188. Hu R, Huffaker TB, Kagele DA, Runtsch MC, Bake E, Chaudhuri AA, et al. MicroRNA-155 confers encephalogenic potential to Th17 cells by promoting effector gene expression. J Immunol. 2013;190(12):5972-80.
189. Rodriguez A, Vigorito E, Clare S, Warren MV, Couttet P, Soond DR, et al. Requirement of bic/microRNA-155 for normal immune function. Science. 2007;316(5824):608-11.
190. Snowden JA, Saccardi R, Allez M, Ardizzone S, Arnold R, Cervera R, et al. Haematopoietic SCT in severe autoimmune diseases: updated guidelines of the European Group for Blood and Marrow Transplantation. Bone Marrow Transplant. 2012;47(6):770-90.
191. Galimberti D, Villa C, Fenoglio C, Serpente M, Ghezzi L, Cioffi SM, et al. Circulating miRNAs as potential biomarkers in Alzheimer's disease. Journal of Alzheimers Disease. 2014;42(4):1261-7.
192. Pasquali L, Lucchesi C, Pecori C, Metelli MR, Pellegrini S, Iudice A, et al. A clinical and laboratory study evaluating the profile of cytokine levels in relapsing remitting and secondary progressive multiple sclerosis. J Neuroimmunol. 2015;278:53-9.
193. Qin H, Zhu X, Liang J, Wu J, Yang Y, Wang S, et al. MicroRNA-29b contributes to DNA hypomethylation of CD4+ T cells in systemic lupus erythematosus by indirectly targeting DNA methyltransferase 1. Journal of dermatological science. 2013;69(1):61-7.
194. Murugaiyan G, da Cunha AP, Ajay AK, Joller N, Garo LP, Kumaradevan S, et al. MicroRNA-21 promotes Th17 differentiation and mediates experimental autoimmune encephalomyelitis. The Journal of clinical investigation. 2015;125(3):1069-80.
195. Cox MB, Cairns MJ, Gandhi KS, Carroll AP, Moscovis S, Stewart GJ, et al. MicroRNAs miR-17 and miR-20a inhibit T cell activation genes and are under-expressed in MS whole blood. PLoS One. 2010;5(8):e12132.
196. Lai RH, Wang MJ, Yang SH, Chen JY. Genomic organization and functional characterization of the promoter for the human suppressor of cytokine signaling 6 gene. Gene. 2009;448(1):64-73.
197. Lai RH, Hsiao YW, Wang MJ, Lin HY, Wu CW, Chi CW, et al. SOCS6, down-regulated in gastric cancer, inhibits cell proliferation and colony formation. Cancer letters. 2010;288(1):75-85.
198. Letellier E, Schmitz M, Baig K, Beaume N, Schwartz C, Frasquilho S, et al. Identification of SOCS2 and SOCS6 as biomarkers in human colorectal cancer. British journal of cancer. 2014;111(4):726-35.
199. Wu K, Hu G, He X, Zhou P, Li J, He B, et al. MicroRNA-424-5p suppresses the expression of SOCS6 in pancreatic cancer. Pathology oncology research : POR. 2013;19(4):739-48.
200. International Multiple Sclerosis Genetics C. IL12A, MPHOSPH9/CDK2AP1 and RGS1 are novel multiple sclerosis susceptibility loci. Genes and immunity. 2010;11(5):397-405.
201. Zhu H, Wang X, Shi H, Su S, Harshfield GA, Gutin B, et al. A genome-wide methylation study of severe vitamin D deficiency in African American adolescents. J Pediatr. 2013;162(5):1004-9 e1.
202. Sanders KA, Benton MC, Lea RA, Maltby VE, Agland S, Griffin N, et al. Next-generation sequencing reveals broad down-regulation of microRNAs in secondary progressive multiple sclerosis CD4+ T cells. Clinical epigenetics. 2016;8(1):87.
203. Aryee MJ, Jaffe AE, Corrada-Bravo H, Ladd-Acosta C, Feinberg AP, Hansen KD, et al. Minfi: a flexible and comprehensive Bioconductor package for the analysis of Infinium DNA methylation microarrays. Bioinformatics. 2014;30(10):1363-9.

204. Hansen K, M, A. minfi: Analyze Illumina's 450K methylation arrays. Bioconductor. 2012.
205. Salehi-Tabar R, Nguyen-Yamamoto L, Tavera-Mendoza LE, Quail T, Dimitrov V, An BS, et al. Vitamin D receptor as a master regulator of the c-MYC/MXD1 network. Proc Natl Acad Sci U S A. 2012;109(46):18827-32.
206. Friedman J, Hastie T, Tibshirani R. Regularization Paths for Generalized Linear Models via Coordinate Descent. J Stat Softw. 2010;33(1):1-22.
207. Chien CH, Sun YM, Chang WC, Chiang-Hsieh PY, Lee TY, Tsai WC, et al. Identifying transcriptional start sites of human microRNAs based on high-throughput sequencing data. Nucleic acids research. 2011;39(21):9345-56.
208. Endo S, Amano M, Nishimura N, Ueno N, Ueno S, Yuki H, et al. Immunomodulatory drugs act as inhibitors of DNA methyltransferases and induce PU.1 up-regulation in myeloma cells. Biochem Biophys Res Commun. 2016;469(2):236-42.
209. Marttila S, Kananen L, Hayrynen S, Jylhava J, Nevalainen T, Hervonen A, et al. Ageing-associated changes in the human DNA methylome: genomic locations and effects on gene expression. BMC Genomics. 2015;16:179.
210. Matsuo R, Asada A, Fujitani K, Inokuchi K. LIRF, a gene induced during hippocampal long-term potentiation as an immediate-early gene, encodes a novel RING finger protein. Biochem Biophys Res Commun. 2001;289(2):479-84.
211. Cree BA, Rioux JD, McCauley JL, Gourraud PA, Goyette P, McElroy J, et al. A major histocompatibility Class I locus contributes to multiple sclerosis susceptibility independently from HLA-DRB1*15:01. PLoS One. 2010;5(6):e11296.
212. Kurata R, Nakaoka H, Tajima A, Hosomichi K, Shiina T, Meguro A, et al. TRIM39 and RNF39 are associated with Behcet's disease independently of HLA-B *51 and -A *26. Biochem Biophys Res Commun. 2010;401(4):533-7.
213. Renauer P, Coit P, Jeffries MA, Merrill JT, McCune WJ, Maksimowicz-McKinnon K, et al. DNA methylation patterns in naive CD4+ T cells identify epigenetic susceptibility loci for malar rash and discoid rash in systemic lupus erythematosus. Lupus Sci Med. 2015;2(1):e000101.
214. Lee Y, Ahn C, Han J, Choi H, Kim J, Yim J, et al. The nuclear RNase III Drosha initiates microRNA processing. Nature. 2003;425(6956):415-9.
215. Fabbri M, Garzon R, Cimmino A, Liu Z, Zanesi N, Callegari E, et al. MicroRNA-29 family reverts aberrant methylation in lung cancer by targeting DNA methyltransferases 3A and 3B. Proc Natl Acad Sci U S A. 2007;104(40):15805-10.
216. Garzon R, Liu S, Fabbri M, Liu Z, Heaphy CE, Callegari E, et al. MicroRNA-29b induces global DNA hypomethylation and tumor suppressor gene reexpression in acute myeloid leukemia by targeting directly DNMT3A and 3B and indirectly DNMT1. Blood. 2009;113(25):6411-8.
217. Morita S, Horii T, Kimura M, Ochiya T, Tajima S, Hatada I. miR-29 represses the activities of DNA methyltransferases and DNA demethylases. Int J Mol Sci. 2013;14(7):14647-58.
218. Ardekani AM, Naeini MM. The Role of MicroRNAs in Human Diseases. Avicenna J Med Biotechnol. 2010;2(4):161-79.
219. Sarkijarvi S, Kuusisto H, Paalavuo R, Levula M, Airla N, Lehtimaki T, et al. Gene expression profiles in Finnish twins with multiple sclerosis. BMC medical genetics. 2006;7:11.

220. Kurzynska-Kokorniak A, Koralewska N, Pokornowska M, Urbanowicz A, Tworak A, Mickiewicz A, et al. The many faces of Dicer: the complexity of the mechanisms regulating Dicer gene expression and enzyme activities. Nucleic acids research. 2015;43(9):4365-80.
221. Wang X, Zhao X, Gao P, Wu M. c-Myc modulates microRNA processing via the transcriptional regulation of Drosha. Sci Rep. 2013;3:1942.
222. Zeis T, Graumann U, Reynolds R, Schaeren-Wiemers N. Normal-appearing white matter in multiple sclerosis is in a subtle balance between inflammation and neuroprotection. Brain. 2008;131(Pt 1):288-303.
223. Eisele S, Krumbholz M, Fischer MT, Mohan H, Junker A, Arzberger T, et al. Prospects of transcript profiling for mRNAs and MicroRNAs using formalin-fixed and paraffin-embedded dissected autoptic multiple sclerosis lesions. Brain pathology. 2012;22(5):607-18.
224. Siebolts U, Varnholt H, Drebber U, Dienes HP, Wickenhauser C, Odenthal M. Tissues from routine pathology archives are suitable for microRNA analyses by quantitative PCR. J Clin Pathol. 2009;62(1):84-8.
225. Bentley-Hewitt KL, Hedderley DI, Monro J, Martell S, Smith H, Mishra S. Comparison of quantitative real-time polymerase chain reaction with NanoString(R) methodology using adipose and liver tissues from rats fed seaweed. N Biotechnol. 2016;33(3):380-6.
226. Mouledous L, Hunt S, Harcourt R, Harry J, Williams KL, Gutstein HB. Navigated laser capture microdissection as an alternative to direct histological staining for proteomic analysis of brain samples. Proteomics. 2003;3(5):610-5.
227. Becker C, Hammerle-Fickinger A, Riedmaier I, Pfaffl MW. mRNA and microRNA quality control for RT-qPCR analysis. Methods. 2010;50(4):237-43.
228. Reis PP, Waldron L, Goswami RS, Xu W, Xuan Y, Perez-Ordonez B, et al. mRNA transcript quantification in archival samples using multiplexed, color-coded probes. BMC Biotechnol. 2011;11:46.
229. Biosystems A. Application Notes: Endogenous Controls for Real-Time Quantitation of miRNA Using TaqMan MicroRNA Assays http://www3.appliedbiosystems.com/cms/groups/mcb_marketing/documents/generaldocuments/cms_044972.pdf2010 [
230. Vlachos IS, Zagganas K, Paraskevopoulou MD, Georgakilas G, Karagkouni D, Vergoulis T, et al. DIANA-miRPath v3.0: deciphering microRNA function with experimental support. Nucleic acids research. 2015;43(W1):W460-6.
231. Vlachos IS, Paraskevopoulou MD, Karagkouni D, Georgakilas G, Vergoulis T, Kanellos I, et al. DIANA-TarBase v7.0: indexing more than half a million experimentally supported miRNA:mRNA interactions. Nucleic acids research. 2015;43(Database issue):D153-9.
232. Wilkins A, Majed H, Layfield R, Compston A, Chandran S. Oligodendrocytes promote neuronal survival and axonal length by distinct intracellular mechanisms: a novel role for oligodendrocyte-derived glial cell line-derived neurotrophic factor. J Neurosci. 2003;23(12):4967-74.
233. Alvarez JI, Saint-Laurent O, Godschalk A, Terouz S, Briels C, Larouche S, et al. Focal disturbances in the blood-brain barrier are associated with formation of neuroinflammatory lesions. Neurobiol Dis. 2015;74:14-24.
234. de Faria O, Jr., Cui QL, Bin JM, Bull SJ, Kennedy TE, Bar-Or A, et al. Regulation of miRNA 219 and miRNA Clusters 338 and 17-92 in Oligodendrocytes. Front Genet. 2012;3:46.
235. Diao HJ, Low WC, Lu QR, Chew SY. Topographical effects on fiber-mediated microRNA delivery to control oligodendroglial precursor cells development. Biomaterials. 2015;70:105-14.

236. Valadi H, Ekstrom K, Bossios A, Sjostrand M, Lee JJ, Lotvall JO. Exosome-mediated transfer of mRNAs and microRNAs is a novel mechanism of genetic exchange between cells. Nat Cell Biol. 2007;9(6):654-9.
237. Hansen TB, Jensen TI, Clausen BH, Bramsen JB, Finsen B, Damgaard CK, et al. Natural RNA circles function as efficient microRNA sponges. Nature. 2013;495(7441):384-8.
238. Freiesleben S, Hecker M, Zettl UK, Fuellen G, Taher L. Analysis of microRNA and Gene Expression Profiles in Multiple Sclerosis: Integrating Interaction Data to Uncover Regulatory Mechanisms. Sci Rep. 2016;6:34512.